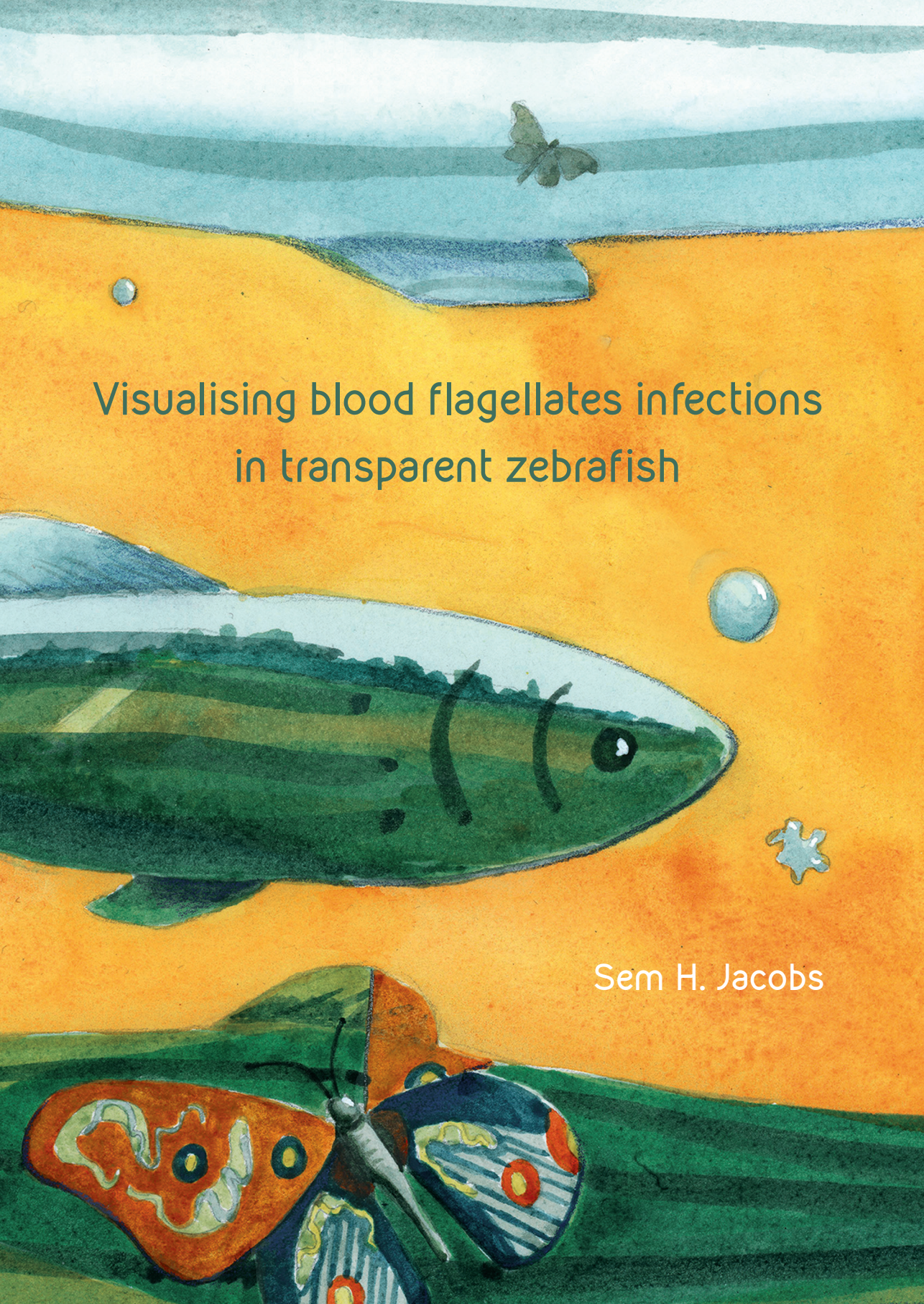

Visualising blood flagellates infections in transparent zebrafish

Sem H. Jacobs

Visualising blood flagellates infections in transparent zebrafish

Sem H. Jacobs

Thesis committee

Promotors
Prof. Dr G.F. Wiegertjes
Professor of Aquaculture and Fisheries
Wageningen University & Research

Dr M. Forlenza
Associate professor, Cell Biology and Immunology Group
Wageningen University & Research

Co-promotor
Dr M.J.M. Lankheet
Associate professor, Experimental Zoology Group
Wageningen University & Research

Other members
Prof. Dr J.M. Wells, Wageningen University & Research
Dr P. Elks, University of Sheffield, UK
Prof. Dr S. Magez, University of Brussels, Belgium
Dr J.M.J. Rebel, Wageningen University & Research

This research was conducted under the auspices of the Graduate School Wageningen Institute of Animal Sciences.

Visualising blood flagellates infections in transparent zebrafish

Sem H. Jacobs

Thesis

submitted in fulfilment of the requirements for the degree of doctor
at Wageningen University
by the authority of the Rector Magnificus,
Prof. Dr A.P.J. Mol,
in the presence of the
Thesis Committee appointed by the Academic Board
to be defended in public
on Friday 5 June 2020
at 01.30 p.m. in the Aula.

Sem H. Jacobs
Visualising blood flagellates infections in transparent zebrafish
228 pages.
PhD thesis, Wageningen University, Wageningen, the Netherlands (2020)
With references, with summary in English and in Dutch
ISBN: 978-94-6395-372-6
DOI: https://doi.org/10.18174/519090

Table of contents

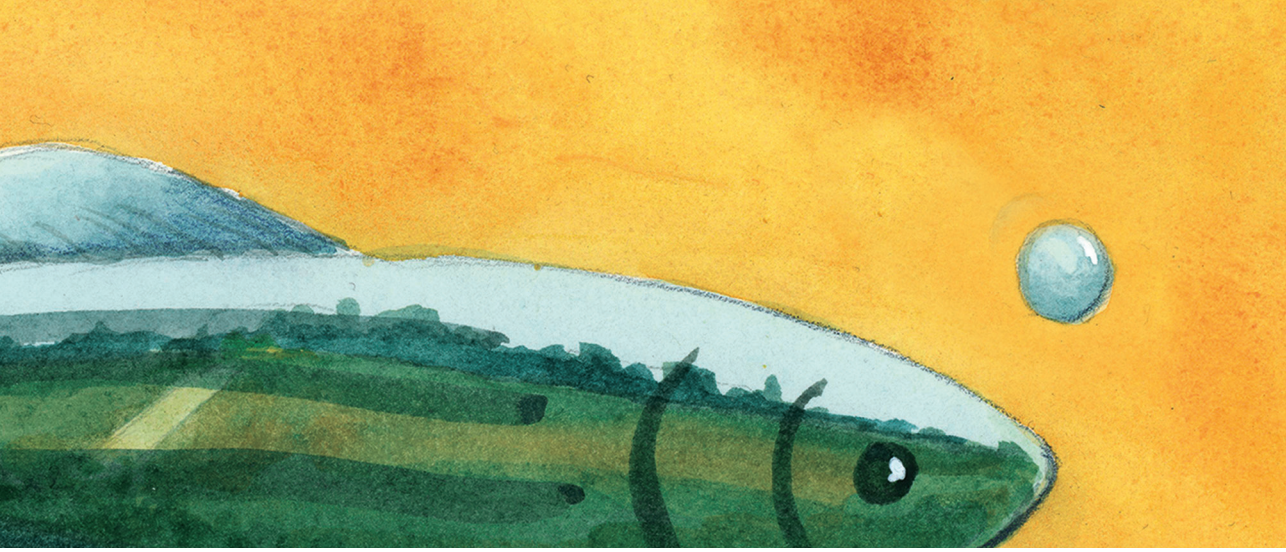

General Introduction

Kinetoplastids

Kinetoplastids are unique protozoa containing a range of omnipresent species, ranging from pathogens of invertebrates, vertebrates and even some plants. These unicellular organisms have a kinetoplastid organelle containing mitochondrial DNA. The kinetoplastid order can be divided in the suborders Trypanosomatida and Bodonidae (**Fig 1**) (Lom, 1979; Lukeš et al., 2014; Simpson et al., 2006).

Trypanosomatids have a single flagellum and can infect animals from all vertebrate classes, including warm-blooded mammals and birds, as well as cold-blooded amphibians, reptiles and fish (Simpson et al., 2006). Trypanosomes are transmitted to their host by a vector, most often an arthropod vector. This requires great adaptation of these trypanosomes to different environments. Stercorarian trypanosomes are transmitted by various blood-sucking insects and develop in the posterior part of the insect gut until they are secreted through the feces (stercus; manure in Latin) of the insect and can then penetrate the skin of the vertebrate host (Uilenberg, 1998; Vickerman, 1985). After infection, stercorarian trypanosomes reside temporarily extracellularly in the blood until they succeed in entering the cells of various tissues and effectively hide from the host immune system (Brener, 1973). The best-known stercorarian trypanosome is *Trypanosoma cruzi*, causing Human American Trypanosomiasis or Chagas´ disease. Salivarian trypanosomes, develop in the midgut of Tsetse-flies (*Glossina* spp.) and are transmitted to their vertebrate host via the saliva of the insect vector (Vickerman, 1985). After infection, salivarian trypanosomes reside extracellular in the blood and in tissue fluids of their vertebrate host. As the infection progresses, the parasites are able to enter the central nervous system, causing neurogenically symptoms which led to the name of the disease, Sleeping Sickness (Losos and Ikede, 1972; Vickerman, 1985). The best-characterized salivarian trypanosomes are *Trypanosoma brucei* species. *T. brucei* is best known for causing Human African Trypanosomiasis (HAT or Sleeping Sickness) and African Animal Trypanosomiasis (AAT) in livestock (Stevens et al., 1998). There are three main *T. brucei* subspecies: *T.b. brucei* (infecting livestock), *T.b. gambiense* and *T.b. rhodesiense* (infecting humans) (Hoare, 1972). The aquatic clade within *Trypanosomatida* includes more than 200 different trypanosomes, affecting fresh and marine fishes (Simpson et al., 2006). One of the most studied aquatic trypanosomes is *Trypanosoma carassii*, previously called *Trypanosoma danilewskyi.* Similar to other trypanosomes, *T. carassii* has a single flagellum (**Fig 2**) (Lom, 1979; Overath et al., 1999, 1998) and infects cyprinids as well as some non-cyprinid freshwater fish (Woo and Ardelli, 2013), where it occurs extracellularly in the blood and tissues of its host (Overath et al., 1999).

Bodonidae, which diverged early in evolution from the well-described suborder Trypanosomatida, have two flagella and while most species are free living in aqueous environments, some are parasitic, affecting either vertebrates or invertebrates (Lukeš et al., 2014; Stevens et al., 2001). *Cryptobia (Trypanoplasma) salmositica* and *Trypanoplasma borreli* are extracellular blood parasites, belonging to the 'Fish cryptobia' clade of the

Parabodonida (**Fig 1**) (Lom, 1979; Losev et al., 2015). *C. salmositica* can infect all species of salmon (*Oncorhynchus* spp.) in freshwater streams or rivers along the west coast of North America and is transmitted by the freshwater leech (*Piscicola salmositica*) (Becker and Katz, 1951; Woo, 1978). *T. borreli* (**Fig 2**), like *T. carassii*, infects cyprinid fish. Both *T. carassii* and *T. borreli* can be transmitted by blood-sucking leeches (*Piscicola geometra* and *Hemiclepsis marginata*) and many fish will carry mixed populations of *T. carassii* and *T. borreli* (Lom, 1979; Lom and Dyková, 1992; Wiegertjes et al., 2005).

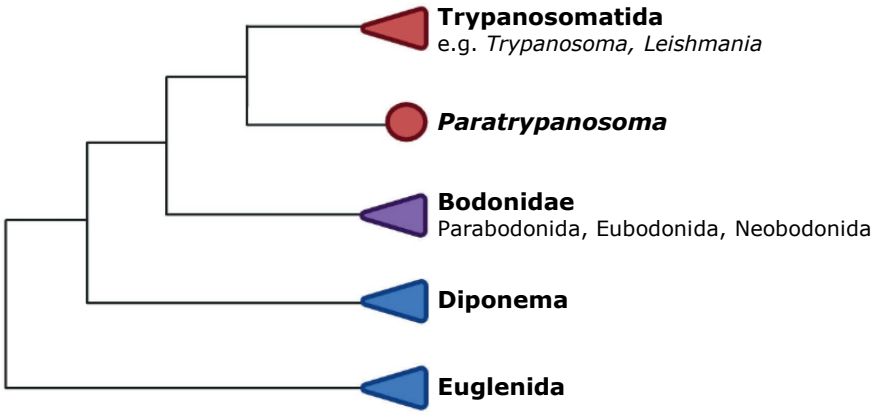

Fig 1. Overview of evolutionary relationships between Trypanosomatida and Bodonidae.
Triangles and circle denote multiple and single known representatives of a clade, respectively. Red, blue and purple depict parasitic, free-living and parasitic/free-living kinetoplastids, respectively (adapted from Lukeš et al., 2014).

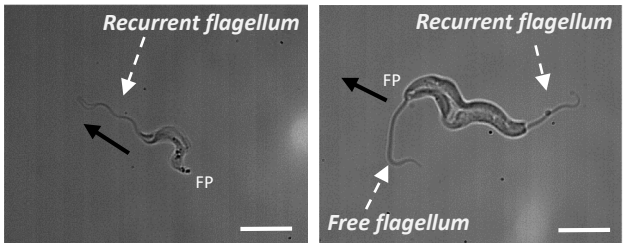

Fig 2. Details of *T. carassii* and *T. borreli* cell body morphology.
Detailed 100x magnification images showing *T. carassii* (left) and *T. borreli* (right). Note the difference in body shape, size and the presence of one flagellum for T. *carassii* and of two flagella for *T. borreli*. The recurrent, cell-attached flagellum of *T. carassii* originates from the flagellar pocket (FP) at the posterior end of the cell body, runs along the cell body, ending free at the anterior (leading) end. The recurrent, cell-attached flagellum of *T. borreli* originates from the flagellar pocket, this time at the anterior end of the cell body, runs along the cell body and protrudes at the posterior end, whereas the non-cell-attached (free) flagellum originates form the flagellar pocket and extend free at the anterior (leading) end. Black arrows indicate swimming direction of the flagellates. Scale bars indicate 10 μm.

Zebrafish as a disease model

Zebrafish are cyprinid fish closely related to common carp and goldfish, both natural hosts to *T. carassii* and/or *T. borreli* (Overath et al., 1998; Steinhagen et al., 1989; Woo and Black, 1984). Zebrafish embryos develop *ex utero*, directly from the single cell stage onwards. Zebrafish embryos and larvae are optically transparent, enabling visualisation of biological processes *in vivo*, in live animals and making zebrafish an attractive vertebrate model species. Zebrafish have been used as a successful model for biomedical, developmental biology, and neurobiology research (Asnani and Peterson, 2014; Blackburn and Langenau, 2014; Cronan and Tobin, 2014; Goessling and North, 2014; Miyares et al., 2014; Nguyen-Chi et al., 2014; Phillips and Westerfield, 2014; Renshaw and Trede, 2012; Schartl, 2014; Torraca et al., 2014; Veinotte et al., 2014; Zon and Cagan, 2014). The success of the zebrafish, especially for host-pathogen interaction studies, is due to several unique aspects: i) the sequential development of the immune system, creating a time frame to study only the early innate immune response without interference of adaptive immunity; ii) the availability of a well annotated genome, which allowed iii) the generation of mutant and transgenic lines including those marking blood vessels and relevant immune cell lineages (Benard et al., 2015; Bertrand et al., 2010; Ellett et al., 2011; Langenau et al., 2004; Lawson and Weinstein, 2002; Page et al., 2013; Petrie-Hanson et al., 2009; Renshaw et al., 2006).

The development from the embryonic zebrafish stage to adult zebrafish lasts approximately 3 months. Zebrafish hatch around 3–4 days post fertilization (dpf) with the end of embryogenesis defined as the protruding mouth stage (around 3 dpf at 28.5°C). The larval development stage follows the embryonic period and has a duration of around 6 weeks. In this period, the larvae greatly increase in length and exhibit various morphological changes into juveniles (around 45 dpf) (**Fig 3**). The juvenile stage closely resembles the adult stage, but sexual maturity takes until approximately 90 dpf (at 28.5°C), when zebrafish are considered adults (Parichy et al., 2009; Singleman and Holtzman, 2014) (**Fig 3**). As stated before, only innate immune cells are present during the first period of 2-7 dpf of embryonic and early larval life, providing a window to study host-pathogen interactions focusing on the innate immune response only. Next, mature T cells will start to leave the thymus and move to peripheral organs, followed by B cell development. Around 2-3 weeks post-hatch, both innate and adaptive immune cells are present in the zebrafish (Langenau et al., 2004; Page et al., 2013; Torraca et al., 2014; Torraca and Mostowy, 2018). The response of innate immune cells, such as macrophages and neutrophils, towards several viral, fungal and bacterial pathogens has been studied in detail using zebrafish (Cronan and Tobin, 2014; García-Valtanen et al., 2017; Meijer, 2016; Nguyen-Chi et al., 2014; Palha et al., 2013; Ramakrishnan, 2013; Renshaw and Trede, 2012; Rosowski et al., 2018; Torraca and Mostowy, 2018). These zebrafish studies, contributed to the knowledge about host-pathogen interaction mechanisms, and in some cases have made it possible to translate findings to clinical applications. In this thesis, we took advantage of the transparency of zebrafish larvae and of the availability of various transgenic lines to visualise the swimming behaviour of *T. carassii* and *T. borreli in vivo* in a vertebrate host and to study in real-time the early events of the innate immune response to these parasites.

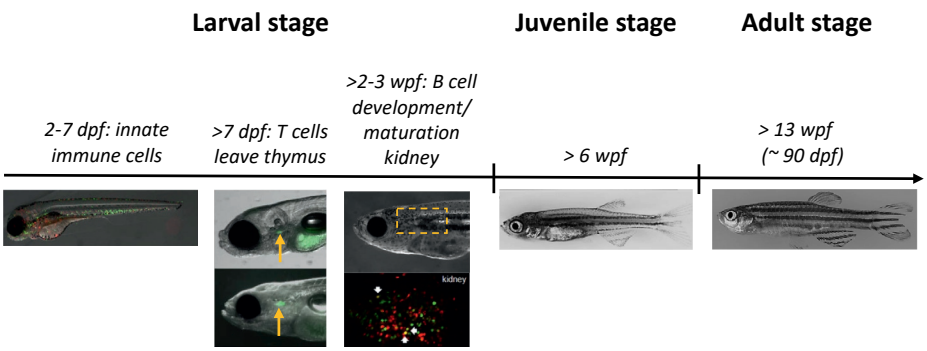

Fig 3. Immune development in zebrafish.
Schematic overview of the immune development of zebrafish. Larval stage lasts approximately 6 weeks. In this stage, during the first 2-7 days post fertilization (dpf), only innate immune cells are present. Next, mature T cells will start to leave the thymus (orange arrow) and move to peripheral organs (>7 dpf), followed by B cell development in the kidney (rectangle) (fluorescent image adapted from Page et al., 2013). Around 2-3 weeks post-hatch, both innate and adaptive immune cells are present in the zebrafish. The juvenile stage lasts until approximately 90 dpf, followed by the adult stage, from 13 wpf onwards, adapted from (Dooley et al., 2013). Images are not in scale.

Early innate immune responses during infection with VSG-containing trypanosomes

African trypanosomes expressing variant surface glycoproteins (VSGs) on their cell surface (VSG^{+}), infect mammalian hosts and cause sequential activation of innate and adaptive immune responses. Early stages of trypanosome infections are associated with production of cytokines, which do not only play a role in resistance, but also in susceptibility of the host to the infection. Analysis of *T. brucei* and *T. congolense* infections in mice revealed that IFNγ is one of the cytokines important in determining the outcome of the infection. As seen during the early phase of the innate response to first peak parasitaemia, IFNγ is secreted first by NK and NKT cells, and subsequently by CD8+ and CD4+ T cells (Cnops et al., 2015; Radwanska et al., 2018; Wu et al., 2017). IFNγ exerts a protective role through the stimulation of phagocytic myeloid cells, leading to TNFα and nitric oxide (NO) secretion (**Fig 4A**). In mice, NO, IFNγ and TNFα play a crucial (direct or indirect) role in limiting trypanosome growth during the first peak of parasitaemia, however uncontrolled expression of the same mediators can result in immunopathology (**Fig 4B, 4C**) (Brunet, 2001; Cnops et al., 2015; Lopez et al., 2008; Magez et al., 2006, 1999; Shi et al., 2003; Sternberg and Mabbott, 1996; Uzonna et al., 1998). *T. brucei brucei* and *T. brucei gambiense* studies revealed that mouse TNFα has a direct trypanolytic effect, mediated by a lectin-like binding domain on the TNF molecule (**Fig 4B**) (Magez et al., 2002, 1998; Sileghem et al., 2001). Nitric oxide (NO) production is a common feature observed during parasitic infections mice model studies, such as malaria, leishmaniasis and toxoplasmosis (reviewed by Brunet, 2001). The aforementioned studies show it is evident that macrophages play a crucial role in determining the outcome of the early innate immune

response to trypanosome infections. A role for neutrophils in the establishment of tsetse fly-mediated trypanosome infections in mouse dermis was recently reported. It was implicated that neutrophils promote the onset of infection and do not significantly contribute to dermal parasite control (Caljon et al., 2018).

Many of the previously described findings were observed in studies taking advantage of several mice models such as trypanosusceptible or trypanotolerant, as well as mutant 'knock-out' mice strains. These studies contributed tremendously to the knowledge about trypanosome biology, how trypanosomes are able to interact with the host and evade the immune system. However, due to lack of transparency, the *in vivo* visualisation of the development of these crucial innate immune responses, at individual level, have not been reported so far. The possibility to visualise in real-time the development of the immune response would allow to directly correlate the host response to the development of the infection.

Fig 4. A balanced innate immune response is crucial during the early phase of trypanosome infections ►

A) Trypanosome infection of mice revealed that IFNγ is one of the cytokines important in determining the outcome of the infection. As seen during early infections, IFNγ is secreted by NK(T) cells, CD8+ and CD4+ T cells (Cnops et al., 2015; Liu et al., 2015; Namangala et al., 2001; Radwanska et al., 2018; Shi et al., 2006; Wu et al., 2017). IFNγ exerts its protective role through direct activation of macrophages, leading to TNFα and nitric oxide (NO) secretion. Activation of macrophages occurs not only in response to IFNγ, but also upon interaction with trypanosome molecules. Cleaving of VSG molecules results in the release of soluble glycosyl-inositol-phosphate VSG (GIP-sVSG) and in the presence of dimyristoyl-glycerol (DMG) moieties on the trypanosome membranes, both of which can directly activate macrophages (Magez et al., 2002, 1998; Sileghem et al., 2001). **B)** TNFα and NO can affect directly and indirectly parasitaemia levels. *T. brucei* and *T. gambiense* studies revealed that mouse TNFα has a direct trypanolytic effect, mediated by a lectin-binding domain on the TNFα molecule (Daulouède et al., 2001; Lucas et al., 1994; Magez et al., 2001). The indirect effects of TNFα are mediated through the induction of inflammatory molecules (such as NO and pro-inflammatory cytokines) and the activation of various immune cells. NO can have direct trypanostatic effects, by affecting trypanosome motility and thus its ability to take up nutrients or remove surface-bound antibodies or complement (Kaushik et al., 1999). **C)** Trypanosomes, through antigenic variation can establish a long-term infection that can last for weeks. However, it is the balance between a controlled release or overexpression of IFNγ, TNFα and NO during the first week, that will determine the outcome of the infection towards either parasitaemia control or immunopathology (Magez et al., 2004, 1999).

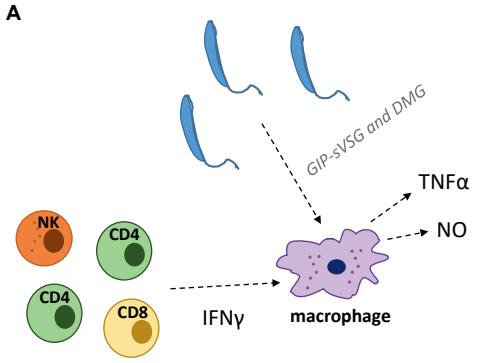
A
GIP-sVSG and DMG
TNFα
NO
NK
CD4
CD4
CD8
IFNγ
macrophage

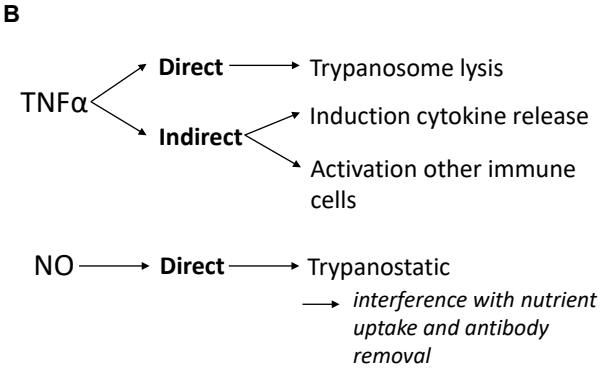
B
TNFα
Direct
Trypanosome lysis
Indirect
Induction cytokine release
Activation other immune cells
NO
Direct
Trypanostatic
interference with nutrient uptake and antibody removal

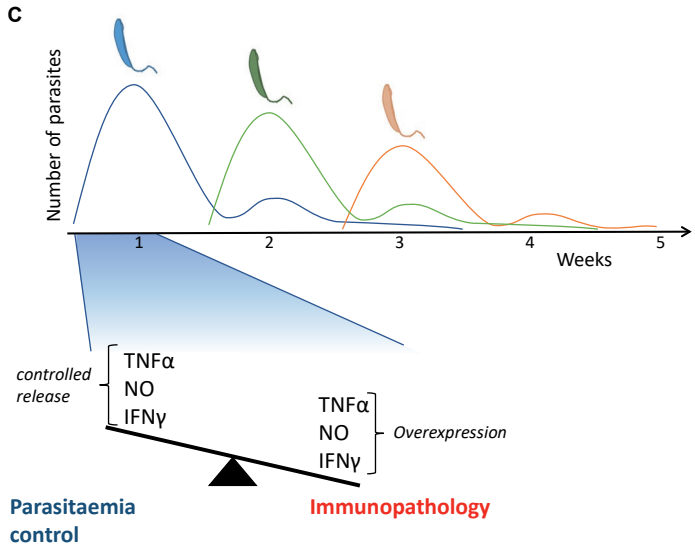
C
Number of parasites
1
2
3
4
5
Weeks
controlled release
TNFα
NO
IFNγ
TNFα
NO
IFNγ
Overexpression
Parasitaemia control
Immunopathology

Early innate immune responses during infections with non-VSG-containing trypanosomes

The majority of *Trypanosoma* species do not have antigenic variation like African trypanosome species. Among the non-VSG-containing (VSG$^-$) trypanosomes we find those causing diseases in humans, including the intracellular *T. cruzi*, and those affecting a range of other mammalian as well as avian, amphibian and fish species. For example, *T. theileri* in ruminants, *T. melophagium* in sheep (Gibson et al., 2010), *T. nabiasi* in rabbits (Grewal, 1957), *T. avium* in birds (Apanius, 1991), *T. rotatorium* in amphibians (Kudo, 1922) and *T. carassii* in fish (Lom and Dyková, 1992) are all extracellular trypanosomes, living in the blood and tissues of their host, which despite the absence of the complex system of antigenic variation typical of African trypanosomes, can still establish long-term infections in the face of the vertebrate immune system. Despite their widespread distribution and ability to affect all vertebrate species, except for studies on the well-characterized intracellular *T. cruzi*, only a hand-full of reports are available describing the immune response to VSG$^-$ trypanosomes. Thus, to our knowledge, it is not known whether any of the abovementioned extracellular trypanosomes rely on a balanced expression of IFNγ, TNFα or NO for their settlement in the host as African trypanosomes do. Thus, considering that *T. cruzi* is an intracellular VSG$^-$ trypanosome, knowledge on the evolution of pathogenicity and associated host immune responses against the more widespread extracellular VSG$^-$ trypanosomes is still very scarce.

All considered, the immune response to the fish trypanosomes *T. carassii*, is perhaps one of the best characterized among all extracellular VSG$^-$ trypanosomes. Interestingly, despite its extracellular nature, the surface coat of *T. carassii* is highly comparable to that of *T. cruzi* (Aguero et al., 2002; Lischke et al., 2000; Overath et al., 2001) displaying carbohydrate-rich glycosylphosphatidylinositol (GPI)-anchored mucin-like glycoproteins. In fish, *in vitro* stimulation of goldfish macrophages with recombinant *T. carassii* heat shock protein (hsp-70), induced the expression and secretion of pro-inflammatory cytokines such as TNFα, IFNγ and the nitric oxide response (Oladiran and Belosevic, 2009). Gene expression study of different tissues (kidney, spleen, liver) of goldfish infected with *T. carassii*, revealed an increase of both pro- and anti-inflammatory cytokines during the acute stage of infection and a delayed upregulation of iNOS related genes (Oladiran et al., 2011). Soluble GPI-anchored proteins derived from *T. carassii* were found to activate carp macrophages *in vitro* via a TLR2-dependent mechanism, triggering the induction of inflammatory genes (Ribeiro et al., 2010). Additionally, goldfish macrophages treated with recombinant *T. carassii* glycoprotein 63 (gp63), a major surface protease (MSP), displayed significant reduction in the expression of inducible nitric oxide synthase (iNOS) and TNFα (TNFa-1 and TNFa-2) (Oladiran and Belosevic, 2012). *T. carassii* infection of carp does not lead to excessive NO production *in vivo* and are associated with an alternative activation of macrophages (*ex vivo*) (Joerink et al., 2006b, 2006a; Saeij et al., 2002). We observed *in vitro* that NO is toxic for *T. carassii* (unpublished observation) and this might be a possible

explanation why *T. carassii* does not induce NO *in vivo*. The results of these studies suggest that macrophages might play a central role during the onset of the immune response during infections with VSG$^-$ trypanosomes and support that *T. carassii* might be an interesting model to study immune responses to extracellular VSG$^-$ trypanosomes. To date, for T. *carassii* infections, the *in vivo* visualisation of the development of the innate immune response, have not been reported. Zebrafish are closely related to common carp, one of the natural hosts of *T. carassii* and would allow for *in vivo* in real-time visualisation of the development of the innate immune response during experimental infections with extracellular VSG$^-$ trypanosomes.

Immune evasion and manipulation strategies of VSG-containing trypanosomes

The cell surface of some African trypanosomes is covered with a layer of variant surface glycoproteins (VSGs). The presence of these surface proteins greatly contributes to a well-known immune evasion mechanism referred to as 'antigenic variation', a strategy based on sequential switching of the major VSG. In fact, VSGs are highly immunogenic and induce specific antibodies' production; by periodically changing their VSGs, a specific population of trypanosomes is no longer recognized by antibodies directed against VSG epitopes displayed on the surface coat of the former population (Antia et al., 1996; Cross, 1996; Morrison et al., 2009; Vickerman, 1969). VSGs are anchored in the trypanosome membrane by glycosylphosphatidylinositol (GPI) anchors, which together form a thick barrier and protect against antibodies or complement molecules that might bind to buried conserved proteins (reviewed by Schwede et al., 2015).

Salivarian trypanosomes remain strictly extracellular in their vertebrate host and are therefore continuously confronted with the hosts' immune response (both innate and adaptive). However, trypanosomes have developed effective mechanisms to evade or manipulate the host immune response. VSG$^+$ trypanosomes infecting mammals, release molecules that are able to dampen the pro-inflammatory response (TNF and NO) by classically activated macrophages (M1), such as Adenylate Cyclase (AdC) and Kinesin Heavy Chain (KHC-1) (reviewed by Stijlemans et al., 2016). AdC is released by 'altruistic' trypanosomes upon phagocytosis and prevents production of TNF (Salmon et al., 2012). KHC-1 release induces IL-10 production and arginase activity by myeloid cells, altogether dampening the pro-inflammatory response and favouring parasite growth and settlement (De Muylder et al., 2013).

Motility of trypanosomes has been shown to be important for cell division, nutrient uptake, but also in immune evasion. *In vitro* studies described that *T. brucei* can clear antibodies, when present at low levels on its surface, during the early stages of infection by using hydrodynamic drag forces generated by directional swimming. The VSG-bound antibodies accumulate in the flagellar pocket at the posterior end and are endocytosed (Engstler et al., 2007). This may support the survival of individual cells during the emergence of a specific humoral immune response and it also gives trypanosomes the time to transform into trypomastigote forms, which are adapted to survive in the mammalian host during the

process of antigenic variation. How dynamic removal of immunoglobulins plays a role *in vivo*, when parasites are swimming in the blood of their host, and whether directional swimming is required for such process, has not been investigated yet.

Immune evasion and manipulation strategies of non-VSG-containing trypanosomes

As previously described, majority of *Trypanosoma* species do not have antigenic variation typical of African trypanosomes, but are still able to maintain long-term infections in their host. Currently, indications of the role of cell surface mucins in immune evasion were observed for non-VSG-containing trypanosomes (VSG^-), such as *T. cruzi, T. theileri* and *T. carassii.* The cell membrane of *T. cruzi*, was shown to be dominated by carbohydrate-rich coats of GPI-anchored mucin-like glycoproteins containing sialic acid (Pereira-Chioccola et al., 2000; Schenkman et al., 1991; Schenkman and Eichinger, 1993). *Trypanosoma theileri* is an extracellular Stercorarian trypanosome, infecting cattle and other Bovinae, and is able to maintain low infection levels for months up until probably the lifetime of the host (Farrar and Klei, 1990; Matthews et al., 1979; Niak, 1978). The surface of *T. theileri* is dominated by a major surface protease (MSP) and four novel protein families. The most abundant protein family on the cell surface seems to be modified by trans-sialidases, indicating that these parasites have a densely packed coat containing sialic acid-modified mucins and proteolytically active MSPs (Kelly et al., 2017). Likewise, some surface proteins of *T. carassii* have been identified and also their cell surface contains mucin-like glycoproteins with sialic acid, and an MSP, gp63 (Aguero et al., 2002; Lischke et al., 2000; Oladiran and Belosevic, 2012; Overath et al., 1999). The formation of this dense sialic acid modified mucin surface coat could well enable the parasites to escape immune recognition, although it has not been formally proven. Additionally, sialic acid and its negative charge are believed to be involved in parasite adherence to erythrocytes and to endothelial cells of the vasculature *in vitro* (Hemphill et al., 1994; Hemphill and Ross, 1995; Pereira-Chioccola et al., 2000). However, the *in vivo* implications and role of sialic acid modified mucins on the cell surface of these VSG^- trypanosomes have not been studied in detail yet. Therefore, an additional or complementary *in vivo* model would allow to study adherence, immune evasion or manipulation strategies by non-VSG-containing trypanosomes in a vertebrate host environment.

Foamy macrophages

For African trypanosome infections, the involvement of innate immune mediators such as IFNγ, TNFα and NO and their role in macrophage activation, has been extensively studied in mouse models, as described before. When looking at the innate immune responses during other intracellular trypanosomatida infections, such as Leishmaniasis (by *Leishmania species*) and Chagas disease (by *T. cruzi*), the involvement of IFNγ, TNFα and NO has been extensively studied as well (reviewed by Kayama and Takeda, 2010; Lopes et al., 2014). These intracellular parasitic infections seem to have one pathological feature in common;

the appearance of foamy macrophages. These (inflammatory) cells have accumulated lipid bodies in their cytoplasm, giving them a typical morphological appearance. Foamy cells have not only been associated with intracellular trypanosomatid infections, but also with several other infectious diseases, including experimental malaria, toxoplasmosis and tuberculosis (reviewed in López-Muñoz et al., 2018; Vallochi et al., 2018).

One of the best characterized functions of the lipid bodies in macrophages and other immune cells, are their capacity to act as sites for increased eicosanoid synthesis. Eicosanoids are non-storable synthesized signalling molecules that control important cellular processes. Some eicosanoids have a central role in the synthesis of inflammatory mediators during infections (Bozza et al., 2009; D'Avila et al., 2011; Melo and Machado, 2001; Melo et al., 2006, 2003; Vallochi et al., 2018). For example, *T. cruzi* infections of mice showed that eicosanoids, like prostaglandins, play a role in parasite survival and escape mechanisms. Prostaglandins are also involved in a wide variety of regulatory activities, including down-regulation of macrophage functions (D'Avila et al., 2011; Toledo et al., 2016). Many studies with the aim to unravel the development and role of lipid bodies or foamy macrophages performed *ex vivo* experiments, upon bleeding or dissection of infected mice. It may be clear that the lipid bodies in foamy macrophages are involved in a variety of cellular processes during intracellular parasite infections. Interestingly, to date, the occurrence of foamy macrophages has not been reported during extracellular trypanosome infections.

Trypanoplasma: early innate immune response and immune evasion and manipulation strategies

T. borreli infections in common carp present an acute infection characterized by increased iNOS activity and pro-inflammatory cytokine gene expression (Forlenza et al., 2008; Saeij et al., 2003, 2002, 2000; Stolte et al., 2008). Further, it was shown that NO contributes to antibody-dependent complement-mediated lysis of *T. borreli in vitro* (Forlenza et al., 2009b). As observed during African trypanosome infections in mice, also during *T. borreli* infections of carp, a balanced TNFα expression was important; inhibition of TNFα resulted in uncontrolled parasitaemia and increased mortality, whereas overexpression of TNFα leads to high mortalities, possibly due to an exacerbated inflammatory response (Forlenza et al., 2009a). Additionally, differential carp macrophage polarization was observed *ex-vivo* after *T. borreli* and *T. carassii* infections, showing a more inflammatory profile for *T. borreli* (Joerink et al., 2007).

Despite the apparent similarities in the early events following trypanosome and trypanoplasma infection in cyprinid fish, a detailed characterization of the early innate immune response and visualisation host-pathogen interaction during trypanoplasma infections has not been performed. Considering the evolutionary position of *T. borreli*, its parasitic nature, and ability to infect the same host as other aquatic trypanosomes (e.g. *T. carassii*), detailed analysis of the *in vivo* kinetics of innate responses in a vertebrates host may provide information on the evolution of pathogenicity of kinetoplastids.

Trypanosome and Trypanoplasma motility

Flagellum motility was shown to be essential for trypanosome survival in all the different environments they inhabit, from the bloodstream of mammals to the gut of the tsetse fly. The flagellum is a multifunctional organelle and its continuous motion is a hallmark of the trypanosome lifestyle (reviewed by Ralston et al., 2009). As stated before, *in vitro* studies describe that *T. brucei* can clear antibodies from its surface by using hydrodynamic drag forces generated by directional swimming (Engstler et al., 2007). In addition, motility is essential for successful cell division, uptake of nutrients, and development in the host (Broadhead et al., 2006; Griffiths et al., 2007; Langousis and Hill, 2014; Ralston et al., 2006; Shimogawa et al., 2018).

Trypanosomes have a single flagellum, which emerges from the posterior side of the body (flagellar pocket), follows the cell body, to which it is attached, and extends free at the anterior end of the cell body. Early studies showed that trypanosome motility is driven by a flagellar wave that initiates at the tip and moves towards the base of the flagellum, at the posterior end of the cell. Hence, the parasite moves forwards, with the flagellum tip leading (Walker, 1961). *In vitro* studies on African trypanosomes have focused on the analysis of qualitative and quantitative traits of trypanosome morphology and motility, and showed the ability of trypanosomes to adapt to the different environments of their hosts (Bargul et al., 2016; Engstler and Stark, 2015; Heddergott et al., 2012; Krüger and Engstler, 2015; Uppaluri et al., 2011). These studies showed for example that the flagellum is responsible for the major propelling force of trypanosomes. Additionally, it was shown that trypanosomes taken from the same population, evidently do not follow an equal, single motility mode and this variation in motility modes is influenced by their cell body shape and stiffness (Heddergott et al., 2012; Uppaluri et al., 2011). The detailed analysis of trypanosome motility, morphology and parasite-host cell interaction has been restricted to *in vitro* or *ex vivo* studies, using conditions that mimic the host environment, for example in blood or tissue taken from naïve or infected animals (Bargul et al., 2016; Beattie and Gull, 1997; Engstler et al., 2007; Heddergott et al., 2012; Hemphill et al., 1994; Hemphill and Ross, 1995; Shimogawa et al., 2018; Skalický et al., 2017; Sunter and Gull, 2016; Wakid and Bates, 2004). Recently, we described an experimental infection of zebrafish (*Danio rerio*) with *Trypanosoma carassii*. This complementary 'transparent' model allowed visualisation of the trypanosome swimming behaviour *in vivo* in a natural vertebrate environment, with the presence blood flow, blood cells and various tissue structures (Dóró et al., 2019, **Chapter 2**).

From the aforementioned studies it becomes clear that ample information is available regarding the morphology, swimming behaviour and flagellar motility of trypanosomes. The same is not true for *Trypanoplasma* species. Trypanoplasma are able to infect the same vertebrate host as other aquatic trypanosomes and have a unique cell body morphology with two flagella (Joerink et al., 2007; Lom, 1979). However, a detailed analysis and description of *T. borreli* swimming behaviour, *in vitro* as well as *in vivo* in a vertebrate host, is currently lacking and will be addressed in this thesis.

Outline of this thesis

Trypanosomes of the *Trypanosoma* genus are blood flagellates, that are important causative agents of diseases of humans, livestock and cold-blooded species, including fish. A controlled activation of the early innate immune response to trypanosome infections was shown to be important for the balance between parasite control and immunopathology. Trypanosome motility is essential for cell division, nutrient uptake and pathogenicity in the vertebrate host. One of the best-studied non-mammalian trypanosomes is *Trypanosoma carassii*, morphologically resembling mammalian trypanosomes. *T. carassii* co-infects cyprinid fish with *Trypanoplasma* species such as *T. borreli,* and currently only few studies have been performed to characterise the morphology, motility and host-pathogen interactions of trypanoplasma. For both trypanosomes and trypanoplasma, *in vivo* studies to visualise the parasite swimming behaviour and host immune response, in a natural host environment, have not been described. The overall **aim of this thesis** was to visualise and characterise blood flagellates infections, by studying: **1)** parasite motility *in vitro* and *in vivo* and **2)** the kinetics of innate immune responses *in vivo*.

Flagellar motility is one of the key elements in the pathogenesis of trypanosomes. To date, analysis of trypanosome motility and swimming behaviour relied on *in vitro* or *ex vivo* studies using conditions that best mimicked the host environment. However, the ability to visualise trypanosome motility *in vivo*, in their natural host environment, would greatly expand our current knowledge. Hence, a detailed *in vivo* description of *T. carassii* swimming behaviour in zebrafish is given in **Chapter 2**. In this thesis we report for the first time a study on trypanosome swimming behaviour in the natural environment of a vertebrate host. Besides reporting swimming behaviours of trypanosomes in the dynamic and complex environment of the blood and tissues, we describe novel anchoring mechanisms of *T. carassii* to host cells and report a novel 'whip-like' movement and backward swimming behaviour *in vivo*, both allowing the parasites to invert swimming direction.

The current knowledge about the early innate immune response upon infection with trypanosomes was obtained from studies performed in several mice models. These showed that a balanced release of innate immune cytokines was crucial during the early acute phase of trypanosome infections. In **Chapter 3** we describe the kinetics of the early innate immune response to *T. carassii*. By using transgenic zebrafish lines marking innate immune cells (macrophages and neutrophils), cytokine-expressing leukocytes and endothelial cells, we show differential immune responses of macrophages and neutrophils and confirm that a controlled early inflammatory immune response is associated with resistance to the infection, whereas an uncontrolled inflammatory response, characterized by the occurrence of pro-inflammatory foamy macrophages, is associated with pathology and susceptibility to the infection.

In nature, many cyprinid fish carry mixed populations of *T. carassii* and *T. borreli*. The biflagellate *T. borreli* is a member of the suborder Bodonids, which diverged early in evolution from the order Trypanosomatida. Although trypanosome swimming behaviour has been extensively described, trypanoplasma swimming behaviour, both *in vivo* and *ex vivo*, remains uncharacterised. To be able to analyse trypanoplasma motility, in **Chapter 4** we performed a novel quantitative analysis comparing *in vitro* the swimming behaviour, cell body characteristics and flagella behaviour of *T. borreli* and *T. carassii.* We show that *T. borreli* has a more heterogeneous and flexible cell body shape than *T. carassii* and that the anterior flagellum of both parasites exhibit comparable behaviours. Furthermore, we established an experimental infection of zebrafish with *T. borreli* and were able to visualise *in vivo* trypanoplasma swimming behaviour in the bloodstream and tissues of a vertebrate host. Finally, we describe the attachment mechanism of the flexible cell body of *T. borreli* to host cells and tissues.

After having characterized in detailed the swimming behaviour of *T. borreli in vitro* and *in vivo*, in **Chapter 5** we report on the *in vivo* visualisation and real-time characterization of the early innate immune response to trypanoplasma infections. By using transgenic zebrafish we were able to show the differential response of macrophages and neutrophils to the infection. Interestingly, as observed also during *T. carassii* infections, we report the occurrence of foamy macrophages and their association with susceptibility to the infection. Together, the results presented in Chapter 3 and 5 provide the first evidence of the occurrence of inflammatory macrophages during extracellular kinetoplastid infections, something that was never reported during mammalian trypanosome infections.

In **Chapter 6**, the general discussion, the outcomes of the previous chapters are placed in a larger framework, and the limitations of the studies as well as the future challenges are discussed. Potential future studies will be described, taking into consideration the strengths and weaknesses of the current thesis. The findings of this thesis paves the way for both, fundamental and applied studies that may contribute to a better understanding of the evolution of pathogenicity of kinetoplastids and demonstrate the complementarity of the zebrafish to mammalian models to study host-parasite interaction.

References

Aguero F, Campo V, Cremona L, Jager A, Noia JM Di, Overath P, Sanchez DO, Frasch AC. 2002. Gene Discovery in the Freshwater Fish Parasite. *Society* **70**:7140–7144. doi:10.1128/IAI.70.12.7140

Antia R, Nowak MA, Anderson RM. 1996. Antigenic variation and the within-host dynamics of parasites. *Proc Natl Acad Sci U S A* **93**:985–989. doi:10.1073/pnas.93.3.985

Apanius V. 1991. Avian trypanosomes as models of hemoflagellate evolution. *Parasitol Today* **7**:87–90. doi:10.1016/0169-4758(91)90203-Z

Bargul JL, Jung J, McOdimba FA, Omogo CO, Adung'a VO, Krüger T, Masiga DK, Engstler M. 2016. Species-Specific Adaptations of Trypanosome Morphology and Motility to the Mammalian Host. *PLoS Pathog* **12**:1–29. doi:10.1371/journal.ppat.1005448

Beattie P, Gull K. 1997. Cytoskeletal architecture and components involved in the attachment of Trypanosoma congolense epimastigotes. *Parasitology* **115** Pt 1:47–55.

Becker CD, Katz M. 1951. Linked references are available on JSTOR for this article : Transmission of the Hemoflagellate , Cryptobia salmositica Katz , 1951 , by a Rhynchobdellid. *J Parasitol* **51**:95–99.

Benard EL, Racz PI, Rougeot J, Nezhinsky AE, Verbeek FJ, Spaink HP, Meijer AH. 2015. Macrophage-expressed perforins Mpeg1 and Mpeg1.2 have an anti-bacterial function in zebrafish. *J Innate Immun* **7**:136–152. doi:10.1159/000366103

Bertrand JY, Chi NC, Santoso B, Teng S, Stainier DYR, Traver D. 2010. Haematopoietic stem cells derive directly from aortic endothelium during development. *Nature* **464**:108–111. doi:10.1038/nature08738

Bozza PT, Magalhães KG, Weller PF. 2009. Leukocyte lipid bodies - Biogenesis and functions in inflammation. *Biochim Biophys Acta - Mol Cell Biol Lipids* **1791**:540–551. doi:10.1016/j.bbalip.2009.01.005

Brener Z. 1973. Biology of Trypanosoma cruzi. *Annu Rev Microbiol* **27**:347–382.

Broadhead R, Dawe HR, Farr H, Griffiths S, Hart SR, Portman N, Shaw MK, Ginger ML, Gaskell SJ, Mckean PG, Gull K. 2006. Flagellar motility is required for the viability of the bloodstream trypanosome **440**:224–227. doi:10.1038/nature04541

Brunet LR. 2001. Nitric oxide in parasitic infections. *Int Immunopharmacol* **1**:1457–1467. doi:10.1016/S1567-5769(01)00090-X

Caljon G, Mabille D, Stijlemans B, De Trez C, Mazzone M, Tacchini-Cottier F, Malissen M, A. Van Ginderachter J, Magez S, De Baetselier P, Van Den Abbeele J. 2018. Neutrophils enhance early Trypanosoma brucei infection onset. *Sci Rep* **8**:1–11. doi:10.1038/s41598-018-29527-y

Cnops J, De Trez C, Stijlemans B, Keirsse J, Kauffmann F, Barkhuizen M, Keeton R, Boon L, Brombacher F, Magez S. 2015. NK-, NKT- and CD8-Derived IFNγ Drives Myeloid Cell Activation and Erythrophagocytosis, Resulting in Trypanosomosis-Associated Acute Anemia. *PLoS Pathog* **11**. doi:10.1371/journal.ppat.1004964

Cronan MR, Tobin DM. 2014. Fit for consumption: zebrafish as a model for tuberculosis. *Dis Model Mech*. doi:10.1242/dmm.016089

Cross GAM. 1996. Antigenic variation in trypanosomes: Secrets surface slowly. *BioEssays* **18**:283–291. doi:10.1002/bies.950180406

D'Avila H, Freire-de-Lima CG, Roque NR, Teixeira L, Barja-Fidalgo C, Silva AR, Melo RCN, DosReis GA, Castro-Faria-Neto HC, Bozza PT. 2011. Host cell lipid bodies triggered by Trypanosoma cruzi infection and enhanced by the uptake of apoptotic cells are associated with prostaglandin E2 generation and increased parasite growth. *J Infect Dis* **204**:951–961. doi:10.1093/infdis/jir432

Daulouède S, Bouteille B, Moynet D, De Baetselier P, Courtois P, Lemesre JL, Buguet A, Cespuglio R, Vincendeau P. 2001. Human Macrophage Tumor Necrosis Factor (TNF)–α Production Induced by Trypanosoma brucei gambiense and the Role of TNF-α in Parasite Control . *J Infect Dis* **183**:988–991. doi:10.1086/319257

De Muylder G, Daulouède S, Lecordier L, Uzureau P, Morias Y, Van Den Abbeele J, Caljon G, Hérin M, Holzmuller P, Semballa S, Courtois P, Vanhamme L, Stijlemans B, De Baetselier P, Barrett MP, Barlow JL, McKenzie ANJ, Barron L, Wynn TA, Beschin A, Vincendeau P, Pays E. 2013. A Trypanosoma brucei Kinesin Heavy Chain Promotes Parasite Growth by Triggering Host Arginase Activity. *PLoS Pathog* **9**:1–14. doi:10.1371/journal.ppat.1003731

Dooley CM, Mongera A, Walderich B, Nüsslein-Volhard C. 2013. On the embryonic origin of adult melanophores: the role of ErbB and Kit signalling in establishing melanophore stem cells in zebrafish. *Development* **140**:1003–1013. doi:10.1242/dev.087007

Dóró É, Jacobs SH, Hammond FR, Schipper H, Pieters RP, Carrington M, Wiegertjes GF, Forlenza M. 2019. Visualizing trypanosomes in a vertebrate host reveals novel swimming behaviours, adaptations and attachment mechanisms. *Elife* **8**:1–25. doi:10.7554/elife.48388

Ellett F, Pase L, Hayman JW, Andrianopoulos A, Lieschke GJ. 2011. mpeg1 promoter transgenes direct macrophage-lineage expression in zebrafish. *Blood* **117**:49–57. doi:10.1182/blood-2010-10-314120.

Engstler M, Pfohl T, Herminghaus S, Boshart M, Wiegertjes G, Heddergott N, Overath P. 2007. Hydrodynamic Flow-Mediated Protein Sorting on the Cell Surface of Trypanosomes 505–515. doi:10.1016/j.cell.2007.08.046

Engstler M, Stark H. 2015. Simulating the Complex Cell Design of Trypanosoma brucei and Its Motility **11**. doi:10.1371/journal.pcbi.1003967

Farrar RG, Klei TR. 1990. Prevalence of Trypanosoma theileri in Louisiana Cattle. *J Parasitol* **76**:734–736. doi:10.2307/3282992

Forlenza M, Magez S, Scharsack JP, Westphal A, Savelkoul HFJ, Wiegertjes GF. 2009a. Receptor-Mediated and Lectin-Like Activities of Carp (Cyprinus carpio) TNF-α. *J Immunol* **183**:5319–5332. doi:10.4049/jimmunol.0901780

Forlenza M, Nakao M, Wibowo I, Joerink M, Arts JAJ, Savelkoul HFJ, Wiegertjes GF. 2009b. Nitric oxide hinders antibody clearance from the surface of Trypanoplasma borreli and increases susceptibility to complement-mediated lysis. *Mol Immunol* **46**:3188–3197. doi:10.1016/j.molimm.2009.08.011

Forlenza M, Scharsack JP, Kachamakova NM, Taverne-Thiele AJ, Rombout JHWM, Wiegertjes GF. 2008. Differential contribution of neutrophilic granulocytes and macrophages to nitrosative stress in a host-parasite animal model. *Mol Immunol* **45**:3178–3189. doi:10.1016/j.molimm.2008.02.025

García-Valtanen P, Martínez-López A, López-Muñoz A, Bello-Perez M, Medina-Gali RM, Ortega-Villaizán MDM, Varela M, Figueras A, Mulero V, Novoa B, Estepa A, Coll J. 2017. Zebra fish lacking adaptive immunity acquire an antiviral alert state characterized by upregulated gene expression of apoptosis, multigene families, and interferon-related genes. *Front Immunol* **8**:121. doi:10.3389/fimmu.2017.00121

Gibson W, Pilkington JG, Pemberton JM. 2010. Trypanosoma melophagium from the sheep ked Melophagus ovinus on the island of St Kilda. *Parasitology* **137**:1799–1804. doi:10.1017/S0031182010000752

Grewal MS. 1957. The life cycle of the British rabbit trypanosome, Trypanosoma nabiasi Railliet, 1895. *Parasitology* **47**:100–118. doi:10.1017/S0031182000021806

Griffiths S, Portman N, Taylor PR, Gordon S, Ginger ML, Gull K. 2007. RNA interference mutant induction in vivo demonstrates the essential nature of trypanosome flagellar function during mammalian infection. *Eukaryot Cell* **6**:1248–1250. doi:10.1128/EC.00110-07

Heddergott N, Krüger T, Babu SB, Wei A, Stellamanns E, Uppaluri S, Pfohl T, Stark H, Engstler M. 2012. Trypanosome Motion Represents an Adaptation to the Crowded Environment of the Vertebrate Bloodstream. *PLoS Pathog* **8**. doi:10.1371/journal.ppat.1003023

Hemphill A, Frame I, Ross CA. 1994. The interaction of Trypanosoma congolense with endothelial cells. *Parasitology* **109**:631–641. doi:10.1017/S0031182000076514

Hemphill A, Ross CA. 1995. Flagellum-mediated adhesion ofTrypanosoma congolense to bovine aorta endothelial cells. *Parasitol Res* **81**:412–420. doi:10.1007/bf00931503

Hoare CA. 1972. The trypanosomes of mammals. A zoological monograph. Blackwell Scientific Publications, 5 Alfred Street, Oxford.

Joerink M, Forlenza M, Ribeiro CMS, de Vries BJ, Savelkoul HFJ, Wiegertjes GF. 2006a. Differential macrophage polarisation during parasitic infections in common carp (Cyprinus carpio L.). *Fish Shellfish Immunol* **21**:561–571. doi:10.1016/j.fsi.2006.03.006

Joerink M, Groeneveld A, Ducro B, Savelkoul HFJ, Wiegertjes GF. 2007. Mixed infection with Trypanoplasma borreli and Trypanosoma carassii induces protection: Involvement of cross-reactive antibodies. *Dev Comp Immunol* **31**:903–915. doi:10.1016/j.dci.2006.12.003

Joerink M, Ribeiro CMS, Stet RJM, Hermsen T, Savelkoul HFJ, Wiegertjes GF. 2006b. Head Kidney-Derived Macrophages of Common Carp (Cyprinus carpio L.) Show Plasticity and Functional Polarization upon Differential Stimulation. *J Immunol* **177**:61–69. doi:10.4049/jimmunol.177.1.61

Kaushik RS, Uzonna JE, Gordon JR, Tabel H. 1999. Innate resistance to Trypanosoma congolense infections: Differential production of nitric oxide by macrophages from susceptible BALB/c and resistant C57B1/6 mice. *Exp Parasitol* **92**:131–143. doi:10.1006/expr.1999.4408

Kayama H, Takeda K. 2010. The innate immune response to Trypanosoma cruzi infection. *Microbes Infect* **12**:511–517. doi:10.1016/j.micinf.2010.03.005

Kelly S, Ivens A, Mott GA, O'Neill E, Emms D, Macleod O, Voorheis P, Tyler K, Clark M, Matthews J, Matthews K, Carrington M. 2017. An alternative strategy for trypanosome survival in the mammalian bloodstream revealed through genome and transcriptome analysis of the ubiquitous bovine parasite trypanosoma (megatrypanum) theileri. *Genome Biol Evol* **9**:2093–2109. doi:10.1093/gbe/evx152

Krüger T, Engstler M. 2015. Flagellar motility in eukaryotic human parasites. *Semin Cell Dev Biol*. doi:10.1016/j.semcdb.2015.10.034

Kudo AR. 1922. On the Protozoa Parasitic in Frogs. *Trans Am Microsc Soc* **41**:59–76. doi:10.1126/science.2.36.296

Langenau DM, Ferrando AA, Traver D, Kutok JL, Hezel JPD, Kanki JP, Zon LI, Thomas Look A, Trede NS. 2004. In vivo tracking of T cell development, ablation, and engraftment in transgenic zebrafish. *Proc Natl Acad Sci U S A* **101**:7369–7374. doi:10.1073/pnas.0402248101

Langousis G, Hill KL. 2014. Motility and more: The flagellum of Trypanosoma brucei. *Nat Rev Microbiol* **12**:505–518. doi:10.1038/nrmicro3274

Lawson ND, Weinstein BM. 2002. In vivo imaging of embryonic vascular development using transgenic zebrafish. *Dev Biol* **248**:307–318. doi:10.1006/dbio.2002.0711

Lischke A, Klein C, Stierhof YD, Hempel M, Mehlert A, Almeida IC, Ferguson MAJ, Overath P. 2000. Isolation and characterization of glycosylphosphatidylinositol-anchored, mucin-like surface glycoproteins from bloodstream forms of the freshwater-fish parasite Trypanosoma carassii. *Biochem J* **345**:693–700. doi:10.1042/0264-6021:3450693

Liu G, Sun D, Wu H, Zhang M, Huan H, Xu J, Zhang X, Zhou H, Shi M. 2015. Distinct contributions of CD4+ and CD8+ T cells to pathogenesis of trypanosoma brucei infection in the context of gamma interferon and interleukin-10. *Infect Immun* **83**:2785–2795. doi:10.1128/IAI.00357-15

Lom J. 1979. Biology of the trypanosomes and trypanoplasms of fishBiology of the Kinetoplastida. pp. 269–337. doi:10.1111/j.1550-7408.1980.tb04245.x

Lom J, Dyková I. 1992. Protozoan parasites of fishes. Amsterdam: Elsevier.

Lopes MF, Costa-Da-Silva AC, Dosreis GA. 2014. Innate immunity to Leishmania infection: Within phagocytes. *Mediators Inflamm* **2014**. doi:10.1155/2014/754965

López-Muñoz RA, Molina-Berríos A, Campos-Estrada C, Abarca-Sanhueza P, Urrutia-Llancaqueo L, Peña-Espinoza M, Maya JD. 2018. Inflammatory and pro-resolving lipids in trypanosomatid infections: A key to understanding parasite control. *Front Microbiol* **9**:1–16. doi:10.3389/fmicb.2018.01961

Lopez R, Demick KP, Mansfield JM, Paulnock DM. 2008. Type I IFNs Play a Role in Early Resistance, but Subsequent Susceptibility, to the African Trypanosomes. *J Immunol* **181**:4908–4917. doi:10.4049/jimmunol.181.7.4908

Losev A, Grybchuk-Ieremenko A, Kostygov AY, Lukeš J, Yurchenko V. 2015. Host specificity, pathogenicity, and mixed infections of trypanoplasms from freshwater fishes. *Parasitol Res* **114**:1071–1078. doi:10.1007/s00436-014-4277-y

Losos GJ, Ikede BO. 1972. Review of Pathology of Diseases in Domestic and Laboratory Animals Caused by Trypanosoma congolense, T. vivax, T. brucei, T. rhodesiense and T. gambiense. *Vet Pathol* **9**:1–71.

Lucas R, Magez S, Leys R De, Fransen L, Lucas R, Magez S, Leys R De, Fransen L, Scheerlinck J, Rampelberg M, Sablon E. 1994. Mapping the Lectin-Like Activity of Tumor Necrosis Factor Published by : American Association for the Advancement of Science Stable URL : http://www.jstor.org/stable/2882928 JSTOR is a not-for-profit service that helps scholars , researchers , and student **263**:814–817.

Lukeš J, Skalický T, Týč J, Votýpka J, Yurchenko V. 2014. Evolution of parasitism in kinetoplastid flagellates. *Mol Biochem Parasitol* **195**:115–122. doi:10.1016/j.molbiopara.2014.05.007

Magez S, Radwanska M, Beschin A, Sekikawa K, De Baetselier P. 1999. Tumor necrosis factor alpha is a key mediator in the regulation of experimental Trypanosoma brucei infections. *Infect Immun* **67**:3128–3132.

Magez S, Radwanska M, Drennan M, Fick L, Baral TN, Brombacher F, Baetselier PD. 2006. Interferon-γ and Nitric Oxide in Combination with Antibodies Are Key Protective Host Immune Factors during Trypanosoma congolense Tc13 Infections . *J Infect Dis* **193**:1575–1583. doi:10.1086/503808

Magez S, Radwanska M, Stijlemans B, Van Xong H, Pays E, De Baetselier P. 2001. A Conserved Flagellar Pocket Exposed High Mannose Moiety Is Used by African Trypanosomes as a Host Cytokine Binding Molecule. *J Biol Chem* **276**:33458–33464. doi:10.1074/jbc.M103412200

Magez S, Stijlemans B, Baral T, De Baetselier P. 2002. VSG-GPI anchors of African trypanosomes: their role in macrophage activation and induction of infection-associated immunopathology. *Microbes Infect* **4**:999–1006. doi:10.1016/S1286-4579(02)01617-9

Magez S, Stijlemans B, Radwanska M, Pays E, Ferguson MAJ, De Beatselier P. 1998. The glycosyl-inositol-phosphate and dimyristoylglycerol moieties of the glycosylphosphatidylinositol anchor of the trypanosome variant-specific surface glycoprotein are distinct macrophage-activating factors. *J Immunol* **160**:1949–1956. doi:10.4049/jimmunol.1301645

Magez S, Truyens C, Merimi M, Radwanska M, Stijlemans B, Brouckaert P, Brombacher F, Pays E, Baetselier PD. 2004. P75 Tumor Necrosis Factor–Receptor Shedding Occurs as a Protective Host Response during African Trypanosomiasis. *J Infect Dis* **189**:527–539. doi:10.1086/381151

Matthews DM, Kingston N, Maki L, Nelms G. 1979. Trypanosoma theileri Laveran, 1902, in Wyoming cattle. *Am J Vet Res* **40**:623–629.

Meijer AH. 2016. Protection and pathology in TB: learning from the zebrafish model. *Semin Immunopathol* **38**:261–273. doi:10.1007/s00281-015-0522-4

Melo RC., Machado CR. 2001. Trypanosoma cruzi: Peripheral Blood Monocytes and Heart Macrophages in the Resistance to Acute Experimental Infection in Rats. *Exp Parasitol* **97**:15–23. doi:10.1006/EXPR.2000.4576

Melo RCN, Ávila HD, Fabrino DL, Almeida PE, Bozza PT. 2003. Macrophage lipid body induction by Chagas disease in vivo: Putative intracellular domains for eicosanoid formation during infection. *Tissue Cell* **35**:59–67. doi:10.1016/S0040-8166(02)00105-2

Melo RCN, Fabrino DL, Dias FF, Parreira GG. 2006. Lipid bodies: Structural markers of inflammatory macrophages in innate immunity. *Inflamm Res* **55**:342–348. doi:10.1007/s00011-006-5205-0

Morrison LJ, Marcello L, McCulloch R. 2009. Antigenic variation in the African trypanosome: Molecular mechanisms and phenotypic complexity. *Cell Microbiol* **11**:1724–1734. doi:10.1111/j.1462-5822.2009.01383.x

Namangala B, Noël W, De Baetselier P, Brys L, Beschin A. 2001. Relative Contribution of Interferon-γ and Interleukin-10 to Resistance to Murine African Trypanosomosis. *J Infect Dis* **183**:1794–1800. doi:10.1086/320731

Nguyen-Chi M, Phan QT, Gonzalez C, Dubremetz JF, Levraud JP, Lutfalla G. 2014. Transient infection of the zebrafish notochord with E. coli induces chronic inflammation. *DMM Dis Model Mech* **7**:871–882. doi:10.1242/dmm.014498

Niak A. 1978. The incidence of Trypanosoma theileri among cattle in Iran. *Trop Anim Health Prod* **10**:26—27. doi:10.1007/bf02235297

Oladiran A, Beauparlant D, Belosevic M. 2011. The expression analysis of inflammatory and antimicrobial genes in the goldfish (Carassius auratus L.) infected with Trypanosoma carassii. *Fish Shellfish Immunol* **31**:606–613. doi:10.1016/j.fsi.2011.07.008

Oladiran A, Belosevic M. 2012. Recombinant glycoprotein 63 (Gp63) of Trypanosoma carassii suppresses antimicrobial responses of goldfish (Carassius auratus L.) monocytes and macrophages. *Int J Parasitol* **42**:621–633. doi:10.1016/j.ijpara.2012.04.012

Oladiran A, Belosevic M. 2009. Trypanosoma carassii hsp70 increases expression of inflammatory cytokines and chemokines in macrophages of the goldfish (Carassius auratus L.). *Dev Comp Immunol* **33**:1128–1136. doi:10.1016/j.dci.2009.06.003

Overath P, Haag J, Lischke A, O'hUigin C. 2001. The surface structure of trypanosomes in relation to their molecular phylogeny. *Int J Parasitol* **31**:468–471. doi:10.1016/S0020-7519(01)00152-7

Overath P, Haag J, Mameza MG, Lischke A. 1999. Freshwater fish trypanosomes: Definition of two types, host control by antibodies and lack of antigenic variation. *Parasitology* **119**:591–601. doi:10.1017/S0031182099005089

Overath P, Ruoff J, Stierhof YD, Haag J, Tichy H, Dyková I, Lom J. 1998. Cultivation of bloodstream forms of Trypanosoma carassii, a common parasite of freshwater fish. *Parasitol Res* **84**:343–347. doi:10.1007/s004360050408

Page DM, Wittamer V, Bertrand JY, Lewis KL, Pratt DN, Delgado N, Schale SE, McGue C, Jacobsen BH, Doty A, Pao Y, Yang H, Chi NC, Magor BG, Traver D. 2013. An evolutionarily conserved program of B-cell development and activation in zebrafish. *Blood* **122**:1–11. doi:10.1182/blood-2012-12-471029

Palha N, Guivel-Benhassine F, Briolat V, Lutfalla G, Sourisseau M, Ellett F, Wang C-H, Lieschke GJ, Herbomel P, Schwartz O, Levraud J-P. 2013. Real-Time Whole-Body Visualization of Chikungunya Virus Infection and Host Interferon Response in Zebrafish. *PLoS Pathog* **9**:e1003619. doi:10.1371/journal.ppat.1003619

Pereira-Chioccola VL, Acosta-Serrano A, De Almeida IC, Ferguson MAJ, Souto-Padron T, Rodrigues MM, Travassos LR, Schenkman S. 2000. Mucin-like molecules form a negatively charged coat that protects Trypanosoma cruzi trypomastigotes from killing by human anti-α-galactosyl antibodies. *J Cell Sci* **113**:1299–1307.

Petrie-Hanson L, Hohn C, Hanson L. 2009. Characterization of rag1 mutant zebrafish leukocytes. *BMC Immunol* **10**:1–8. doi:10.1186/1471-2172-10-8

Radwanska M, Vereecke N, Deleeuw V, Pinto J, Magez S. 2018. Salivarian trypanosomosis: A review of parasites involved, their global distribution and their interaction with the innate and adaptive mammalian host immune system. *Front Immunol* **9**:1–20. doi:10.3389/fimmu.2018.02253

Ralston KS, Kabututu ZP, Melehani JH, Oberholzer M, Hill KL. 2009. The Trypanosoma brucei Flagellum: Moving Parasites in New Directions . *Annu Rev Microbiol* **63**:335–362. doi:10.1146/annurev.micro.091208.073353

Ralston KS, Lerner AG, Diener DR, Hill KL. 2006. Flagellar Motility Contributes to Cytokinesis in Trypanosoma brucei and Is Modulated by an Evolutionarily Conserved Dynein Regulatory System † **5**:696–711. doi:10.1128/EC.5.4.696

Ramakrishnan L. 2013. The zebrafish guide to tuberculosis immunity and treatment. *Cold Spring Harb Symp Quant Biol* **78**:179–192. doi:10.1101/sqb.2013.78.023283

Renshaw SA, Loynes CA, Trushell DMI, Elworthy S, Ingham PW, Whyte MKB. 2006. A transgenic zebrafish model of neutrophilic inflammation. *Blood* **108**:3976–3978. doi:10.1182/blood-2006-05-024075

Renshaw SA, Trede NS. 2012. A model 450 million years in the making: zebrafish and vertebrate immunity. *Dis Model Mech* **5**:38–47. doi:10.1242/dmm.007138

Ribeiro CMS, Pontes MJSL, Bird S, Chadzinska M, Scheer M, Verburg-van Kemenade BML, Savelkoul HFJ, Wiegertjes GF. 2010. Trypanosomiasis-induced Th17-like immune responses in carp. *PLoS One* **5**:e13012. doi:10.1371/journal.pone.0013012

Rosowski EE, Knox BP, Archambault LS, Huttenlocher A, Keller NP, Wheeler RT, Davis JM. 2018. The zebrafish as a model host for invasive fungal infections. *J Fungi* **4**. doi:10.3390/jof4040136

Saeij JPJ, de Vries BJ, Wiegertjes GF. 2003. The immune response of carp to Trypanoplasma borreli: Kinetics of immune gene expression and polyclonal lymphocyte activation. *Dev Comp Immunol* **27**:859–874. doi:10.1016/S0145-305X(03)00083-1

Saeij JPJ, Stet RJM, Groeneveld A, Verburg-Van Kemenade LBM, Van Muiswinkel WB, Wiegertjes GF. 2000. Molecular and functional characterization of a fish inducible-type nitric oxide synthase **51**:339–346. doi:10.1007/s002510050628

Saeij JPJ, Van Muiswinkel WB, Groeneveld A, Wiegertjes GF. 2002. Immune modulation by fish kinetoplastid parasites: A role for nitric oxide. *Parasitology* **124**:77–86. doi:10.1017/S0031182001008915

Salmon D, Vanwalleghem G, Morias Y, Denoeud J, Krumbholz C, Lhommé F, Bachmaier S, Kador M, Gossmann J, Dias FBS, De Muylder G, Uzureau P, Magez S, Moser M, De Baetselier P, Van Den Abbeele J, Beschin A, Boshart M, Pays E. 2012. Adenylate cyclases of Trypanosoma brucei inhibit the innate immune response of the host. *Science (80-)* **337**:463–466. doi:10.1126/science.1222753

Schenkman S, Eichinger D. 1993. Trypanosoma cruzi trans-sialidase and cell invasion. *Parasitol Today* **9**:218–222. doi:10.1016/0169-4758(93)90017-A

Schenkman S, Jiang MS, Hart GW, Nussenzweig V. 1991. A novel cell surface trans-sialidase of trypanosoma cruzi generates a stage-specific epitope required for invasion of mammalian cells. *Cell* **65**:1117–1125. doi:10.1016/0092-8674(91)90008-M

Schwede A, Macleod OJS, MacGregor P, Carrington M. 2015. How Does the VSG Coat of Bloodstream Form African Trypanosomes Interact with External Proteins? *PLoS Pathog* **11**:1–18. doi:10.1371/journal.ppat.1005259

Shi M, Pan W, Tabel H. 2003. Experimental African trypanosomiasis: IFN-γ mediates early mortality. *Eur J Immunol* **33**:108–118. doi:10.1002/immu.200390013

Shi M, Wei G, Pan W, Tabel H. 2006. Experimental African Trypanosomiasis: A Subset of Pathogenic, IFN-γ-Producing, MHC Class II-Restricted CD4 + T Cells Mediates Early Mortality in Highly Susceptible Mice . *J Immunol* **176**:1724–1732. doi:10.4049/jimmunol.176.3.1724

Shimogawa MM, Ray SS, Kisalu N, Zhang Y, Geng Q, Ozcan A, Hill KL. 2018. Parasite motility is critical for virulence of African trypanosomes. *Sci Rep* **8**:1–11. doi:10.1038/s41598-018-27228-0

Sileghem M, Saya R, Grab DJ, Naessens J. 2001. An accessory role for the diacylglycerol moiety of variable surface glycoprotein of African trypanosomes in the stimulation of bovine monocytes. *Vet Immunol Immunopathol* **78**:325–339. doi:10.1016/S0165-2427(01)00241-0

Simpson AGB, Stevens JR, Lukeš J. 2006. The evolution and diversity of kinetoplastid flagellates. *Trends Parasitol* **22**:168–174. doi:10.1016/j.pt.2006.02.006

Skalický T, Dobáková E, Wheeler RJ, Tesařová M, Flegontov P, Jirsová D, Votýpka J, Yurchenko V, Ayala FJ, Lukeš J. 2017. Extensive flagellar remodeling during the complex life cycle of *Paratrypanosoma* , an early-branching trypanosomatid. *Proc Natl Acad Sci* **114**:201712311. doi:10.1073/pnas.1712311114

Steinhagen D, Kruse P, Korting W. 1989. The Parasitemia of Cloned Trypanoplasma borreli Laveran and Mesnil , 1901 , in Laboratory- Infected Common Carp (Cyprinus carpio L .) Author (s): Dieter Steinhagen , Peter Kruse and Wolfgang Körting Source : The Journal of Parasitology , Vol . 75 , No. *J Parasitol* **75**:685–689.

Sternberg JM, Mabbott NA. 1996. Nitric oxide-mediated suppression of T cell responses during Trypanosoma brucei infection: Soluble trypanosome products and interferon-γ are synergistic inducers of nitric oxide synthase. *Eur J Immunol*. doi:10.1002/eji.1830260306

Stevens JR, Harvey PH, Nee S. 2001. The Molecular Evolution of Trypanosomatidae. *Adv Parasitol* **48**:2–55.

Stevens JR, Noyens HA, Dover GA, Gibson WC. 1998. The ancient and divergent origins of the human pathogenic trypanosomes , Trypanosoma brucei and T . cruzi. *Parasitology* **18**:107–116.

Stijlemans B, Caljon G, Van Den Abbeele J, Van Ginderachter JA, Magez S, De Trez C. 2016. Immune evasion strategies of Trypanosoma brucei within the mammalian host: Progression to pathogenicity. *Front Immunol* **7**. doi:10.3389/fimmu.2016.00233

Stolte EH, Savelkoul HFJ, Wiegertjes G, Flik G, Lidy Verburg-van Kemenade BM. 2008. Differential expression of two interferon-γ genes in common carp (Cyprinus carpio L.). *Dev Comp Immunol* **32**:1467–1481. doi:10.1016/j.dci.2008.06.012

Sunter JD, Gull K. 2016. The Flagellum Attachment Zone : ' The Cellular Ruler ' of Trypanosome Morphology **32**.

Toledo DAM, D'Avila H, Melo RCN. 2016. Host lipid bodies as platforms for intracellular survival of protozoan parasites. *Front Immunol* **7**:1–6. doi:10.3389/fimmu.2016.00174

Torraca V, Masud S, Spaink HP, Meijer AH. 2014. Macrophage-pathogen interactions in infectious diseases: New therapeutic insights from the zebrafish host model. *DMM Dis Model Mech*. doi:10.1242/dmm.015594

Torraca V, Mostowy S. 2018. Zebrafish Infection: From Pathogenesis to Cell Biology. *Trends Cell Biol* **28**:143–156. doi:10.1016/j.tcb.2017.10.002

Uilenberg G. 1998. A field guide for The Diagnosis, Treatment and Prevention of African Animal Trypansomosis.

Uppaluri S, Nagler J, Stellamanns E, Heddergott N, Herminghaus S, Engstler M, Pfohl T. 2011. Impact of microscopic motility on the swimming behavior of parasites: Straighter Trypanosomes are more directional. *PLoS Comput Biol* **7**:1–8. doi:10.1371/journal.pcbi.1002058

Uzonna JE, Kaushik RS, Godon J., Tabel H. 1998. Experimental Murine Trypanosoma congolense Infections. I. Administration of Anti-IFN- γ Antibodies Alters Trypanosome-Susceptible Mice to a Resistant-Like Phenotype. *J Immunol* **161**:5507–5515. doi:10.4049/jimmunol.1301645

Vallochi AL, Teixeira L, Oliveira K da S, Maya-Monteiro CM, Bozza PT. 2018. Lipid Droplet, a Key Player in Host-Parasite Interactions. *Front Immunol* **9**:1022. doi:10.3389/fimmu.2018.01022

Vickerman K. 1985. Developmental Cycles and Biology of Pathogenic Trypanosomes. *Br Med Bull* **41**:105–114. doi:10.1093/oxfordjournals.bmb.a072036

Vickerman K. 1969. On the Surface Coat and Flagellar Adhesion in Trypanosomes. *J Cell Sci* **5**:163–193.

Wakid MH, Bates PA. 2004. Flagellar attachment of Leishmania promastigotes to plastic film in vitro. *Exp Parasitol* **106**:173–178. doi:10.1016/j.exppara.2004.03.001

Walker PJ. 1961. Organization of Function in Trypanosome Flagella. *Nature* **189**:1017–1018. doi:10.1038/1891017a0

Wiegertjes GF, Forlenza M, Joerink M, Scharsack JP. 2005. Parasite infections revisited. *Dev Comp Immunol* **29**:749–758. doi:10.1016/j.dci.2005.01.005

Woo PTK. 1978. The division process of Cryptobia salmositica in experimentally infected rainbow trout (Salmo gairdneri). *Can J Zool* **56**:1514–1518.

Woo PTK, Ardelli BF. 2013. Immunity against selected piscine flagellates. *Dev Comp Immunol* **43**:268–279. doi:10.1016/j.dci.2013.07.006

Woo PTK, Black GA. 1984. Trypanosoma danilewskyi: Host Specificity and Host's Effect on Morphometrics. *J Parasitol* **70**:788. doi:10.2307/3281762

Wu H, Liu G, Shi M. 2017. Interferon gamma in African trypanosome infections: Friends or foes? *Front Immunol* **8**:4–10. doi:10.3389/fimmu.2017.01105

CHAPTER 2

Visualizing trypanosomes in a vertebrate host reveals novel swimming behaviours, adaptations and attachment mechanisms

Éva Dóró[1$], Sem H. Jacobs[1], Ffion R. Hammond[1#], Henk Schipper[2], Remco P.M. Pieters[2], Mark Carrington[3], Geert F. Wiegertjes[1,4], Maria Forlenza[1*]

[1] Cell Biology and Immunology Group, Department of Animal Sciences, Wageningen University & Research, Wageningen, The Netherlands

[2] Experimental Zoology Chair Group, Department of Animal Sciences, Wageningen University & Research, Wageningen, The Netherlands

[3] Department of Biochemistry, University of Cambridge, Tennis Court Road, Cambridge, UK

[4] Aquaculture and Fisheries Group, Department of Animal Sciences, Wageningen University & Research, Wageningen, The Netherlands

[$] Current address: Institute of Transdisciplinary Discoveries, Medical School, Faculty of Medicine, University of Pécs, Pécs, Hungary

[#] Current address: Department of Infection, Immunity & Cardiovascular Disease, University of Sheffield, Sheffield, United Kingdom

Elife 8 (2019), p. 1–25.

Abstract

Trypanosomes are important disease agents of humans, livestock and cold-blooded species, including fish. The cellular morphology of trypanosomes is central to their motility, adaptation to the host's environments and pathogenesis. However, visualizing the behaviour of trypanosomes resident in a live vertebrate host has remained unexplored. In this study, we describe an infection model of zebrafish (*Danio rerio*) with *Trypanosoma carassii*. By combining high spatio-temporal resolution microscopy with the transparency of live zebrafish, we describe in detail the swimming behaviour of trypanosomes in blood and tissues of a vertebrate host. Besides the conventional tumbling and directional swimming, *T. carassii* can change direction through a 'whip-like' motion or by swimming backward. Further, the posterior end can act as an anchoring site *in vivo*. To our knowledge, this is the first report of a vertebrate infection model that allows detailed imaging of trypanosome swimming behaviour *in vivo* in a natural host environment.

Introduction

Trypanosoma is a genus of flagellated protozoa, and most species proliferate in the blood and tissue fluids of their host. The best-known and most commonly studied trypanosomes are those that cause human diseases: Human African Trypanosomiasis caused by *Trypanosoma brucei* and American Trypanosomiasis caused by *T. cruzi.* However, trypanosomes infect animals from all vertebrate classes, including warm-blooded mammals and birds as well as cold-blooded amphibians, reptiles and fish (Simpson et al., 2006).

African trypanosomes, such as *Trypanosoma brucei*, are exclusively extracellular and are continuously exposed to the innate, humoral and cellular immune systems. *T. brucei* has become a textbook example of antigenic variation based on low frequency switches of the expressed variant surface glycoprotein (VSG) that dominates the cell surface and allows the population to escape the host adaptive immune system. In addition, individual cell survival is favoured by a process that cleans the cell surface of low levels of bound immunoglobulins through endocytosis and degradation (Engstler et al., 2007; Forlenza et al., 2009). Trypanosome motility is an integral part of this process as the hydrodynamic drag on antibody-VSG complexes, caused by the forward swimming motion of the cell, results in accumulation of the complexes at the posterior pole, close to the flagellar pocket, where endocytosis occurs (Engstler et al., 2007). In addition, motility is essential for successful cell division, immune evasion and development in the host (Broadhead et al., 2006; Griffiths et al., 2007; Ralston et al., 2006; Shimogawa et al., 2018).

In vitro studies using African trypanosomes have focused on the characterization of qualitative and quantitative parameters of trypanosome morphology and motility and emphasized the ability of trypanosome species to adapt to the various environments of their mammalian hosts (Alizadehrad et al., 2015; Bargul et al., 2016; Heddergott et al., 2012; Krüger and Engstler, 2015). Thus far, detailed analysis of swimming behaviour, morphology and trypanosome-host cell interaction has been restricted to *ex vivo*, using conditions that best mimic the host environment, as for example in blood taken from naïve or infected animals (Bargul et al., 2016; Beattie and Gull, 1997; Engstler et al., 2007; Heddergott et al., 2012; Hemphill and Ross, 1995; Shimogawa et al., 2018; Skalický et al., 2017; Sunter and Gull, 2016; Wakid and Bates, 2004). It has not been feasible to recreate complex *in vivo* microenvironments, which, in the case of the vertebrate host, includes the streaming of the blood, vessels with heterogeneous size and endothelium composition, as well as changes occurring during the course of an infection, for example from to the onset of anaemia. It still remains a challenge to mimic *in vitro* the dynamic conditions of the crowded and fast-moving blood stream in which trypanosomes live. Given the importance of motility for trypanosome survival, analysis of trypanosome swimming behaviour *in vivo*, in a vertebrate host environment, is important to fully understand trypanosome biology and pathogenesis.

Quantitative and qualitative approaches *in vivo* are hindered by the lack of transparency of mammalian vertebrate hosts. Nevertheless, using transgenic trypanosomes expressing a luciferase reporter protein it has been possible to monitor overall trypanosome distribution and to quantify total trypanosome load in mice (Burrell-saward et al., 2015; Capewell et al., 2016; Goyard et al., 2014; McLatchie et al., 2013). Fluorescent trypanosomes have been used *in vivo* to visualize their presence in mouse skin, a possible reservoir of trypanosomes in the late phase of infection (Capewell et al., 2016). Although the sensitivity of both systems allows for indirect visualization of trypanosome location or distribution, low spatio-temporal resolution and the lack of transparency of deep tissues limits the possibility for qualitative and quantitative analysis of trypanosome swimming behaviour *in vivo*. Finally, using a combination of multicolour light sheet fluorescence microscopy and high-speed fluorescence microscopy it has been possible to analyse the infection process and swimming behaviour of *T. brucei ex vivo*, in dissected tissues of the partially transparent tsetse fly vector (Gibson and Peacock, 2019; Schuster et al., 2017; Wang and Belosevic, 1994). Nevertheless, to date, no method is available to study with sufficient resolution trypanosome swimming behaviour *in vivo* in a vertebrate host environment.

In the current study, we have used *Trypanosoma carassii* infection of zebrafish, *Danio rerio*, to visualize trypanosome movement in the bloodstream and tissues of a vertebrate host. *T. carassii* infects a broad range of cyprinid fish (Overath et al., 1998), is transmitted by blood-sucking leeches (i.e., *Hemiclepsis marginata*) (Lom and Dyková, 1992), and lives extracellularly in the blood and tissue fluids of the fish (Haag et al., 1998; Lom and Dyková, 1992). *T. carassii* can establish a long-term infection characterized by polyclonal B cell activation and recurrent waves of parasitaemia, without the expression of a uniform VSG-like surface coat (Agüero et al., 2002; Joerink et al., 2007; Overath et al., 2001, 1999). Phylogenetically, *T. carassii* belongs to the aquatic clade of Trypanosoma, a sister group that diverged from the Trypanosomatid lineage prior to the divergence of the Stercorarian and Salivarian trypanosomes that infect mammals (Simpson et al., 2006; Stevens, 2008). Morphologically, *T. carassii* isolated from fish has a single flagellum that emerges from the flagellar pocket at the cell posterior, is attached to the cell body and extends free at the anterior end, defining the anterior-posterior axis.

Zebrafish have been used as a model for developmental biology, as well as biomedical and neurobiology research (Asnani and Peterson, 2014; Blackburn and Langenau, 2014; Cronan and Tobin, 2014; Goessling and North, 2014; Miyares et al., 2014; Nguyen-Chi et al., 2014; Phillips and Westerfield, 2014; Renshaw and Trede, 2012; Schartl, 2014; Torraca et al., 2014; Veinotte et al., 2014; Zon and Cagan, 2014) and are a fresh water cyprinid fish closely related to many of the natural hosts of *T. carassii.* The great advantage of zebrafish is the transparency of the larvae, and of some juvenile and adult stages. Furthermore, mutant and transgenic lines including those marking blood vessels and

relevant immune cell lineages are available (Benard et al., 2015; Bertrand et al., 2010; Ellett et al., 2010; Langenau et al., 2004; Lawson and Weinstein, 2002; Page et al., 2013; Petrie-Hanson et al., 2009; Renshaw et al., 2006).

The transparency of the zebrafish allows high-resolution, real-time imaging of trypanosome movement and host-parasite interaction *in vivo,* under conditions that exactly represent the natural environment during infection. In this study, by combining *T. carassii* infection of transparent zebrafish with high-speed microscopy, we provide the first description of trypanosome swimming behaviour *in vivo* in a vertebrate host. Our observations reveal that trypanosomes can rapidly adapt their swimming behaviour to the heterogeneous host environments. It was not possible to assign one preferred swimming behaviour to trypanosomes in either the blood stream, tissues or other body fluids. Conditions such as the presence or absence of the blood flow or of red blood cells, the speed of the flow, the size of the blood vessel, the type of endothelium or epithelium lining the vessels or the tissues, as well as the compactness of the tissues, all influenced the swimming behaviour. Furthermore, we show that trypanosomes can change direction through backwards swimming and through a 'whip-like' motion. Finally, we were able to capture a novel mechanism through which trypanosomes attach to host cells or tissues. These observations greatly expand our knowledge on trypanosome swimming behaviour and show that trypanosomes can rapidly adapt to match the host environment.

Material and methods

Key Resource Table

Reagent type (species) or resource	Designation	Source or reference	Identifiers	Additional information
gene (*Danio rerio*)	*elongation factor-1a (ef1a)*	NA	ZDB-GENE-990415-52	template for primers for RQ-PCR analysis
gene (*Trypanosoma carassii*)	*heat-shock protein-70* (*hsp70*)	NA	GeneBank-FJ970030.1	template for primers for RQ-PCR analysis
strain, strain background (*Cyprinus carpio*)	Wild type common carp, R3xR8 strain	doi:10.1016/0044-8486(95)91961-T		
strain, strain background (*Danio rerio*)	Wild type zebrafish, AB strain	European Zebrafish Resource Center (EZRC)	https://www.ezrc.kit.edu/index.php	
strain, strain background (*Danio rerio*)	casper strain	doi:10.1016/j.stem.2007.11.002		optically transparent
strain, strain background (*Danio rerio*)	*Tg(fli:egfp)^{y1}* (*casper)*	doi:10.1038/nrg888		optically transparent line, marking the vasculature with green fluorescent protein
strain, strain background (*Trypanosoma carassii*)	TsCc-NEM strain	doi:10.1007/s004360050408		

Zebrafish lines and maintenance

Zebrafish were kept and handled according to the Zebrafish Book (zfin.org) and animal welfare regulations of The Netherlands. Adult zebrafish were reared at the aquatic research facility of Wageningen University & Research (Carus). Zebrafish embryos and larvae were raised in egg water (0.6 g/L sea salt, Sera Marin, Heinsberg, Germany) at 27°C with a 12:12 light-dark cycle. From 5 days post fertilisation (dpf) until 14 dpf, larvae were fed once a day with Tetrahymena. Larvae older than 10 dpf were also fed daily with dry feed ZM-100 (zmsystem, UK). The zebrafish lines used in this study included: wild type AB, optically transparent casper lines (White et al., 2008), transgenic *Tg(fli:egfp)^{y1}* line marking the vasculature (Lawson and

Weinstein, 2002) *or crosses thereof.* All animals were handled in accordance with good animal practice as defined by the European Union guidelines for handling of laboratory animals (http://ec.europa.eu/environment/ chemicals/lab_animals/home_en.htm). All animal work at Wageningen University was approved by the local experimental animal committee (DEC number 2014095).

***Trypanosoma carassii* culture**

Trypanosoma carassii (strain TsCc-NEM) was previously cloned and characterized (Overath et al., 1998) and maintained in our laboratory by syringe passage through common carp (*Cyprinus carpio*, R3xR8 strain; Irnazarow, 1995). To this end, adult common carp were infected by intraperitoneal injection of 1 x 10^4 *T. carassii*; approximately 3 weeks post-infection and before the parasitaemia reached 1x10^6/ml, carp were euthanized in 0.6 g/l tricaine methane sulfonate (TMS, Crescent Research Chemicals) and bled *via* the caudal vein using a final concentration of 10-20 Units heparin/ml of blood. Trypanosomes in blood where imaged immediately or blood was kept at 4°C overnight in siliconized tubes. The following morning, trypanosomes were enriched at the interface between the red blood cells and plasma, and this buffy coat was recovered and centrifuged at 600xg for 8 minutes at room temperature. Trypanosomes were resuspended in RPMI without glutamine and phenol red (Lonza, Verviers, Belgium). To separate trypanosomes from red blood cells, the suspension was loaded on top of a 100% Ficoll-Paque layer (GE Healthcare, Uppsala, Sweden) and centrifuged at room temperature for 20 min, at 800xg. Cells at the interphase were transferred to a new 50 ml tube and washed with RPMI. Trypanosomes were then resuspended at a density of 5x10^5-1x10^6/ml and cultured in 75 or 165 cm^2 flasks in complete medium: 22.5% MEM with glutamine and phenol red (Gibco), 22.5% Leibovitz's L-15 medium without L-glutamine, with phenol red (Lonza, Verviers, Belgium), 45% Hanks' Balanced Salt solution (HBSS) with phenol red (Lonza, Verviers, Belgium), 10% sterile water, completed with 10% pooled carp serum, 2% 200 mM glutamine (Fisher Scientific) and 1% penicillin-streptomycin solution (10.000:10.000, Fisher Scientific). Cultures were incubated at 27°C without CO_2. Trypanosomes were kept at a density below 5x10^6/ml and subcultured one to three times a week. Using this medium, *T. carassii* was kept in culture without losing infectivity for up to 2 months. For zebrafish infection, trypanosomes were cultured for 1 week and never longer than 3 weeks.

Zebrafish infection with *Trypanosoma carassii* and morbidity signs

Cultured trypanosomes were centrifuged at 800xg for 5 minutes and resuspended in 2% polyvinylpyrrolidone (PVP, Sigma-Aldrich) prior to injection. PVP was used to increase the viscosity of the medium to assure a homogenous trypanosome solution throughout the injection period. Trypanosome number in 1-2 nl drop size varied depending on the intended dose and was monitored at the beginning and after 50 injections using a Bürker counting

chamber. Prior to injection, 5 dpf zebrafish larvae were anaesthetized with 0.017% Ethyl 3-aminobenzoate methanesulfonate (MS-222, Tricaine, Sigma-Aldrich) in egg water, and injected intravenously. Experimental groups received either *T. carassii* resuspended in PVP solution or PVP solution alone as a negative control. Injected larvae were directly transferred into pre-warmed egg water and kept in the incubator at 27°C. Viability was monitored daily. During the course of the optimization of the infection model, we noticed that some fish displayed lethargic behaviour and no escape reflex to a pipette, such fish usually had a high parasitaemia leading to death. These clinical signs were therefore used to monitor morbidity and the progression of infection. When necessary, fish were removed from the experiment and euthanized with an overdose of anaesthetic (0.4% MS-222).

Real-time quantitative PCR

At various time points after infection, three to six zebrafish larvae were sacrificed by an overdose of anaesthetic, pooled and transferred to RNA later (Ambion). Total RNA isolation was performed with the Qiagen RNeasy Micro Kit (QIAgen, Venlo, The Netherlands) according to manufacturer's protocol. Next, 250-500 ng of total RNA was used as template for cDNA synthesis using SuperScript III Reverse Transcriptase and random hexamers (Invitrogen, Carlsbad, CA, USA), following the manufacturer's instructions with an additional DNase step using DNase I Amplification Grade (Invitrogen, Carlsbad, CA, USA). cDNA was then diluted 25 times to serve as template for real-time quantitative PCR (RT-qPCR) using Rotor-Gene 6000 (Corbett Research, QIAgen), as previously described (Forlenza et al., 2012, 2008). Primers for zebrafish *elongation factor-1a* (*ef1a* Fw: 3'-CTGGAGGCCAGCTCAAACAT-5' and RV: 3'-ATCAAGAAGAGTAGTAGTACCG-5'; ZDB-GENE-990415-52) and *T. carassii heat-shock protein-70* (FW: 3'-CAGCCGGTGGAGCGCGT-5' 3'-AGTTCCTTGCCGCCGAAGA-5'; GeneBank-FJ970030.1) were obtained from Eurogentec (Liège, Belgium). Gene expression was normalized to the *ef1a* housekeeping gene and expressed relative to the time point PVP control.

High-speed light microscopy, image and video analysis

For imaging of *T. carassii* swimming behaviour *in vitro*, the high-speed camera was mounted on an automated DM6b upright digital microscope (Leica Microsystems), controlled by Leica LASX software (version 3.4.2.) and equipped with 100x oil (NA 1.32), 40x (NA 0.85, DIC) and 20x (NA 0.8, DIC) short distance objectives (Leica Microsystems). For high-speed light microscopy a three grey-scale (12 bits) Photron APX-RS High Speed Camera (Photron, resolution (128 x 16) to (1024 x 1024) pixels), with Leica HC 1x Microscope C-mount Adapter was used, controlled by Photron FASTCAM Viewer (PFV) software (version 3.5.1). Images were acquired at a resolution of 900 x 900 or 768 x 880 pixels depending on the C-mount adapter. Trypanosomes were transferred to non-coated microscopic slides (Superforst, Thermo Scientific), covered with a 24 x 50 mm coverslip and imaged immediately and for no longer than 10 min.

Prior to imaging of *T. carassii* swimming behaviour *in vivo*, the high-speed camera was mounted on a DMi8 inverted digital microscope (Leica Microsystems), controlled by Leica LASX software (version 3.4.2.) and equipped with 40x(NA 0.6) and 20x(NA 0.4) long distance objectives (Leica Microsystems). For high-speed light microscopy a three grey-scale (8 bits) Mikrotron EoSens MC1362 (Mikrotron GmbH, resolution 1280 x 1024 pixels), with Leica HC 1x Microscope C-mount Camera Adapter was used, controlled by XCAP-Std software (version 3.8, EPIX inc.). Images were acquired at a resolution of 900 x 900 or 640 x 640 pixels. Zebrafish larvae were anaesthetised with 0.017% MS-222 and embedded in UltraPure LMP Agarose (Invitrogen) on a microscope slide (1.4-1.6 mm) with a well depth of 0.5-0.8 mm (Electron Microscopy Sciences). Upon solidification of the agarose, the specimen was covered with 3-4 drops of egg water containing 0.017% MS-222, by a 24 x 50 mm coverslip and imaged immediately.

For all high-speed videos, image series were acquired at 240–500 frames per second (fps) and analysed using a PFV software (version 3.2.8.2) or MiDAS Player v5.0.0.3 (Xcite, USA); 240-250 fps were found optimal for imaging of trypanosome swimming behaviour *in vitro*, whereas 480-500 fps were used for *in vivo* imaging of infected zebrafish. Quantification of trypanosome length, swimming speed and directionality was performed with ImageJ-Fijii (version 1.51n) using the MTrack plug-in. For livestream light microscopy (acquisitions at 20 fps) a DFC3000G camera (Leica Microsystems) was mounted on the DMi8 inverted digital microscope and controlled by the Leica LASX software. Images were acquired at a resolution of 720x576 or 1296 x 966 pixels.

For fluorescence microscopy of *Tg(fli1:egfp)*^{y1} casper lines, marking the zebrafish vasculature in green, the Zeiss LSM-510 confocal microscope, with a 20x long-distance objective was used with the following settings: laser excitation = 488nm with 73% transmission; HFT filter = 488nm; BP filter = 505-550; detection gain = 800; amplifier offset = -0.01; amplifier gain = 1.1; bright field channel was opened with Detection Gain = 130; frame size (pixels) = 2048 x 2048; pinhole = 300 (optical slice < 28.3µm, pinhole ø = 6.26 airy units). Videos were produced using CyberLink PowerDirector 16.

Results

Characterization of *T. carassii* swimming behaviour *in vitro*

Previous *in vitro* studies reported on the heterogeneity in swimming behaviour of African trypanosomes, and on how this was dependent on the viscosity of the culture medium or host blood (Bargul et al., 2016; Engstler et al., 2007; Heddergott et al., 2012). To investigate the swimming behaviour of *T. carassii* in fish blood or culture medium, we used high spatio-temporal resolution microscopy. For the initial description of trypanosome swimming behaviour *in vitro*, we adopted the classification and quantification method described previously (Bargul et al.,

2016): *persistent swimmers*, trypanosomes exhibiting a directional movement covering several hundreds of micrometres; *tumblers*, trypanosomes exhibiting a non-directional movement and travelling no further than their body length; and *intermediate swimmers,* trypanosomes alternating periods of directional and non-directional movement.

Analysis of the swimming behaviour of trypanosomes in blood of infected carp revealed that up to 96.4% of *T. carassii* could be classified as *tumblers* (**Fig 1A-B** and **Video 1**, 00:00 - 45:19 sec). The remaining trypanosomes (3.5%) behaved as *intermediate swimmers* (**Video 1**, 00:00 - 45:19 sec), and only 0.1% could be classified as *persistent swimmers* (**Fig 1A-B** and **Video 1**, 45:19 - 58:03 sec). Persistent swimmers showed an average speed of 32 µm/sec and could cover a 'straight-line' distance of up to 418 µm in 20 seconds, whereas intermediate swimmers showed a lower average speed of 14 µm/sec (**Fig 1B**). Although tumblers did not move any distance greater than their body length (~23 ± 2.4 µm, **Fig 1C**), they were still very mobile. Taking advantage of the spatio-temporal resolution of high-speed videography, the speed of displacement of the posterior end of tumblers was 14 µm/sec, similar to that of intermediate swimmers (**Fig 1B**).

Comparison of the movement of freshly isolated trypanosomes kept in either carp serum or culture medium revealed comparable swimming behaviour (**Video 1**, 00:58 sec - 1:15 min). Culture in medium or serum for a period of up to 2 months did not alter morphology, the proportions of tumblers, intermediate or persistent swimmers (data not shown), suggesting that the swimming behaviour is an intrinsic property of trypanosomes in blood.

In freshly drawn blood from infected carp, trypanosomes were observed anchored to red blood cells or to leukocytes. Attachment always occurred through their posterior end leaving the flagellum free to move (**Fig 2** and **Video 2**, 00:00 – 00:28 sec). Similarly, also when cultured, trypanosomes could attach to the flask or glass surface through their posterior end (**Video 2**, 00:28 – 00:55 sec). Whether the site of attachment coincided with the cell membrane, flagellum base, or neck of the flagellar pocket was not readily clarified with the current image resolution. Finally, trypanosomes were also observed to alternate between forward and backward swimming (**Video 2**, 00:55 sec - 1:15 min).

Establishment of a *Trypanosoma carassii* infection model in zebrafish

To observe the swimming behaviour of *T. carassii* in a host, we developed an infection model in transparent zebrafish larvae. First, the susceptibility and kinetics of parasitaemia were determined. Infection of 5 day-post-fertilization (dpf) zebrafish resulted in an acute infection associated with low survival (**Fig 3A**) and high parasitaemia (**Fig 3B**), independent of the infection dose. This confirms that zebrafish, similarly to other cyprinid fish, are susceptible to *T. carassii* infection.

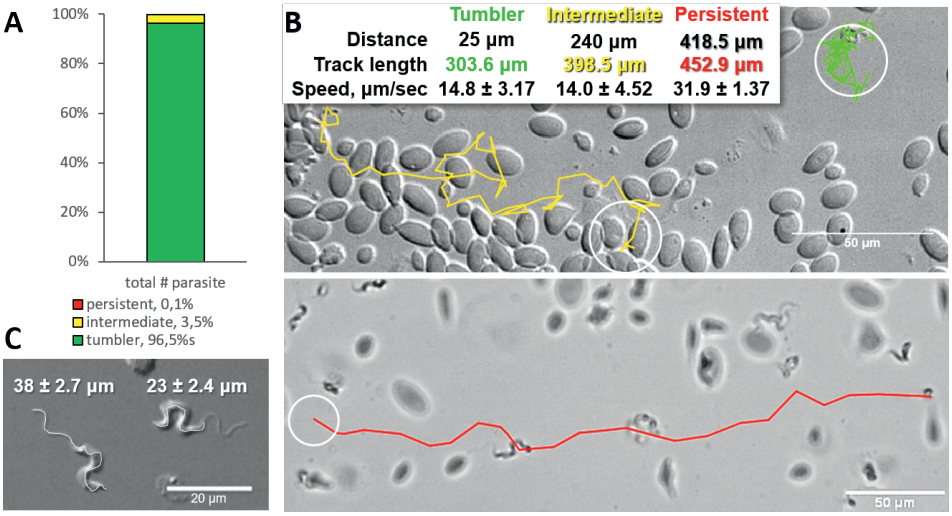

Fig 1. Majority of trypanosomes in freshly drawn blood are tumblers.
Blood was freshly drawn from carp and *T. carassii* swimming behaviour analysed immediately using high resolution microscopy at 240 frames per second (fps). **A)** Relative percentage of tumblers, and intermediate or persistent swimmers (defined in the text) was calculated over a total number of 944 *T. carassii*, isolated from 6 different carp infections and imaged over 60 independent acquisitions. **B)** Representative tracks of a tumbler (green), intermediate (yellow) and persistent (red) swimmer. The diameter of the circles (23 µm) indicates the average cell-body size of a trypanosome as also shown in C. The inset table summarizes the straight-line distance covered by the trypanosome (between the first and last track point); the total track length, i.e. the path covered by the trypanosome in approximately 20 seconds of acquisition time, indicated in matching colours; and the average speed (µm/sec) was calculated on a selection of the acquisitions used in A. For tumblers, the displacement of the posterior end was used as tracking point. **C)** Detailed image of two trypanosomes indicating the total body length including the flagellum (left) and the total cell-body length excluding the flagellum (right). Measurements were acquired on high resolution images of at least 10 freshly isolated trypanosomes obtained from 4 independent infections, using more than 20 frames within the same acquisition. Quantification of trypanosome length, swimming speed and directionality was performed with ImageJ-Fiji using the MTrack plug-in. ***Video 1*** displays high-speed videos of the swimming behaviour of tumblers, intermediate and persistent swimmers in carp blood, or of trypanosomes in serum or culture medium.

Video 1. Swimming behaviour of *T. carassii* in freshly drawn carp blood, or blood diluted with either carp serum or culture medium, showing representative tumblers, intermediate and persistent swimmers.

In vivo, T. carassii rapidly adapts its swimming behaviour to the heterogenous blood environment

Having established that *T. carassii* can infect zebrafish, we took advantage of the transparency of zebrafish larvae to characterize trypanosome swimming behaviour *in vivo*. Zebrafish larvae were infected at 5 dpf with 200 *T. carassii* per fish and imaged using either live

stream imaging (20 fps) or high spatio-temporal resolution microscopy (500 fps) at various time points after infection and in differently-sized blood vessels. When parasitaemia was low, typically early during infection, trypanosomes were most readily detected in small to medium-sized blood vessels with reduced blood flow and a lower density of red blood cells, such as the tail tip loop or intersegmental capillaries (ISCs). In the tail tip loop, trypanosomes were dragged passively by the blood stream along with red blood cells (**Fig 4A** and **Video 3**, 00:00 – 00:42 sec) and were seen to either curl or stretch the cell body as well as occasionally propel their flagellum in the same or opposite direction to the blood flow (**Video 3**, 00:42 sec - 01:57 min) but were never seen swimming faster than the flow. ISCs are narrow, with a diameter equivalent to a single red blood cell. In ISCs, trypanosomes were elongated with their flagellum in the opposite direction to the blood flow (**Fig 4B** and **Video 3**, 01:57 - 02:49 min); the diameter of the vessel, the speed of the flow and the presence of colliding red blood cells within the ISC, force the trypanosomes to passively move forward in the direction of the flow.

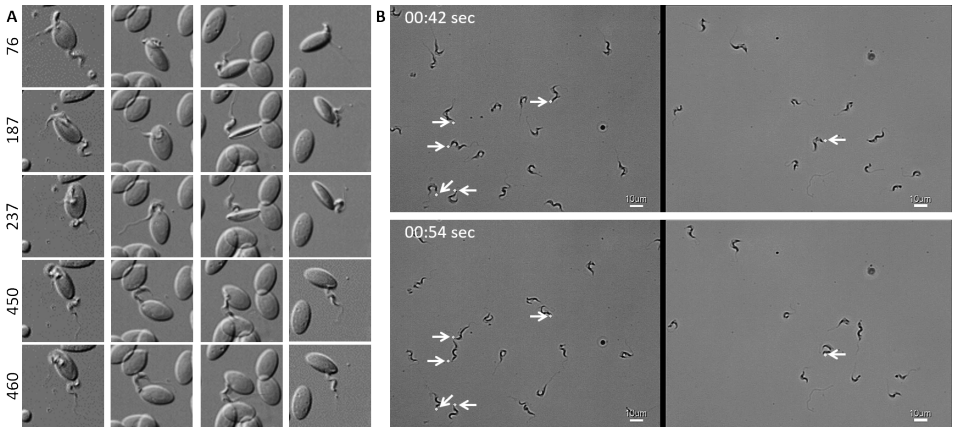

Fig 2. *T. carassii* attaches to cells or surfaces through its posterior end leaving the flagellum free to move.

A) Blood was freshly drawn from carp and trypanosomes swimming behaviour immediately imaged using high resolution microscopy at 240 frames fps. Images are frames (indicated by the numbers) of four different locations within the same field of view, selected from the corresponding ***Video 2***. Note how the posterior end of the parasites is attached to the red blood cell and the flagellum is free to move. **B)** Selected frames from ***Video 2***, at the indicated time points, showing how *T. carassii* can also adhere to glass surfaces through the posterior end (white arrow) leaving the body and flagellum free to move.

Video 2. *T. carassii* attaches to cells or surfaces through its posterior end leaving the flagellum free to move. Trypanosomes were also observed to swim backwards.

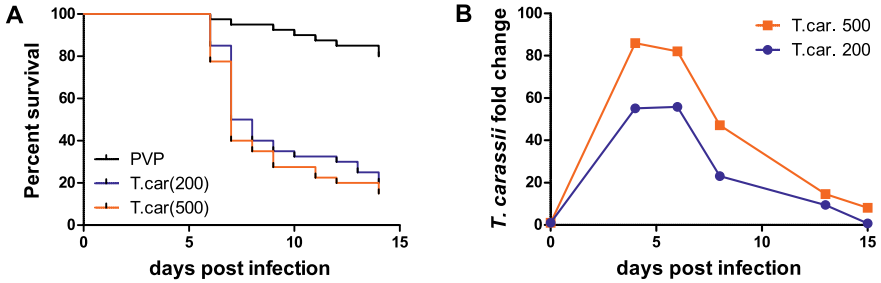

Fig 3. Zebrafish larvae are susceptible to *T. carassii* infection.
Zebrafish larvae (5 dpf) were injected with the indicated number of *T. carassii* per fish. PVP was used as injection control. **A)** Kinetics of zebrafish larval survival. Fish (n=40/group) were observed daily for signs of infection and survival. **B)** Kinetics of parasitaemia. Trypanosome levels were quantified by real-time quantitative-PCR using *T. carassii hsp70*-specific primers. RNA of five fish was pooled at each time point. Expression was normalized relative to the host house-keeping gene *elongation factor-1 alpha* and expressed relative to fish injected with the corresponding trypanosome dose at time point zero.

In larger diameter vessels with a strong blood flow and higher density of red blood cells, such as the cardinal caudal vein (**Video 3**, 02:49 - 04:11 min) or artery (**Video 3**, 04:11 - 04:37 min), detection and description of swimming behaviour was greatly aided by the use of high spatio-temporal resolution microscopy. In these vessels as well, trypanosomes are dragged passively by the blood stream, curling among the densely packed red blood cells. In real time speed, only the occasional trypanosome was seen to slow down by rolling or bouncing against the vessel in the peripheral cell-free layer (**Fig 4C** and **Video 3**, 03:53 - 04:11 min). In general, the typical tumbling movement described *in vitro* was not observed in the fish, except for those locations where the blood flow was highly reduced or absent as in sharp turns of the tail tip (**Video 3**, 04:37 - 05:09 min), and in locations where leukocytes adhering to the endothelium would create a local disturbance of the flow rate allowing trypanosomes to tumble (**Video 3**, 05:09 - 05:24 min).
Physiological changes in the blood flow or red blood cells density associated with the infection, allowed visualization of additional swimming behaviours in blood vessels. For example, in cases where the blood flow was temporarily interrupted, trypanosomes were able to swim directionally, repeatedly invert direction, or tumble (**Fig 5A** and **Video 4**, 00:00 - 01:23 min). In cases where the blood flow continued but red blood cells were occluded, trypanosomes were able to persistently swim against the blood flow (**Fig 5B**, and **Video 4**, 01:23 - 02:13 min). We did not attempt to distinguish, *in vivo*, between intermediate and persistent swimmers because physical factors such as the presence of red blood cells, the length of a capillary or the stability of the blood flow could all interfere with the directionality

of their movement. Instead, all trypanosomes observed to swim directionally in the blood, independent of the distance covered before changing direction, were considered swimmers. Altogether, we observed that *T. carassii* can adopt different swimming behaviours all greatly influenced by the blood flow, size of the blood vessel and presence of red blood cells. Most frequently, in blood vessels with an intact blood flow and high density of red blood cells, trypanosomes are dragged passively by the flow along with red blood cells, in a curling motion. Occasionally, when the blood flow or the number of red blood cells is reduced, trypanosomes can swim directionally and persistently (swimmers) in blood vessels. This indicates that, at least *in vivo*, it is not possible to assign a specific swimming behaviour to trypanosomes in blood vessels; on the contrary, trypanosomes rapidly adapt their swimming behaviour to changes in micro-environmental conditions.

Trypanosomes can attach *in vivo* by anchoring through their posterior end

In addition to being dragged passively within blood vessels, trypanosomes could often be seen attached to the endothelium on the dorsal luminal side of the cardinal caudal vein (referred to as caudal vein, **Fig 6A**). Remarkably, despite the strong blood flow, attachment (anchoring) could last for several seconds (**Video 5**, 0:00 - 01:11 min) and involved a small area of the posterior end of the trypanosome, leaving the cell body and the flagellum free to move (**Video 5**, 01:11 - 01:59 min). Although anchoring could be observed already at 1 dpi, it was more easily detected at later stages of the infection. Anchoring was not the only mode of attachment, trypanosomes were also seen crawling along the vessel wall involving the entire cell body (**Fig 6B** and **Video 5**, 01:59 - 02:38 min). Within blood vessels, anchoring occurred exclusively at the dorsal side of the caudal vein, whereas crawling could occur anywhere in the vein. No attachment or crawling was observed in arteries or capillaries, independently of the speed of the blood flow.

Altogether, our observations show that *T. carassii* attaches to host cells through their posterior end, both *in vitro* (**Video 2**) and *in vivo*, leaving the flagellum free to move, and suggest that the posterior end acts as an anchoring site. Whether the exact anchoring site corresponds to the flagellum base or to the neck of the flagellar pocket and whether it may possibly favour extravasation, could not be confirmed under the current conditions and will be the focus of further investigation.

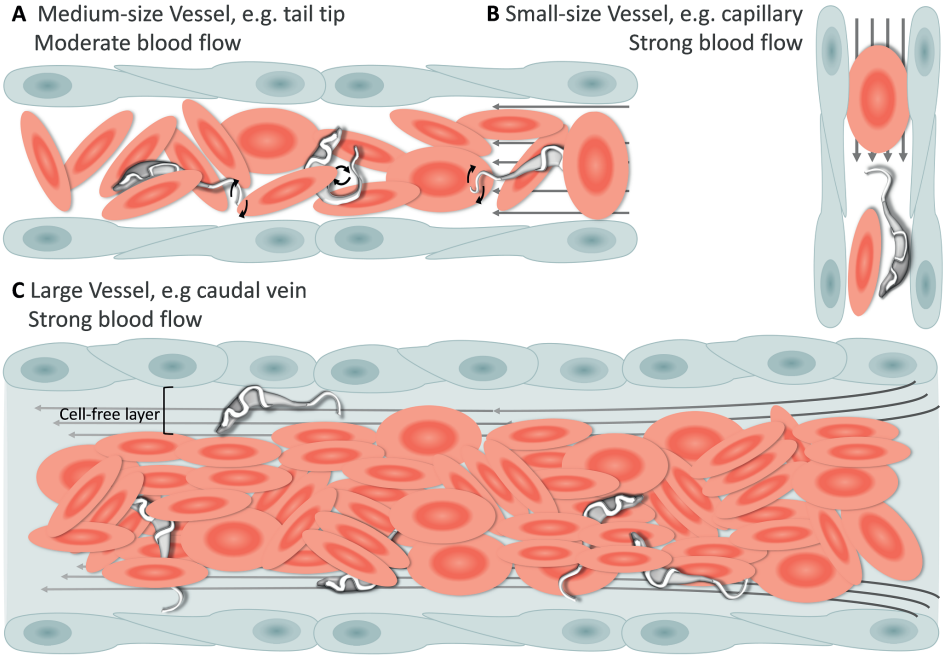

Fig 4. Schematic representation of *T. carassii* swimming behaviour in blood vessels of various sizes.

In general, in vessels with an intact blood flow (grey arrows) and a normal number of red blood cells (RBC), trypanosomes are dragged passively by the flow along with RBC. Under these conditions, trypanosomes were never seen swimming directionally against the flow or faster than RBC. **A)** In medium-sized blood vessels with moderate flow, while being dragged passively by the flow, trypanosomes can either curl or stretch their body, as well as occasionally propel their flagellum in the same or opposite direction to the blood flow. **B)** In small-sized blood vessels of one-cell diameter, such as intersegmental capillaries (ISC), trypanosomes are pushed forward by the blood flow and by colliding RBC. **C)** In large-sized blood vessels, the blood flow is very strong and the density of RBC high, making it more difficult to detect trypanosomes without the aid of high-speed microscopy. Only the occasional trypanosome that would slow down by bouncing against the vessel wall would be visible in the cell-free layer. ***Video 3*** contains high-speed videos showing details of the trypanosome movements schematically depicted above.

Video 3. Swimming behaviour of *T. carassii* in small, medium and large sized vessels with an intact blood flow. Under these conditions, trypanosomes are dragged passively by the flow or pushed forward by colliding RBC.

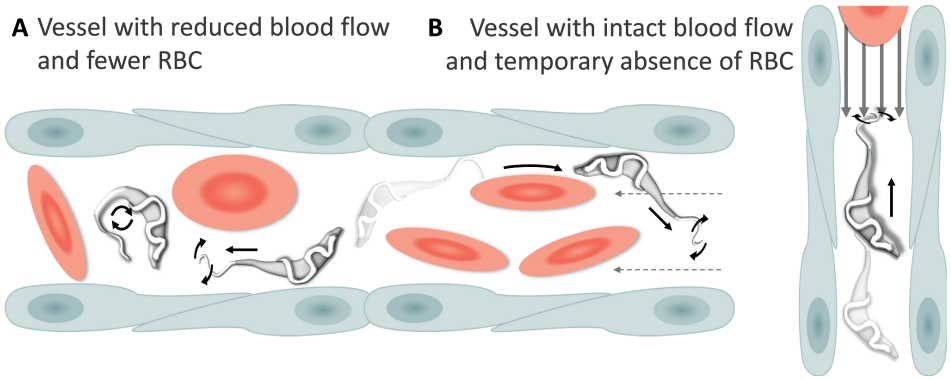

Fig 5. Schematic representation of *T. carassii* swimming behaviour in blood vessels with altered blood flow or RBC number.

A) Blood vessels with a reduced blood flow (dashed arrows) and fewer RBC. **B)** Blood vessels with an intact blood flow (grey arrows) but with a temporary absence of RBC. In both cases, trypanosomes can swim directionally (black straight arrows) by propelling the flagellum (distorted circular arrows) in the same or opposite direction of the flow or can tumble (circular arrows). ***Video 4*** contains high-speed videos showing trypanosome movement in medium-sized blood vessels and in capillaries as schematically depicted.

Video 4. Swimming behaviour of *T. carassii* in medium-sized blood vessels with interrupted blood flow, or in capillaries with intact blood flow and reduced number of red blood cells. Under these conditions, trypanosomes can repeatedly invert direction, swim directionally or tumble.

T. carassii movement in fluids outside the blood vessels and in tissues

A characteristic of *T. carassii* infections is extravasation from blood vessels into surrounding tissues and tissue fluids (Haag et al., 1998; Lom and Dyková, 1992). In zebrafish, this was observed at 1 dpi and allowed us to investigate the swimming behaviour in tissue fluids other than blood, including those of the peritoneal and heart cavities. In these locations, we could thus evaluate the swimming behaviour of trypanosomes in the absence of red blood cells and of blood flow. In these environments, the swimming behaviour was similar to that observed *in vitro* (**Video 1** and **Fig 1**), where the majority of the trypanosomes were tumblers (**Fig 7** and **Video 6**, 00:00 – 00:42 sec). In a field of view of more than 100 trypanosomes in the peritoneal cavity, only 3 persistent swimmers could be identified (**Fig 7B** and **Video 6**, 00:42 sec - 01:35 min). Furthermore, trypanosomes were seen anchored by their posterior end to cells of the peritoneal membrane in a manner similar to that observed in the caudal vein (**Video 6**, 00:34 – 00:42 sec).

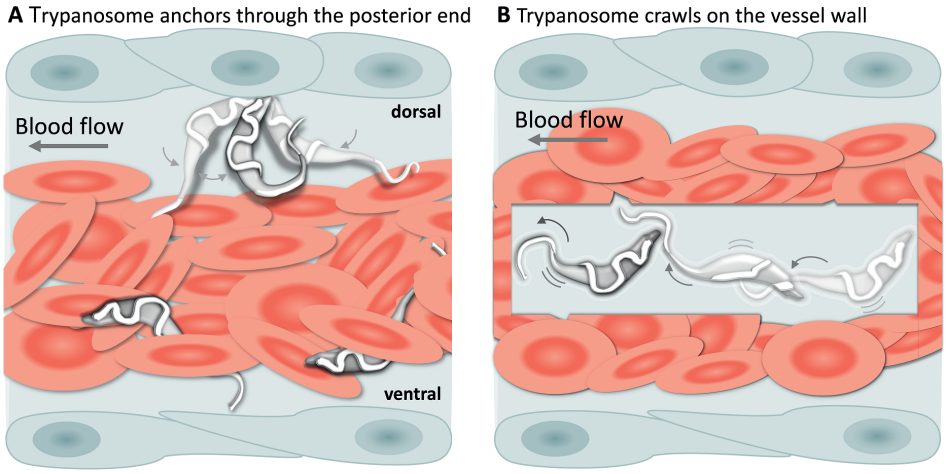

Fig 6. *T. carassii* attachment to the blood vessel wall.
A) *T. carassii* anchor themselves by their posterior end, leaving the cell body and the flagellum free to move. Anchoring occurred only to the dorsal luminal side of the caudal vein and was not observed in other blood vessels. **B)** Trypanosomes crawl along the vessel wall of the caudal vein; the transparent square allows visualization of trypanosomes through the pack of RBC. Crawling occurred everywhere in the vein and involved the entire cell body. ***Video 5*** contains high-speed videos showing anchored and crawling *T. carassii* in the caudal vein as schematically depicted above.

Video 5. *T. carassii* anchor to the dorsal luminal side of the caudal vein and crawl along the vessel wall of veins.

Next, we analysed the swimming behaviour of *T. carassii* in tissues: the tail tip, fins, muscle and interstitial space lining the blood vessels. Here, we observed no apparent consistency in swimming behaviour, and trypanosomes alternated between directional and non-directional swimming depending on the compactness of the tissue. For example, in the compact tissue of the fins, most trypanosomes were directional swimmers (**Fig 8A-B**) although their path can often be interrupted or hindered by the compactness of the tissue. Swimmers moved at an average speed of 47.5 μm/sec, covering up to 187 μm, before disappearing from the view or colliding with an obstacle that resulted in a change in direction (**Video 7**, 0 – 47 sec). Similar to the observations made *in vitro* (**Video 2**), trypanosomes could invert their swimming direction by swimming backwards (**Fig 8A-B** and **Video 7**, 00:47 sec - 01:07 min). *In vivo*, backward swimming was only observed in the fins.
In the interstitial space lining the cardinal blood vessels (artery and vein), trypanosomes swim directionally or tumble (**Video 8**, 00:00 – 00:23 sec), but can also use the space between cells to pin themselves and effectively invert swimming direction in a 'whip-like' motion, a movement distinct from the more random tumbling movement. (**Video 8**, 00:23 sec - 01:17 min). Such 'whip-like' movement was also observed for trypanosomes swimming in ISC in

which the blood flow is absent, and in more compact tissues such as the fin (**Fig 8C** and **Video 8**, 01:17 - 02:18 min). The 'whip-like' motion combines the swing of the flagellum along one plane, similar to the movement of tumblers on a glass surface (**Video 1**), accompanied by a 180° rotation of the cell body along a third axis. This is indeed possible only *in vivo* where the cylindrical form of a capillary or interstitial space within a tissue, allow the very flexible trypanosome's cell body to move in three dimensions. Furthermore, in compact tissues that do not present a ready passage for trypanosomes, the persistent swimming translates into a drilling (auger) movement, which in some cases can lead to an enlargement of the space between somatic cells (**Fig 8D** and **Video 8**, 02:18 - 03:52 min).

Altogether, in tissues and tissue fluids *T. carassii* can adopt all swimming movements and can adhere through the posterior end to endothelial cells of the peritoneal cavity. Besides the previously described tumbling and directional (forward) swimming, trypanosomes were also able to invert direction through a 'whip-like' motion or by backward swimming.

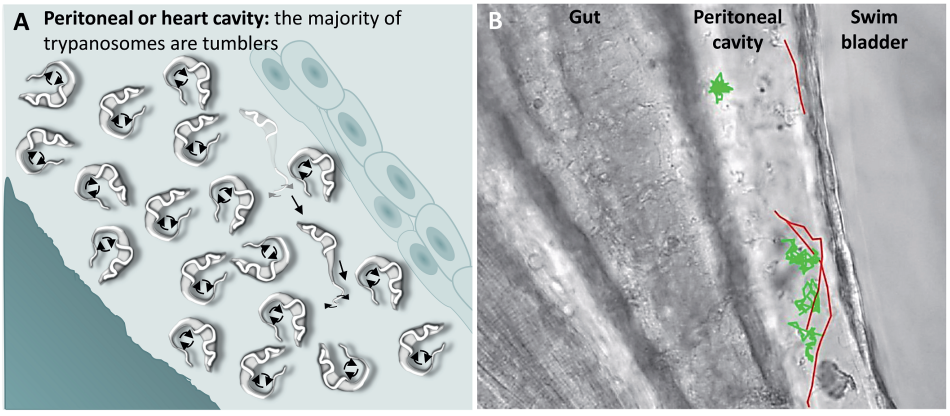

Fig 7. ***T. carassii* swimming behaviour in tissue fluids outside blood.**

A) Schematic representation of *T. carassii* swimming in the peritoneal or heart cavity, both environments without hydrodynamic flow and red blood cells; here, most of the trypanosomes are tumblers, only occasionally a persistent swimmer could be observed. **B)** Selected frame from ***Video 6***, capturing trypanosomes in the peritoneal cavity. More than 100 trypanosomes are present but are not all in focus in the selected frame; the majority are tumblers. The tracks of four representative tumblers (green) and of the only three persistent swimmers (red) are shown. ***Video 6***, contain high-speed videos showing the location and swimming behaviours described above.

Video 6. Swimming behaviour of *T. carassii* extravasated from blood vessels into tissue fluids that lack blood flow and RBC. These include the peritoneal and heart cavity.

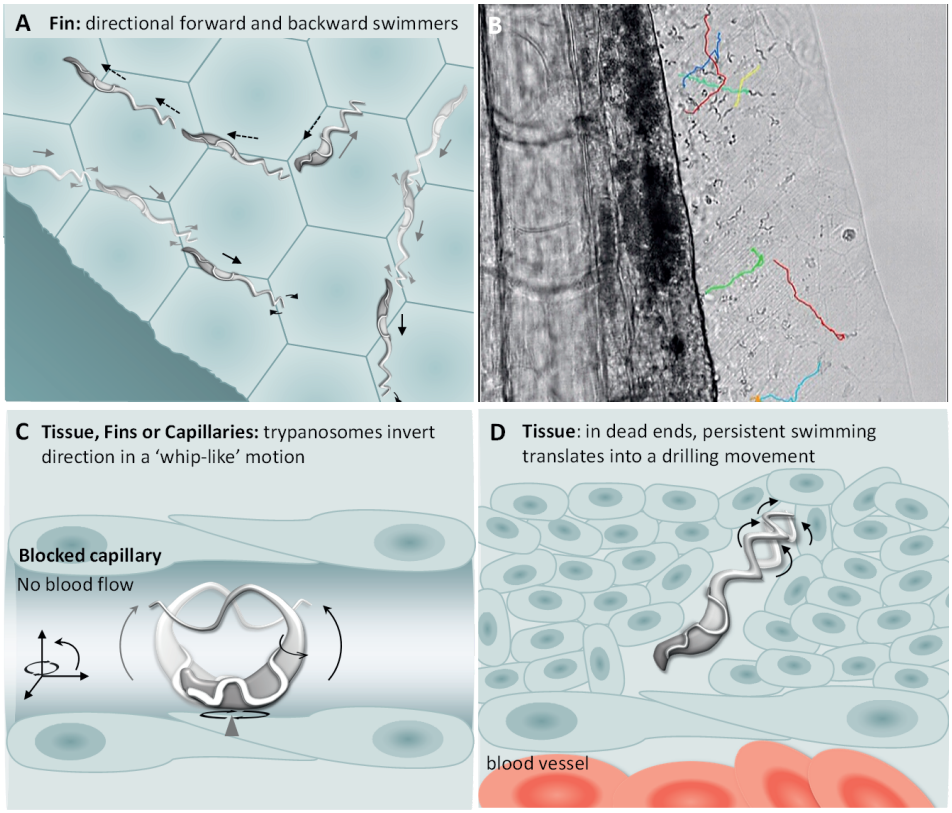

Fig 8. ***T. carassii*** **swimming behaviour in tissues.**
A) Schematic representation of *T. carassii* swimming in compact tissues such as those in the fins. Most trypanosomes are directional swimmers and both, forward and backward swimming was observed. **B)** Selected frame from ***Video 7*** showing the tracks of representative persistent swimmers identified in the fins. **C)** In less compact tissues and in capillaries without blood flow, trypanosomes could invert their swimming direction in a 'whip-like' motion using the available three-dimensional space of the capillary or tissue. The 'whip-like' motion combines the swing of the flagellum along one plane (thin arc arrows), accompanied by a 180° rotation of the flexible cell body along a third axis (rotational arrows). **D)** In tissues where trypanosomes reach dead ends such as the interstitial space between vessels, persistent forward swimming translates into a drilling (auger) movement. ***Video 7*** and ***Video 8*** contain high-speed videos showing all locations and swimming behaviours schematically depicted above.

Video 7. Swimming behaviour of *T. carassii* in the narrow spaces of the fins, capturing persistent forward and backward swimmers.

Video 8. Swimming behaviour of *T. carassii* in various tissues.

Progression of *T. carassii* infection and associated clinical signs

Physiological changes associated with the progression of the infection can affect the conditions within blood vessels or host tissues, and thus influence trypanosome behaviour. In addition to extravasation (**Video 6- Video 8**), which occurred as early as 1 dpi, we observed onset of anaemia and vasodilation of blood vessels.

Non-infected larvae have a strong and steady blood flow, with all blood vessels packed with red blood cells (**Fig 9A**). In contrast, infected larvae progressively showed a decrease in the ratio between red blood cells and trypanosomes from 1 to 8 dpi (**Fig 9B-C**), until in some cases red blood cells disappeared completely (**Fig 9D** and **Video 9**). Anaemia therefore is a hallmark of late stages of *T. carassii* infection in zebrafish larvae.

Highly infected fish that are anaemic also showed vasodilation, a clinical sign typical of advanced stages of infection (> 3 dpi) with *T. carassii* (**Fig 10A-C**), most obviously observed in the caudal vein. The degree of vasodilation differed between individuals and in extreme cases the diameter of the caudal vein could be up to three times larger than that of control fish (**Fig 10D**). Vasodilation also occurs in the caudal artery but to a lesser extent (not shown). Interestingly, while the dilated blood vessels of larvae are packed with trypanosomes and have limited circulation, the number of extravasated trypanosomes is very low (**Video 9**).

Fig 9. Onset of anaemia during *T. carassii* infection. ►

Zebrafish larvae (5 dpf) were infected with 200 *T. carassii* or injected with PVP as non-infected control. Images are selected frames depicting the caudal artery, extracted from high-speed videos where trypanosomes (white open-arrow heads) and red blood cells (RBC, black open-arrow heads) were identified and tracked. **A)** Artery of a control, non-infected, fish. Only RBC are present. **B)** Artery of an infected fish, 1 dpi, showing a high ratio of RBC:trypanosomes. This frame corresponds to seconds 04:20-04:23 in ***Video 3***, where the same trypanosomes were tracked. **C)** Artery of an infected fish, 6 dpi, showing a reduced ratio of RBC:trypanosomes, indicating the onset of anaemia. **D)** Artery of an infected fish suffering from severe anaemia, 8 dpi, where only trypanosomes are present. The frame is extracted from the corresponding ***Video 9***. Scale bars indicate 25 µm.

Video 9. Anaemia is a hallmark of *T. carassii* infection.

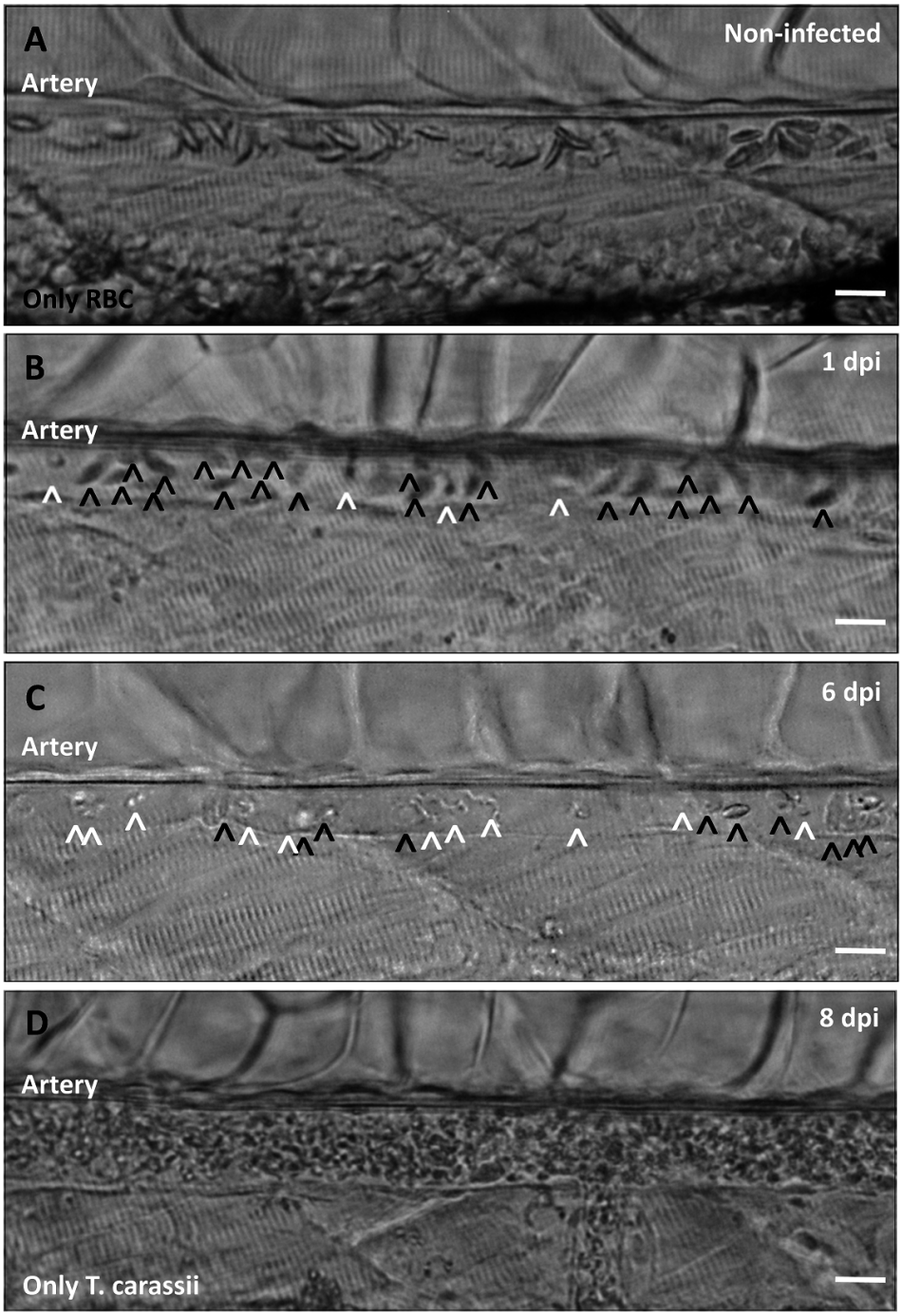
A
Artery
Non-infected
Only RBC
B
Artery
1 dpi
C
Artery
6 dpi
D
Artery
8 dpi
Only T. carassii

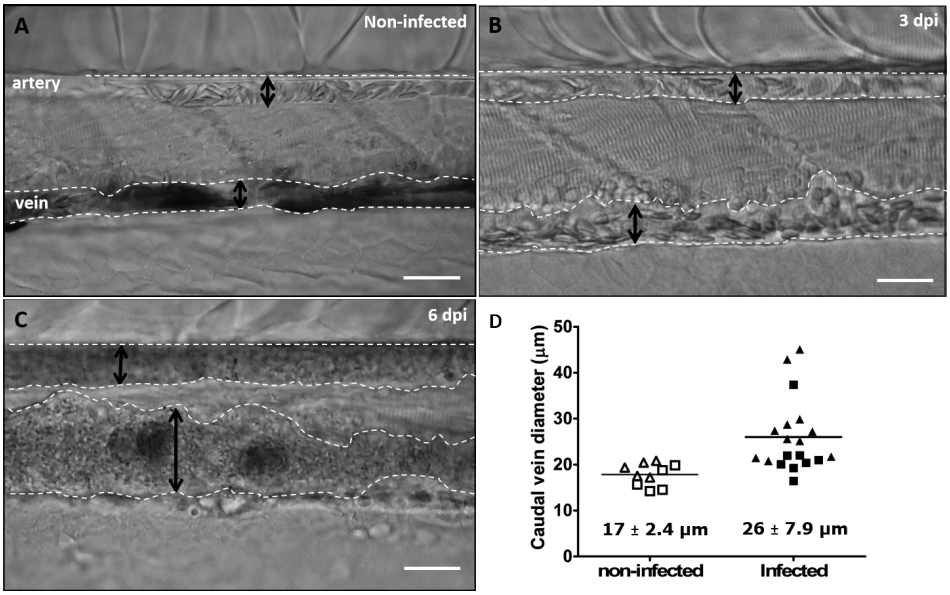

Fig 10. Advanced stages of *T. carassii* infection lead to vasodilation of the caudal vein.
Wild type zebrafish larvae (5 dpf) were infected with 200 *T. carassii* or injected with PVP as non-infected control. Images are selected frames from high-speed videos. **A-C)** Representative images of caudal artery and caudal vein (dashed lines) region at various time points after infection. Scale bars indicate 50 µm. **D)** Maximum diameter of the caudal vein in non-infected (open symbols) and infected individuals (closed symbols) at 2-3 dpi (squares) and 6-8 dpi (triangles). Each value is the average of at least 3 measurements taken at different locations within the caudal vein of the same individual. Numbers indicate average and standard deviation.

Discussion

In this study we describe a trypanosome infection model in zebrafish. By combining the transparency of zebrafish larvae with high spatio-temporal resolution microscopy, we were able to describe in detail the *in vivo* swimming behaviour of *T. carassii* in blood, tissues and tissue fluids of a vertebrate host. In addition to non-directional tumbling and directional forward swimming, we also describe how *in vivo* trypanosomes can reverse direction through a 'whip-like' motion or by swimming backwards. Finally, we report a novel observation that the posterior end of *T. carassii*, possibly coinciding with the flagellum base or flagellar pocket's neck, can act as an anchoring site. To our knowledge this is the first report of the swimming behaviour of trypanosomes *in vivo* in a vertebrate host environment.
Knowledge of trypanosome-host cell interaction, movement, and tropism in vertebrate hosts is important to understand trypanosome biology and pathology. To date, detailed analysis

of trypanosome swimming behaviour and interaction with vertebrate host cells has only been possible using isolated blood or conditions that best mimic those of the host blood or tissues. Although the current *in vitro* approaches have brought a wealth of information on the quantitative aspects of trypanosomes motility and potential immune evasion strategies, they could not fully reproduce the streaming nature of the blood, the heterogeneity of the blood stream between and within vessel, the different sizes of blood vessels between which trypanosomes regularly alternate, the different types of endothelium lining arteries and veins and finally, the changes that occur in the blood due to the infection itself.

In this study, we first investigated the motion of *T. carassii* in infected carp blood. Based on a previously proposed descriptions of the swimming behaviour of salivarian trypanosomes in mouse blood (Bargul et al., 2016; Shimogawa et al., 2018), clearly more than 90% of *T. carassii* could be classified as tumblers, and this was independent of whether they were in whole blood, diluted in serum or culture medium. Our observations are in agreement with a previous study reporting that directional persistent swimming was not a prominent feature of *T. brucei* in whole blood from an immunocompetent infected mouse (Shimogawa et al., 2018) but are in contrast with the study by Bargul and colleagues in which up to 30% persistent swimmers and 45% intermediate swimmers could be observed in blood films from immunosuppressed infected mice (Bargul et al., 2016). Differences in *T. brucei* strains, host immune status as well as the use of whole blood or blood films may account for the observed discrepancies. Nevertheless, both studies could not reproduce the streaming of the blood and thus, the observation where made under static conditions.

Our initial *in vitro* observations led to the suggestion that the tumbling behaviour might be an intrinsic property of *T. carassii* in the bloodstream. However, our subsequent *in vivo* observations showed that this applies only to trypanosomes swimming in fluids with highly reduced or absent flow, for example the peritoneal fluid or blood in vessels in which the flow was slow or absent (**Fig 7A** and **Video 9**). In contrast, analysis of the swimming behaviour of *T. carassii* in the zebrafish blood stream revealed that it is not possible to assign a single or predominant swimming behaviour. In vessels with a normal blood flow and in the presence of red blood cells, trypanosomes were dragged passively by the flow along with red blood cells. In the centre of large vessels, such as the cardinal artery or cardinal vein, the velocity of the flow does not allow either tumbling or directional swimming against or faster than the flow. Similarly, in narrow intersegmental capillaries (ISCs), trypanosomes are forced to move forward because of streaming of the blood or the presence of colliding red blood cells. Under these conditions, trypanosomes were never seen swimming faster than the passive movement of red blood cells as previously suggested (Heddergott et al., 2012; Langousis and Hill, 2014). Furthermore, since trypanosomes are carried along with red blood cells by the flow, it is difficult to envisage how the red blood cells could represent anything more than very occasional obstacles or surfaces for mechanical interactions that would favour forward swimming (Bargul et al., 2016; Heddergott et al., 2012). At the periphery of the cardinal vein,

there is a cell-free layer where the number of red blood cells and the speed of the blood flow is reduced (Bagchi, 2007). Here trypanosomes could clearly slow themselves down by crawling, rolling or by temporarily anchoring themselves to the dorsal endothelium (further discussed below). However, in arteries or small capillaries, adherence to the epithelium was never observed, even when the flow was reduced or completely absent. This suggests that not only the velocity of the flow but also the type of endothelium influences trypanosome swimming behaviour.

Physiological changes occur as the infection progresses that modify conditions within blood vessels. The flow is strongly reduced or interrupted and the density of red blood cells is reduced by obstruction of blood vessels or anaemia. In these conditions, directional swimmers were observed that swam faster than the flow and others that swam against the flow, or that repeatedly changed direction within blood vessels (**Video 4**). Taken together, our observations show that it is not possible to generalize the swimming behaviour of trypanosomes in blood as they can rapidly adopt different swimming behaviours: tumbling, directional swimming or anchoring. These behaviours are all largely influenced by the size and type of vessel, the speed of the flow, the presence, or not, of red blood cells as well as the highly dynamic microenvironment within a vessel, as for example the centre compared to the periphery, and the type of endothelium.

Outside of the blood, it has been suggested that the directionality of swimming is influenced by the density or compactness of the tissue (Bargul et al., 2016; Sun et al., 2018; Wheeler et al., 2013). Our observation of swimming behaviour in various tissues revealed that it is the size of the interstitial space through which the trypanosome has to swim that largely determines whether it will swim directionally, tumble or both. For example, within the compact tissue of the fins, where the space below epithelial cells is very narrow (mesenchyme) and the basement membrane is not deformable (Mateus et al., 2012), the vast majority of trypanosomes swim directionally. This observation is in agreement with the swimming behaviour described for procyclic forms of *T. brucei* swimming through microfluidic devices smaller than their maximum cell diameter, mimicking potential size-limiting environments within host tissues (Sun et al., 2018). In zebrafish fins, the space can be so restrictive that to invert direction the trypanosome is obliged to swim backwards (**Video 7**). Backward swimming was previously observed *in vitro* or *ex vivo* for *T. brucei* motility mutants or for wild type trypanosomes swimming in high-density medium or in whole blood (Bargul et al., 2016; Baron et al., 2007; Branche, 2006; Engstler et al., 2007; Heddergott et al., 2012; Shimogawa et al., 2018) and *ex vivo*, for procyclic and mesocyclic stages of *T. brucei* parasites swimming in confined spaces within the midgut of the tsetse fly (Schuster et al., 2017). The observation of *T. carassii* swimming in zebrafish tissues is the first report of backward swimming in a vertebrate host environment.

In the less compact areas of the fins or in the tissue lining the blood vessels, in addition to directional swimmers (forward or backwards), tumblers and trypanosomes that repeatedly inverted direction through a whip-like motion were observed (**Video 8**). When directional

swimmers reached dead ends, the persistent forward swimming translated into either a drilling movement similar to the movement described for *T. brucei* in dead-end spaces within the midgut of the tsetse fly (Schuster et al., 2017), or backwards swimming as observed in the fins. Altogether, these observations indicate that trypanosomes can adopt several swimming behaviours and that these are largely influenced by the compactness and confinement offered by the tissue.

Perhaps one of the most interesting observations is the discovery that trypanosomes can anchor themselves to the vein endothelium by their posterior end, leaving the flagellum and the entire cell body free to move. Anchoring was observed as soon as 30 min to 1h after *T. carassii* injection into zebrafish larvae, and by 1 dpi extravasation was observed. Under the current conditions, it was not possible to ascertain whether this adhesion mechanism favours or is even required for extravasation. So far, we have been unable to capture the exact moment of extravasation.

The anchoring site on the posterior of the trypanosome leaves the cell body and flagellum free to move (**Video 2** and **Video 5**) so it seems likely that the adhesion on the trypanosome occurs via the flagellum base or the neck of the flagellar pocket itself. The presence of specific adhesion molecules would at least partly explain how *T. carassii* can very rapidly anchor themselves, upon sudden collision with the endothelium, and remain in position for more than 15 s despite the very rapid blood flow and collisions with blood cells. Anchoring was only observed in the cardinal vein but trypanosomes were seen crawling on vein endothelium (**Video 5**) through dynamic interactions that involved the cell membrane, not just the flagellum membrane, suggesting that the molecules required for whole-cell adherence might be different from those required for anchoring through the posterior end. This is reminiscent of leukocyte rolling, which also occurs only in veins and not in arteries. Altogether, the possibility to observe *T. carassii* behaviour both *in vitro* and *in vivo,* in the presence or absence of a strong hydrodynamic flow, and at various locations within the vertebrate host, demonstrated how the environmental conditions, especially the presence or absence of a flow, strongly influence the ability of the trypanosome to attach and the duration of the attachment.

T. carassii anchors to zebrafish cells in a manner clearly distinct from that described for other trypanosomes. The major difference being the lack of extensive interaction between the trypanosome's flagellum membrane and the host cell or artificial surface. Stable interaction involving large portions of the flagellum membrane have been described among others for haptomonads stages (surface-attached) of *Paratrypanosoma confusum*, or *Leishmania* promastigotes (**Fig 11A**) (Skalický et al., 2017; Wakid and Bates, 2004). In these liberform parasites (flagellum not laterally attached to the cell), adhesion occurs through an attachment pad forming from the bulge at the base of the flagellum. At least *in vitro*, the formation of the pad takes approximately 1h, causing extensive remodelling of the flagellum itself, and effectively anchors the parasites to the surface, and in the case of *P. confusum*, also favours

their division (Skalický et al., 2017). Similarly, *T. brucei* epimastigotes divide while attached to the brush border of the salivary gland epithelium through extensive outgrowths of the non-cell-attached anterior part of the flagellum membrane (**Fig 11B**) (Beattie and Gull, 1997; Langousis and Hill, 2014; Schuster et al., 2017). Such adhesion mechanism was only recently captured *ex vivo* through high-speed videography of dissected tsetse fly salivary glands; however, the exact moment of attachment and the time required to establish the stable interaction *in vivo*, were not reported (Schuster et al., 2017). *T. congolense* was reported to adhere *in vitro* to bovine aorta endothelial (BAE) cell monolayers *via* extensive membrane protrusions (filopodia) of the membrane-attached flagellum (**Fig 11C**) (Beattie and Gull, 1997; Hemphill and Ross, 1995), an interaction that was shown to involve sialic acid residues on BAE cells (Hemphill et al., 1994). Although adhesion was observed already at 1h, the filopodia increased in size over a period of 24-48h. Whether such type of interaction occurs with similar kinetics also *in vivo*, in vessels with an intact blood flow, is yet to be confirmed. All the above attachment mechanisms are clearly geared towards creating a very stable interaction with a surface to either establish a permanent infection in the salivary glands of the insect host, or to possibly adhere to the vertebrate host endothelium. They all involve extensive modifications of the flagellum membrane that occur over time to increase the contact area between the (para)trypanosomes and the surface. Most of these interactions, however, were observed *in vitro* for (para)trypanosomes cultivated on glass or plastic surfaces or endothelial cell monolayers and studied by means of scanning or transmission electron microscopy, as well as *in vitro* binding assays (Beattie and Gull, 1997; Hemphill and Ross, 1995; Hemphill et al., 1994; Skalický et al., 2017; Vickerman, 1969; Wakid and Bates, 2004). Therefore, to what extent the kinetics of interaction and the size of the contact area described also apply to the more dynamic *in vivo* environment is yet to be ascertained. The interactions between *T. carassii* and zebrafish cells was limited to the tip of the posterior end of the trypanosome body (**Fig 11D**), leaving the entire flagellum and trypanosome's cell body free to rapidly move (**Video 2**). Despite the small surface involved, anchoring occurred very rapidly, suggesting a very strong, yet dynamic, type of interaction, the duration of which was influenced by the presence or absence of a strong hydrodynamic flow as well as colliding red blood cells. Given the *in vivo* dynamic conditions within a blood vessel, it seems unlikely that *T. carassii* would establish stable interactions that involve large portions of the trypanosome cell surface, as for example described *in vitro* for *T. congolense*. We were unable to determine whether the anchoring area of *T. carassii* corresponds to the flagellum base, flagellar pocket neck or to the cell body membrane. Nevertheless, since *T. carassii* adherence to red blood cells and to glass surfaces was also observed *in vitro,* it will be possible to investigate the adhesion mechanism at high resolution in the future.

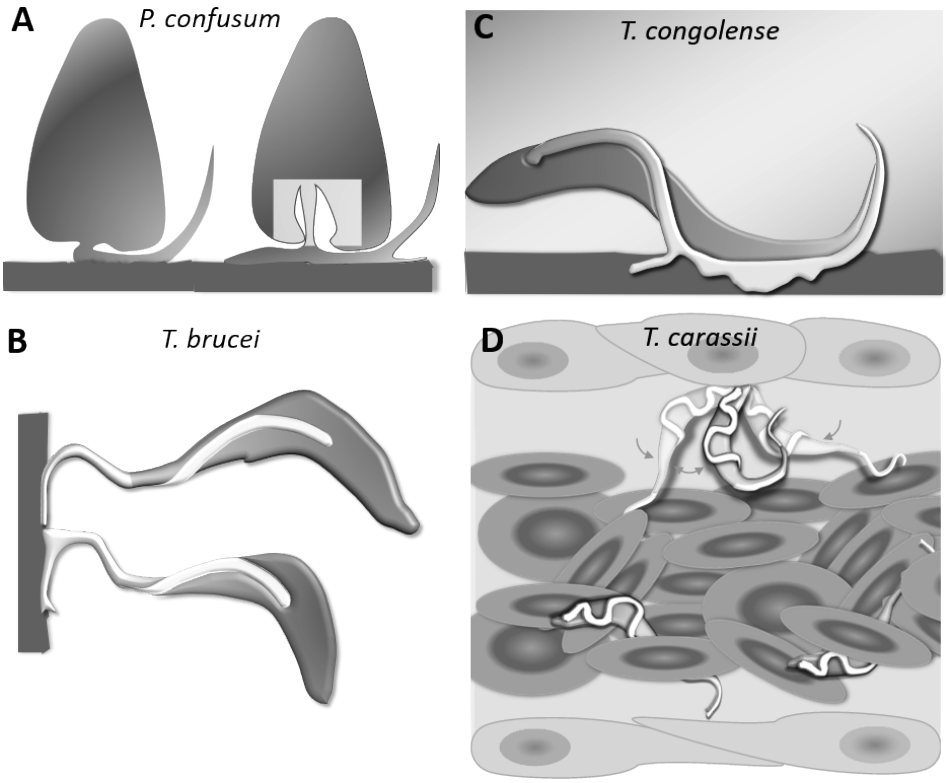

Fig 11: **Schematic drawing depicting the attachment of various trypanosome species.**
A) Haptomonads stages of *Paratrypanosoma confusum*: adhesion occurs through an attachment pad forming from the bulge at the base of the flagellum involving extensive remodelling of the flagellum membrane (based on: Skalický et al., 2017). The square indicates the location of the flagellar pocket. **B)** *T. brucei* epimastigotes attached through the flagellum to the brush border of the salivary gland epithelium (based on (Beattie and Gull, 1997; Schuster et al., 2017; Vickerman and Tetley, 1990). **C)** *T. congolense* adhesion to bovine aorta endothelial cell line *via* extensive membrane protrusions (filopodia) of the membrane-attached flagellum (based on (Beattie and Gull, 1997; Hemphill and Ross, 1995). **D)** *T. carassii* attached through the posterior end, leaving the cell body and flagellum free to move, as also shown in Fig 5.

In conclusion, we described for the first time the swimming behaviour of a trypanosome *in vivo* in the natural environment of a vertebrate host. We reported on the complex and heterogeneous environment in which the trypanosomes reside and how this highly influences the swimming behaviour. We describe how it is not possible to assign specific behaviours to trypanosomes swimming in any of the host compartments, as the trypanosomes were extremely effective in rapidly adapting their motion to the highly dynamic host environment. We describe backward swimming and a whip-like movements that allowed trypanosomes

to invert direction as well as identifying the posterior end as a novel anchoring site that allows the cell to adhere to host cells in a manner different from those described to date for other trypanosomes. Altogether, establishment of the *T. carassii* zebrafish infection model in combination with the genetic tractability of the zebrafish and of trypanosomes, represent a unique possibility to address questions related to: 1) trypanosome swimming behaviour *in vivo* in the natural environment of a vertebrate host, 2) host-pathogen interaction, 3) trypanosome biology, 4) the effect of specific immune factors on the progression of the infection, 5) the effect of drugs on both the trypanosome and the host and 6) immune evasion strategies of trypanosomes that do not present antigenic variation. For all these reasons, the *T. carassii*-zebrafish model holds the promise to become a valuable complementary model to those currently available, to study the complex biology of trypanosome and their interaction with the vertebrate host.

Acknowledgments

This work was supported by the FishForPharma FP7 People: Marie Curie Initial Training Network, project number PITN-GA-2011-289209 and the Dutch Research Council (NWO), project number 022.004.005. The authors wish to thank the CARUS-ARF Aquatic Research Facility of Wageningen University for fish rearing and husbandry.

References

Agüero F, Campo V, Cremona L, Jäger A, Di Noia JM, Overath P, Sánchez DO, Frasch AC. 2002. Gene discovery in the freshwater fish parasite Trypanosoma carassii: Identification of trans-sialidase-like and mucin-like genes. *Infect Immun* **70**:7140–7144. doi:10.1128/IAI.70.12.7140-7144.2002

Alizadehrad D, Krüger T, Engstler M, Stark H. 2015. Simulating the Complex Cell Design of Trypanosoma brucei and Its Motility. *PLoS Comput Biol* **11**:e1003967. doi:10.1371/journal.pcbi.1003967

Asnani A, Peterson RT. 2014. The zebrafish as a tool to identify novel therapies for human cardiovascular disease. *Dis Model Mech* **7**:763–767. doi:10.1242/dmm.016170

Bagchi P. 2007. Mesoscale simulation of blood flow in small vessels. *Biophys J*. doi:10.1529/biophysj.106.095042

Bargul JL, Jung J, McOdimba FA, Omogo CO, Adung'a VO, Krüger T, Masiga DK, Engstler M. 2016. Species-Specific Adaptations of Trypanosome Morphology and Motility to the Mammalian Host. *PLOS Pathog* **12**:e1005448. doi:10.1371/journal.ppat.1005448

Baron DM, Kabututu ZP, Hill KL. 2007. Stuck in reverse: loss of LC1 in Trypanosoma brucei disrupts outer dynein arms and leads to reverse flagellar beat and backward movement. *J Cell Sci* **120**:1513–20. doi:10.1242/jcs.004846

Beattie P, Gull K. 1997. Cytoskeletal architecture and components involved in the attachment of Trypanosoma congolense epimastigotes. *Parasitology* **115**:47–55. doi:10.1017/S0031182097001042

Benard EL, Racz PI, Rougeot J, Nezhinsky AE, Verbeek FJ, Spaink HP, Meijer AH. 2015. Macrophage-expressed perforins Mpeg1 and Mpeg1.2 have an anti-bacterial function in zebrafish. *J Innate Immun* **7**:136–152. doi:10.1159/000366103

Bertrand JY, Chi NC, Santoso B, Teng S, Stainier DYR, Traver D. 2010. Haematopoietic stem cells derive directly from aortic endothelium during development. *Nature* **464**:108–111. doi:10.1038/nature08738

Blackburn JS, Langenau DM. 2014. Zebrafish as a model to assess cancer heterogeneity, progression and relapse. *Dis Model Mech* **7**:755–762. doi:10.1242/dmm.015842

Branche C. 2006. Conserved and specific functions of axoneme components in trypanosome motility. *J Cell Sci* **119**:3443–3455. doi:10.1242/jcs.03078

Broadhead R, Dawe HR, Farr H, Griffiths S, Hart SR, Portman N, Shaw MK, Ginger ML, Gaskell SJ, McKean PG, Gull K. 2006. Flagellar motility is required for the viability of the bloodstream trypanosome. *Nature* **440**:224–227. doi:10.1038/nature04541

Burrell-saward H, Rodgers J, Bradley B, Croft SL, Ward TH. 2015. A sensitive and reproducible in vivo imaging mouse model for evaluation of drugs against late-stage human African trypanosomiasis. *J Antimicrob Chemother* **70**:510–517. doi:10.1093/jac/dku393

Capewell P, Cren-Travaillé C, Marchesi F, Johnston P, Clucas C, Benson RA, Gorman T-A, Calvo-Alvarez E, Crouzols A, Jouvion G, Jamonneau V, Weir W, Stevenson ML, O'Neill K, Cooper A, Swar NK, Bucheton B, Ngoyi DM, Garside P, Rotureau B, MacLeod A. 2016. The skin is a significant but overlooked anatomical reservoir for vector-borne African trypanosomes. *Elife* **5**:157–167. doi:10.7554/eLife.17716

Cronan MR, Tobin DM. 2014. Fit for consumption: zebrafish as a model for tuberculosis. *Dis Model Mech*. doi:10.1242/dmm.016089

Ellett F, Pase L, Hayman JW, Andrianopoulos A, Lieschke GJ. 2010. mpeg1 promoter transgenes direct macrophage-lineage expression in zebrafish. *Blood* **117**:e49–e56. doi:10.1182/blood-2010-10-314120

Engstler M, Pfohl T, Herminghaus S, Boshart M, Wiegertjes G, Heddergott N, Overath P. 2007. Hydrodynamic Flow-Mediated Protein Sorting on the Cell Surface of Trypanosomes. *Cell* **131**:505–515. doi:10.1016/j.cell.2007.08.046

Forlenza M, De Carvalho Dias JDA, Veselý T, Pokorová D, Savelkoul HFJ, Wiegertjes GF. 2008. Transcription of signal-3 cytokines, IL-12 and IFN alpha beta, coincides with the timing of CD8 alpha beta up-regulation during viral infection of common carp (Cyprinus carpio L). *Mol Immunol* **45**:1531–1547.

Forlenza M, Kaiser T, Savelkoul HFJ, Wiegertjes GF. 2012. The use of real-time quantitative PCR for the analysis of cytokine mRNA levels.Methods in Molecular Biology (Clifton, N.J.). pp. 7–23. doi:10.1007/978-1-61779-439-1_2

Forlenza M, Nakao M, Wibowo I, Joerink M, Arts JAJ, Savelkoul HFJ, Wiegertjes GF. 2009. Nitric oxide hinders antibody clearance from the surface of Trypanoplasma borreli and increases susceptibility to complement-mediated lysis. *Mol Immunol* **46**:3188–97. doi:10.1016/j.molimm.2009.08.011

Gibson W, Peacock L. 2019. Fluorescent proteins reveal what trypanosomes get up to inside the tsetse fly. *Parasit Vectors* **12**:6. doi:10.1186/s13071-018-3204-y

Goessling W, North TE. 2014. Repairing quite swimmingly: advances in regenerative medicine using zebrafish. *Dis Model Mech* **7**:769–776. doi:10.1242/dmm.016352

Goyard S, Dutra PL, Deolindo P, Autheman D, D'Archivio S, Minoprio P. 2014. In vivo imaging of trypanosomes for a better assessment of host-parasite relationships and drug efficacy. *Parasitol Int* **63**:260–268. doi:10.1016/j.parint.2013.07.011

Griffiths S, Portman N, Taylor PR, Gordon S, Ginger ML, Gull K. 2007. RNA interference mutant induction in vivo demonstrates the essential nature of trypanosome flagellar function during mammalian infection. *Eukaryot Cell*. doi:10.1128/EC.00110-07

Haag J, O'hUigin C, Overath P. 1998. The molecular phylogeny of trypanosomes: evidence for an early divergence of the Salivaria. *Mol Biochem Parasitol* **91**:37–49. doi:10.1016/S0166-6851(97)00185-0

Heddergott N, Krüger T, Babu SB, Wei A, Stellamanns E, Uppaluri S, Pfohl T, Stark H, Engstler M. 2012. Trypanosome Motion Represents an Adaptation to the Crowded Environment of the Vertebrate Bloodstream. *PLoS Pathog* **8**:e1003023. doi:10.1371/journal.ppat.1003023

Hemphill a, Ross C a. 1995. Flagellum-mediated adhesion of Trypanosoma congolense to bovine aorta endothelial cells. *Parasitol Res* **81**:412–20. doi:10.1007/BF00931503

Hemphill A, Frame I, Ross CA. 1994. The interaction of Trypanosoma congolense with endothelial cells. *Parasitology* **109 (Pt 5**:631–41.

Irnazarow I. 1995. Genetic variability of Polish and Hungarian carp lines. *Aquaculture* **129**:215. doi:10.1016/0044-8486(95)91961-T

Joerink M, Groeneveld A, Ducro B, Savelkoul HFJ, Wiegertjes GF. 2007. Mixed infection with Trypanoplasma borreli and Trypanosoma carassii induces protection: Involvement of cross-reactive antibodies. *Dev Comp Immunol* **31**:903–915. doi:10.1016/j.dci.2006.12.003

Krüger T, Engstler M. 2015. Flagellar motility in eukaryotic human parasites. *Semin Cell Dev Biol*. doi:10.1016/j.semcdb.2015.10.034

Langenau DM, Ferrando AA, Traver D, Kutok JL, Hezel J-PD, Kanki JP, Zon LI, Look AT, Trede NS, Alt FW, Travert D, Zont L 1. 2004. In vivo Tracking of T Cell Development, Ablation, and Engraftment in Transgenic In vivo tracking of T cell development, ablation, and engraftment in transgenic zebrafish. *Source Proc Natl Acad Sci United States Am* **101**:7369–7374.

Langousis G, Hill KL. 2014. Motility and more: the flagellum of Trypanosoma brucei. *Nat Rev Microbiol* **12**:505–18. doi:10.1038/nrmicro3274

Lawson ND, Weinstein BM. 2002. In vivo imaging of embryonic vascular development using transgenic zebrafish. *Dev Biol* **248**:307–318. doi:10.1006/dbio.2002.0711

Lom J, Dyková I. 1992. Protozoan Parasites of Fishes In: Lom J, Dyková I, editors. Developments in Aquaculture and Fisheries Science. Amsterdam: Elsevier. p. 33.

Mateus R, Pereira T, Sousa S, de Lima JE, Pascoal S, Saúde L, Jacinto A. 2012. In Vivo Cell and Tissue Dynamics Underlying Zebrafish Fin Fold Regeneration. *PLoS One* **7**:e51766. doi:10.1371/journal.pone.0051766

McLatchie AP, Burrell-Saward H, Myburgh E, Lewis MD, Ward TH, Mottram JC, Croft SL, Kelly JM, Taylor MC. 2013. Highly Sensitive In Vivo Imaging of Trypanosoma brucei Expressing "Red-Shifted" Luciferase. *PLoS Negl Trop Dis* **7**:e2571. doi:10.1371/journal.pntd.0002571

Miyares RL, de Rezende VB, Farber SA. 2014. Zebrafish yolk lipid processing: a tractable tool for the study of vertebrate lipid transport and metabolism. *Dis Model Mech* **7**:915–927. doi:10.1242/dmm.015800

Nguyen-Chi M, Phan QT, Gonzalez C, Dubremetz J-F, Levraud J-P, Lutfalla G. 2014. Transient infection of the zebrafish notochord with E. coli induces chronic inflammation. *Dis Model Mech* **7**:871–82. doi:10.1242/dmm.014498

Overath P, Haag J, Lischke A, O'HUigin C. 2001. The surface structure of trypanosomes in relation to their molecular phylogeny. *Int J Parasitol* **31**:468–471.

Overath P, Haag J, Mameza MG, Lischke A. 1999. Freshwater fish trypanosomes: Definition of two types, host control by antibodies and lack of antigenic variation, Parasitology. doi:10.1017/S0031182099005089

Overath P, Ruoff J, Stierhof YD, Haag J, Tichy H, Dyková I, Lom J. 1998. Cultivation of bloodstream forms of Trypanosoma carassii, a common parasite of freshwater fish. *Parasitol Res* **84**:343–347. doi:10.1007/s004360050408

Page DM, Wittamer V, Bertrand JY, Lewis KL, Pratt DN, Delgado N, Schale SE, McGue C, Jacobsen BH, Doty A, Pao Y, Yang H, Chi NC, Magor BG, Traver D. 2013. An evolutionarily conserved program of B-cell development and activation in zebrafish. *Blood* **122**:e1–e11. doi:10.1182/blood-2012-12-471029

Petrie-Hanson L, Hohn C, Hanson L. 2009. Characterization of rag1 mutant zebrafish leukocytes. *BMC Immunol* **10**:8. doi:10.1186/1471-2172-10-8

Phillips JB, Westerfield M. 2014. Zebrafish models in translational research: tipping the scales toward advancements in human health. *Dis Model Mech* **7**:739–743. doi:10.1242/dmm.015545

Ralston KS, Lerner AG, Diener DR, Hill KL. 2006. Flagellar motility contributes to cytokinesis in Trypanosoma brucei and is modulated by an evolutionarily conserved dynein regulatory system. *Eukaryot Cell*. doi:10.1128/EC.5.4.696-711.2006

Renshaw SA, Loynes CA, Trushell DMI, Elworthy S, Ingham PW, Whyte MKB. 2006. A transgenic zebrafish model of neutrophilic inflammation. *Blood* **108**:3976–3978. doi:10.1182/blood-2006-05-024075

Renshaw SA, Trede NS. 2012. A model 450 million years in the making: zebrafish and vertebrate immunity. *Dis Model Mech* **5**:38–47. doi:10.1242/dmm.007138

Schartl M. 2014. Beyond the zebrafish: diverse fish species for modeling human disease. *Dis Model Mech* **7**:181–92. doi:10.1242/dmm.012245

Schuster S, Krüger T, Subota I, Thusek S, Rotureau B, Beilhack A, Engstler M. 2017. Developmental adaptations of trypanosome motility to the tsetse fly host environments unravel a multifaceted in vivo microswimmer system. *Elife* **6**. doi:10.7554/eLife.27656

Shimogawa MM, Ray SS, Kisalu N, Zhang Y, Geng Q, Ozcan A, Hill KL. 2018. Parasite motility is critical for virulence of African trypanosomes. *Sci Rep* **8**:9122. doi:10.1038/s41598-018-27228-0

Simpson AGB, Stevens JR, Lukes J. 2006. The evolution and diversity of kinetoplastid flagellates. *Trends Parasitol* **22**:168–174.

Skalický T, Dobáková E, Wheeler RJ, Tesařová M, Flegontov P, Jirsová D, Votýpka J, Yurchenko V, Ayala FJ, Lukeš J. 2017. Extensive flagellar remodeling during the complex life cycle of Paratrypanosoma, an early-branching trypanosomatid. *Proc Natl Acad Sci U S A* **114**:11757–11762. doi:10.1073/pnas.1712311114

Stephen A. Renshaw, Catherine A. Loynes, Daniel M.I. Trushell, Stone Elworthy, Philip W. Ingham and MKBW. 2002. Atransgenic zebrafish model of neutrophilic inflammatio. *Blood* **99**:672–679. doi:10.1182/blood.V99.2.672

Stevens JR. 2008. Kinetoplastid phylogenetics, with special reference to the evolution of parasitic trypanosomes. *Parasite* **15**:226–232. doi:10.1051/parasite/2008153226

Sun SY, Kaelber JT, Chen M, Dong X, Nematbakhsh Y, Shi J, Dougherty M, Lim CT, Schmid MF, Chiu W, He CY. 2018. Flagellum couples cell shape to motility in Trypanosoma brucei. *Proc Natl Acad Sci U S A* **115**:E5916–E5925. doi:10.1073/pnas.1722618115

Sunter JD, Gull K. 2016. The Flagellum Attachment Zone: "The Cellular Ruler" of Trypanosome Morphology. *Trends Parasitol* **32**:309–324. doi:10.1016/j.pt.2015.12.010

Torraca V, Masud S, Spaink HP, Meijer AH. 2014. Macrophage-pathogen interactions in infectious diseases: new therapeutic insights from the zebrafish host model. *Dis Model Mech* **7**:785–797. doi:10.1242/dmm.015594

Veinotte CJ, Dellaire G, Berman JN. 2014. Hooking the big one: the potential of zebrafish xenotransplantation to reform cancer drug screening in the genomic era. *Dis Model Mech* **7**:745–754. doi:10.1242/dmm.015784

Vickerman K. 1969. ON THE SURFACE COAT AND FLAGELLAR ADHESION IN TRYPANOSOMES. *J Cell Sci* **5**:163.

Vickerman K, Tetley L. 1990. Flagellar Surfaces of Parasitic Protozoa and Their Role in Attachment In: Bloodgood RA, editor. Ciliary and Flagellar Membranes. Boston, MA: Springer US. pp. 267–304. doi:10.1007/978-1-4613-0515-6_11

Wakid MH, Bates PA. 2004. Flagellar attachment of Leishmania promastigotes to plastic film in vitro. *Exp Parasitol* **106**:173–178. doi:10.1016/j.exppara.2004.03.001

Wang R, Belosevic M. 1994. Cultivation of Trypanosoma danilewskyi (Laveran & Mesnil, 1904) in serum-free medium and assessment of the course of infection in goldfish, Carassius auratus (L.). *J Fish Dis* **17**:47–56. doi:10.1111/j.1365-2761.1994.tb00344.x

Wheeler RJ, Gluenz E, Gull K. 2013. The Limits on Trypanosomatid Morphological Diversity. *PLoS One* **8**:e79581. doi:10.1371/journal.pone.0079581

White RM, Sessa A, Burke C, Bowman T, LeBlanc J, Ceol C, Bourque C, Dovey M, Goessling W, Burns CE, Zon LI. 2008. Transparent Adult Zebrafish as a Tool for In Vivo Transplantation Analysis. *Cell Stem Cell*. doi:10.1016/j.stem.2007.11.002

Zon L, Cagan R. 2014. From fish tank to bedside in cancer therapy: an interview with Leonard Zon. *Dis Model Mech* **7**:735–8. doi:10.1242/dmm.016642

CHAPTER 3

Differential response of macrophages and neutrophils to trypanosome infections in zebrafish: occurrence of foamy macrophages

Sem H. Jacobs[1,2], Éva Dóró[1,*], Ffion R. Hammond[1,#], Marleen Scheer[1], Mai E. Nguyen- Chi[3], Georges Lutfalla[3], Geert F. Wiegertjes[1,4], Maria Forlenza[1]

[1] Cell Biology and Immunology Group, Department of Animal Sciences, Wageningen University & Research, Wageningen, The Netherlands
[2] Experimental Zoology Group, Department of Animal Sciences, Wageningen University & Research, Wageningen, The Netherlands
[3] DIMNP, CNRS, University of Montpellier, Montpellier, France
[4] Aquaculture and Fisheries Group, Department of Animal Sciences, Wageningen University & Research, Wageningen, The Netherlands
[*] current address: Institute of Physiology, Faculty of Medicine, University of Pécs, Pécs, Hungary
[#] current address: Department of Infection, Immunity & Cardiovascular Disease, University of Sheffield, Sheffield, United Kingdom

Manuscript submitted

Abstract

A tight regulation of the early innate immune response to trypanosome infections is critical to strike a balance between parasite control and inflammation-associated pathology. How the arms race between trypanosomes and their mammalian host exactly unfolds in the early phase of infection, is currently unknown. This is largely due to the inability to concomitantly visualise, *in vivo*, parasites, host cells and their activation state. We recently reported the establishment of a trypanosome infection model in larval zebrafish using the fish-specific *Trypanosoma carassii.* By combining the transparency of zebrafish larvae with high-resolution high-speed microscopy, we were able to reveal novel attachment mechanisms and adaptation strategies of trypanosomes *in vivo* in the natural environment of a vertebrate host. In the present work, we once again take advantage of the transparency of zebrafish larvae and of the availability of transgenic lines marking innate immune cells to study the *T. carassii* infection in a vertebrate host. We developed a clinical scoring system based on, among others, *in vivo* monitoring of parasitaemia that allowed us to consistently identify high- and low-infected individuals and to simultaneously characterize their differential innate response. Between high- and low-infected individuals, not only did macrophage and neutrophil number and distribution differ, but also macrophage morphology and activation state. Interestingly, exclusively in the cardinal caudal vein of high-infected fish, large granular macrophages rich in lipid droplets appeared. These were confirmed to be foamy macrophages characterized by a strong pro-inflammatory profile, assessed using *il1β* and *tnfa* transgenic zebrafish lines, and were associated with susceptibility to the infection. Altogether, our data provide an *in vivo* characterization of the differential response of innate immune cells to trypanosome infection and identify foamy macrophages as cells potentially associated with an exacerbated immune response. To our knowledge this is the first report of the occurrence of foamy macrophages during an extracellular trypanosome infection.

Introduction

Trypanosomes of the *Trypanosoma* genus are protozoan haemoflagellates that can infect animals from all vertebrate classes, including warm-blooded mammals and birds as well as cold-blooded amphibians, reptiles and fish. This genus contains human and animal pathogens all transmitted by biting flies, including the intracellular *Trypanosoma cruzi* (causing Human American Trypanosomiasis or Chagas' disease), *Leishmania species* (causing Leishmaniasis), the extracellular *T. brucei rhodesiense* and *T. brucei gambiense* (causing Human African Trypanosomiasis or Sleeping Sickness) and *T. congolense*, *T. vivax* and *T. b. brucei* (causing Animal African Trypanosomiasis or Nagana) (Radwanska et al., 2018; Simpson et al., 2006). Among these, salivarian trypanosomes such as *T. brucei* ssp. live extracellularly in the bloodstream or tissue fluids of their host. For example, *T. vivax* can multiply rapidly and is evenly distributed throughout the cardiovascular system, *T. congolense* tends to aggregate in small blood vessels, whereas *T. brucei* especially can extravasate and multiply in interstitial tissues (reviewed by Magez and Caljon, 2011). Pathologically, anaemia appears to be a factor common to infections with most if not all trypanosomes although with different underlying causative mechanisms. These include, among others, erythrophagocytosis by macrophages (Cnops et al., 2015; Guegan et al., 2013), hemodilution (Naessens, 2006), erythrolysis through intermembrane transfer of variant surface glycoprotein (VSG) from trypanosomes to erythrocytes (Rifkin and Landsberger, 1990), oxidative stress from free radicals (Mishra et al., 2017) and mechanical damage through direct interaction of trypanosomes with erythrocytes surface (Boada-Sucre et al., 2016).

Immunologically, infections with trypanosomes are often associated with dysfunction and pathology related to exacerbated innate and adaptive immune responses (reviewed by Radwanska et al., 2018; Stijlemans et al., 2016). Initially it was believed that antibody-dependent complement-mediated lysis was the major protective mechanisms involved in early parasite control (Krettli et al., 1979; Musoke and Barbet, 1977). However, later studies revealed that at low antibody levels, trypanosomes can efficiently remove surface-bound antibodies through an endocytosis-mediated mechanisms (Engstler et al., 2007), and that complement C5-deficient mice are able to control the first-peak parasitaemia similarly to wild type mice (La Greca et al., 2014). Instead, innate immune mediators such as IFNγ, TNFα and nitric oxide (NO) were shown to be indispensable for the control of first-peak parasitaemia, through direct and indirect mechanisms (reviewed by Radwanska et al., 2018). In the early phase of infection, the timely induction of IFNγ by NK, NKT and $CD8^+$ cells (Cnops et al., 2015) followed by the production of TNFα and NO by IFNγ-primed macrophages (Baral et al., 2007; Iraqi et al., 2001; Lopez et al., 2008; Lucas et al., 1994b; Magez et al., 1993, 2007, 2006, 2001, 1999; O'Gorman et al., 2006; Sternberg and Mabbott, 1996; Wu et al., 2017) leads to effective control of first-peak parasitaemia. Glycosyl-inositol-phosphate soluble variant surface glycoproteins (GPI-VSG) released from the surface of trypanosomes were

found to be the major inducers of TNFα in macrophages, and that such response could be primed by IFNγ (Coller et al., 2003; Magez et al., 2002). When macrophages would encounter GPI-VSG prior to IFNγ exposure however, their TNFα and NO response would dramatically be reduced (Coller et al., 2003) which, depending on the timing, could either lead to macrophage unresponsiveness or prevent exacerbated inflammatory responses during the first-peak of parasite clearance. Altogether, these data made clear that an early innate immune response is crucial to control the acute phase of trypanosome infection, but that its tight regulation is critical to ensure parasite control as opposed to pathology.

All aforementioned findings took advantage of the availability of several mice models for trypanosome infection using trypanosusceptible or trypanotolerant as well as mutant 'knock-out' mice strains. Although mice cannot be considered natural hosts of trypanosomes and do not always recapitulate all features of natural infections, the availability of such models allowed to gain tremendous insights into the general biology of trypanosomes, their interaction with and evasion of the host immune system, as well as into various aspects related to vaccine failure, antigenic variation, and (uncontrolled) inflammation (Magez and Caljon, 2011). The use of knock-out strains for example, shed specific light on the role of various cytokines, particularly TNFα, IFNγ and IL-10, in the control of parasitaemia and in the induction of pathological conditions during infection (reviewed in Magez and Caljon, 2011). It would be ideal to be able to follow, *in vivo*, the early host responses to the infection and visualise the trypanosome responses to the host's attack. However, due to the lack of transparency of most mammalian hosts, this has not yet been feasible.

We recently reported the establishment of an experimental trypanosome infection of zebrafish (*Danio rerio*) with the fish-specific trypanosome *Trypanosoma carassii* (Dóró et al., 2019, **Chapter 2**). In the latter study, by combining *T. carassii* infection of transparent zebrafish with high-resolution high-speed microscopy, we were able to describe in detail the swimming behaviour of trypanosomes *in vivo*, in the natural environment of blood and tissues of a live vertebrate host. This led to the discovery of novel attachment mechanisms as well as trypanosome's swimming behaviours that otherwise would not have been observed *in vitro* (Dóró et al., 2019). Previous studies in common carp (*Cyprinus carpio*), goldfish (*Carrassius aurata*) and more recently zebrafish, demonstrated that infections with *T. carassii* presents many of the pathological features observed during human or animal trypanosomiasis, including a pro-inflammatory response during first-peak parasitaemia (Kovacevic et al., 2015; Oladiran et al., 2011; Oladiran and Belosevic, 2009a) polyclonal B and T cell activation (Joerink et al., 2004, 2007; Lischke et al., 2000; Ribeiro et al., 2010; Woo and Ardelli, 2014) and anaemia (Dóró et al., 2019; Islam and Woo, 1991; McAllister et al., 2019). These shared features among human and animal (including fish) trypanosomiases suggest a commonality in (innate) immune responses to trypanosomes across different vertebrates.

Zebrafish are fresh water cyprinid fish closely related to many of the natural hosts of *T. carassii* (Kent et al., 2006; Simpson et al., 2006) and are a powerful model species owing to, among others, their genetic tractability, large number of transgenic lines marking several immune cell types, knock-out mutant lines and most importantly, the transparency of developing embryos allowing high-resolution *in vivo* visualisation of cell behaviour (Benard et al., 2015; Bertrand et al., 2010; Ellett et al., 2011; Langenau et al., 2004; Lawson and Weinstein, 2002; Page et al., 2013; Petrie-Hanson et al., 2009; Renshaw et al., 2006; White et al., 2008). During the first 2-3 weeks of development, zebrafish are devoid of mature T and B lymphocytes and thus offer a window of opportunity to study innate immune responses (Torraca et al., 2014; Torraca and Mostowy, 2018), especially those driven by neutrophils and macrophages. The response of macrophages and neutrophilic granulocytes towards several viral, fungal and bacterial pathogens has been studied in detail using zebrafish (Cronan and Tobin, 2014; García-Valtanen et al., 2017; Nguyen-Chi et al., 2014; Palha et al., 2013; Ramakrishnan, 2013; Renshaw and Trede, 2012; Rosowski et al., 2018; Torraca and Mostowy, 2018), but never before in the context of trypanosome infections.

Taking advantage of the recently established zebrafish-*T. carassii* infection model and of the availability of zebrafish transgenic lines marking macrophages and neutrophils as well as *il1b*- and *tnfa*-expressing cells, in the current study, we describe the early events of the innate immune response of zebrafish to *T. carassii* infections. Based on a novel clinical scoring system relying, amongst other criteria, on *in vivo* real-time monitoring of parasitaemia, we could consistently segregate larvae in high- and low-infected individuals without having to sacrifice the larvae. Between these individuals we always observed a marked differential response between macrophages and neutrophils, especially with respect to their proliferative capacity and redistribution in tissues or major blood vessels during infection. Significant differences were observed in the inflammatory response of macrophages in high- and low-infected individuals and in their susceptibility to the infection. In low-infected individuals, despite an early increase in macrophage number, a mild inflammatory response strongly associated with control of parasitaemia and survival to the infection was observed. Conversely, exclusively in the cardinal caudal vein of high-infected individuals, we describe the occurrence of large, granular macrophages, reminiscent of foamy macrophages (Vallochi et al., 2018), characterized by a strong inflammatory profile and association to susceptibility to the infection. This is the first report of the occurrence of foamy macrophages during an extracellular trypanosome infection.

Materials and methods

Zebrafish lines and maintenance

Zebrafish were kept and handled according to the Zebrafish Book (zfin.org) and local animal welfare regulations of The Netherlands. Zebrafish embryo and larvae were raised in egg water (0.6 g/L sea salt, Sera Marin, Heinsberg, Germany) at 27°C with a 12:12 light-dark cycle. From 5 days post fertilisation (dpf) until 14 dpf larvae were fed Tetrahymena once a day. From 10 dpf larvae were also daily fed dry food ZM-100 (ZM systems, UK). The following zebrafish lines used in this study: transgenic *Tg(mpx:GFP)*^{i114} (Renshaw et al., 2006), *Tg(kdrl:hras-mCherry)*^{s896} *referred as Tg(kdrl:caax-mCherry)* (Chi et al., 2008), *Tg(fli1:eGFP)*^{y1} (Lawson and Weinstein, 2002), *Tg(mpeg1:eGFP)*^{gl22}, (Ellett et al., 2011), *Tg(mpeg1.4:mCherry-F)*^{ump2Tg}, *Tg*(*il1b:eGFP-F)*^{ump3Tg}, (Nguyen-Chi et al., 2014), *Tg(tnfa:eGFP-F)*^{ump5Tg} (Nguyen-Chi et al., 2015) or crosses thereof. The latter three transgenic zebrafish lines express a farnesylated (membrane-bound) mCherry (mCherry-F) or eGFP (eGFP-F) under the control of the *mpeg1, il1b* or *tnfa* promoter, respectively.

Trypanosoma carassii culture and infection of zebrafish larvae

Trypanosoma carassii (strain TsCc-NEM) was cloned and characterized previously (Overath et al., 1998) and maintained in our laboratory by syringe passage through common carp (*Cyprinus carpio*) as described previously (Dóró et al., 2019, **Chapter 2**). Blood was drawn from infected carp and kept at 4°C overnight in siliconized tubes. Trypanosomes enriched at the interface between the red blood cells and plasma were collected and centrifuged at 800xg for 8 minutes at room temperature. Trypanosomes were resuspended at a density of 5 x 10^5-1 x 10^6 ml and cultured in 75 or 165 cm^2 flasks at 27°C without CO_2 in complete medium as described previously (Dóró et al., 2019, **Chapter 2**). *T. carassii* were kept at a density below 5 x 10^6/ml, and sub-cultured 1-3 times a week. In this way *T. carassii* could be kept in culture without losing infectivity for up to 2 months. The carp white blood cells eventually present in the enriched trypanosome fraction immediately after isolation, died within the first 3-5 days of culture and were removed prior to *T. carassii* injection into zebrafish. Cells were centrifuged at 800xg for 5 minutes in a 50 ml Falcon tube and the tube was subsequently tilted in a 20^0 angle in relation to the table surface, facilitating the separation of the motile trypanosomes along the conical part of the tube from the static pellet of white blood cells at the bottom of the tube.

For zebrafish infection, trypanosomes were cultured for 1 week and no longer than 3 weeks. Infection of zebrafish larvae was performed as described previously (Dóró et al., 2019, **Chapter 2**). Briefly, prior to injection, 5 days post fertilization (dpf) zebrafish larvae were anaesthetized with 0.017% Ethyl 3-aminobenzoate methanesulfonate (MS-222, Tricaine, Sigma-Aldrich) in egg water. *T. carassii* parasites were resuspended in 2% polyvinylpyrrolidone (PVP, Sigma-Aldrich) and injected (n=200) intravenously in the Duct of Cuvier.

Clinical scoring system of the severity of infection

Careful monitoring of the swimming behaviour of zebrafish larvae after infection (5 dpf onwards) as well as *in vivo* observation of parasitaemia development in transparent larvae, led to the observation that larvae could generally be segregated into high- and low-infected individuals from 4 days post infection (dpi) onwards. To objectively assign zebrafish to either one of these two groups, we developed a clinical scoring system (**Fig 1**). The first criterion looked at the escape reflex upon contact with a pipette and was sufficient to identify high-infected individuals as those not reacting to the pipet (slow swimmers). To categorize the remaining individuals, an infection score based on counting parasite:blood cell ratios in 100 events passing through the intersegmental capillary (ISC) above the cloaca was developed. The infection scores on a scale from 1 to 10 were assigned as follows: 1=no parasites observed, 2=1-10% parasite, 3=11-20% parasite, 4=21-30% parasite, 5=31-40% parasite, 6=41-55% parasite, 7=56-70% parasite, 8=71-85% parasite, 9=86-99%, 10=no blood cells observed. Larvae with infection scores between 1-3 were categorized as low-infected while scores between 6-10 were categorized as high infected. Larvae with scores 4-5 were reassessed 1 day later, at 5 dpi, and then categorised as high- or low-infected. Next to that, the swimming behaviour of larvae was observed and compared to the control group. Heartbeat of the larvae was monitored and noted if it was slower than the control. The diameter of the cardinal caudal vein in the trunk area after the cloaca region was measured in ImageJ (version 1.49o) to quantify the degree of vasodilation. Eventual blockage of tail tip vessel-loop was also noted. Extravasation and the location of extravasated parasites (e.g. fins, muscle, intraperitoneal cavity, and interstitial space lining the blood vessels) was recorded.

Real-time quantitative PCR

Zebrafish were sacrificed by an overdose of MS-222 anaesthetic (50 mg/L). At each time point 3-6 zebrafish larvae were sacrificed and pooled. Pools were transferred to RNA later (Ambion), kept at 4°C overnight and then transferred to -20°C for further storage. Total RNA isolation was performed with the Qiagen RNeasy Micro Kit (QIAgen, Venlo, The Netherlands) according to manufacturer's protocol. Next, 250-500 ng total RNA was used as template for cDNA synthesis using SuperScript III Reverse Transcriptase and random hexamers (Invitrogen, Carlsbad, CA, USA), following the manufacturer's instructions with an additional DNase step using DNase I Amplification Grade (Invitrogen, Carlsbad, CA, USA). cDNA was then diluted 25 times to serve as template for real-time quantitative PCR (RT-qPCR) using Rotor-Gene 6000 (Corbett Research, QIAgen), as previously described (Forlenza et al., 2012). Primers (**Table 1**) were obtained from Eurogentec (Liège, Belgium). Gene expression was normalized to the expression of *elongation factor-1 alpha* (*ef1a*) housekeeping gene and expressed relative to the PVP control at the same time point or to 0 days post injection (dpi) time point.

Table 1. List of primers used in this study

Gene name	Fw primer 5'-3'
ef1a	CTGGAGGCCAGCTCAAACAT
T. car. hsp70	CAGCCGGTGGAGCGCGT
il-1β	TTGTGGGAGACAGACAGTGC
il10_1	ACTTGGAGACCATTCTGCC
tnfa_1	AAGTGCTTATGAGCCATGC
tnfb	AAACAACAAATCACCACACC
il6_1	ACTCCTCTCCTCAAACCT
arg 2	GGTGGGAGCAGGACACAC

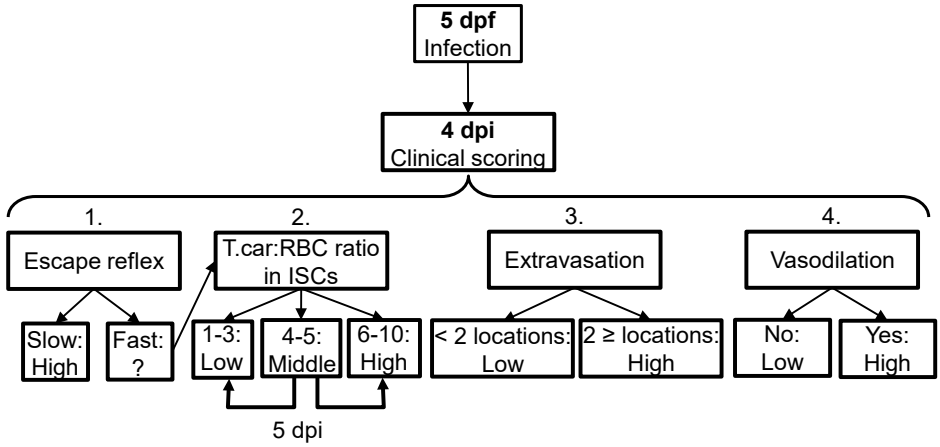

Fig 1. Schematic overview of clinical scoring system to determine individual infection levels of *T. carassii*-infected zebrafish larvae.

Zebrafish larvae infected with *T. carassii* can be analysed at 4 dpi, and based on up to 4 different parameters including visual monitoring of larval behaviour, parasite numbers, location or vasodilation, larvae could be segregated into high- and low-infected individuals. See details in the text in the corresponding Materials & Methods section.

In vivo imaging and videography of zebrafish

Prior to imaging, zebrafish larvae were anaesthetised with 0.017% MS-222 (Sigma-Aldrich). For total fluorescence acquisition, double transgenic *Tg(mpeg1.4:mCherry-F;mpx:GFP)* were positioned on preheated flat agar plates (1% agar in egg water with 0.017% MS-222) and imaged with Fluorescence Stereo Microscope (Leica M205 FA). The image acquisition settings were as following: Zoom: 2.0 - 2.2, Gain: 1, Exposure time (ms): 70 (BF)/700 (GFP)/1500 (mCherry), Intensity: 60 (BF)/700 (GFP)/700 (mCherry), Contrast: 255/255 (BF)/ 70/255 (GFP)/ 15/255 (mCherry).

RV primer 5'-3'	Acc. number (zfin.org)
ATCAAGAAGAGTAGTAGTACCG	ZDB-GENE-990415-52
AGTTCCTTGCCGCCGAAGA	FJ970030.1 (GeneBank)
GATTGGGGTTTGATGTGCTT	ZDB-GENE-040702-2
CACCATATCCCGCTTGAGTT	ZDB-GENE-051111-1
CTGTGCCCAGTCTGTCTC	ZDB-GENE-050317-1
ACACAAAGTAAAGACCATCC	ZDB-GENE-050601-2
CATCTCTCCGTCTCTCAC	ZDB-GENE-120509-1
TGTCCCGCATGGAGAAGTACT	ZDB-GENE-030131-1334

Alternatively, anaesthetised larvae were embedded in UltraPure LMP Agarose (Invitrogen) and positioned on the coverglass of a 35 mm petri dish, (14 mm microwell, coverglass No. 0 (0.085-0.13mm), MatTek corporation) prior to imaging. A Roper Spinning Disk Confocal (Yokogawa) on Nikon Ti Eclipse microscope with 13x13 Photometrics Evolve camera (512 x 512 Pixels 16 x 16 micron) equipped with a 40x (1.30 NA, 0.24 mm WD) OI objective, was used with the following settings: GFP excitation: 491nm, emission: 496-560nm, digitizer: 200 MHz (12-bit); 561 BP excitation: 561nm; emission: 570-620nm, digitizer: 200 MHz (12-bit); BF: digitizer: 200 MHz (12-bit). Z-stacks of 1 or 0.5 µm. An Andor-Revolution Spinning Disk Confocal (Yokogawa) on a Nikon Ti Eclipse microscope with Andor iXon888 camera (1024 x 1024 Pixels 13 x 13 micron) equipped with 40x (0.75 NA, 0.66 mm WD) objective, 40x (1.15 NA, 0.61-0.59 mm WD) WI objective, 20x (0.75 NA, 1.0 mm WD) objective and 10x (0.50 NA, 16 mm WD) objective was used with the following settings: Dual pass 523/561: GFP excitation: 488nm, emission: 510-540nm, EM gain: 20-300ms, digitizer: 10 MHz (14-bit); RFP excitation: 561nm; emission: 589-628nm, EM gain: 20-300ms, digitizer: 10 MHz (14-bit); BF DIC EM gain: 20-300ms, digitizer: 10 MHz (14-bit). Z-stacks of 1 µm. Images were analysed with ImageJ-Fiji (version 1.52p).

High-speed videography of *T. carassii* swimming behaviour *in vivo* was performed as described previously (Dóró et al., 2019, **Chapter 2**). Briefly, the high-speed camera was mounted on a DMi8 inverted digital microscope (Leica Microsystems), controlled by Leica LASX software (version 3.4.2.) and equipped with 40x (NA 0.6) and 20x (NA 0.4) long distance objectives (Leica Microsystems). For high-speed light microscopy a (8 bits) EoSens MC1362 (Mikrotron GmbH, resolution 1280 x 1024 pixels), with Leica HC 1x Microscope C-mount Camera Adapter, was used, controlled by XCAP-Std software (version 3.8, EPIX inc.). Images were acquired at a resolution of 900 x 900 or 640 x 640 pixels. Zebrafish larvae were anaesthetised with 0.017% MS-222 and embedded in UltraPure LMP Agarose (Invitrogen) on a microscope slide (1.4-1.6 mm) with a well depth of 0.5-0.8 mm (Electron Microscopy Sciences). Upon solidification of the agarose, the specimen was covered with

3-4 drops of egg water containing 0.017% MS-222, by a 24 x 50 mm coverslip and imaged immediately. For all high-speed videography, image series were acquired at 480–500 frames per second (fps) and analysed using a PFV software (version 3.2.8.2) or MiDAS Player v5.0.0.3 (Xcite, USA).

Fluorescence quantification

Quantification of total cell fluorescence in zebrafish larvae was performed in ImageJ (version 1.49o) using the free-form selection tool and by accurately selecting the larvae area. Owing to the high auto-fluorescence of the gut or gut content, and large individual variation, the gut area was excluded from the total fluorescence signal. Area integrated intensity and mean grey values of each selected larva were measured by the software. To correct for the background, three consistent black areas were selected in each image. Analysis was performed using the following formula: corrected total cell fluorescence (CTCF) = Integrated density – (Area X Mean background value).

EdU proliferation assay and immunohistochemistry

iCLICK™ EdU (5- ethynyl-2'- deoxyuridine, component A) from ANDY FLUOR 555 Imaging Kit (ABP Biosciences) at a stock concentration of 10 mM, was diluted in PVP to 1.13 mM. Infected *Tg(mpeg1:eGFP)* or *Tg(mpx:GFP)* larvae were injected in the heart cavity at 3 dpi (8dpf) with 2 nl of solution, separated in high- and low-infected individuals at 4 dpi and euthanized 6-8 hours later (30-32h after EdU injection) with an overdose of anaesthetic (0.4% MS-222 in egg water). Following fixation in 4% paraformaldehyde (PFA, Thermo Scientific) in PBS, o/n at 4°C, larvae were washed three times in buffer A (0.1% (v/v) tween-20, 0.05% (w/v) azide in PBS), followed by dehydration: 50% MeOH in PBS, 80% MeOH in H_20 and 100% MeOH, for 15 min each, at room temperature (RT), with gentle agitation. To remove background pigmentation, larvae were incubated in bleach solution (5% (v/v) H_2O_2 and 20% (v/v) DMSO in MeOH) for 1hr at 4°C, followed by rehydration: 100% MeOH, 80% MeOH in H2O, 50% MeOH in PBS for 15 min each, at room temperature (RT), with gentle agitation. Next, larvae were incubated three times for 5 minutes each in buffer B (0.2%(v/v) triton-x100, 0.05% azide in PBS) at RT with gentle agitation followed by incubation in EdU iCLICK™ development solution for 30 min at RT in the dark and three rapid washes with buffer B.

The described EdU development led to loss of GFP signal in the transgenic zebrafish. Therefore, to retrieve the position of neutrophils or macrophages, wholemount immunohistochemistry was performed. Larvae were blocked in 0.2% triton-x100, 10% DMSO, 6% (v/v) normal goat serum and 0.05% azide in PBS, for 3 hrs, at RT with gentle agitation. Next, the primary antibody Chicken anti-GFP (Aves labs.Inc., 1:500) in Antibody buffer (0.2% tween-20, 0.1% heparin, 10% DMSO, 3% normal goat serum and 0.05% azide in PBS) was added and incubated overnight (o/n) at 37°C. After three rapid and three 5 minutes washes in buffer C (0.1% tween-20, 0.1% (v/v) heparin in PBS), at RT with gentle

agitation, the secondary antibody goat anti-chicken-Alexa 488 (Abcam, 1:500) was added in Antibody buffer and incubated o/n at 37°C. After three rapid and three 5 minutes washes in buffer C, at RT with gentle agitation, larvae were imaged with Andor Spinning Disk Confocal Microscope.

BODIPY injection

BODIPY™ FL pentanoic acid (BODIPY-FL5, Invitrogen) was diluted in DMSO to a 3 mM stock solution. Stock solution was diluted 100x (30 µM) with PVP. Infected larvae 3 dpi (8 dpf) were injected with 1 nl of the solution i.p. (heart cavity) and imaged 18-20 hours later.

Statistical analysis

Analysis of gene expression and total fluorescence data were performed in GraphPad PRISM 5. Statistical analysis of gene expression data was performed on Log(2) transformed values followed by One-way ANOVA and Dunnett's multiple comparisons test. Analysis of Corrected Total Cell Fluorescence was performed on Log(10) transformed values followed by Two-way ANOVA and Bonferroni multiple comparisons post-hoc test. Analysis of EdU^+ macrophages was performed on Log(10) transformed values followed by One-way ANOVA and Bonferroni multiple comparisons post-hoc test. In all cases, $p<0.05$ was considered significant.

Results

Susceptibility of zebrafish larvae to *T. carassii* infection

We recently reported the establishment of a trypanosome infection in zebrafish larvae using a natural fish parasite, *Trypanosoma carassii* (Dóró et al., 2019, **Chapter 2**). To further investigate the immune response to *T. carassii* infection, we first investigated the kinetics of susceptibility of zebrafish larvae as well as the kinetics of expression of various immune-related genes. Similar to what was previously reported, *T. carassii* infection of 5 dpf zebrafish larvae leads to approximately 10-20% survival by 15 days post infection (dpi) with the highest incidence of mortality between 4 and 7dpi (**Fig 2A**). The onset of mortality coincided with the peak of parasitaemia as assessed by real-time quantitative gene expression analysis of a *T. carassii*-specific gene (**Fig 2B**). A preliminary gene expression analysis of a panel of immune-related genes, did not reveal a specific response triggered by the infection. Except for a mild upregulation of *il6*, other prototypical pro-inflammatory genes including *tnfa, tnfb* and *il1b* and regulatory molecules such as *il10* or *arginase*, were not significantly regulated by the infection (**Supplementary Fig 1**). As the analysis was performed on pools of whole larvae, this may have obscured tissue-specific responses. Furthermore, although up to 5 larvae were pooled at each sampling point and up to 3 pools were analysed at each time point, a large variation in the response was observed. Nevertheless, we consistently observed 10-

20% survival in the *T. carassii*-infected group, suggesting that zebrafish larvae can control *T. carassii* infection. This observation prompted us to investigate the kinetics of parasitaemia and development of (innate) immune responses at the individual level.

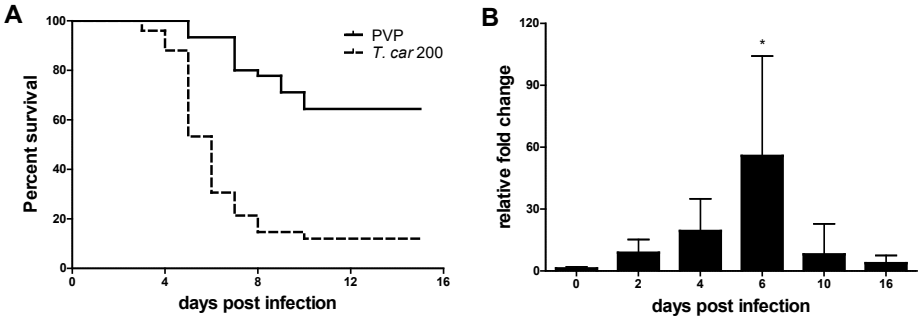

Fig 2. *T. carassii* infection of larval zebrafish.
A) *Tg(mpeg1.4:mCherry-F;mpx:GFP)* larvae (5 dpf) were injected intravenously with *n*=200 *T. carassii*/fish or with PVP as control and survival was monitored over a period of 15 days. **B)** *Tg(mpeg1.4:mCherry-F;mpx:GFP)* zebrafish (5 dpf) were treated as in A and sampled at various time points. At each time point, 3-6 pools of 3-5 larvae were sampled for real-time quantitative PCR analysis. Relative fold change of the *T. carassii*-specific *heat-shock protein-70* (*hsp70*) was normalised to the zebrafish-specific *ef1α* and expressed relative to the parasite injected group at time point 0h. Bars indicate average and standard deviation (SD) on n=3-6 pools per time point.

Clinical signs of *T. carassii* infection and clinical scoring system

To characterize the response to *T. carassii* infection in individual zebrafish larvae, we developed a clinical scoring system to determine individual infection levels, enabling us to group together individual larvae based on severity of infection. From 4 dpi onwards, we could consistently sort larvae into groups of high- or low-infected individuals based on *in vivo* observations, without the need to sacrifice animals (**Supplementary Video 1**). Infection levels were categorised using four criteria: 1) escape reflex (slow vs fast) upon contact with a pipette tip, 2) infection scores (1-10, see details in Materials and Methods), based on the ratio of blood cells and parasites passing through an intersegmental capillary (ISC) in 100 events (**Fig 3A** and **3B**) (**Supplementary Video 1,** 00:06-00:39 sec), 3) extravasation, based on the presence of parasites outside of blood vessels (**Fig 3C**) (**Supplementary Video 1,** 00:40-1:20 sec) and 4) vasodilation, based on the diameter of the cardinal caudal vein (**Fig 3D** and **3E**). The first criterion defined all individuals with a minimal escape reflex (slow swimmers) as high-infected individuals: they were mostly located at the bottom of the tank and showed minimal reaction upon direct contact with a pipette. Larvae with a normal escape reflex (fast swimmers) however, were not exclusively low-infected individuals. Therefore, a second

criterion was used based on trypanosome counting in ISC (**Supplementary Video 1,** 00:06-00:39 sec). Individuals with an infection score between 1-3 were categorized as low-infected and always survived the infection (see Materials and Methods). Individuals with an infection score between 6-10 were categorized as high-infected and generally succumbed to the infection. Individuals with an intermediate score (4-5) could go both ways: they either showed a delayed parasitaemia and later developed high parasitaemia (common) or recovered from the infection (rare). The third criterion clearly identified high-infected individuals as those showing extensive extravasation at two or more of the following locations: peritoneal cavity (**Fig 3C**) (**Supplementary Video 1**, 00:40-00:59 sec), interstitial space lining the blood vessels, muscle tissue (**Supplementary Video 1**, 01:00-01:07 sec) or fins (**Supplementary Video 1**, 01:08-01:20 sec), in particular the anal fin. At these locations, in high-infected individuals, trypanosomes could accumulate in high numbers, filling up all available spaces. Extravasation however could also occur in low-infected individuals, but to a lesser extent. The fourth criterion, vasodilation of the cardinal caudal vein associated with high numbers of trypanosomes in the blood vessels, was a definitive sign of high infection level, and never occurred in low-infected larvae. To validate our scoring system, expression of a *T. carassii*-specific gene was analysed in pools of larvae classified as high- or low-infected. As expected, in individuals categorized as high-infected, *T. carassii*-specific gene expression increased more than 60-fold whereas in low-infected individuals the increase was less than 20-fold (**Fig 3F**). Altogether these data show that *T. carassii* infects zebrafish larvae, but that the infection can develop differently among individuals, leading to different outcomes. The clinical scoring system based on numerous criteria is suitable to reliably separate high- and low-infected larvae to further investigate individual immune responses.

***T. carassii* infection induces a strong macrophage response in zebrafish larvae**

After having established a method to determine infection levels in each larva, we next investigated whether a differential innate immune response would be mounted in high- and low-infected fish. To this end, using double-transgenic *Tg(mpeg1.4:mCh-F;mpx:GFP)* zebrafish, we first analysed macrophage and neutrophil responses in whole larvae by quantifying total cell fluorescence in high- and low-infected individuals (**Fig 4**). Total neutrophil response (total green fluorescence) was not significantly affected by the infection (**Fig 4A** and **4C**). In contrast, the macrophage response (total red fluorescence) increased significantly in infected individuals from 3 dpi onwards, and was most prominent in the head region and along the cardinal caudal vein (**Fig 4B**). In low-infected larvae, a significant increase in red fluorescence was observed already by 5 dpi and remained high up until 9 dpi; in high-infected larvae, despite a marginal but not significant increase at 5 and 7 dpi, significant differences were observed at day 9 after infection (**Fig 4C**). Interestingly, no significant differences were observed between high- or low-infected individuals, suggesting that despite the differences in trypanosome levels (**Fig 3F**), macrophages respond to the presence and not to the number of trypanosomes.

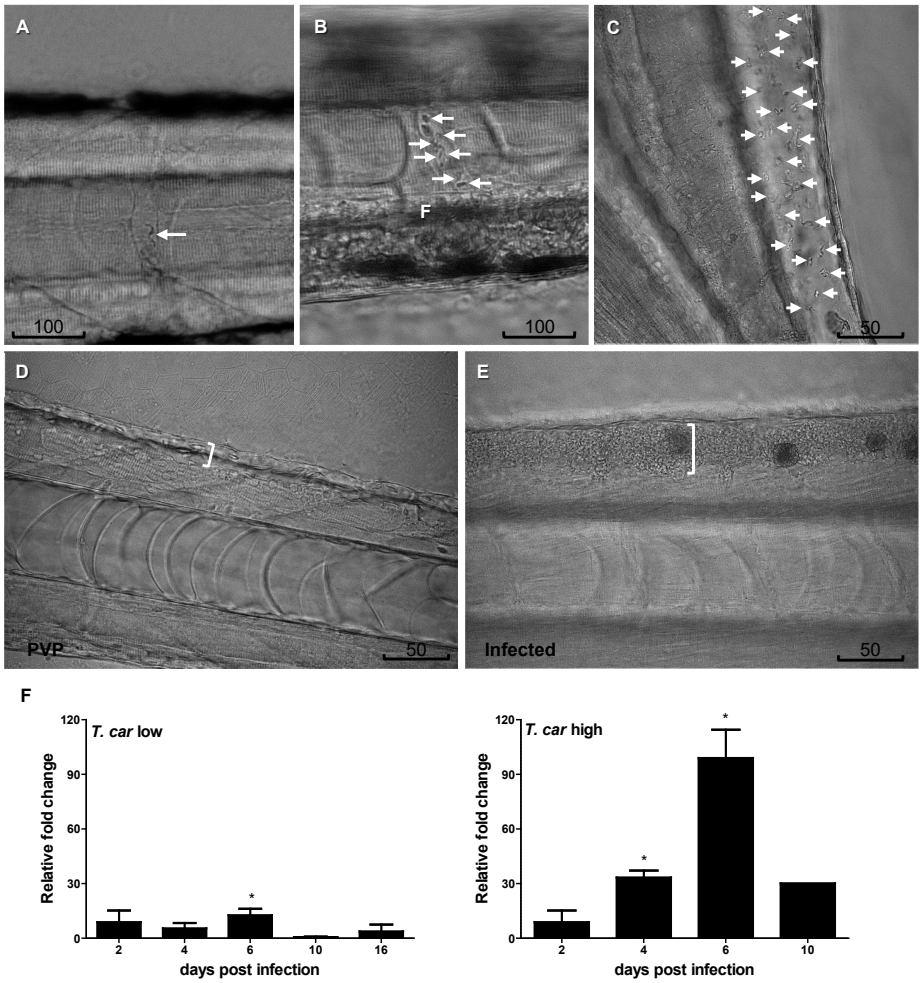

Fig 3. Progression of *T. carassii* infection in zebrafish larvae.

Tg(mpeg1.4:mCherry-F;mpx:GFP) 5 dpf zebrafish were injected with *n*=200 *T. carassii* or with PVP and imaged at 2 dpi (**A**), 5 dpi (**B-C**), 7 dpi (**D-E**) or sampled at various time points after infection (**F**). Shown are representative images of intersegmental capillaries (ISC) containing various number of *T. carassii* (white arrows) (**A-B**); extravasated *T. carassii* (only some indicated with white arrows) in the intraperitoneal cavity (**C**); cardinal caudal vein diameter in PVP (**D**) or in *T. carassii*-infected larvae (**E**). Square brackets indicate the diameter of the cardinal caudal vein. Frames are extracted from high-speed videos acquired with a Leica DMi8 inverted microscope at a 40x magnification. **F)** *T. carassii* infection level. High- and low-infected individuals were separated from 4 dpi onwards based on our clinical scoring criteria. At each time point, 3 pools of 3-5 larvae were sampled for subsequent real-time quantitative gene expression analysis. Each data point represents the mean of 3 pools, except for the high-infected group at 10 dpi where only one pool could be made due to low survival. Relative fold change of the *hsp70* was normalised relative to the zebrafish-specific *ef1a* housekeeping gene and expressed relative to the trypanosome-injected group at time point 0h.

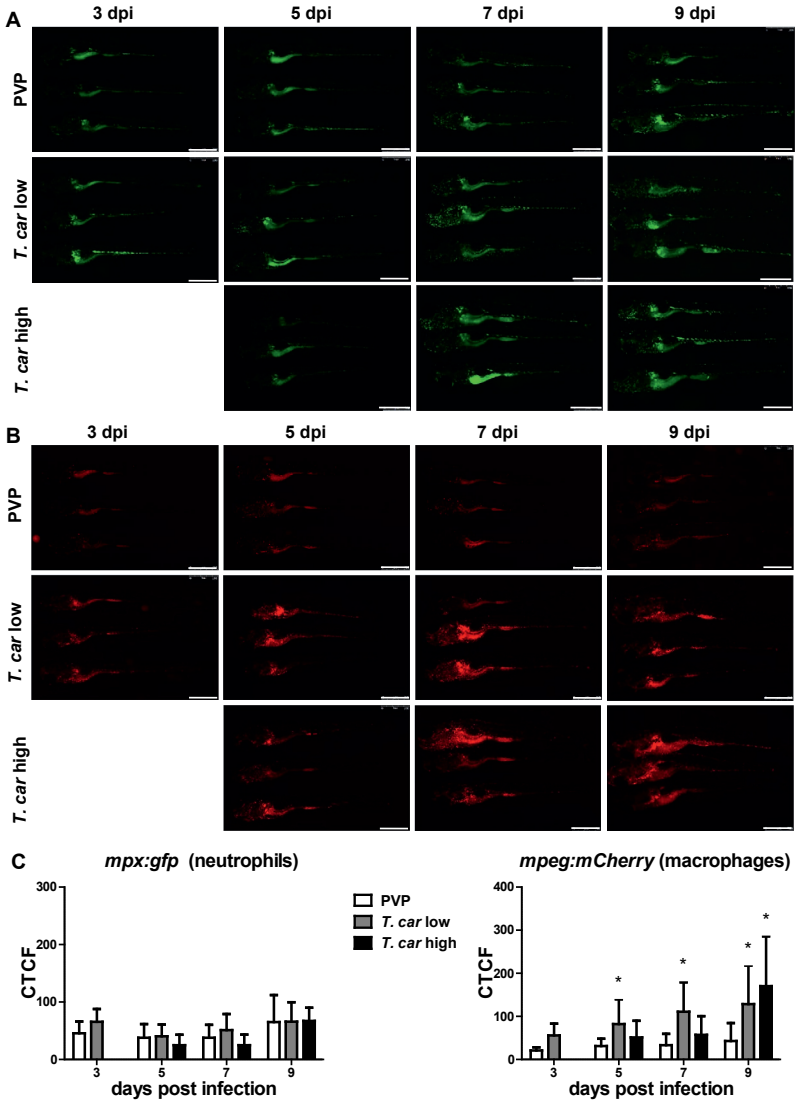

Fig 4. Macrophages respond more prominently than neutrophils to *T. carassii* infection. *Tg(mpeg1.4:mCherry-F;mpx:GFP)* were injected intravenously at 5 dpf with *n*=200 *T. carassii* or with PVP. At 4 dpi larvae were separated in high- and low-infected individuals. **A-B)** At the indicated time points, images were acquired with Leica M205FA Fluorescence Stereo Microscope with 1.79x zoom. Images are representatives of n=3-44 larvae per group, depending on the number of high- or low-infected larvae categorized at each time point. Scale bar indicates 750 µm. **C)** Corrected Total Cell Fluorescence (CTCF) quantification of infected and non-infected larvae. Bars represent average and standard deviation of red and green fluorescence in n=5-44 whole larvae, from 2 independent experiments. * indicates significant differences ($P<0.05$) to the respective PVP control as assessed by Two-Way ANOVA followed by Bonferroni post-hoc test.

***T. carassii* infection promotes macrophage and neutrophil proliferation**

The increase in overall red fluorescence can be indicative of activation of the *mpeg* promotor driving mCherry expression, but also of macrophage proliferation. To address the latter hypothesis, *Tg(mpeg1:eGFP)* or *Tg(mpx:GFP*) zebrafish larvae were infected with *T. carassii*, and subsequently injected with iCLICK™ EdU for identification of proliferating cells. With respect to proliferation, developing larvae display a generalized high rate of cell division throughout the body that increases overtime particularly in hematopoietic organs such as the thymus or the head kidney. Thus, for a more sensitive quantification of the proliferative response of macrophages and neutrophils in response to the infection, EdU was injected at 3 dpi (8 dpf), and at 4 dpi, larvae were separated in high- and low-infected individuals, followed by fixation and whole mount immunohistochemistry 6-8h later (30-32h after EdU injection). This allowed evaluating the macrophage and neutrophil response right at the onset of the macrophage response observed in **Fig 4C** and concomitantly with the development of differences in parasitaemia. As expected, EdU^+ nuclei could be identified throughout the body of developing larvae. When specifically looking at proliferating macrophage (**Fig 5**) and neutrophils (**Fig 6**) we selected the area of the head (left panels) and trunk (right panels) region, where previously (**Fig 4B**) the highest increase in red fluorescence was observed.

When analysing the macrophage response, a higher number of macrophages were observed in the head and trunk of both high- and low-infected larvae (**Fig 5A**, 10x magnifications). In the head, macrophages were scattered throughout the region but in infected larvae they were most abundant in the area corresponding to the haematopoietic tissue (head kidney), posterior to the branchial arches, indicative of progenitors proliferation. In the trunk, macrophages were scattered throughout the tissue, and in high-infected larvae in particular, macrophages also clustered in the cardinal caudal vein (**Fig 5A**, right panels). In agreement with previous results (**Fig 4C**), quantification of total green fluorescence confirmed a significant increase in the head and trunk of low-infected larvae. In high-infected individuals, a significant increase was observed in the trunk, whereas in the head the number of macrophages was clearly elevated although not significantly when compared to the PVP-injected controls (**Fig 5B**). In all groups, total cell fluorescence in the head region was significantly higher than that in the trunk region (**Fig 5B**), and thus largely contributed to the total cell fluorescence previously measured in whole larvae (**Fig 4C**).

Given the high number of macrophages in the head region, their heterogeneous morphology, the thickness of the tissue and the overall high number of EdU^+ nuclei, it was not possible to reliably count single (EdU^+) macrophages in this area. Therefore, when analysing the degree of proliferation, we focused on the trunk region only. There, EdU^+ macrophages could be observed in all groups, and in agreement with the total cell fluorescence measured in the same region (**Fig 5B**), their number was higher in

high- and low-infected individuals compared to PVP-injected controls (**Fig 5C** and **Supplementary Video 2**). No significant difference was observed between high- and low-infected fish, confirming that macrophages react to the presence and not to the number of trypanosomes. Within the trunk region of high-infected larvae, a large proportion of macrophages were observed around and inside the cardinal caudal vein, the majority of which were EdU^+ (**Supplementary Fig 2A**), suggesting that in high-infected larvae, proliferating macrophages migrated to the vessels. Altogether, these data confirm that *T. carassii* infection triggers macrophage proliferation and that proliferation is higher in low-infected individuals compared to high-infected fish, possibly due to a higher haematopoietic activity triggered in low-infected larvae.

When analysing the neutrophil response, in agreement with the previous observation, the number of neutrophils in the head and trunk regions was not apparently different between infected and non-infected larvae (**Fig 6A**). Neutrophils were scattered throughout the head region, but differently from what observed for macrophages, their number did not increase in the area corresponding to the haematopoietic tissue. Quantification of total cell fluorescence in the head and trunk revealed no significant differences between groups (**Fig 6B** and **Supplementary Video 3**). Interestingly, quantification of EdU^+ neutrophils in the trunk region, revealed that while in PVP-injected individuals EdU^+ neutrophils were rarely observed, in infected fish, a significant, although low number of neutrophils had proliferated (**Fig 6C**). These data indicate that neutrophils also respond to the infection by proliferating, but their number is relatively low and may have not significantly contributed to changes in total cell fluorescence. Conversely to macrophages, within the analysed trunk region, neutrophils were never observed within the cardinal caudal vein, and independently of whether they proliferated (EdU^+) or not, were mostly observed lining the vessel (**Supplementary Fig 2B**). Altogether, these data indicate that independent of the trypanosome number, *T. carassii* triggers a differential macrophage and neutrophil proliferation, where macrophages respond more prominently than neutrophils to the infection.

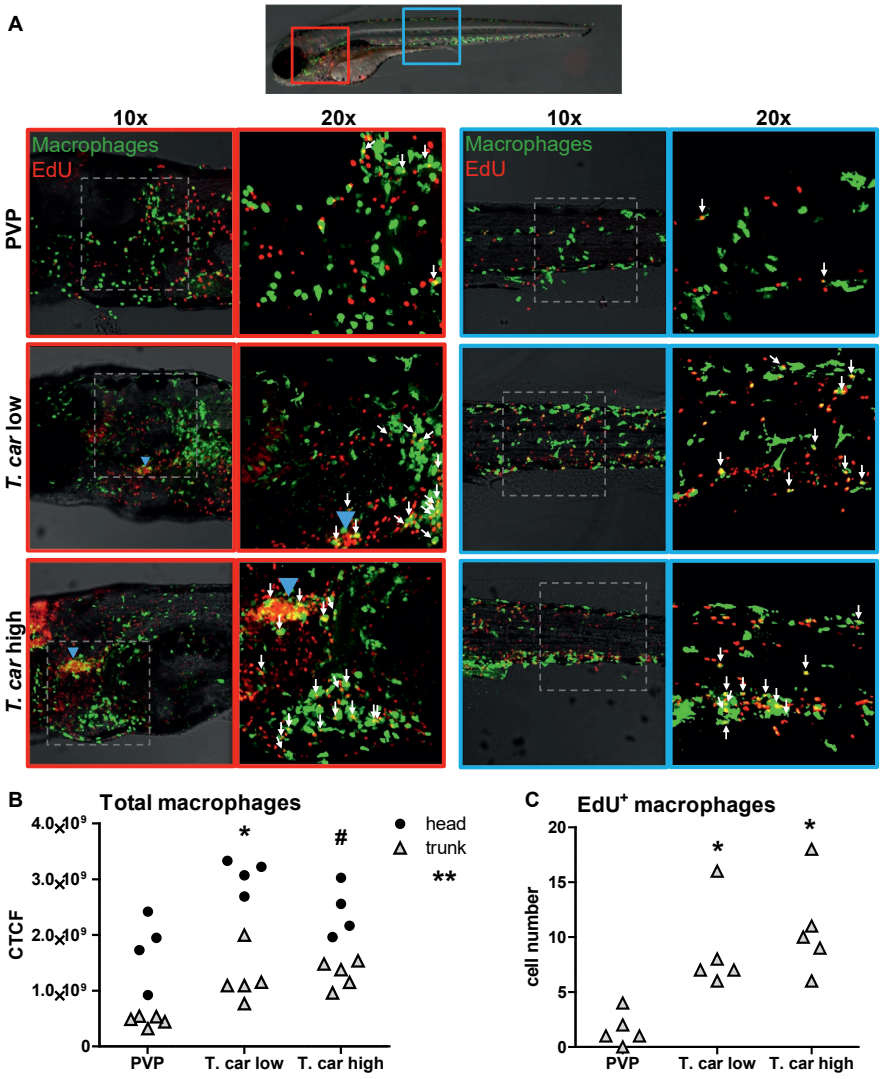
A
10x
20x
10x
20x
Macrophages
EdU
Macrophages
EdU
PVP
T. car low
T. car high
B
Total macrophages
CTCF
4.0x10^9
3.0x10^9
2.0x10^9
1.0x10^9
0
PVP
T. car low
T. car high
head
trunk
*
#
**
C
EdU+ macrophages
cell number
20
15
10
5
0
PVP
T. car low
T. car high
*
*

◂ Fig 5. *T. carassii* infection triggers macrophage proliferation.
Tg(mpeg1:eGFP) zebrafish larvae were infected intravenously at 5 dpf with n=200 *T. carassii* or with PVP control (n=5 larvae per group, from four independent experiments). At 3 dpi, larvae received 2 nl 1.13mM iCLICK™ EdU, at 4 dpi were separated in high- and low-infected individuals and were imaged after fixation and whole mount immunohistochemistry 6-8h later (30-32h after EdU injection, ~9 dpf). Larvae were fixed and treated with iCLICK EdU ANDY FLUOR 555 (Red) development to identify EdU^+ nuclei and with anti-GFP antibody to retrieve the position of macrophages, as described in the material and methods section. Larvae were imaged with Andor Spinning Disc Confocal Microscope using 10x and 20x magnification. **A)** Representative maximum projections of the head (left panels, red boxes) and trunk (right panels, blue boxes) regions capturing macrophages (green) and EdU^+ nuclei (red) in PVP control, low- and high-infected zebrafish. In the PVP control group, EdU^+ nuclei and GFP^+ macrophages only rarely overlapped (white arrows, 20x), indicating limited proliferation of macrophages. In low- and high-infected individuals, the number of EdU^+ macrophages increased (white arrows, 20x), indicating proliferation of macrophages in response to *T. carassii* infection. Blue arrowhead in the head of low- and high-infected larvae, indicates the position of the thymus, an actively proliferating organ at this time point. The identification of EdU^+ macrophages (white arrows) was performed upon detailed analysis of the separate stacks used to generate the overlay images, and are provided in **Supplementary Video 2**. **B)** Corrected total cell fluorescence (CTCF) calculated in the head (circles) and trunk (triangles) region. Symbols indicate individual larvae. * indicates significant differences of both, the head and trunk region to the respective PVP controls; # indicates significant differences of the trunk to the respective PVP control; ** indicates significant differences between CTCF in the head and trunk regions, as assessed by Two-Way ANOVA followed by Bonferroni post-hoc test. **C)** Number of EdU^+ macrophages in the trunk region of infected and non-infected larvae. Symbols indicate individual larvae. * indicates significant differences to the PVP control as assessed by One-Way ANOVA followed by Bonferroni post-hoc test.

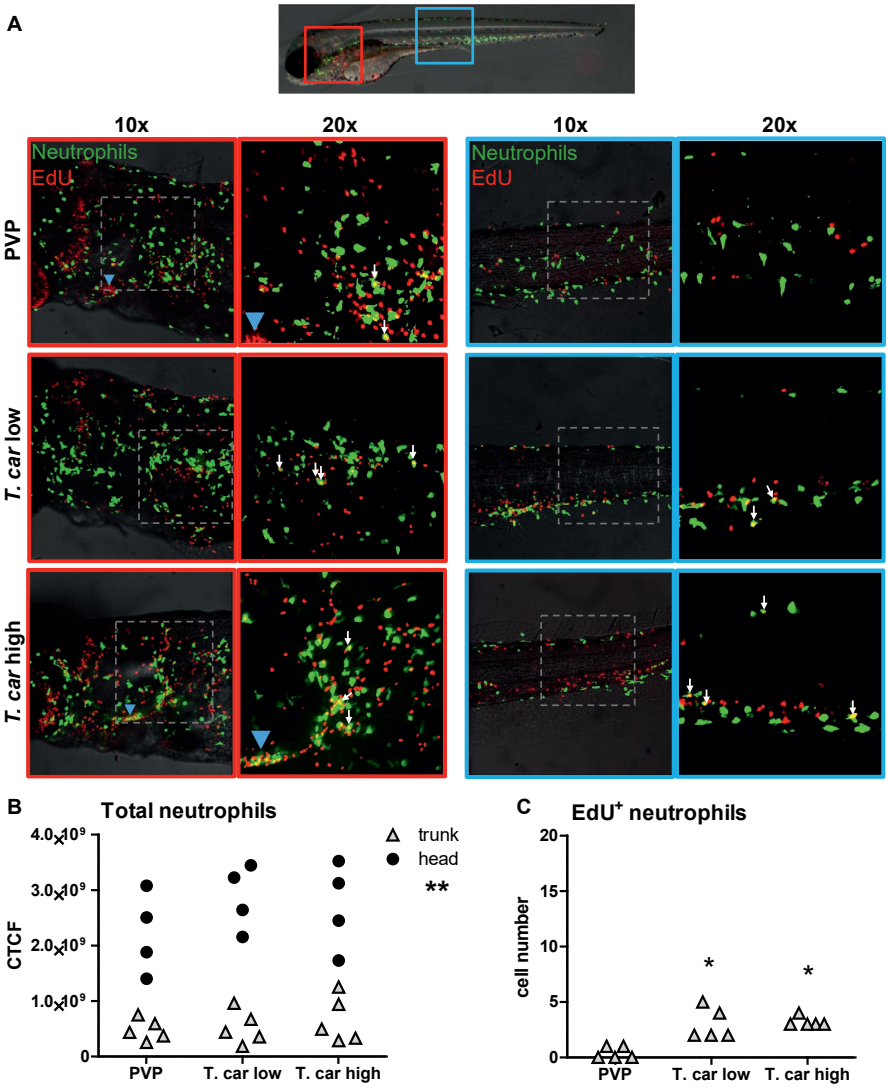
A
10x
20x
10x
20x
Neutrophils
EdU
PVP
T. car low
T. car high
B
Total neutrophils
CTCF
4.0x10⁹
3.0x10⁹
2.0x10⁹
1.0x10⁹
0
trunk
head
**
PVP
T. car low
T. car high
C
EdU⁺ neutrophils
cell number
20
15
10
5
0
*
*
PVP
T. car low
T. car high

◂ **Fig 6. *T. carassii* infection triggers neutrophil proliferation.**
Tg(mpx:GFP) were treated as described in Fig 5 (n=5 larvae per group, from four independent experiments). **A)** Representative maximum projections of the head (left panels, red boxes) and trunk (right panels, blue boxes) region capturing neutrophils (green) and EdU$^+$ nuclei (red) in PVP, low- and high-infected zebrafish. The images acquired at a 20x magnification show that in all groups, EdU$^+$ nuclei and GFP$^+$ neutrophils only rarely overlapped (white arrows), and was marginally higher in infected than in non-infected PVP controls. Detailed analysis of the separate stacks selected to compose the overlay image of the head region of the high-infected larva (bottom left panel), revealed that none of the neutrophils in the area indicated by the blue arrowhead (thymus) were EdU$^+$ (**Supplementary Video 3**). **B)** Corrected total cell fluorescence (CTCF) calculated in the head (circles) and trunk (triangles) region. Symbols indicate individual larvae. ** indicates significant differences between CTCF in the head and trunk regions, as assessed by Two-Way ANOVA followed by Bonferroni post-hoc test. **C)** Number of EdU$^+$ neutrophils in the trunk region of infected and non-infected larvae. Symbols indicate individual larvae. * indicates significant differences to the PVP control as assessed by One-Way ANOVA followed by Bonferroni post-hoc test.

Differential distribution of neutrophils and macrophages in high- and low-infected zebrafish larvae

After having established that *T. carassii* infection triggers macrophage, and to a lesser extent, neutrophil proliferation, we next investigated whether a differential distribution of these cells would occur during infection. Considering the haematic nature of the trypanosome and the kinetics of parasitaemia, we focused on the cardinal caudal vein at 4 dpi, a time point at which clear differences in parasitaemia (**Fig 3**) and a differential distribution of macrophages and neutrophils (**Fig 5-6** and **Supplementary Fig 2**) were observed between high- and low-infected larvae. To this end, crosses between transgenic lines marking the blood vessels and those marking either macrophages or neutrophils were used. *Tg(kdrl:caax-mCherry;mpx:GFP)* or *Tg(fli1:eGFP x mpeg1.4:mCherry-F*) were infected with *T. carassii*, separated in high- and low-infected larvae at 4 dpi and imaged with Roper Spinning Disk Confocal Microscope using 40x magnification. Longitudinal and orthogonal images of the vessel were analysed to visualise the exact location of cells along the cardinal caudal vein (**Fig 7** and **Supplementary Video 4**). In PVP controls, both macrophages and neutrophils were exclusively located outside the vessel in close contact with the endothelium or in the tissue adjacent the cardinal caudal vein. In infected fish, while neutrophils remained exclusively outside the vessel (**Fig 7**, left panel), macrophages could be seen both inside (white arrows) and outside (blue arrows) the vessel (**Fig 7**, right panel). Whilst in low-infected individuals macrophage morphology was similar to that observed in non-infected fish, in high-infected larvae, macrophages inside the vessel clearly had a more rounded morphology. Altogether these data indicate that differently from neutrophils, macrophages increase in number in infected fish, are recruited inside the cardinal caudal vein and, depending on the infection level, their morphology can be greatly affected.

***T. carassii* infection triggers the formation of foamy macrophages in high-infected fish**

Between control and high- or low-infected larvae, clear differences could be observed in macrophage morphology and location when examined in greater detail. In control fish, macrophages generally exhibited an elongated and dendritic morphology, were very rarely observed inside the vessel and were mostly located along the vessel endothelium, in the tissue lining the cardinal vessels or in the ventral fin (**Fig 8A**, left). A similar morphology and distribution were observed in low-infected larvae (not shown). Strikingly, in high-infected larvae, we consistently observed large, dark, granular and round macrophages located almost exclusively inside the cardinal vein on the dorsal luminal side. These dark macrophages were clearly visible already in bright field images due to their size, colour and location, and could be present as single cells or as aggregates (**Fig 8A**, right). The occurrence of these large macrophages increased with the progression of the infection and was exclusive to high-infected individuals (**Supplementary Video 5**) since they were never observed in low-infected or control larvae.

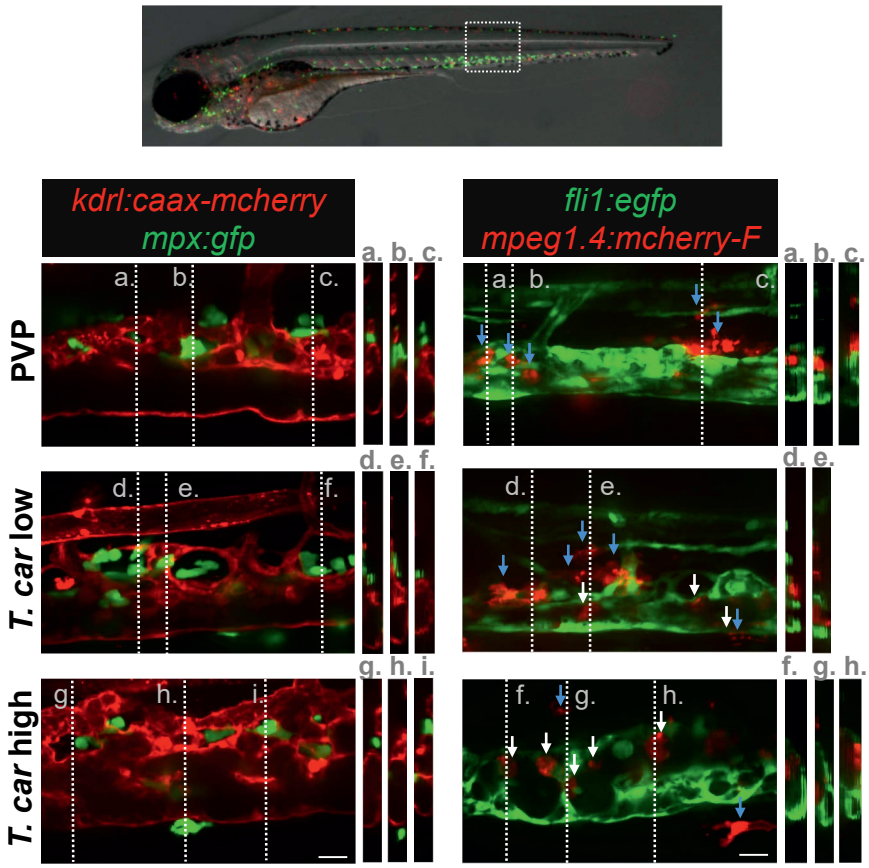

The rounded morphology, size and dark appearance of these cells was reminiscent of that of foamy macrophages. Therefore, to further investigate the nature of these cells, the green fluorescent fatty acid BODIPY-FLC5 was used to track lipid accumulation in infected larvae (**Fig 8B**). Interestingly, administration of BODIPY-FL5 in high-infected larvae, one day prior to the expected appearance of the large macrophages, revealed the accumulation of lipids in these cells (**Supplementary Video 6**). Macrophages without this large, dark, granular appearance did not show lipid accumulation. This result therefore confirms that the large, rounded, granular macrophages in the cardinal caudal vein are indeed foamy macrophages.

Foamy macrophages have a pro-inflammatory activation state

To further investigate the activation state of foamy macrophages, we made use of the *Tg(tnfa:eGFP-F;mpeg1.4:mCherry-F)* and *Tg(il1b:eGFP-F x mpeg1.4:mCherry-F)* double transgenic zebrafish lines, having macrophages in red and *tnfa*- or *Il1b*-expressing cells in green (**Fig 9** and **10**). We first focused on the time point at which the foamy macrophages were most clearly present in highly infected individuals, 4 dpi. Our results clearly show that all large foamy macrophages, were strongly positive for *tnfa*, suggesting an inflammatory activation state (**Fig 9A**). Interestingly, not only the large foamy macrophages within the vessel, but also dendritic or lobulated macrophages outside or lining the vessel showed various degrees of activation. Macrophages that were still partly in the vessel (**Fig 9B**, yellow arrowhead) displayed higher *tnfa* expression than macrophages lining the outer endothelium (white arrow heads). This could suggest that the presence of *T. carassii* components within the vessels might trigger macrophage activation.

◂ **Fig 7. Macrophages are recruited into the cardinal caudal vein of high-infected zebrafish larvae.** *Tg(kdrl:caax-mCherry;mpx:GFP)* and *Tg(fli1:eGFP x mpeg1.4:mCherry-F*) zebrafish larvae (n=5 larvae per group, from two independent experiments) were injected intravenously at 5 dpf with n=200 *T. carassii* or with PVP. At 4 dpi larvae were separated in high- and low-infected groups and imaged with a Roper Spinning Disk Confocal Microscope using 40x magnification. Scale bars indicate 25 µm. **Left panel**: representative images of the longitudinal view of the cardinal caudal vein (red), capturing the location of neutrophils (green). Orthogonal views of the locations marked with grey dashed lines (a,b,c,d,e,f,g,h,i), confirm that in all groups, neutrophils are present exclusively outside the vessel. **Right panel**: representative images of the longitudinal view on the vessel, capturing the position of macrophages (red) outside (blue arrowheads) or inside (white arrowheads) the vessel (green). Orthogonal views of the locations marked with grey dashed lines (a,b,c,d,e,f,g,h) confirm that in PVP controls, macrophages are present exclusively outside the vessel (blue arrows); in low-infected larvae, most macrophages are outside the vessel (blue arrows) having an elongated or dendritic morphology, although seldomly rounded macrophages can be observed within the vessel (white arrows); in high-infected larvae, although macrophages with dendritic morphology can be seen outside the vessel, the majority of the macrophages resides inside the vessel, clearly having a rounded morphology. **Supplementary Video 4** provides the stacks used for the orthogonal views.

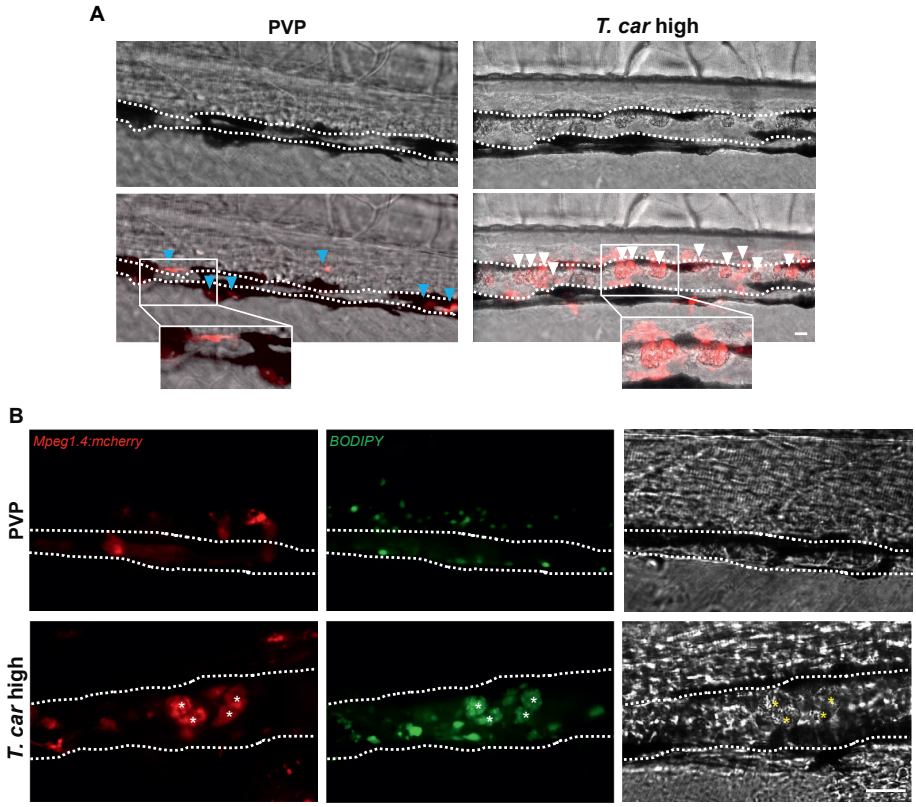

Fig 8. The large macrophages inside the cardinal caudal vein of high-infected zebrafish are foamy macrophages. A) *Tg(mpeg1.4:mCherry-F; mpx:GFP*) zebrafish larvae were infected intravenously at 5 dpf with *n*=200 *T. carassii* or with PVP (n=5 larvae per group) and imaged at 7 dpi using an Andor Spinning Disc Confocal Microscope at a 20x magnification. Representative images from three independent experiments are shown, with blue arrowheads pointing at macrophages outside the vessel and white arrowheads indicating large round macrophages inside the cardinal vein (dashed line). Scale bar indicates 25 µm. **B)** *Tg(mpeg1.4:mCherry-F)* were treated as in A (n=5 larvae per group). At 3 dpi, larvae received 1 nl of 30 µM BODIPY-FLC5 and were imaged 18-20 hours later using a Roper Spinning Disc Confocal Microscope at a 40x magnification. Representative images from three independent experiments are shown. Scale bar indicates 25 µm. **Supplementary Video 6** provides the stacks used in B.

Similarly to what was observed for *tnfa* expression, all foamy macrophages within the vessel were also positive for *il1b* (**Fig 9C**, asterisk), confirming their pro-inflammatory profile. Interestingly, not only macrophages but also endothelial cells (a selection is indicated by white arrows) were strongly positive for *il1b*. Outside the vessel, cells that were mCherry negative but strongly positive for *Il1b* could also be observed (**Fig 9C**, blue arrow); given their position outside the vessel, these are most likely neutrophils.

Altogether these data indicate that foamy macrophages occur in high-infected larvae and have a strong pro-inflammatory profile.

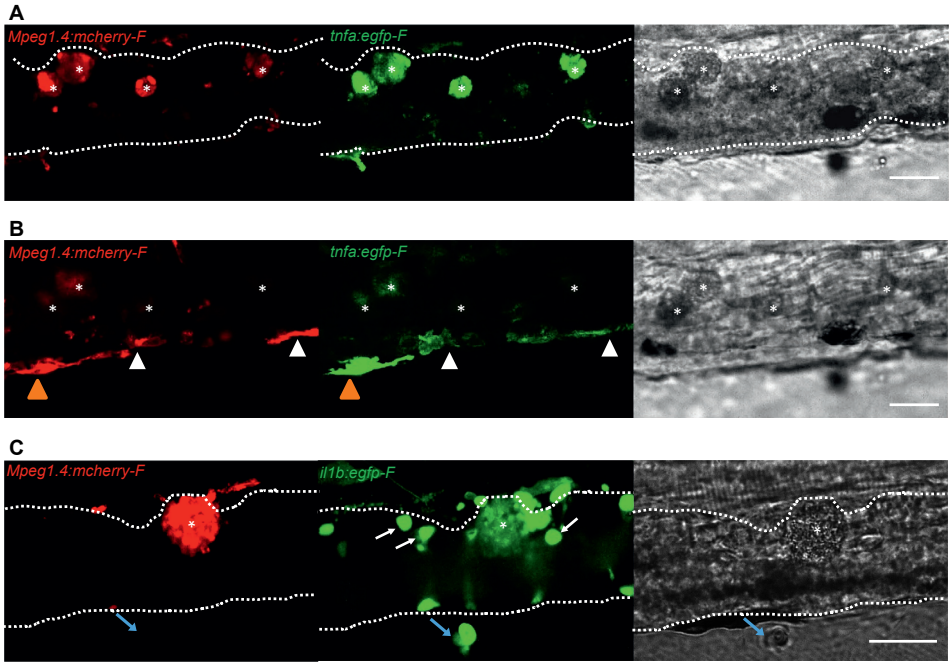

Fig 9. Foamy macrophages have an inflammatory profile.

Tg(tnfa:eGFP-F;mpeg1.4:mCherry-F) **A-B**) or *Tg(il1b:eGFP-F x mpeg1.4:mcherry-F)* **C**) zebrafish larvae (5dpf), were injected with n=200 *T. carassii* or with PVP. At 4 dpi, high-infected individuals were imaged with an Andor (**A-B**) or Roper (**C**) Spinning Disk Confocal Microscope using 40x magnification. Scale bar indicates 25 μm. Foamy macrophages (asterisks) were easily identified within the cardinal caudal vessel (dashed lines) and were strongly positive for *tnfa* (**A**) and *il1b* (**C**) expression (GFP signal). **B**) Same as in A, but a few stacks up, focusing on the cells lining the endothelium. Macrophages that were partly inside and partly outside the vessel (yellow arrowhead) were also strongly positive for *tnfa*, whereas macrophages lining the outer endothelium had a lower *tnfa* expression (white arrowheads). **C**) A foamy macrophage (asterisk) within the cardinal caudal vessel (dashed lines) was positive for *il1b*. Endothelial cells were also strongly positive for *il1b*, a selection of which is indicated by white arrows. A mCherry-negative-Il1b positive cell is present outside the vessel (blue arrow). Given its position, it is likely to be a neutrophil.

High-infected zebrafish have a strong inflammatory profile associated with susceptibility to infection

When comparing the overall inflammatory state in high- and low-infected larvae it was apparent that high-infected individuals generally exhibited a higher pro-inflammatory response than low-infected larvae (**Fig 10**). Although *tnfa*- and *il1b*-positive macrophages could be seen in low-infected individuals, these were generally few (**Fig 10A** and **10B**, middle panels) and a higher number of *tnfa*- and *il1b*-expressing cells was observed in high-infected larvae (**Fig 10A** and **10B**, right panels). In these fish, *il1b* and *tnfa* expression was observed not only in (foamy) macrophages (asterisk), but also in mCherry negative cells outside the vessel (blue arrow, likely neutrophils) and in endothelial cells lining the vessel (bright green). As mentioned earlier, high-infected individuals are not able to control parasitaemia and generally succumbed to the infection. Altogether, these results suggest that in high-infected individuals, uncontrolled parasitaemia leads to an exacerbated pro-inflammatory response leading to susceptibility to the infection. Low-infected individuals however, with increased macrophage number and moderate cytokine responses, are able to control parasitaemia and to recover from the infection.

Fig 10. High-infected zebrafish have a strong inflammatory profile. ►
Zebrafish larvae (5 dpf), either (**A**) *Tg(tnfa:eGFP-F x mpeg1.4:mCherry-F*) (n= 8-13 larvae per group from four independent experiments), or (**B**) *Tg(il1b:eGFP-F; mpeg1.4:mCherry-F)* (n=7-8 larvae per group from two independent experiments), were infected as described in Fig 7. At 3 dpi, larvae were separated in high- and low-infected individuals and at 4 dpi imaged with a Roper Spinning Disk Confocal Microscope. Scale bar indicate 25 µm. **A)** In non-infected PVP controls (left panel), several macrophages can be observed outside the vessel but none was positive for *tnfa*. In low-infected individuals (middle panel) macrophages were present inside and outside the vessel. Except the occasional macrophage showing *tnfa*-egfp expression (white arrowhead), they generally did not exhibit strong GFP signal. In high-infected individuals however, foamy macrophages (asterisks) as well as endothelial cells (bright green cells) or other leukocytes, were strongly positive for *tnfa*-egfp expression. **B)** *il1b-egfp* expression was generally low in non-infected PVP controls. In low-infected larvae *il1b* positive macrophages were rarely observed (white arrowhead). In both high- and low-infected fish, some endothelium cells in the cardinal caudal vein show high *il1b*-egfp expression (bright green cells in middle and right panel). In high-infected individual however (right panel), foamy macrophages inside the vessel (asterisks) as well as other macrophages lining the vessel (white arrowhead) and leukocytes in the tissue (blue arrow), were positive for *il1b*-egfp expression.

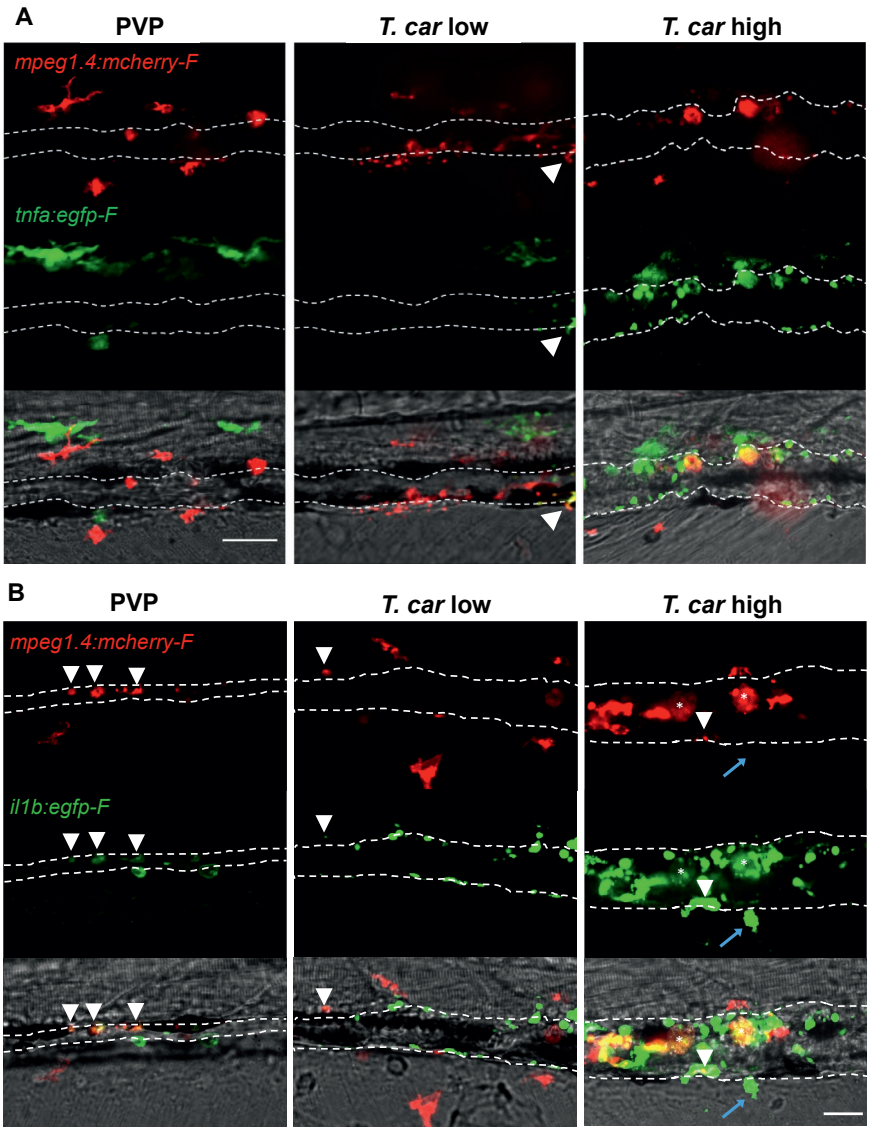
A
PVP
T. car low
T. car high
mpeg1.4:mcherry-F
tnfa:egfp-F
B
PVP
T. car low
T. car high
mpeg1.4:mcherry-F
il1b:egfp-F

Discussion

In this study we describe the differential response of macrophages and neutrophils, *in vivo*, during the early phase of trypanosome infection of larval zebrafish. Considering the prominent role of innate immune factors in determining the balance between pathology and control of first-peak parasitaemia in mammalian models of trypanosomiasis (Magez and Caljon, 2011; Radwanska et al., 2018; Stijlemans et al., 2017), the use of transparent zebrafish larvae, devoid of a fully developed adaptive immune system, allowed us to investigate *in vivo* the early events of the innate immune response to *T. carassii* infection. After having established a clinical scoring system of infected larvae, we were able to consistently differentiate high- and low-infected individuals, each associated with opposing susceptibility to the infection. In high-infected larvae, which fail to control first-peak parasitaemia, we observed a strong inflammatory response associated with the occurrence of foamy macrophages and susceptibility to the infection. Conversely, in low-infected individuals, which succeeded in controlling parasitaemia, we observed a moderate inflammatory response associated with resistance to the infection. Altogether these data confirm that also during trypanosome infection of zebrafish, innate immunity is sufficient to control first-peak parasitaemia and that a controlled inflammatory response is beneficial to the host.

Using transgenic lines marking macrophages and neutrophils, total cell fluorescence and cell proliferation analysis revealed that *T. carassii* infection triggers a marked macrophage proliferation, particularly in the haematopoietic region and in low-infected individuals. Although to a much lesser extent, neutrophils also responded to the infection by proliferating. The total number of neutrophils however, was comparatively low and likely did not contribute to the total cell fluorescence measured in our whole larvae analysis. Although neutrophils were recently implicated in promoting the onset of tsetse fly-mediated trypanosome infections in mouse dermis, macrophage-derived immune mediators, such as NO and TNFα were confirmed to played a more prominent role in the control of first-peak parasitaemia and in the regulation of the overall inflammatory response (Caljon et al., 2018).

The observation that in low-infected individuals the number of macrophages was significantly increased by 4-5 dpi, the time point at which clear differences in parasitaemia were apparent between the two infected groups, suggests a role for macrophages, or for macrophage-derived factors in first-peak parasitaemia control. Phagocytosis however, can be excluded as one of the possible contributing factors since motile *T. carassii*, similar to other extracellular trypanosomes (Caljon et al., 2018; Saeij et al., 2003; Scharsack et al., 2003), cannot be engulfed by any innate immune cell. A strong inflammatory response is also not required for trypanosomes control, since in low-infected individuals, only moderate *il1b* or *tnfα* expression was observed, mostly in macrophages, as assessed using transgenic zebrafish reporter lines. Our data are in agreement with several previous studies using trypanoresistant (BALB/c) or trypanosusceptible (C57Bl/6) mice that revealed the double-edge sword of pro-inflammatory

mediators such as TNFα or IFNγ during trypanosome infection in mammalian models (reviewed by Radwanska et al., 2018; Stijlemans et al., 2007). These studies showed that a timely but controlled expression of IFNγ, TNFα and NO, contributed to trypanosomes control via direct (Daulouede et al., 2001; F Iraqi et al., 2001; Lucas et al., 1994) or indirect mechanisms (Kaushik et al., 1999; Magez et al., 2007, 2006; Mansfield and Paulnock, 2005; Namangala et al., 2001; Noël et al., 2002). Conversely, in individuals in which an uncontrolled inflammatory response took place, immunosuppression and inflammation-related pathology occurred (Namangala et al., 2009, 2001; Noël et al., 2004; Stijlemans et al., 2016). The stark contrast between the mild inflammatory response observed in low-infected individuals and the exacerbated response observed in high-infected larvae, strongly resembles the opposing responses generally observed in trypanoresistant or trypanosusceptible animal models. Owing to the possibility to monitor the infection at the individual level, it was possible to observe such responses within one population of outbred zebrafish larvae. Although we were unable to investigate the specific role of Tnfα during *T. carassii* infection of zebrafish, due to the unavailability of *tnfα*-/- zebrafish lines or the unsuitability of morpholinos for transient knock-down at late stages of development, we previously reported that recombinant zebrafish (as well as carp and trout) Tnfα, are all able to directly lyse *T. brucei* (Forlenza et al., 2009). In the same study, we reported that also during trypanoplasma (kinetoplastid) infection of common carp, soluble as well as transmembrane carp Tnfα play a crucial role in both trypanosome control and susceptibility to the infection. Thus, considering the evolutionary conservation of the lectin-like activity among vertebrate's TNFα (Daulouede et al., 2001; Forlenza et al., 2009; Lucas et al., 1994a; Magez et al., 1997) it is possible that the direct lytic activity of zebrafish Tnfα may have played a role in the control of first-peak parasitaemia in low-infected individuals. In the future, using *tnfα*-/- zebrafish lines, possibly in combination with *ifnγ* reporter or *ifnγ*-/- lines, it will be possible to investigate in detail the relative contribution of these inflammatory mediators in the control of parasitaemia as well as onset of inflammation.

There are multiple potential explanations for the inability of high-infected larvae to control parasitaemia and the overt inflammatory response. Using various comparative mice infection models, it became apparent that while TNFα production is required for parasitaemia control, a timely shedding of TNFα-R2 receptors is necessary to limit the TNFα-mediated infection-associated immunopathology (Radwanska et al., 2018). Furthermore, during *T. brucei* infection in mice and cattle, continuous cleavage of membrane glycosylinositolphosphate (GIP)-anchored VSG (mVSG-GPI) leads to shedding of the soluble VSG-GPI (sVSG-GPI), while the dimyristoylglycerol compound (DMG) is left in the membrane. While the galactose-residues of sVSG-GIP constituted the minimal moiety required for optimal TNFα production, the DMG compound of mVSG contributed to macrophage overactivation (TNFα and IL-1β secretion) (Magez et al., 2002, 1998; Sileghem et al., 2001). Although *T. carassii* was shown to possess a surface dominated by GPI-anchored carbohydrate-rich mucin-like glycoproteins, not subject to antigenic variation (Lischke et al., 2000; Overath et al., 2001), components of its excreted/

secreted proteome, together with phospholipase C-cleaved GPI-anchored surface proteins, have all been shown to play a role in immunogenicity (Joerink et al., 2007), inflammation (Oladiran and Belosevic, 2009b, 2009a; Ribeiro et al., 2010) as well as immunosuppression (Oladiran and Belosevic, 2012). Thus, the overactivation caused by the presence of elevated levels of pro-inflammatory trypanosome-derived moieties, combined with the lack of a timely secretion of regulatory molecules (e.g. soluble TNFR2) that could control the host response, may have all contributed to the exacerbated inflammation observed in high-infected individuals.

Given the differential response observed in high- and low-infected individuals, especially with respect to macrophage distribution and activation, we attempted to investigate the specific role of macrophages in the protection or susceptibility to *T. carassii* infection. To this end, the use of a cross between the *Tg(mpeg1:Gal4FF)*^{gl2} (Ellett et al., 2011) and the *Tg(UAS-E1b:Eco.NfsB-mCherry)*^{c26} (Davison et al., 2007) line, which would have allowed the timed metronidazole (MTZ)-mediated depletion of macrophages in zebrafish larvae, was considered. Unfortunately, *in vitro* analysis of the effect of MTZ on the trypanosome itself, revealed that trypanosomes are susceptible to MTZ, rendering the *nfsB* line not suitable to investigate the role of macrophages (nor neutrophils) during this particular type of infection. Alternatively, we attempted to administer liposome-encapsulated clodronate (Lipo-clodronate) as described previously (Nguyen-Chi et al., 2017; Phan et al., 2018; Travnickova et al., 2015). In our hands however, administration of 5 mg/ml Lipo-clodronate (3 nl) to 5 dpf larvae (instead of 2-3 dpf larvae), led to the rapid development of oedema.

Besides differences between the overall macrophage and neutrophil (inflammatory) response, the differential distribution of these cells was investigated *in vivo* during an ongoing infection, utilising the transparency of the zebrafish and the availability of transgenic lines marking the vasculature. Neutrophils were never observed inside cardinal caudal vein although in infected individuals they were certainly recruited and were observed in close contact with the outer vessel's endothelium. Conversely, macrophages could be seen both outside and inside the vessel and the total proportion differed between high- and low-infected individuals. While in low-infected individuals the majority of macrophages recruited to the cardinal caudal vein remained outside the vessel's in close contact with the endothelium, in high-infected individuals the majority of macrophages were recruited inside the caudal vein and were tightly attached to the luminal vessel wall. To our knowledge, such detailed description of the relative (re)distribution of neutrophils and macrophages, *in vivo*, during a trypanosome infection, has not been reported before.

Interestingly, exclusively in high-infected individuals, by 4 dpi large, round, dark and granular cells were observed, already under the bright field view, in the lumen of the cardinal caudal vein. These cells were confirmed to be foamy macrophages with high cytoplasmic lipid content. Foam cells, or foamy macrophages have been named after the lipid bodies accumulated in their cytoplasm leading to their typical enlarged morphological appearance

(Dvorak et al., 1983), but are also distinguished by the presence of diverse cytoplasmic organelles (Melo et al., 2003). They have been associated with several (intracellular) infectious diseases, including Leishmaniasis, Chagas disease, experimental malaria, toxoplasmosis and tuberculosis, (reviewed in López-Muñoz et al., 2018; Vallochi et al., 2018), but never before with (extracellular) trypanosome infection. For example, during *T. cruzi* infection of rat, increased numbers of activated monocytes or macrophages were reported in the blood or heart (Melo and Machado, 2001). Interestingly, trypanosome uptake was shown to directly initiate the formation of lipid bodies in macrophages, leading to the appearance of foamy macrophages (D'Avila et al., 2011). During human *Mycobacterium tuberculosis* infections, foamy macrophages play a role in sustaining the presence of bacteria and contribute to tissue cavitation enabling the spread of the infection (Russell et al., 2009). Independently of the disease, it is clear that foamy macrophages are generally associated with inflammation, since their cytoplasmic lipid bodies are a source of eicosanoids, strong mediators of inflammation (Melo et al., 2006; Wymann and Schneiter, 2008). In turn, inflammatory mediators such as Prostaglandin E2 benefit trypanosome survival, as shown in *Trypanosoma*, *Leishmania*, *Plasmodium*, and *Toxoplasma* infections (reviewed in Vallochi et al., 2018). Our results are consistent with these reports as we show the occurrence of foamy macrophages exclusively in individuals that developed high parasitaemia, characterized by a strong pro-inflammatory response, and ultimately succumbed to the infection. Although we did not systematically investigate the exact kinetics of parasitaemia development in correlation with foamy macrophages occurrence, during our *in vivo* monitoring, we consistently observed that the increase in trypanosome number preceded the appearance of foamy macrophages. It is possible that, in high-infected individuals, foamy macrophages are formed due to the necessity to clear the increasing concentration of circulating trypanosome-derived moieties or of dying trypanosomes. The interaction with trypanosome-derived molecules, including soluble surface (glycol)proteins or trypanosome DNA, may not only be responsible for the activation of pro-inflammatory pathways, but also for a change in cell metabolism. The occurrence of foamy macrophages has been reported for intracellular trypanosomatids (*T. cruzi, Leishmania*), and arachidonic acid-derived lipids were reported to act as regulators of the host immune response and trypanosome burden during *T. brucei* infections (López-Muñoz et al., 2018). To our knowledge our study is the first to report the presence of foamy macrophages during an extracellular trypanosome infection.

The possibility to detect the occurrence of large, granular cells already in the bright field and the availability of transgenic lines that allowed us to identify these cells as macrophages, further emphasizes the power of the zebrafish model. It allowed us to visualise *in vivo*, in real time, not only their occurrence but also their differential distribution with respect to other macrophages or neutrophils. Observations that we might have missed if we for example were to bleed an animal, perform immunohistochemistry or gene expression analysis. In fact, gene expression analysis, even on pools of high- and low-infected larvae, failed to detect

the differential activation state of the two groups (data not shown), which instead was easily visible upon microscopical analysis. Thus, the possibility to separate high- and low-infected animals without the need to sacrifice them, allowed us to follow at the individual level the progression of the infection and the ensuing differential immune response.
In the future it will be interesting to analyse the transcription profiles of sorted macrophage populations from high- and low-infected larvae. Given the marked heterogeneity in macrophage activation observed especially within high-infected individuals, single-cell transcriptome analysis, of foamy macrophages in particular, may provide insights in the differential activation state of the various macrophage phenotypes. Furthermore, the zebrafish has already emerged as a particularly valuable animal model to study inflammation and host-pathogen interaction and can be a powerful complementary tool to examine macrophage plasticity and polarization *in vivo*, by truly reflecting the complex nature of the environment during an ongoing infection in a live host. Finally, the availability of (partly) transparent adult zebrafish lines (Antinucci and Hindges, 2016; White et al., 2008), may aid the *in vivo* analysis of macrophage activation in adult individuals.
Altogether, in this study we describe the innate immune response of zebrafish larvae to *T. carassii* infection. The transparency and availability of various transgenic zebrafish lines, enabled us to establish a clinical scoring system that allowed us to monitor parasitaemia development and describe the differential response of neutrophils and macrophages at the individual level. Interestingly, for the first time in an extracellular trypanosome infection, we report the occurrence of foamy macrophages, characterized by a high lipid content and strong inflammatory profile, associated with susceptibility to the infection. Our model paves the way to investigate which mediators of the trypanosomes are responsible for the induction of such inflammatory response as well as study the condition that lead to the formation of foamy macrophages *in vivo*.

Acknowledgments
This work was supported by the FishForPharma FP7 People: Marie Curie Initial Training Network, project number PITN-GA-2011-289209 and the Dutch Research Council (NWO), project number 022.004.005. Dr. Christelle Langevin from Institut National de la Recherche Agronomique (INRA) is greatly acknowledged for her assistance with immunohistochemical analysis. The authors like to thank Dr. Danilo Pietretti and Dr. Sylvia Brugman from the Cell Biology and Immunology Group, Wageningen University & Research for technical support with the RQ-PCR analysis or fruitful discussions, and CARUS Aquatic Research Facility of Wageningen University for fish rearing and husbandry. Furthermore, the authors like to thank Dr. Norbert de Ruijter from the Wageningen Light Microscopy Centre, and the Montpellier Resources Imagerie facility for their assistance.

References

Antinucci P, Hindges R. 2016. A crystal-clear zebrafish for in vivo imaging. *Sci Rep* **6**:1–10. doi:10.1038/srep29490

Baral TN, De Baetselier P, Brombacher F, Magez S. 2007. Control of Trypanosoma evansi Infection Is IgM Mediated and Does Not Require a Type I Inflammatory Response . *J Infect Dis* **195**:1513–1520. doi:10.1086/515577

Benard EL, Racz PI, Rougeot J, Nezhinsky AE, Verbeek FJ, Spaink HP, Meijer AH. 2015. Macrophage-expressed perforins Mpeg1 and Mpeg1.2 have an anti-bacterial function in zebrafish. *J Innate Immun* **7**:136–152. doi:10.1159/000366103

Bertrand JY, Chi NC, Santoso B, Teng S, Stainier DYR, Traver D. 2010. Haematopoietic stem cells derive directly from aortic endothelium during development. *Nature* **464**:108–111. doi:10.1038/nature08738

Boada-Sucre AA, Rossi Spadafora MS, Tavares-Marques LM, Finol HJ, Reyna-Bello A. 2016. Trypanosoma vivax Adhesion to Red Blood Cells in Experimentally Infected Sheep. *Patholog Res Int* **2016**. doi:10.1155/2016/4503214

Caljon G, Mabille D, Stijlemans B, Trez C De, Mazzone M, Tacchini-cottier F, Malissen M, Ginderachter JA Van, Magez S, Baetselier P De, Abbeele J Van Den. 2018. Neutrophils enhance early Trypanosoma brucei infection onset 1–11. doi:10.1038/s41598-018-29527-y

Chi NC, Shaw RM, Val S De, Kang G, Jan LY, Black BL, Stainier DYR. 2008. Expression and Atrioventricular Canal Formation. *Genes Dev* 734–739. doi:10.1101/gad.1629408.734

Cnops J, De Trez C, Stijlemans B, Keirsse J, Kauffmann F, Barkhuizen M, Keeton R, Boon L, Brombacher F, Magez S. 2015. NK-, NKT- and CD8-Derived IFNγ Drives Myeloid Cell Activation and Erythrophagocytosis, Resulting in Trypanosomosis-Associated Acute Anemia. *PLoS Pathog* **11**. doi:10.1371/journal.ppat.1004964

Coller SP, Mansfield JM, Paulnock DM. 2003. Glycosylinositolphosphate Soluble Variant Surface Glycoprotein Inhibits IFN-γ-Induced Nitric Oxide Production Via Reduction in STAT1 Phosphorylation in African Trypanosomiasis. *J Immunol* **171**:1466–1472. doi:10.4049/jimmunol.171.3.1466

Cronan MR, Tobin DM. 2014. Fit for consumption: zebrafish as a model for tuberculosis. *Dis Model Mech*. doi:10.1242/dmm.016089

D'Avila H, Freire-de-Lima CG, Roque NR, Teixeira L, Barja-Fidalgo C, Silva AR, Melo RCN, DosReis GA, Castro-Faria-Neto HC, Bozza PT. 2011. Host cell lipid bodies triggered by Trypanosoma cruzi infection and enhanced by the uptake of apoptotic cells are associated with prostaglandin E2 generation and increased parasite growth. *J Infect Dis* **204**:951–961. doi:10.1093/infdis/jir432

Daulouede S, Bouteille B, Moynet D, De Baetselier P, Courtois P, Lemesre JL, Buguet A, Cespuglio R, Vincendeau P. 2001. Human macrophage tumor necrosis factor (TNF)-alpha production induced by Trypanosoma brucei gambiense and the role of TNF-alpha in parasite control. *J Infect Dis* **183**:988–991.

Davison JM, Akitake CM, Goll MG, Rhee JM, Gosse N, Baier H, Halpern ME, Leach SD, Parsons MJ. 2007. Transactivation from Gal4-VP16 transgenic insertions for tissue-specific cell labeling and ablation in zebrafish. *Dev Biol* **304**:811–824. doi:10.1016/j.ydbio.2007.01.033

Dóró É, Jacobs SH, Hammond FR, Schipper H, Pieters RP, Carrington M, Wiegertjes GF, Forlenza M. 2019. Visualizing trypanosomes in a vertebrate host reveals novel swimming behaviours, adaptations and attachment mechanisms. *Elife* **8**:1–25. doi:10.7554/elife.48388

Dvorak AM, Dvorak HF, Peters SP, Shulman ES, MacGlashan DW, Pyne K, Harvey VS, Galli SJ, Lichtenstein LM. 1983. Lipid bodies: cytoplasmic organelles important to arachidonate metabolism in macrophages and mast cells. *J Immunol* **131**:2965–76.

Ellett F, Pase L, Hayman JW, Andrianopoulos A, Lieschke GJ. 2011. mpeg1 promoter transgenes direct macrophage-lineage expression in zebrafish. *Blood* **117**:49–57. doi:10.1182/blood-2010-10-314120.

Engstler M, Pfohl T, Herminghaus S, Boshart M, Wiegertjes G, Heddergott N, Overath P. 2007. Hydrodynamic Flow-Mediated Protein Sorting on the Cell Surface of Trypanosomes 505–515. doi:10.1016/j.cell.2007.08.046

Forlenza M, Kaiser T, Savelkoul HFJ, Wiegertjes GF. 2012. The use of real-time quantitative PCR for the analysis of cytokine mRNA levels.Methods in Molecular Biology (Clifton, N.J.). pp. 7–23. doi:10.1007/978-1-61779-439-1_2

Forlenza M, Magez S, Scharsack JP, Westphal A, Savelkoul HFJ, Wiegertjes GF. 2009. Receptor-Mediated and Lectin-Like Activities of Carp (Cyprinus carpio) TNF-α. *J Immunol* **183**:5319–5332. doi:10.4049/jimmunol.0901780

García-Valtanen P, Martínez-López A, López-Muñoz A, Bello-Perez M, Medina-Gali RM, Ortega-Villaizán M del M, Varela M, Figueras A, Mulero V, Novoa B, Estepa A, Coll J. 2017. Zebra fish lacking adaptive immunity acquire an antiviral alert state characterized by upregulated gene expression of apoptosis, multigene families, and interferon-related genes. *Front Immunol* **8**. doi:10.3389/fimmu.2017.00121

Guegan F, Plazolles N, Baltz T, Coustou V. 2013. Erythrophagocytosis of desialylated red blood cells is responsible for anaemia during Trypanosomavivax infection. *Cell Microbiol* **15**:1285–1303. doi:10.1111/cmi.12123

Iraqi F, Sekikawa K, Rowlands J, Teale A. 2001. Susceptibility of tumour necrosis factor-alpha genetically deficient mice to Trypanosoma congolense infection. *Parasite Immunol* **23**:445–451.

Islam A, Woo P. 1991. Anemia and its mechanism in goldfish Carassius auratus infected with Trypanosoma danilewskyi. *Dis Aquat Organ* **11**:37–43. doi:10.3354/dao011037

Joerink M, Groeneveld A, Ducro B, Savelkoul HFJ, Wiegertjes GF. 2007. Mixed infection with Trypanoplasma borreli and Trypanosoma carassii induces protection: Involvement of cross-reactive antibodies. *Dev Comp Immunol* **31**:903–915. doi:10.1016/j.dci.2006.12.003

Joerink M, Saeij J, Stafford J, Belosevic M, Wiegertjes G. 2004. Animal models for the study of innate immunity: protozoan infections in fish In: Flik G, Wiegertjes GF, editors. Host-Parasite Interactions. Taylor & Francis. p. (55):67-89.

Kaushik RS, Uzonna JE, Gordon JR, Tabel H. 1999. Innate resistance to Trypanosoma congolense infections: Differential production of nitric oxide by macrophages from susceptible BALB/c and resistant C57B1/6 mice. *Exp Parasitol* **92**:131–143. doi:10.1006/expr.1999.4408

Kent ML, Lom J, Dyková I, Dykova I. 2006. Protozoan Parasites of Fishes. *J Parasitol* **79**:673. doi:10.2307/3283600

Kovacevic N, Hagen MO, Xie J, Belosevic M. 2015. The analysis of the acute phase response during the course of Trypanosoma carassii infection in the goldfish (Carassius auratus L.). *Dev Comp Immunol* **53**:112–122. doi:10.1016/j.dci.2015.06.009

Krettli AU, Weisz-Carrington P, Nussenzweig RS. 1979. Membrane-bound antibodies to bloodstream Trypanosoma cruzi in mice: Strain differences in susceptibility to complement-mediated lysis. *Clin Exp Immunol* **37**:416–423.

La Greca F, Haynes C, Stijlemans B, De Trez C, Magez S. 2014. Antibody-mediated control of Trypanosoma vivax infection fails in the absence of tumour necrosis factor. *Parasite Immunol* **36**:271–276. doi:10.1111/pim.12106

Langenau DM, Ferrando AA, Traver D, Kutok JL, Hezel JPD, Kanki JP, Zon LI, Thomas Look A, Trede NS. 2004. In vivo tracking of T cell development, ablation, and engraftment in transgenic zebrafish. *Proc Natl Acad Sci U S A* **101**:7369–7374. doi:10.1073/pnas.0402248101

Lawson ND, Weinstein BM. 2002. In vivo imaging of embryonic vascular development using transgenic zebrafish. *Dev Biol* **248**:307–318. doi:10.1006/dbio.2002.0711

Lischke A, Klein C, Stierhof YD, Hempel M, Mehlert A, Almeida IC, Ferguson MAJ, Overath P. 2000. Isolation and characterization of glycosylphosphatidylinositol-anchored, mucin-like surface glycoproteins from bloodstream forms of the freshwater-fish parasite Trypanosoma carassii. *Biochem J* **345**:693–700. doi:10.1042/0264-6021:3450693

López-Muñoz RA, Molina-Berríos A, Campos-Estrada C, Abarca-Sanhueza P, Urrutia-Llancaqueo L, Peña-Espinoza M, Maya JD. 2018. Inflammatory and pro-resolving lipids in trypanosomatid infections: A key to understanding parasite control. *Front Microbiol* **9**:1–16. doi:10.3389/fmicb.2018.01961

Lopez R, Demick KP, Mansfield JM, Paulnock DM. 2008. Type I IFNs Play a Role in Early Resistance, but Subsequent Susceptibility, to the African Trypanosomes. *J Immunol* **181**:4908–4917. doi:10.4049/jimmunol.181.7.4908

Lucas R, Magez S, De Leys R, Fransen L, Scheerlinck JP, Rampelberg M, Sablon E, De Baetselier P. 1994a. Mapping the lectin-like activity of tumor necrosis factor. *Science (80-)*. doi:10.1126/science.8303299

Lucas R, Magez S, Leys R De, Fransen L, Lucas R, Magez S, Leys R De, Fransen L, Scheerlinck J, Rampelberg M, Sablon E. 1994b. Mapping the Lectin-Like Activity of Tumor Necrosis Factor Published by : American Association for the Advancement of Science Stable URL : http://www.jstor.org/stable/2882928 JSTOR is a not-for-profit service that helps scholars , researchers , and student **263**:814–817.

Magez S., Lucas R, Darji A, Bajyana Songa E, Hamers R, Baetselier P de. 1993. Murine tumour necrosis factor plays a protective role during the initial phase of the experimental infection with Trypanosoma brucei brucei. *Parasite Immunol* **15**:635–641. doi:10.1111/j.1365-3024.1993.tb00577.x

Magez S, Caljon G. 2011. Mouse models for pathogenic African trypanosomes: Unravelling the immunology of host-parasite-vector interactions. *Parasite Immunol*. doi:10.1111/j.1365-3024.2011.01293.x

Magez S, Geuskens M, Beschin A, del Favero H, Verschueren H, Lucas R, Pays E, de Baetselier P. 1997. Specific uptake of tumor necrosis factor-alpha is involved in growth control of Trypanosoma brucei. *J Cell Biol* **137**:715–727.

Magez S, Radwanska M, Beschin A, Sekikawa K, De Baetselier P. 1999. Tumor necrosis factor alpha is a key mediator in the regulation of experimental Trypanosoma brucei infections. *Infect Immun* **67**:3128–3132.

Magez S, Radwanska M, Drennan M, Fick L, Baral TN, Allie N, Jacobs M, Nedospasov S, Brombacher F, Ryffel B, Baetselier PD. 2007. Tumor Necrosis Factor (TNF) Receptor–1 (TNFp55) Signal Transduction and Macrophage-Derived Soluble TNF Are Crucial for Nitric Oxide–Mediated Trypanosoma congolense Parasite Killing . *J Infect Dis* **196**:954–962. doi:10.1086/520815

Magez S, Radwanska M, Drennan M, Fick L, Baral TN, Brombacher F, Baetselier PD. 2006. Interferon-γ and Nitric Oxide in Combination with Antibodies Are Key Protective Host Immune Factors during Trypanosoma congolense Tc13 Infections . *J Infect Dis* **193**:1575–1583. doi:10.1086/503808

Magez S, Radwanska M, Stijlemans B, Van Xong H, Pays E, De Baetselier P. 2001. A Conserved Flagellar Pocket Exposed High Mannose Moiety Is Used by African Trypanosomes as a Host Cytokine Binding Molecule. *J Biol Chem* **276**:33458–33464. doi:10.1074/jbc.M103412200

Magez S, Stijlemans B, Baral T, De Baetselier P. 2002. VSG-GPI anchors of African trypanosomes: their role in macrophage activation and induction of infection-associated immunopathology. *Microbes Infect* **4**:999–1006. doi:10.1016/S1286-4579(02)01617-9

Magez S, Stijlemans B, De Baetselier P, Radwanska M, Pays E, Ferguson MAJ. 1998. The glycosylinositol-phosphate and dimyristoylglycerol moieties of the glycosylphosphatidylinositol anchor of the trypanosome variant-specific surface glycoprotein are distinct macrophage-activating factors. *J Immunol*.

Mansfield JM, Paulnock DM. 2005. Regulation of innate and acquired immunity in African trypanosomiasis. *Parasite Immunol* **27**:361–371. doi:10.1111/j.1365-3024.2005.00791.x

McAllister M, Phillips N, Belosevic M. 2019. Trypanosoma carassii infection in goldfish (Carassius auratus L.): changes in the expression of erythropoiesis and anemia regulatory genes. *Parasitol Res*. doi:10.1007/s00436-019-06246-5

Melo RC., Machado CR. 2001. Trypanosoma cruzi: Peripheral Blood Monocytes and Heart Macrophages in the Resistance to Acute Experimental Infection in Rats. *Exp Parasitol* **97**:15–23. doi:10.1006/EXPR.2000.4576

Melo RCN, Ávila HD, Fabrino DL, Almeida PE, Bozza PT. 2003. Macrophage lipid body induction by Chagas disease in vivo: Putative intracellular domains for eicosanoid formation during infection. *Tissue Cell* **35**:59–67. doi:10.1016/S0040-8166(02)00105-2

Melo RCN, Fabrino DL, Dias FF, Parreira GG. 2006. Lipid bodies: Structural markers of inflammatory macrophages in innate immunity. *Inflamm Res* **55**:342–348. doi:10.1007/s00011-006-5205-0

Mishra RR, Senapati SK, Sahoo SC. 2017. Trypanosomiasis induced oxidative stress and hematobiochemical alteration in cattle. *Artic J Entomol Zool Stud* **5**:721–727.

Musoke AJ, Barbet AF. 1977. Activation of complement by variant-specific surface antigen of Trypanosoma brucei. *Nature* **270**:438–440.

Naessens J. 2006. Bovine trypanotolerance: A natural ability to prevent severe anaemia and haemophagocytic syndrome? *Int J Parasitol* **36**:521–528. doi:10.1016/j.ijpara.2006.02.012

Namangala B, De Baetselier P, Beschin A. 2009. Both Type-I and Type-II Responses Contribute to Murine Trypanotolerance. *J Vet Med Sci* **71**:313–318.

Namangala B, Noel W, De Baetselier P, Brys L, Beschin A. 2001. Relative contribution of interferon-gamma and interleukin-10 to resistance to murine African trypanosomosis. *J Infect Dis* **183**:1794–1800.

Nguyen-Chi M, Laplace-Builhé B, Travnickova J, Luz-Crawford P, Tejedor G, Lutfalla G, Kissa K, Jorgensen C, Djouad F. 2017. TNF signaling and macrophages govern fin regeneration in zebrafish larvae. *Cell Death Dis* **8**:e2979. doi:10.1038/cddis.2017.374

Nguyen-Chi M, Laplace-Builhe B, Travnickova J, Luz-Crawford P, Tejedor G, Phan QT, Duroux-Richard I, Levraud JP, Kissa K, Lutfalla G, Jorgensen C, Djouad F. 2015. Identification of polarized macrophage subsets in zebrafish. *Elife* **4**:1–14. doi:10.7554/eLife.07288

Nguyen-Chi M, Phan QT, Gonzalez C, Dubremetz JF, Levraud JP, Lutfalla G. 2014. Transient infection of the zebrafish notochord with E. coli induces chronic inflammation. *DMM Dis Model Mech* **7**:871–882. doi:10.1242/dmm.014498

Noël W, Hassanzadeh G, Raes G, Namangala B, Daems I, Brys L, Brombacher F, Baetselier PD, Beschin A. 2002. Infection stage-dependent modulation of macrophage activation in Trypanosoma congolense-resistant and -susceptible mice. *Infect Immun* **70**:6180–6187.

Noël W, Raes G, Ghassabeh GH, De Baetselier P, Beschin A. 2004. Alternatively activated macrophages during parasite infections. *Trends Parasitol* **20**:126–133. doi:10.1016/j.pt.2004.01.004

O'Gorman GM, Park SDE, Hill EW, Meade KG, Mitchell LC, Agaba M, Gibson JP, Hanotte O, Naessens J, Kemp SJ, MacHugh DE. 2006. Cytokine mRNA profiling of peripheral blood mononuclear cells from trypanotolerant and trypanosusceptible cattle infected with Trypanosoma congolense. *Physiol Genomics* **28**:53–61. doi:10.1152/physiolgenomics.00100.2006

Oladiran A, Beauparlant D, Belosevic M. 2011. The expression analysis of inflammatory and antimicrobial genes in the goldfish (Carassius auratus L.) infected with Trypanosoma carassii. *Fish Shellfish Immunol* **31**:606–613. doi:10.1016/j.fsi.2011.07.008

Oladiran A, Belosevic M. 2012. Recombinant glycoprotein 63 (Gp63) of Trypanosoma carassii suppresses antimicrobial responses of goldfish (Carassius auratus L.) monocytes and macrophages. *Int J Parasitol* **42**:621–633. doi:10.1016/j.ijpara.2012.04.012

Oladiran A, Belosevic M. 2009a. Trypanosoma carassii hsp70 increases expression of inflammatory cytokines and chemokines in macrophages of the goldfish (Carassius auratus L.). *Dev Comp Immunol* **33**:1128–1136. doi:10.1016/j.dci.2009.06.003

Oladiran A, Belosevic M. 2009b. Trypanosoma carassii calreticulin binds host complement component C1q and inhibits classical complement pathway-mediated lysis. *Dev Comp Immunol* **34**:396–405. doi:10.1016/j.dci.2009.11.005

Overath P, Haag J, Lischke A, O'HUigin C. 2001. The surface structure of trypanosomes in relation to their molecular phylogeny. *Int J Parasitol* **31**:468–471.

Overath P, Ruoff J, Stierhof YD, Haag J, Tichy H, Dyková I, Lom J. 1998. Cultivation of bloodstream forms of Trypanosoma carassii, a common parasite of freshwater fish. *Parasitol Res* **84**:343–347. doi:10.1007/s004360050408

Page DM, Wittamer V, Bertrand JY, Lewis KL, Pratt DN, Delgado N, Schale SE, McGue C, Jacobsen BH, Doty A, Pao Y, Yang H, Chi NC, Magor BG, Traver D. 2013. An evolutionarily conserved program of B-cell development and activation in zebrafish. *Blood* **122**:1–11. doi:10.1182/blood-2012-12-471029

Palha N, Guivel-Benhassine F, Briolat V, Lutfalla G, Sourisseau M, Ellett F, Wang C-H, Lieschke GJ, Herbomel P, Schwartz O, Levraud J-P. 2013. Real-Time Whole-Body Visualization of Chikungunya Virus Infection and Host Interferon Response in Zebrafish. *PLoS Pathog* **9**:e1003619. doi:10.1371/journal.ppat.1003619

Petrie-Hanson L, Hohn C, Hanson L. 2009. Characterization of rag1 mutant zebrafish leukocytes. *BMC Immunol* **10**:1–8. doi:10.1186/1471-2172-10-8

Phan QT, Sipka T, Gonzalez C, Levraud JP, Lutfalla G, Nguyen-Chi M. 2018. Neutrophils use superoxide to control bacterial infection at a distance. *PLoS Pathog* **14**:1–29. doi:10.1371/journal.ppat.1007157

Radwanska M, Vereecke N, Deleeuw V, Pinto J, Magez S. 2018. Salivarian trypanosomosis: A review of parasites involved, their global distribution and their interaction with the innate and adaptive mammalian host immune system. *Front Immunol* **9**:1–20. doi:10.3389/fimmu.2018.02253

Ramakrishnan L. 2013. The zebrafish guide to tuberculosis immunity and treatment. *Cold Spring Harb Symp Quant Biol* **78**:179–192. doi:10.1101/sqb.2013.78.023283

Renshaw SA, Loynes CA, Trushell DMI, Elworthy S, Ingham PW, Whyte MKB. 2006. A transgenic zebrafish model of neutrophilic inflammation. *Blood* **108**:3976–3978. doi:10.1182/blood-2006-05-024075

Renshaw SA, Trede NS. 2012. A model 450 million years in the making: zebrafish and vertebrate immunity. *Dis Model Mech* **5**:38–47. doi:10.1242/dmm.007138

Ribeiro CMS, Pontes MJSL, Bird S, Chadzinska M, Scheer M, Verburg-van Kemenade BML, Savelkoul HFJ, Wiegertjes GF. 2010. Trypanosomiasis-induced Th17-like immune responses in carp. *PLoS One* **5**:e13012. doi:10.1371/journal.pone.0013012

Rifkin MR, Landsberger FR. 1990. Trypanosome variant surface glycoprotein transfer to target membranes: A model for the pathogenesis of trypanosomiasis. *Proc Natl Acad Sci U S A* **87**:801–805. doi:10.1073/pnas.87.2.801

Rosowski EE, Knox BP, Archambault LS, Huttenlocher A, Keller NP, Wheeler RT, Davis JM. 2018. The zebrafish as a model host for invasive fungal infections. *J Fungi* **4**. doi:10.3390/jof4040136

Russell DG, Cardona P-J, Kim M-J, Allain S, Altare F. 2009. Foamy macrophages and the progression of the human tuberculosis granuloma. *Nat Immunol* **10**:943–948. doi:10.1038/ni.1781

Saeij JPJ, Groeneveld A, Van Rooijen N, Haenen OLM, Wiegertjes GF. 2003. Minor effect of depletion of resident macrophages from peritoneal cavity on resistance of common carp Cyprinus carpio to blood flagellates. *Dis Aquat Organ* **57**:67–75. doi:10.3354/dao057067

Scharsack JP, Steinhagen D, Kleczka C, Schmidt JO, Körting W, Michael RD, Leibold W, Schuberth HJ. 2003. Head kidney neutrophils of carp (Cyprinus carpio L.) are functionally modulated by the haemoflagellate Trypanoplasma borreli. *Fish Shellfish Immunol* **14**:389–403. doi:10.1006/fsim.2002.0447

Sileghem M, Saya R, Grab DJ, Naessens J. 2001. An accessory role for the diacylglycerol moiety of variable surface glycoprotein of African trypanosomes in the stimulation of bovine monocytes. *Vet Immunol Immunopathol* **78**:325–339. doi:10.1016/S0165-2427(01)00241-0

Simpson AGB, Stevens JR, Lukeš J. 2006. The evolution and diversity of kinetoplastid flagellates. *Trends Parasitol* **22**:168–174. doi:10.1016/j.pt.2006.02.006

Sternberg JM, Mabbott NA. 1996. Nitric oxide-mediated suppression of T cell responses during Trypanosoma brucei infection: Soluble trypanosome products and interferon-γ are synergistic inducers of nitric oxide synthase. *Eur J Immunol*. doi:10.1002/eji.1830260306

Stijlemans B, Caljon G, Van Den Abbeele J, Van Ginderachter JA, Magez S, De Trez C. 2016. Immune evasion strategies of Trypanosoma brucei within the mammalian host: Progression to pathogenicity. *Front Immunol* **7**. doi:10.3389/fimmu.2016.00233

Stijlemans B, Guilliams M, Raes G, Beschin A, Magez S, De Baetselier P. 2007. African trypanosomosis: from immune escape and immunopathology to immune intervention. *Vet Parasitol* **148**:3–13.

Stijlemans B, Radwanska M, Trez C De, Magez S. 2017. African trypanosomes undermine humoral responses and vaccine development: Link with inflammatory responses? *Front Immunol* **8**:582. doi:10.3389/fimmu.2017.00582

Torraca V, Masud S, Spaink HP, Meijer AH. 2014. Macrophage-pathogen interactions in infectious diseases: New therapeutic insights from the zebrafish host model. *DMM Dis Model Mech*. doi:10.1242/dmm.015594

Torraca V, Mostowy S. 2018. Zebrafish Infection: From Pathogenesis to Cell Biology. *Trends Cell Biol* **28**:143–156. doi:10.1016/j.tcb.2017.10.002

Travnickova J, Tran Chau V, Julien E, Mateos-Langerak J, Gonzalez C, Lelievre E, Lutfalla G, Tavian M, Kissa K. 2015. Primitive macrophages control HSPC mobilization and definitive haematopoiesis. *Nat Commun* **6**:6227. doi:10.1038/ncomms7227

Vallochi AL, Teixeira L, Oliveira K da S, Maya-Monteiro CM, Bozza PT. 2018. Lipid Droplet, a Key Player in Host-Parasite Interactions. *Front Immunol* **9**:1022. doi:10.3389/fimmu.2018.01022

White RM, Sessa A, Burke C, Bowman T, LeBlanc J, Ceol C, Bourque C, Dovey M, Goessling W, Burns CE, Zon LI. 2008. Transparent Adult Zebrafish as a Tool for In Vivo Transplantation Analysis. *Cell Stem Cell* **2**:183–189. doi:10.1016/j.stem.2007.11.002

Woo PTK, Ardelli BF. 2014. Immunity against selected piscine flagellates. *Dev Comp Immunol* **43**:268–279. doi:10.1016/j.dci.2013.07.006

Wu H, Liu G, Shi M. 2017. Interferon gamma in African trypanosome infections: Friends or foes? *Front Immunol* **8**:4–10. doi:10.3389/fimmu.2017.01105

Wymann MP, Schneiter R. 2008. Lipid signalling in disease. *Nat Rev Mol Cell Biol*. doi:10.1038/nrm2335

Supplementary data

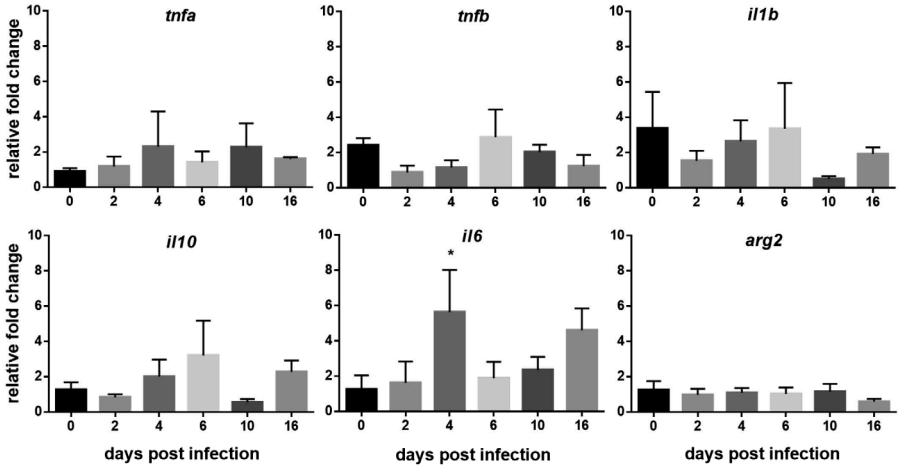

Supplementary Fig 1. Gene expression analysis on pooled larvae, is not sufficiently sensitive to reveal differences in immune response to *T. carassii* infection at different time points after infection. *Tg(mpeg1.4:mCherry-F;mpx:GFP)* zebrafish (5 dpf) were injected intravenously with 200 *T. carassii* or PVP control and sampled at various time points. At each time point 3-6 pools of 3-5 larvae were sampled for real-time quantitative PCR analysis. Relative fold change was normalised to the zebrafish-specific *ef1a* and expressed relative to the respective PVP-injected group. Bars indicate average and standard deviation (SD) on n=3-6 pools per time point.

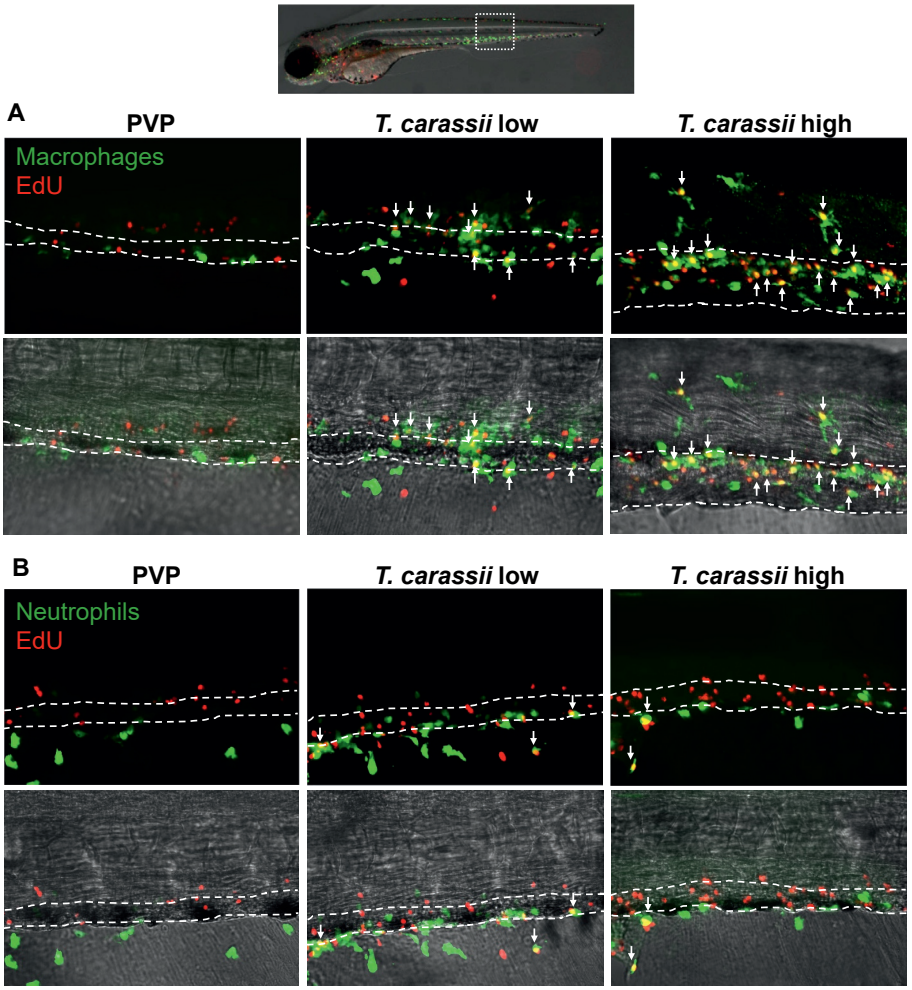

Supplementary Fig 2. Differential distribution of EdU+ macrophages and neutrophils along the caudal vein of high- and low-infected larvae. Zebrafish were treated as described in figure 5. **A)** A high number of macrophages can be seen around and inside the caudal vein. Especially in high-infected individuals, the majority of cells within the vessel was EdU+, suggesting that in these larvae, proliferating macrophages migrated to the vessels. **B)** Neutrophils were never observed within the caudal vein and, independently of whether they proliferated (EdU+) or not, were mostly observed lining the vessel.

CHAPTER 4

Swimming behaviour of the biflagellate *Trypanoplasma borreli*, a comparison to the uniflagellate *Trypanosoma carassii*

Sem H. Jacobs[1,2,#], Martin J.M. Lankheet[2,#], Kaylee S.E. van Dijk[1], Felipe Arditti[1,3], Remco P.M. Pieters[2], Henk Schipper[2], Geert F. Wiegertjes[1,4], Maria Forlenza[1]

[1] Cell Biology and Immunology Group, Department of Animal Sciences, Wageningen University & Research, Wageningen, The Netherlands

[2] Experimental Zoology Group, Department of Animal Sciences, Wageningen University & Research, Wageningen, The Netherlands

[3] Mechatronics Engineering Department, University of São Paulo, Brazil

[4] Aquaculture and Fisheries Group, Department of Animal Sciences, Wageningen University & Research, Wageningen, The Netherlands

[#] The authors equally contributed to the work.

Manuscript in preparation

Abstract

Trypanoplasma borreli is a protozoan parasite member of the suborder Bodonids, which diverged early in evolution from the order Trypanosomatida. *T. borreli* lives extracellularly in the blood and tissues of cyprinid fish and is often observed co-infecting with *Trypanosoma carassii.* Differently from trypanosomes, *T. borreli* has two flagella. Although the swimming behaviour and flagellar motility of trypanosomes has been well characterized, for biflagellate trypanoplasma this has remained largely unknown. In this study, we performed a quantitative analysis to compare *in vitro* the swimming behaviour, cell body characteristics and flagella behaviour of *T. borreli* and *T. carassii*. Although the anterior flagellum of both parasites exhibits comparable behaviour*, T. borreli* was observed to have a more variable and flexible cell body shape than *T. carassii* and showed a higher degree of directionality in its motion. Next, we established an experimental infection of zebrafish larvae with *T. borreli* that allowed us to visualise *in vivo* trypanoplasma swimming behaviour in the bloodstream and tissues of a vertebrate host. We show that both parasites are able to anchor themselves to host tissues and cells and that their attachment occurs via different parts of their cell body. Our study provides the first detailed characterization of the swimming behaviour of a biflagellate *in vitro* as well as *in vivo* in a vertebrate host. Considering the evolutionary position of *T. borreli*, their unique cell body morphology with two flagella, and their ability to infect the same host as other aquatic trypanosomes, our analysis may contribute to the understanding of the evolution of pathogenicity of kinetoplastids.

Introduction

The Trypanosoma genus contains human and animal pathogens, all transmitted by biting flies, including those that cause human diseases: Human African Trypanosomiasis caused by *Trypanosoma brucei* and American Trypanosomiasis caused by *T. cruzi* (Radwanska et al., 2018; Simpson et al., 2006). Trypanosomes have a single flagellum, which emerges from the posterior side, is attached to the body along the length of the cell body and extends freely at the anterior end of the cell body (Heddergott et al., 2012). The flagellum is a multifunctional organelle and its constant motion is a characteristic of the trypanosome lifestyle (reviewed by Ralston et al., 2009). Flagellum motility has shown to be essential for trypanosome survival in all the different environments they inhabit, from the bloodstream of mammals to the gut of the tsetse fly vector. In fact, it is important for cell division, infectivity and survival in the host. (Broadhead et al., 2006; Engstler et al., 2007; Griffiths et al., 2007; Langousis and Hill, 2014; Ralston et al., 2006; Shimogawa et al., 2018). *In vitro* studies on African trypanosomes have used methods such as high-speed videography and mathematical modelling to analyse parameters of trypanosome morphology and motility, and showed that trypanosomes are specialised in adapting to the various host's environments (Bargul et al., 2016; Engstler and Stark, 2015; Heddergott et al., 2012; Krüger and Engstler, 2015; Rodríguez et al., 2009; Uppaluri et al., 2011).

One of the best-studied non-mammalian trypanosomes is *Trypanosoma carassii*, which presents many morphological features of mammalian trypanosomes (Dóró et al., 2019; Lom, 1979; Overath et al., 1999, 1998). *T. carassii* is transmitted by blood-sucking leeches (*Hemiclepsis sp.*) to cyprinid fish, where it occurs extracellularly in the blood and tissues (**Chapter 3**, Dóró et al., 2019; Haag et al., 1998; Lom and Dyková, 1992; Overath et al., 1999). *T. carassii* is regularly observed co-infecting fish with *Trypanoplasma spp* (e.g. *T. borreli* in cyprinid fish) (Joerink et al., 2007; Lom, 1979). *T. borreli* is part of the Parabodonidae family, which diverged early in evolution from the well-described order Trypanosomatida (Hughes and Piontkivska, 2003; Lom, 1979; Simpson et al., 2006). Interestingly, while trypanosomes are parasites affecting all vertebrate species, members of the trypanoplasma (and cryptobia) species are mostly found in the aquatic environment, the majority of which are free-living non-parasitic protozoa (Simpson et al., 2006). Exceptions are *T. borreli*, *Cryptobia salmositica* and *C. bullock* (Hughes and Piontkivska, 2003; Woo and Thomas, 1991). *T. borreli* is an extracellular blood flagellate, also transmitted by blood-sucking leeches *(Piscicola sp.)* to cyprinid fish (Lom, 1979; Lukeš et al., 2014; Steinhagen et al., 1989). *T. borreli* causes cryptobiosis in cyprinid fish, characterised by anaemia and splenomegaly, and infects both wild and farmed fish (Bunnajirakul et al., 2000; Lom, 1979; Losev et al., 2015; Steinhagen et al., 1990; Woo, 2003). Trypanoplasma, differently from trypanosomes, have two flagella: one free flagellum that emerges from the anterior side of the cell body (flagellar pocket), and one recurrent (cell-attached) flagellum emerging from the same anterior side, running along the cell body and extending free at the posterior end (Lom, 1979).

Interestingly, although a wealth of information is available regarding morphology, swimming behaviour, flagellar motility and host-pathogen interaction of trypanosomes, very little is known about *Trypanoplasma* (*Cryptobia*) species. Considering their evolutionary position, parasitic nature, unique cell body possessing two flagella, and ability to infect the same vertebrate host as other aquatic trypanosomes, detailed analysis of *T. borreli* swimming behaviour, *in vitro* as well as *in vivo* in a vertebrate host, may aid understanding the evolution of pathogenicity of kinetoplastids.

Recently, we reported the establishment of a *T. carassii* infection model in zebrafish, a cyprinid fish closely related to the natural hosts of *T. carassii* and *T. borreli*. By combining the transparency of zebrafish larvae with high-speed videography, we were able to visualise, for the first time *in vivo,* novel swimming behaviours, attachment mechanisms and adaptation strategies of trypanosomes in the blood and tissues of a vertebrate host (Dóró et al., 2019, **Chapter 2**).

In the current study, we compared the motility of the biflagellate *T. borreli* with that of the uniflagellate *T. carassii*. Using high spatio-temporal resolution microscopy, we performed a detailed quantitative analysis comparing motility, cell body characteristics and flagella behaviour of *T. borreli* and *T. carassii in vitro.* Next, we established an experimental infection of zebrafish with *T. borreli* and for the first time visualised the *in vivo* swimming behaviour of a biflagellate in the blood and tissues of a vertebrate host. We show that the anterior flagellum of both parasites exhibits comparable behaviours, although one is cell-attached in *T. carassii* and the other is cell-free in *T. borreli*. Yet, the dynamics of their motions are very different. *T. borreli* has a more flexible, and dynamically changing, cell body shape than *T. carassii* and it swims more directional. Additionally, we show that also *T. borreli* is able to anchor itself to the vessel endothelium *in vivo*, and that attachment involves the cell body and neither of the two flagella. Our study provides the first detailed characterization of the swimming behaviour of a biflagellate *in vitro* and *in vivo* in a vertebrate host.

Materials and methods

Zebrafish lines and maintenance

Wild type zebrafish (AB strain) were kept and handled according to the Zebrafish Book (zfin.org) and animal welfare regulations of The Netherlands. Adult zebrafish were reared at the aquatic research facility of Wageningen University & Research (Carus). Zebrafish embryos and larvae were raised at 27°C with a 12:12 light-dark cycle in egg water (0.6 g/L sea salt, Sera Marin, Heinsberg, Germany). From 5 days post fertilisation (dpf) until 14 dpf, larvae were fed once a day with Tetrahymena. Larvae older than 10 dpf also received dry feed ZM-100 (zmsystem, UK) daily. All animals were handled in accordance with good animal practice as defined by the European Union guidelines for handling of laboratory animals (http://ec.europa.eu/environment/ chemicals/lab_animals/home_en.htm).

Trypanoplasma borreli and _Trypanosoma carassii_ culture and _T. borreli_ infection of zebrafish

Trypanoplasma borreli and *Trypanosoma carassii* (strain TsCc-NEM) were cloned and characterised previously (Steinhagen et al., 1989 and Overath et al., 1998) and maintained in our laboratory by syringe passage through common carp (*Cyprinus carpio*) as described previously (Dóró et al., 2019; Forlenza et al., 2008). *T. borreli and T. carassii* were kept at a density below $5x10^6$/ml, and sub-cultured 1-3 times a week. In this way, *T. borreli and T. carassii* could be kept in culture without losing infectivity for up to 1-2 months.

Prior to zebrafish infection, *T. borreli* were cultured for 1 week and no longer than 3 weeks. Parasites and any remaining white blood cell still present in the culture were centrifuged at 800 x g for 5 minutes in a 50 ml Falcon tube and the tube was subsequently tilted at a 20^0 angle relative to the table plane, facilitating the separation of the motile trypanosomes along the conical part of the tube from the static pellet of remaining white blood cells at the bottom. To study the swimming behaviour of *T. borreli in vivo* we established an experimental infection of zebrafish larvae, as described previously for *T. carassii* (Dóró et al., 2019). Briefly, zebrafish larvae (5 days post fertilisation (dpf)) were anaesthetised in 0.017% Ethyl 3-aminobenzoate methanesulfonate (MS-222, Tricaine, Sigma-Aldrich) in egg water and injected in the Duct of Cuvier with *n*= 200 *T. borreli*. Injected larvae were directly transferred into pre-warmed egg water and kept at 27°C. Viability was monitored daily. Lethargic fish showing no escape reflex to a pipette, were confirmed to be heavily infected upon microscopic analysis. The escape reflex was therefore used to monitor morbidity and the progression of infection. When necessary, fish were removed from the experiment and euthanized with an overdose of anaesthetic (0.4% MS-222).

High-speed light microscopy

For imaging of *T. borreli* and *T. carassii in vitro*, a volume of 7 µl of *T. borreli* and *T. carassii* culture (2-3 x 10^6 cells/ml) were transferred to non-coated microscopic slides (Superforst, Thermo Scientific), covered with a 24 x 50 mm coverslip. In this way one to three parasites could be imaged at the same time. Imaging started immediately and lasted for no longer than 10 minutes. A Photron APX-RS high-speed camera was mounted on an automated DM6b upright digital microscope (Leica Microsystems with Leica HC 1x Microscope C-mount Adapter), equipped with 100x oil objective (NA 1.32) (Leica Microsystems) and controlled by Leica LASX software (version 3.4.2.). 12-Bits greyscale images were obtained at a resolution of 768 x 880 pixels, and frame rate of 250 frames per second (fps). The spatial and temporal resolution in these videos were sufficient to analyse both cell body and flagella movements in detail.

High-speed videography of *T. borreli* swimming behaviour *in vivo* was performed as described previously (Dóró et al., 2019). Zebrafish larvae were anaesthetised in 0.017% MS-222 in egg water, embedded in 1.5% UltraPure LMP Agarose (Invitrogen) and positioned on the cover glass of a 35 mm petri dish (14 mm microwell, coverglass No. 0 (0.085-0.13mm),

MatTek corporation). The high-speed camera was mounted with a Leica HC 1x Microscope C-mount on a DMi8 inverted digital microscope (Leica Microsystems), controlled by Leica LASX software (version 3.4.2.) and equipped with 40x (NA 0.6) and 20x (NA 0.4) long distance objectives (Leica Microsystems). Images were acquired at 500 fps. In all cases, Photron FASTCAM Viewer (PFV) software (version 3.5.1) was used to control the camera and save the images. All high-speed videos were analysed using the PFV software (version 4.0.1.0) or MiDAS Player (version 5.0.0.3, Xcite, USA). All videos were produced using CyberLink PowerDirector-16.

Analysis of *T. borreli* and *T. carassii* swimming behaviour

High-speed movies were analysed in Python, using the OpenCV image processing toolbox. Parasites were detected and analysed in each frame, and their cell body and flagellum/a were tracked from frame to frame to quantify their motion (**Fig 1A**). To detect parasites in the image we first applied a Canny edge detection (**Fig 1B**), translating high contrasts in the greyscale image into a binary black and white image (**Fig 1C**). The filter extracted both the cell body and the flagellum/a of the parasite. To fill the empty space in between the edges and convert line patterns into solid objects, we applied a dilation and erosion to the image (**Fig 1D**). This solidifies the cell body and the flagellum/a, without affecting cell body size or thickness of flagellum/a. In the case of multiple parasites in one image, we tracked the motions of the parasites using a Kalman filter to keep track of their identity, and analysed each individual parasite separately. Flagellum/a were identified by means of an erosion followed by dilation, and labelling the parts that have been removed as the flagella. The erosion and dilation parameters were chosen to remove the thin flagella, while minimally affecting the bodies. Next, we determined the attachment points of the flagellum/a to the body as the overlap between a slightly inflated cell body and the previously detected flagellum/a. These attachment points were used to parameterize the flagellum/a, by means of an axis reconstruction, starting at the attachment point and ending at the tip of the flagellum. This provides information on the length of the flagellum (**Fig 2A**), as well as the location relative to the cell body. In case the procedure provided more than the number of flagellum/a expected (one for *T. carassii*, two for *T. borreli*) we selected the largest one(s). For *T. borreli* we identified the two flagella without identity swaps, by tracking the motion of their end points from frame to frame based on a nearest neighbour assessment, and distinguished the two flagella based on their mean length throughout the movie.

For the cells body without flagellum/a we determined the contour, the centre of mass (COM), the length-width ratio and the orientation of the long axis. Motion of the cell body was quantified as displacement of the COM. Cell body shape distortions were quantified by the length-width ratio (based on an ellipsoid fitted to the contour), and by the distance of the COM relative to the cell body contour (**Fig 2A**). Locations of the COM outside the cell body corresponded to negative distances. The directionality of movement was quantified as the

distance between the start and end-point of motion, divided by the length of the actual path taken (**Fig 2B**). We calculated directionality for several time intervals (between start point and end point) of 40, 80, 120, 160, 200 and 240 frames), equivalent to 0.16, 0.32, 0.48, 0.64, 0.80 and 0.96 seconds. For each interval a mean and a standard deviation was calculated by sliding the interval, frame by frame, across the full time-line of a track (with a minimum of 1000 frames (4 seconds).

To quantify the dynamics of motion parameters, we used the Fast Fourier transform (FFT). The FFT translates a time signal, e.g. speed as a function of time, into its frequency components. It describes fluctuations of the signal as a function of frequency; fast changes contribute to high-frequency components, slow changes to low-frequency components. The Fourier transform is a convenient signal processing tool as it provides a way to compare the dynamics of motion parameters, in case the motions are pseudo random and not synchronised.

Statistical analysis of motion parameters

Each separate track in a movie was considered an independent measurement. To compare motion parameters of the tracks of the *T. borreli* and *T. carassii*, we used a linear model with parasite type as fixed effect. Statistical analyses were performed in R (Rstudio, R-3.4.3).

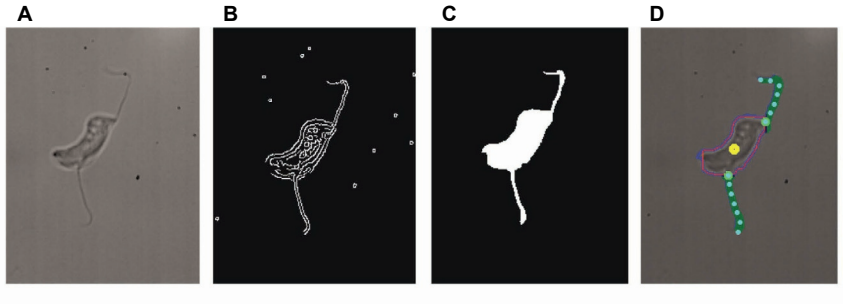

Fig 1. Illustration of image analysis steps.

A) Original image of a *T. borreli* parasite, a greyscale image at 100x magnification. **B)** Result of a Canny edge detection, a binary image highlighting high intensity gradients. **C)** A solid silhouette comprising cell body and flagella, after dilation and erosion. **D)** Original image with annotations: the blue contour shows the complete parasite including cell body and flagella, the red contour shows just the cell body with the centre of mass indicated by the yellow circle, the green filled contours show the two flagella, and the light-green circles show the equidistant points quantifying the flagella. The larger dot near the cell body indicates the point of insertion of the flagella on the cell body.

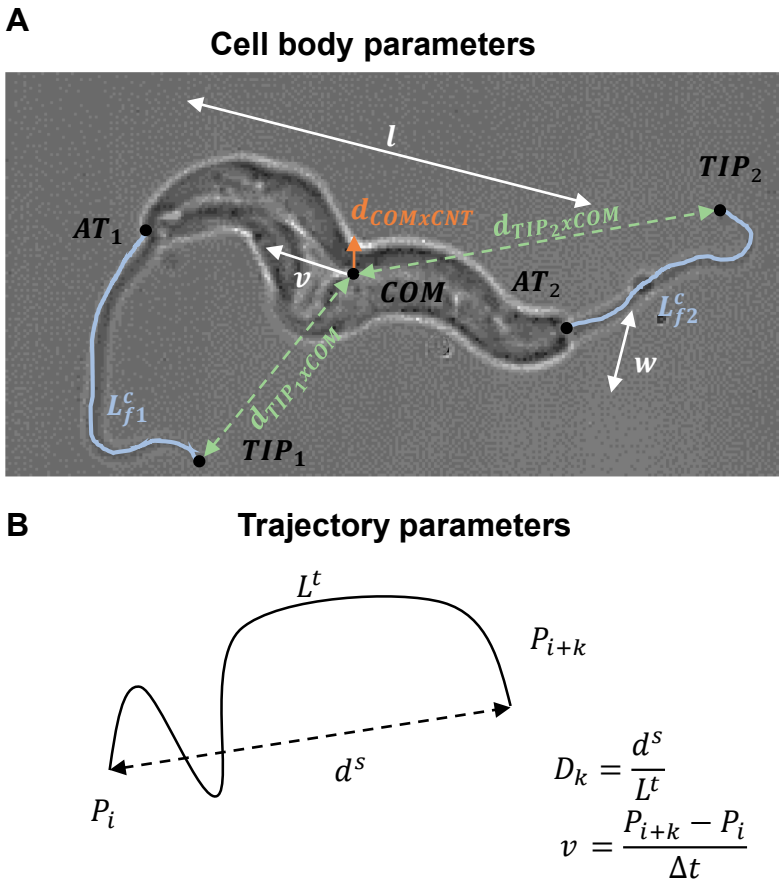

Fig 2. Cell body and trajectory parameters used to analyse and compare the swimming behaviour of T. *borreli* and *T. carassii*.

A) Parameters used to study the cell body characteristics. *l* = length of cell body, *w* = width cell body, *COM* = centre of mass, *v* = speed COM, v_l= longitudinal speed, v_b= orthogonal speed, $d_{COMxCNT}$ = distance centre of mass to contour, $AT_{1/2}$ = attachment point flagellum/ point where flagellum leaves cell body, $TIP_{1/2}$= tip of flagellum, $L^c_{f\,1/2}$ =length of contour of flagellum, $d^s_{f\,1/2}$= straight distance from TIP to AT, $d_{TIP_{1/2}xCOM}$ = distance TIP to COM. **B)** Parameters used to study the trajectory. P_i = position COM in frame i, P_{i+k}= position COM in frame i+k, L^t= tracked trajectory length from P_i to P_{i+k}, d^s = straight distance from P_i to P_{i+k}, D_k= directionality until frame k, *v*= speed, Δ*t*= time interval.

Results

Directional swimming and crumpling are typical *T. borreli* swimming behaviours

Here we aim to describe and compare the motility of the biflagellate *T. borreli* to that of the uniflagellate *T. carassii* by analysing their swimming trajectories, cell body characteristics and flagella behaviour *in vitro*. *Trypanoplasma borreli* has two flagella, an anterior and a posterior, whereas *T. carassii* has one flagellum, and have a considerable difference in cell body size with *T. borreli* being twice the size as *T. carassii* (**Fig 3**). Trypanosomes, like *T. carassii*, have the flagellar pocket at the posterior end from which the recurrent flagellum emerges and then runs along the cell body, ending free at the anterior (leading) end. Trypanoplasma, like *T. borreli,* have their flagellar pocket at the anterior end from which both flagella originate; the recurrent flagellum runs from the flagellar pocket along the cell body and ends free at the posterior (trailing) end, whereas the non-cell attached flagellum is free to move at the anterior (leading) end of the parasite (**Fig 3** and **Video 1**).

In vitro, T. borreli motility was characterized by two typical behaviours: 1) directional swimming interrupted by 2) crumpling, followed by directional swimming, most often in a direction different from the previous one. When swimming directionally, *T. borreli* had an elongated cell body and waves originating from the flagellar pocket at the anterior end propagated posteriorly through the recurrent flagellum along the cell body (**Fig 4A** and **Video 1**). When directional swimming was interrupted, the cell body shape changed from elongated into a wrinkled shape, in a way that resembles the crumpling of a sheet of paper into a ‘paper ball’ (**Fig 4B** and **Video 1**). After this, the trypanoplasma would elongate itself again and resume swimming directionally, most often in a different direction (**Fig 4B** and **Video 1**).

Interestingly, we observed that *T. borreli*, similarly to *T. carassii* (**Chapter 2**, Dóró et al., 2019), can anchor itself to the glass surface as well as to red blood cells or leukocytes (**Video 2**). While *T. carassii* attached through a discrete area at the posterior tip of the cell body leaving both, the cell body and the flagellum free to move, *T. borreli* attached through the cell membrane at a location central to its cell body. This effectively anchored the centre of the cell body to the surface while leaving both flagella free to move (**Video 2**). To quantitatively compare swimming patterns of *T. borreli* and *T. carassii*, we next analysed changes in cell body shape, motility and flagellum behaviour.

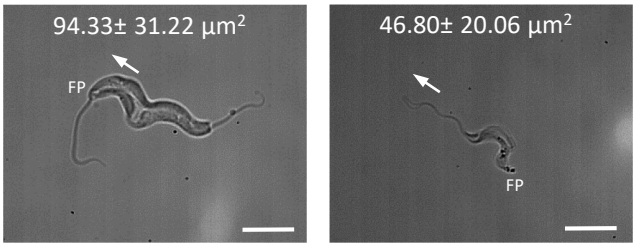

Fig 3. Biflagellate *T. borreli* and uniflagellate *T. carassii*.

Images (100x magnification) of freshly isolated parasites showing the major morphological differences between *T. borreli* (left) and *T. carassii* (right), indicating the mean cell body surface area, excluding the flagella, calculated over n=41 *T. borreli* and n=33 *T. carassii*. The flagellar pocket (FP) indicates the anterior end of *T. borreli*, and the posterior end of *T. carassii*; arrows indicate the swimming direction. Scale bar indicates 10 µm.

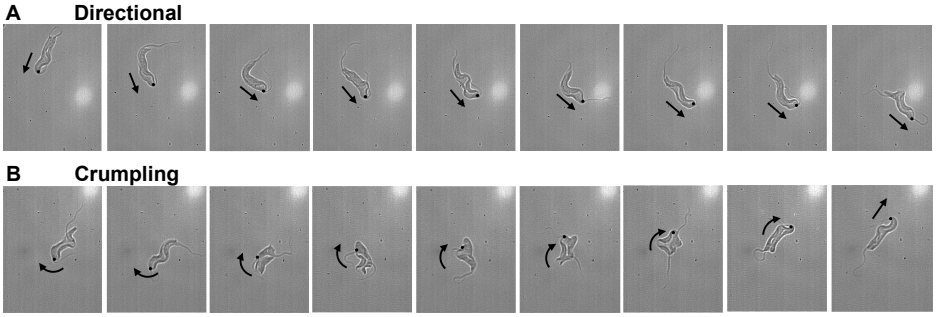

Fig 4. *T. borreli* alternates between directional swimming and crumpling.

T. borreli motility *in vitro* is characterized by **A)** directional swimming followed by **B)** changes in cell body shape that entail wrinkling of the cell membrane in a manner resembling the crumpling of a sheet of paper into a 'paper ball'. After this, *T. borreli* elongates itself again and resumes swimming directionally, in this case, in a direction different from the original one. Arrows indicate swimming direction; black dot indicates the anterior end of the parasite for easier orientation. Images are frames selected from the corresponding **Video 1**.

T. borreli* swims more directionally than *T. carassii

We quantitatively analysed the trajectory's parameters by measuring the directionality (D) of the centre of mass (COM) considering the distance (d) between two points on the trajectory and the actual length (L) of the path between the two points (**Fig 5A**). For *T. borreli* and *T. carassii* we first compared the changes in directionality during varying time intervals (**Fig 5C**), followed by comparison of the time-averaged directionality values (**Fig 5D**).

When looking at the trajectories of one representative *T. borreli* and *T. carassii* (**Fig 5B**), we see that both parasites alternate between periods of directional swimming and tumbling. Overall, we observe that *T. borreli* swims directionally for longer periods than *T. carassii* and that the trajectory of *T. carassii* shows more frequent tumbling behaviour. This is supported by the detailed analysis of directionality showing that during longer time intervals, *T. borreli* has higher (average) directionality values (0.80 and 0.96 s, orange and red lines/bars) and thus swims more directional than *T. carassii* (**Fig 5C** and **5D**). For short time intervals however (0.16 and 0.32 s, dark and light blue lines/ bars), both parasites show larger fluctuations indicating fast changes in swimming directionality (**Fig 5C** and **5D**; dark blue and light blue lines/bars). For both parasites, the time-averaged directionality values are higher for the shorter time intervals (e.g. 0.16 and 0.32 s, dark and light blue bars), and decrease with the length of the interval (e.g. 0.80 and 0.96 s, orange and red bars) (**Fig 5D**). Thus, during short time intervals the rapid changes in swimming direction have a larger impact on directionality values than during longer time intervals. In fact, both parasites can rapidly change swimming direction, which is typical of a low Reynolds number regime in which inertial forces are irrelevant.

Finally, with respect to the directionality at population level, we quantitatively compared the mean directionality values at each time interval for all analysed parasites (**Fig 5E**). At all time intervals, *T. borreli* shows higher values than *T. carassii*, confirming that *T. borreli* swims more directionally than *T. carassii* (**Fig 5E**). Whereas the mean directionality values for *T. borreli* are somewhat normally distributed, with nearly equal number of values above and below the median value (**Fig 5E**), for *T. carassii*, a group of parasites can be observed showing very low directionality, especially during longer time intervals (at 0.80 and 0.96 s) (**Fig 5E**). These low directionality values correspond with tumbling behaviour and indicate that more tumblers were observed for *T. carassii* than for *T. borreli*.

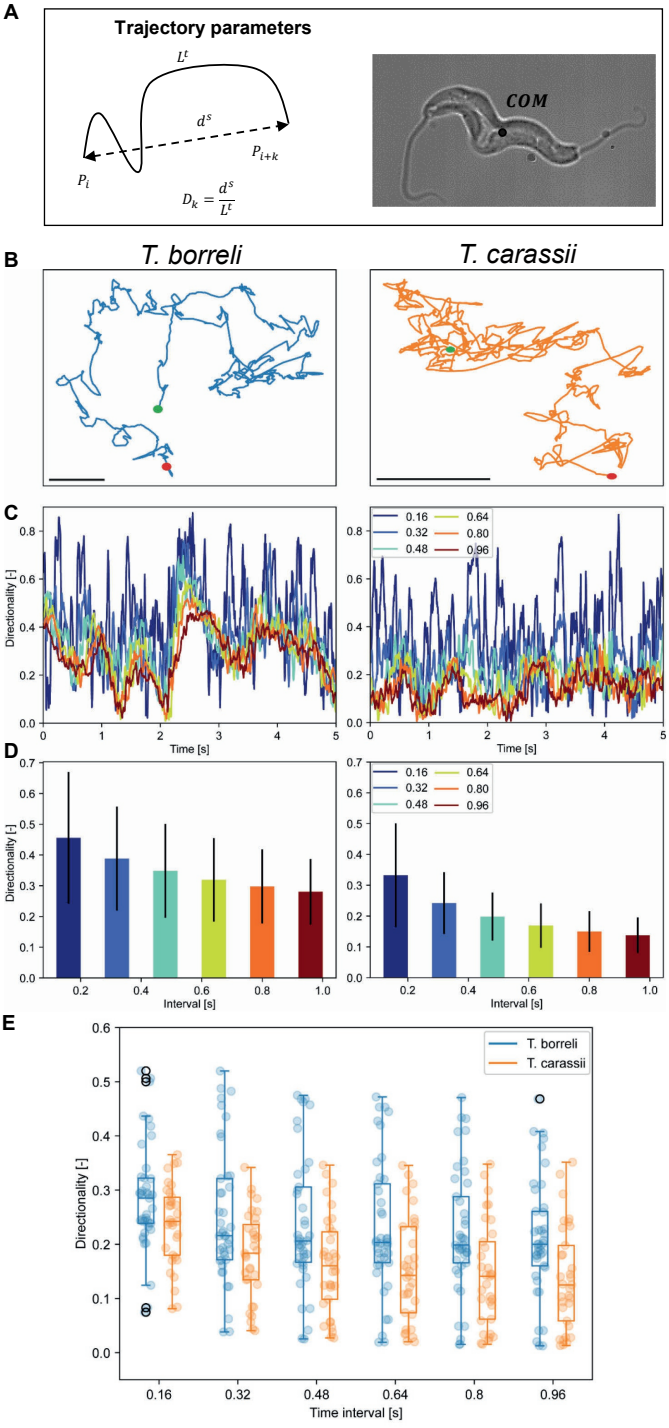
A
Trajectory parameters
L^t
d^s
P_{i+k}
P_i
$D_k = \frac{d^s}{L^t}$
COM
B
T. borreli
T. carassii
C
Directionality [-]
Time [s]
0.16
0.32
0.48
0.64
0.80
0.96
D
Directionality [-]
Interval [s]
E
Directionality [-]
Time interval [s]
T. borreli
T. carassii

◂ Fig 5. *T. borreli* swims more directional than *T. carassii.*
A) Overview of parameters used to analyse the trajectory and directionality. *COM* = centre of mass, P_i = position COM in frame i, P_{i+k} = position COM in frame i+k, L^t = tracked trajectory length from P_i to P_{i+k}, d^s = straight distance from P_i to P_{i+k}, D_k = directionality for interval duration k. **B)** Representative examples of trajectories for *T. borreli* (left) and *T. carassii* (right). Green and red spots mark the start and the end of the trajectory, respectively. Scale bar represents 5 μm. **C)** Change of directionality in time (5 seconds) for the examples in B. Different lines correspond to different time intervals (k corresponding to 40, 80, 120, 160, 200 and 240 frames of the corresponding high-speed video; equivalent to 0.16, 0.32, 0.48, 0.64,0.8 and 0.96 seconds). A time-line is obtained by sifting an interval of duration k, frame by frame, along the length of the recorded track. Measurements for different time intervals are aligned by their mid-point. **D)** Time-averaged directionality values of the data shown in C. Error bars represent standard deviations. **E)** Boxplots showing the distribution of the mean values of the directionality (as shown for the examples in D) for all *T. borreli* (n=41) and T. *carassii* (n=33). Scatterplots indicate the mean directionality value of individual parasites (with minimum trajectory length of 4 seconds). Black circles indicate outliers.

T. borreli swimming behaviour is dominated by slow variations in speed

In addition to analysing differences in directionality of swimming, we also analysed the changes in speed, irrespective of the swimming direction. Speed was quantified by displacements of the COM. Analysing representative examples of *T. borreli* and *T. carassii*, we observed for both parasites large and mostly irregular fluctuations in their speed (**Fig 6A**), indicating that both parasites have highly variable swimming speeds. To compare the fluctuations in speed, we calculated the corresponding Fourier transforms (**Fig 6B**), which describe the fluctuations of the signal as a function of frequency: fast changes in speed contribute to high-frequency components, whereas slow changes in speed to low-frequency components. Analysis of the changes in speed of a representative *T. borreli* revealed that it has broad fluctuations in swimming speed, dominated by slow variations in speed (**Fig 6B**, large speed amplitudes at low frequency). Conversely, the variations in speed of *T. carassii* showed no clear predominance for fast or slow changes (**Fig 6B**, comparable speed amplitude at low and high frequencies). These observations were supported when analysing the variations in speed at population level (**Fig 6C**). On average, *T. borreli* shows slightly higher values at all frequencies than *T. carassii,* but the difference is most prominent at the lower frequencies, corroborating our observation that *T. borreli* movements are dominated by relatively slow changes in speed (**Fig 6C**). Larger speed variations for *T. borreli* than *T. carassii* were also reflected in larger standard deviations of the speeds (**Fig 6D**, right), whereas the mean speeds on population level for *T. borreli* (v=31.18±9.44 μm/s) and *T. carassii* (v=27.46±12.35 μm/s) were comparable (**Fig 6D**, left).

Altogether, our analysis demonstrated that on average the two parasites swim at a comparable mean speed, but that *T. borreli* has larger variations in speed than *T. carassii*, and that these variations predominantly occur slowly.

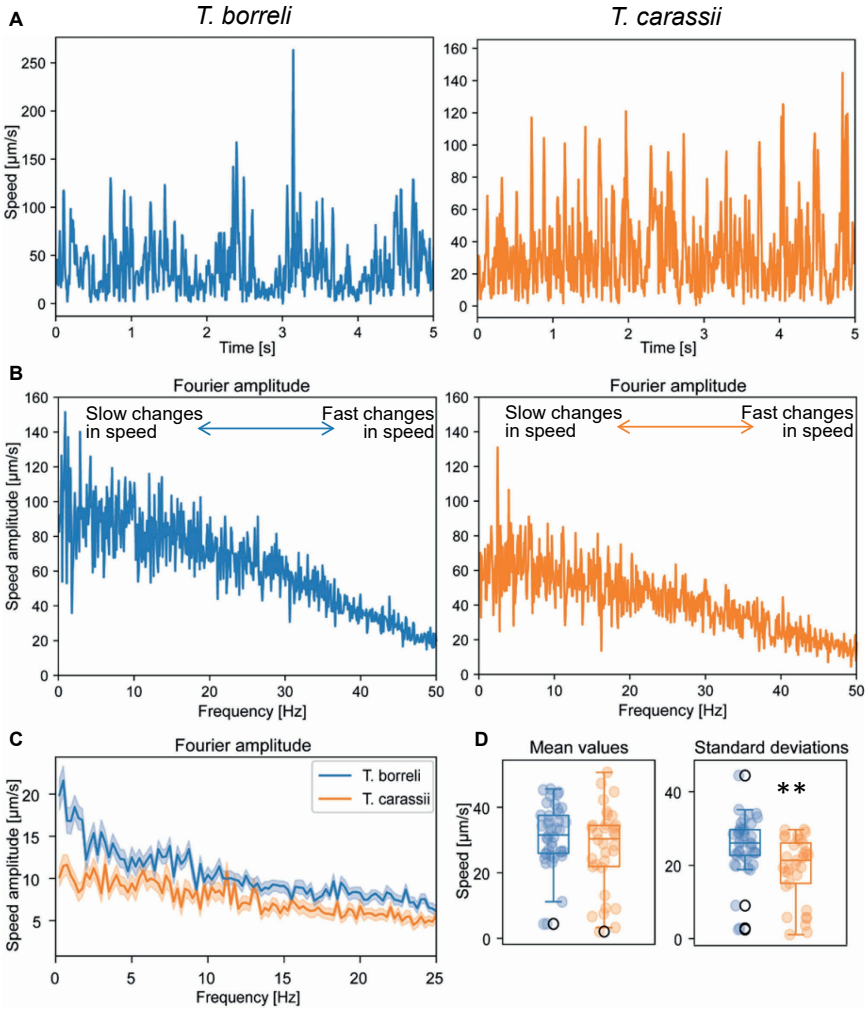

Fig 6. *T. borreli* swimming behaviour is dominated by larger variations in speed, which occur slowly compared to *T. carassii*.

A) Representative examples of swimming speed for *T. borreli* (left) and for *T. carassii* (right) calculated over a 5 seconds interval. Swimming speed was quantified by the frame-by-frame displacement of the COM **B)** Fourier transform of the changes in speed of the representative examples shown in A, describing the amplitude of speed variations as a function of frequency. Fast changes in speed contribute to high-frequency components, whereas slow changes in speed contribute to low-frequency components **C)** Fourier transforms averaged for *T. borreli* (n=41) and *T. carassii* (n=33). Confidence intervals (shades) show standard errors of the mean. Trajectories were analysed over a period of 4 seconds. **D)** Boxplots of the mean speeds (left) and corresponding standard deviations (right) of all analysed parasites as mentioned in C. Scatter plots show individual data points. ** indicates significant differences ($P<0.01$) between means as assessed by Linear Mixed Model without random effects. Black circles indicate outliers for the box plots.

T. borreli* has a more variable and flexible cell body shape than *T. carassii

The changes in direction and speed as previously described occur owing to changes in cell body shape and movements of the flagella. To compare changes in cell body shape, we analysed three different parameters (**Fig 7A**): (1) surface area of the cell body's silhouette, (2) the length-width ratio of an ellipsoid fitted to the body contour without the flagella, and (3) the distance between the centre of mass (COM) and the cell body contour (CNT). The length-width ratio and COM-CNT distance are highly sensitive to both elongation and curvature. For each parameter we determined the mean values and corresponding standard deviations for all analysed parasites (**Fig 7B-D**). In addition, we quantified the changes in cell body shape by means of a frequency analysis (Fourier transforms) as performed for speed (**Fig 7E-F**).

As expected, the mean surface area of the cell body's silhouette of *T. borreli* (94.33± 31.22 μm^2*)*, was significantly larger than that of *T. carassii* (46.80± 20.06 μm^2) (**Fig 7B**, left). *T. borreli* showed higher variation in surface area than *T. carassii*, as indicated by the larger standard deviations (**Fig 7B**, right). This result confirms our visual observations (**Video 1**) that *T. borreli* has a more flexible and variable cell body shape whereas *T. carassii* has a more rigid and invariable cell body.

Analysis of length-width ratio revealed that, on average, *T. borreli* has a more elongated cell body than *T. carassii* (**Fig 7C**, left). When considering the variation of the length-width ratio, *T. borreli* showed higher standard deviations than *T. carassii* (**Fig 7C**, right), substantiating the cell body's surface area observations. Whereas the mean surface area of *T. borreli* was significantly larger than that of *T. carassii*, no significant differences were observed in the distance COM-CNT between two parasites (**Fig 7D**, left). *T. borreli*, however, showed substantially higher variations in COM-CNT distance (**Fig 7D**, right), which supports the finding that *T. borreli* has a more flexible cell body than *T. carassii.*

The fluctuations in all aforementioned parameters (surface area of the cell body's silhouette, length-width ratio and distance COM-CNT), characterised by the Fourier transforms, show a comparable trend as observed for the speed: *T. borreli* shows relatively slow changes in all analysed cell body parameters (large amplitudes especially at low frequency) (**Fig 7E-G,** blue line). Conversely, cell body parameters of *T. carassii* remained predominantly unchanged (low amplitudes with little variation across frequency) (**Fig 7B-D**, right), confirming its rigidity. If changes occurred, they showed no clear predominance for fast or slow changes (**Fig 7E-G**). The similarity in cell body shape parameters suggests that they may arise from a common underlying pattern of cell body movements.

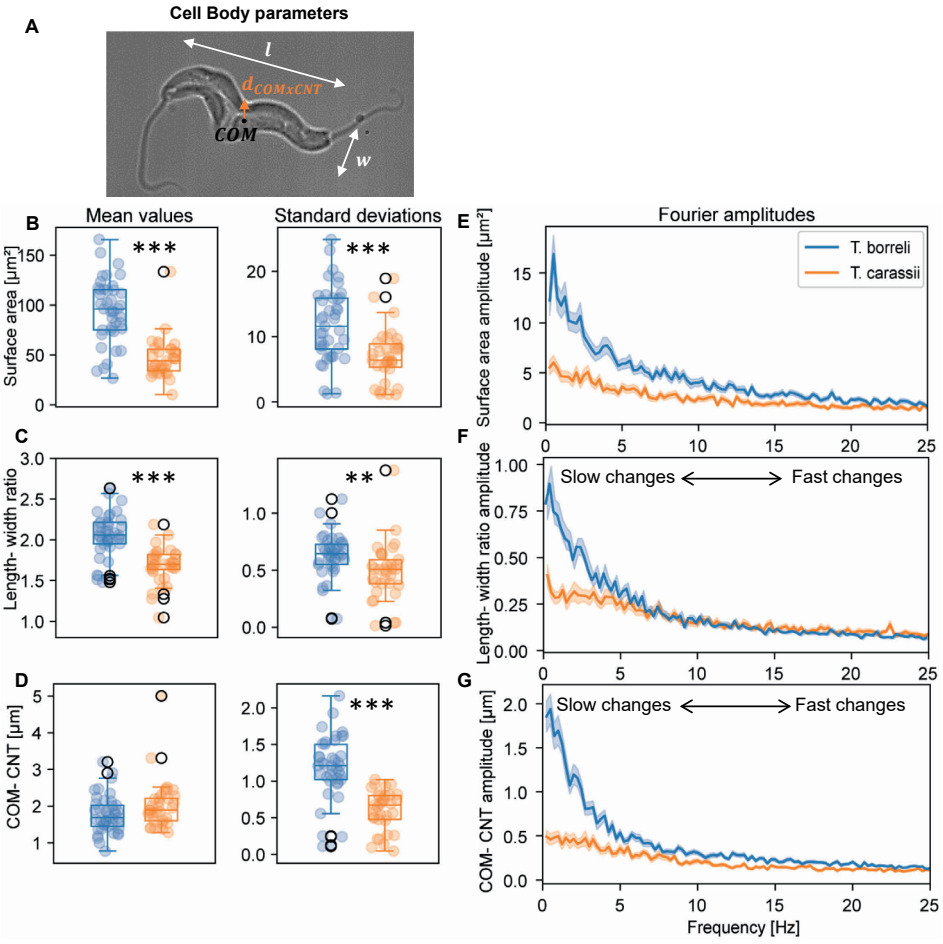

Fig 7. *T. borreli* has a large, flexible and elongated cell body in comparison to *T. carassii*.
A) Overview of parameters used to analyse the cell body. *l* = length of cell body, *w* = width cell body, *COM* = centre of mass, $d_{COMxCNT}$ = distance centre of mass to contour. **B-D-left)** Boxplots of the mean surface area of the cell body's silhouette (B), mean length-width ratio (C), and mean distance between centre of mass (COM) to contour (CNT) (D) calculated over n=41 *T. borreli* and n=33 *T. carassii*. **B-D-right)** Boxplots of the standard deviations of the corresponding aforementioned parameters measured for all analysed parasites. Scatter plots show individual data points. * indicates significant differences (**= P<0.01, ***=P<0.001) between means as assessed by Linear Mixed Model without random effects. Black circles indicate outliers for the boxplots. Trajectories were analysed over a period of 4 seconds. **E-G)** Fourier transforms averaged for all analysed parasites, providing the average changes in cell body's surface area (E), length-width ratio (F), and distance between centre of mass (COM) to contour (CNT) (G). Confidence intervals (shades) show standard errors of the mean. Trajectories were analysed over a period of 4 seconds. These transforms describe the fluctuations of the aforementioned parameters as a function of frequency; fast changes contribute to high-frequency components, slow changes to low-frequency components.

The anterior flagellum of *T. borreli* and *T. carassii* have a comparable behaviour

As previously described, *T. carassii* has one flagellum whereas T. *borreli* has two flagella; both parasites have a cell-attached flagellum that emerges from the flagellar pocket, runs through the cell body and ends free at the opposite end. Trypanosomes, like *T. carassii*, have the flagellar pocket at the posterior end, where the cell-attached flagellum originates. This cell-attached flagellum runs along the cell body ending free at the anterior (leading) end. For *T. borreli,* both flagella originate from a single flagellar pocket that is located at the anterior end of the parasite. The recurrent flagellum runs from the flagellar pocket along the cell body and ends free at the posterior end, whereas the non-cell-attached flagellum is free to move at the anterior (leading) end of the parasite (**Fig 8A**). To gain insight in the role of the flagella, we analysed three parameters: (1) flagella length, measured as the length of (the portion of) the flagellum that is not attached to the cell body; (2) distance from the flagellum tip to the COM and; (3) the speed of the tip of the flagellum (**Fig 8B**).

Measurements of flagellum length confirmed our visual observations (**Fig 8A-B**) that the anterior (non-cell-attached) flagellum of *T. borreli* is longer than the posterior flagellum (**Fig 8C**, blue and green bars) and is comparable in length to the anterior flagellum of *T. carassii* (**Fig 8C**, orange bars). In fact, the anterior flagellum of *T. borreli* and *T. carassii* could reach lengths ≥17.5 µm whereas the posterior flagellum of *T. borreli* was only seldomly longer than 10 µm.

By analysing the distance of the flagellum tip to the COM (**Fig 8D**), we can compare differences in flagella movements with respect to the cell body; for example, whether it freely swings in front (or behind) the parasite or whether it is more often close to or away from the cell body. For the shorter, posterior flagellum of *T. borreli*, we found relatively short distances, as expected for the shorter length of the flagellum. (Fig 8D, green bars). This is depicted by the left-skewed distribution resulting from the frequent low distance values (**Fig 8D**, green bars). The curve for the longer, anterior flagellum of *T. borreli* had a more symmetric distribution, suggesting that this flagellum makes large amplitude movements with the tip moving towards and away from the COM (**Fig 8D**, blue bars). The anterior flagellum of *T. carassii* showed a distribution similar to the anterior flagellum of *T. borreli*, although it is slightly more skewed towards lower values (**Fig 8D**, orange bars). This indicates that the anterior flagellum tip of *T. carassii* is more often close to the COM than the anterior flagellum tip of *T. borreli* is, consistently with the tumbling behaviour of *T. carassii* reported earlier (**Fig 5**).

The distributions of flagellum tip speeds revealed that the anterior flagellum of *T. borreli* moved more frequently at lower speed than the posterior flagellum tip of *T. borreli* (**Fig 8E**, blue and green bars). The posterior flagellum of *T. borreli* showed relatively higher occurrence of middle speed range. In other words, it moves at a more constant, average speed with fewer deviations into the low speed range. The tip speed of the

anterior flagellum of *T. carassii* displayed comparable speeds to the anterior flagellum of *T. borreli* (**Fig 8E**, orange and green bars). Altogether these three parameters indicate that the behaviour of the anterior (non-cell-attached) flagellum of *T. borreli* is similar to that of the anterior (cell-attached) flagellum of *T. carassii.* In addition, *T. borreli* has a cell-attached posterior flagellum that behaves differently than the non-cell-attached anterior flagellum.

Swimming behaviour of *T. borreli* in the vasculature

After performing a novel quantitative analysis to compare the *in vitro* swimming behaviour, cell body characteristics and flagella behaviour of *T. borreli* and *T. carassii.* Next, made use of the transparency of zebrafish larvae to visualise *in vivo T. borreli* swimming behaviour in the dynamic environments of a vertebrate host. These included the blood, and upon extravasation, tissues and tissue fluids of zebrafish. To this end, 5 dpf zebrafish were infected with *T. borreli* and imaged at various time points after infection using either live stream imaging (20/22 fps) or high spatio-temporal resolution microscopy (500 fps). Early during infection (1-2 days post infection (dpi)), when parasitaemia is still low, *T. borreli* could be observed in large-size vessels such as the cardinal caudal vein and artery (**Video 3**). Detection of *T. borreli* in large-size vessels with an intact blood flow and high density of red blood cells (RBC), was strongly aided by the use of high-speed microscopy. Under these conditions, *T. borreli* were generally passively dragged by the flow along with RBC (**Video 3**). Already at this early time point, *T. borreli* extravasate and can be detected in the interstitial tissue between the cardinal vessels. Interestingly, in small vessels of one-cell diameter, such as the intersegmental capillaries (ISCs), *T. borreli* was seldomly observed. In fact, as seen in **Video 3**, several parasites pass through the vein and artery, but none enters the capillary. Later during the infection (>3 dpi), as the number of parasites increases and the number of RBC decreases due to the onset of anaemia, *T. borreli* could be detected in ISCs; it had an elongated cell body shape and moved forward in the direction of the flow along with RBC (**Video 3**).

The use of high-speed videography also allowed visualisation of additional swimming behaviours of *T. borreli* in the blood. In the cardinal caudal vein, we detected several *T. borreli* that were able to (temporarily) resist the blood flow and either tumble on the vessels wall or anchor themselves to the vein endothelium (**Video 4**). Anchoring of *T. borreli* occurred in a manner similar to that described *in vitro* (**Video 2**). Both flagella and the flexible cell body were free to move suggesting that the flagella do not serve as anchoring sites. At the current resolution however, it was not possible to ascertain the exact anchoring point *in vivo*. Anchoring or tumbling was never observed in arteries or capillaries, independently of the speed of the blood flow (**Video 4**).

Movements of *T. borreli* in fluids outside the blood vessels and in tissues

We observed *T. borreli* extravasation as early as 1h after injection (not shown), but it was widespread from 2 dpi onwards. Extravasation allowed us to study the motility and behaviour in tissues and fluids outside the blood vessels, in the absence of red blood cells and blood flow. Locations for extravasation included, but were not limited to, the interstitial space lining the cardinal vessels, intraperitoneal cavity, heart cavity, muscle tissue, and fins (**Video 5**). Interestingly, when *T. borreli* was in the interstitial spaces lining the cardinal vein or in stationary fluids without hydrodynamic flow and blood cells, it mostly adopted a tumbling behaviour (**Video 5**). In the compact tissue of the anal or pectoral fins however, the biflagellate adopted an elongated form, swimming directionally in the narrow spaces of the fin epithelium. When the path of the parasite was interrupted, it crumpled (as previously observed *in vitro*) and effectively inverted its swimming direction (**Video 5**). The flexibility of the cell body of *T. borreli*, allowed it to navigate through variable gaps in the compact tissue of the fins.

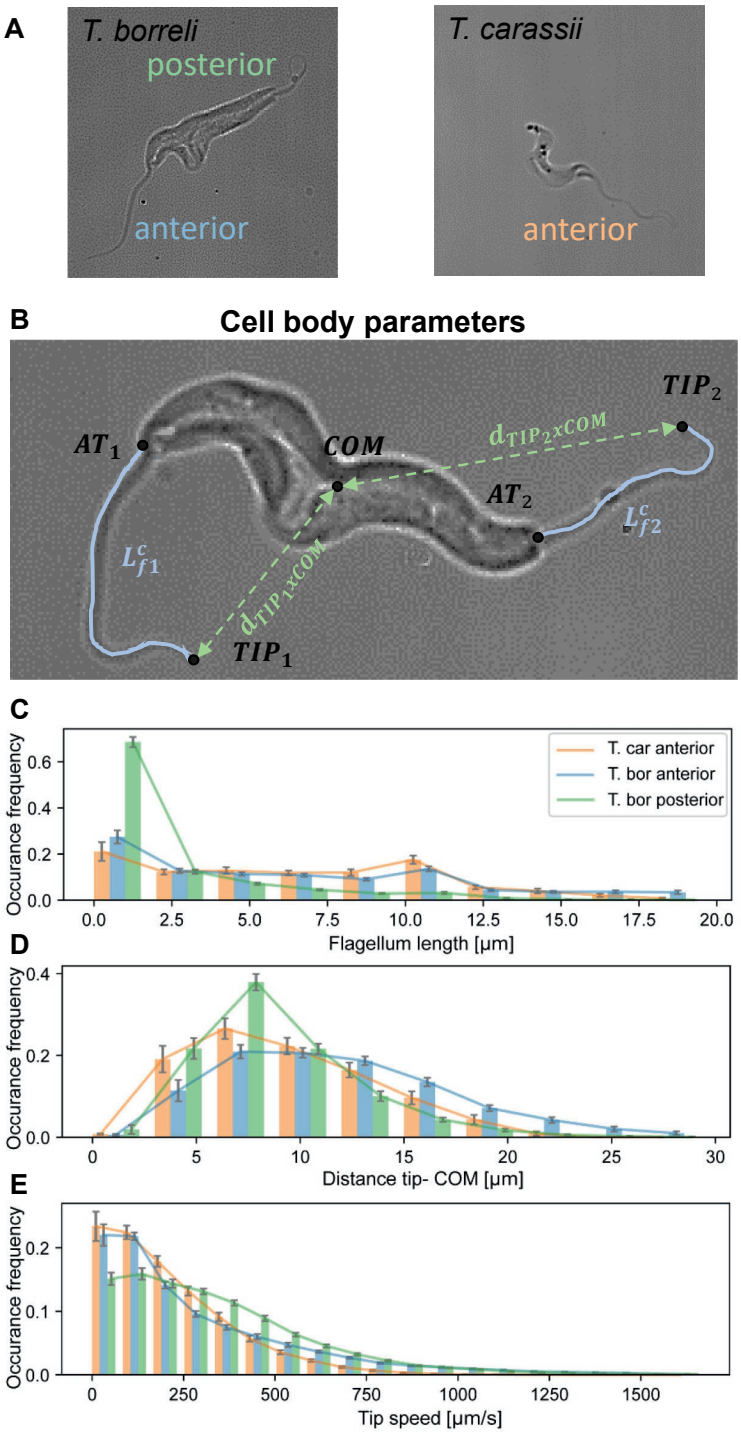
A
T. borreli
posterior
anterior
T. carassii
anterior
B
Cell body parameters
TIP_2
AT_1
COM
d_{TIP_2xCOM}
AT_2
L^c_{f2}
L^c_{f1}
d_{TIP_1xCOM}
TIP_1
C
Occurance frequency
T. car anterior
T. bor anterior
T. bor posterior
Flagellum length [µm]
D
Occurance frequency
Distance tip- COM [µm]
E
Occurance frequency
Tip speed [µm/s]

◂ Fig 8. Comparable anterior flagella behaviour.
A) Representative images indicating the anterior (blue) and posterior (green) flagellum of *T. borreli* and the anterior (orange) flagellum of *T. carassii*. **B)** Overview of the parameters used to analyse flagella behaviour; for simplicity only *T. borreli* is shown. *T. borreli* is oriented as in A. *COM* = centre of mass, $AT_{1/2}$ = point were flagellum leaves the cell body, $TIP_{1/2}$ = tip of flagellum, $L^{c}_{f\,1/2}$ =length of contour of flagellum, $d^{s}_{f\,1/2}$ = straight distance from TIP to AT, $d_{TIP_{1/2}xCOM}$ = distance TIP to COM. **C-E)** Flagellum length (C), distance of flagellum tip to centre of mass (COM) (D)**,** and tip speed (E) plotted against the normalised frequency of occurrence. The bars are coloured according to the flagella as explained in A. Trajectories were analysed over a period of minimum 2 seconds.

Discussion

In this study we describe for the first time motility of the biflagellate trypanoplasma and compare it to the motility of the uniflagellate trypanosome, by analysing the swimming trajectories, cell body shape dynamics and flagella behaviour *in vitro*. In addition, we established an experimental infection of zebrafish larvae with *T. borreli* that allowed us to visualise its movements *in vivo* in the bloodstream and tissues of a vertebrate host.

The swimming behaviour of *T. borreli* was characterised by directional swimming interrupted by “crumpling”, similar to the wrinkling of a paper ball, which allowed *T. borreli* to change its swimming direction. The “crumpling” movement is unlike any other observed for (uniflagellate) trypanosomes, e.g. *T. carassii*. We showed that *T. borreli* has larger variations in speed compared to *T. carassii,* and these were predominantly slow fluctuations. Further, *T. borreli* has on average a larger, more flexible and elongated cell body in comparison to *T. carassii.* Remarkably, the behaviour of the anterior (non-cell-attached) flagellum of *T. borreli*, behaved in a similar manner as the anterior (cell-attached) flagellum of *T. carassii*. We observed *T. borreli* was able to anchor itself both *in vitro*, to glass surface or cells, and *in vivo* to the vessel wall through its cell membrane, leaving both flagella free to move. By combining the transparency of zebrafish larvae with high spatio-temporal resolution microscopy, we were able to analyse the *in vivo* swimming behaviour of *T. borreli* in blood, tissues and tissue fluids of a vertebrate host. We observed that *T. borreli* was able to (temporarily) resist the blood flow and either tumble on the vessels wall or anchor itself to the vein endothelium of the cardinal caudal vein.

We observed *in vitro* that the motility of *T. borreli* has characterised by broad, low-frequency fluctuations in speed. The fluctuations in speed of *T. carassii*, had a uniform distribution, with no clear predominance for fast or slow changes. A similar trend was observed for the analysed cell body shape parameters. The correlation between speed and cell body shape was expected, since in an environment dominated by viscous forces (low Reynolds number), inertia plays no role and speed changes instantaneously follow variations in shape (Purcell,

1977).

Despite the differences in speed fluctuation for *T. borreli* and *T. carassii*, the mean speed of the parasites was very similar (31.18 µm/s for *T. borreli* and 27.46 µm/s for *T. carassii*). The cell body size, which was analysed via 2D measurement of the cell body surface area, was on average two times larger size for *T. borreli* than for *T. carassii*. Based on these data one might expect substantially higher power requirements (which is equal to speed times force, where force scales with cell body size), and hence energy consumption, for *T. borreli* compared to *T. carassii*. However, we observed that *T. borreli* had slower variations in its speed and cell body shape (low frequencies observed in the Fourier transform analysis) than *T. carassii*. These slow variations corresponded to more directional swimming, especially over longer time intervals. Such an increase in directionality might (partly) compensate for the larger energy consumption. For a more detailed analysis of power requirements, 3D measurements and extensive Computational Fluid Dynamics simulations could be performed, which fall beyond the scope of the present analysis.

As suggested before by Uppaluri et al (2011), trypanosome cell body shape can be interpreted as an indicator for directionality, since more directional movements are related to a more elongated cell body. For *T. borreli* we observed an elongated cell body shape, alternated with periods in which the cell body shape changed from elongated into a “crumpled paper ball”. This “crumpling” movement of *T. borreli* was not observed for *T. carassii*, and to our knowledge was never described for other trypanosome species. The observed difference in cell body flexibility is supported by differences in cell body morphology and cytoskeleton architecture. The rigid cell body of trypanosomes has asymmetric chirality, with the single cell-attached flagellum running around the body and creating torsion in the cell body. The cell-attached flagellum of trypanoplasma runs along the flexible cell body and therefore does not create torsion (Wheeler, 2017). The cytoskeleton of *T. borreli*, has three microtubular bands, which form an incomplete corset that reinforces the cell body (Gibson, 2017), whereas trypanosomes have a complete corset formed out of subpellicular microtubules that encase the entire cell body. The crosslinking of these subpellicular microtubules are important in the rigidness of the cell body (Cunha Vidal and De Souza, 2017). Despite the “crumpling” of the cell body, the mean length-width ratio for *T. borreli* was larger than that for *T. carassii*, indicating a more elongated cell body shape. Moreover, this corresponded to a higher directionality of swimming. The observation that more elongated cell bodies move more directionally thus also extends to the biflagellate *T. borreli*.

The “crumpling” movements as observed for *T. borreli* were also reflected in the distance between the centre of mass (COM) and the contour (CNT) of the parasites. The distance is large for a contracted cell body and small for an elongated cell body. The measured values showed a significantly larger variation in *T. borreli* than in *T. carassii*, in accordance with our visual observations. *T. borreli*, therefore, has a larger and more flexible cell body, but still shows, on average, a higher length-width ratio and higher directionality than *T. carassii*. This

is different from the finding described for trypanosomes (*T. brucei*), where more directional movements corresponded to higher cell body stiffness (Uppaluri et al., 2011). Presumably the second flagellum plays a major role in both directionality and cell body shape in *T. borreli*. It allows for a larger and more flexible cell body in combination with a more elongated shape and higher degree of directionality.

Despite the observed differences in motility, the propelling mechanism for *T. borreli* and *T. carassii* appears to be comparable. For *T. brucei* it has been described that the flagellum tip speed is in general larger than the speed of the centre of mass of the parasite (Uppaluri et al., 2011), and we observed this for *T. borreli* and *T. carassii* as well. The major propelling force of trypanosome movement is produced by the tip-to-base beat of the flagellum (Bargul et al., 2016; Heddergott et al., 2012). We observed that the anterior flagellum of *T. borreli* and *T. carassii* exhibit overall comparable behaviours. When analysing the distance of the flagellum tip to the COM, which gives indications about the behaviour of the flagellum with respect to the cell body, we observed that the anterior flagellum tip of *T. carassii* is moderately more frequently close to the COM than the anterior flagellum tip of *T. borreli* is. This finding might reflect the observation that *T. carassii* more frequently displays a tumbling behaviour, whereas *T. borreli* moves more often directionally. Interestingly, although the anterior flagella show comparable behaviours, the anterior flagellum of *T. carassii* is the recurrent, cell-attached flagellum (creating torsion of the cell body), while the anterior flagellum of *T. borreli* is the free flagellum.

T. brucei motility aids individual cell survival by clearing the cell surface of bound immunoglobulins (when in low levels). The VSG-bound antibodies accumulate in the flagellar pocket at the posterior end and are endocytosed (Engstler et al., 2007). Additionally, trypanosomes, and likely also trypanoplasma, continuously replenish their membrane, since the flagellar pocket is the only site of endocytosis (reviewed by Field and Carrington, 2009; Langousis and Hill, 2014). We previously reported that for *T. borreli* antibody accumulation at the flagellar pocket and subsequent clearance does occur (Forlenza et al., 2009). Because the flagellar pocket of T. *borreli* is located at the anterior pole of the cell body, the accumulation of antibodies at the flagellar pocket might therefore be supported by membrane recycling and endocytosis.

In a previous study, we were able to visualise, for the first time *in vivo,* novel swimming behaviours, attachment and adaptation strategies of *Trypanosomes* in the vertebrate host blood and tissue (Dóró et al., 2019, **Chapter 2**). In our current study, we observed that *T. borreli* could anchor themselves as well *in vitro* and *in vivo*, although the way they anchor differed from *T. carassii.* Attachment of *T. carassii* always occurred through their posterior end, leaving the flagellum and the entire cell body free to move (Dóró et al., 2019). Attachment of *T. borreli* involved the cell membrane at a location centre to its cell body, allowing *T. borreli* to move and change its flexible cell body shape, since the non-attached part of the cell body can move freely. Attachment in this way leaves both the anterior and posterior ends of the

cell body with the two flagella free to move. The different ways of attachment of these two parasites could be related to their differences in cell body shape. *T. carassii* has a more rigid cell body, than *T. borreli*. The attachment of *T. carassii* and *T. borreli* did not seem to involve extensive modifications of the cell membrane, since the anchoring could occur very rapidly, and was able to withstand the strong blood stream as well as the colliding blood cells.

When analysing *T. borreli* and *T. carassii in vivo,* we observed some similarities in their swimming behaviour. Both parasites were passively dragged by the blood flow and were able to attach, although via different parts of their cell body, to the endothelium of the cardinal caudal vein, which may possibly favour extravasation from blood vessels into surrounding tissues. When extravasated in cavities, such as hart cavity or peritoneal cavity, both parasites were observed to adopt tumbling swimming behaviour, whereas in tissues, such as fins, muscle and interstitial space lining the blood vessels, both were observed to swim more directional. Yet, some of the differences in cell body shape did seem to influence the parasite behaviour *in vivo.* In small vessels of one-cell diameter, such as the intersegmental capillaries (ISCs), *T. borreli* was seldomly observed. Only later during the infections, when the numbers of *T*. *borreli* increased in the vasculature, we could observe them in these small vessels. *T. carassii* however*,* was frequently observed in these small vessels, already early during infection (Dóró et al., 2019). Additionally, we observed that *T. borreli* was able to (temporarily) resist the blood flow and either tumble on the vessels wall of the cardinal caudal vein, while *T. carassii* was only observed to be able to slow themselves down by crawling and rolling on the vessel wall of the cardinal caudal vein when the number of blood cells and speed of flow was reduced (Dóró et al., 2019). These observations possibly reflect the differences in cell body size of these two parasites. In dense tissue, *T. carassii* were observed to invert their swimming direction by backward swimming (Dóró et al., 2019), while *T. borreli* were observed to invert their swimming direction by “crumpling” their cell bodies. This different way of changing their swimming direction in dense tissue are presumably related to the combination of a more flexible cell body and the use of a second flagellum for *T. borreli*. It would be interesting in the future to perform a comparative and quantitative analysis, to investigate whether the differences in cell body size, shape and flexibility as well as attachment strategy, aid in for example speed and efficacy of extravasation.

In conclusion, the biflagellate *T. borreli* shows *in vitro* distinctly different motility compared to the uniflagellate *T. carassii*. Whereas their anterior flagellum behaviour is very similar, they differ in directionality, speed fluctuations and of cell body shape variations, and these differences also lead to different *in vivo* behaviours. However, we also saw similarities in their behaviours *in vivo*, such as the ability to extravasate and anchor themselves to the dorsal side of the cardinal caudal vein. The biflagellate *T. borreli*, therefore adopted a different set of optimizations to successfully establish infections in a vertebrate host. The current study provides the first detailed characterization of the swimming behaviour of a biflagellate *in vitro* and *in vivo* in a vertebrate host and may aid in understanding the evolution of pathogenicity

of kinetoplastids.

Acknowledgments

This work was supported by the Dutch Research Council (NWO), project number 022.004.005. The authors wish to thank the CARUS Aquatic Research Facility of Wageningen University for fish rearing and husbandry.

References

Bargul JL, Jung J, McOdimba FA, Omogo CO, Adung'a VO, Krüger T, Masiga DK, Engstler M. 2016. Species-Specific Adaptations of Trypanosome Morphology and Motility to the Mammalian Host. *PLoS Pathog* **12**:1–29. doi:10.1371/journal.ppat.1005448

Broadhead R, Dawe HR, Farr H, Griffiths S, Hart SR, Portman N, Shaw MK, Ginger ML, Gaskell SJ, Mckean PG, Gull K. 2006. Flagellar motility is required for the viability of the bloodstream trypanosome **440**:224–227. doi:10.1038/nature04541

Bunnajirakul S, Steinhagen D, Hetzel U, Körting W, Drommer W. 2000. A study of sequential histopathology of Trypanoplasma borreli (Protozoa: Kinetoplastida) in susceptible common carp Cyprinus carpio. *Dis Aquat Organ* **39**:221–229. doi:10.3354/dao039221

Cunha Vidal J, De Souza W. 2017. Morphological and Functional Aspects of Cytoskeleton of Trypanosomatids JulianaCytoskeleton - Structure, Dynamics, Function and Disease. p. 53. doi:http://dx.doi.org/10.5772/57353

Dóró É, Jacobs SH, Hammond FR, Schipper H, Pieters RP, Carrington M, Wiegertjes GF, Forlenza M. 2019. Visualizing trypanosomes in a vertebrate host reveals novel swimming behaviours, adaptations and attachment mechanisms. *Elife* **8**:1–25. doi:10.7554/elife.48388

Engstler M, Pfohl T, Herminghaus S, Boshart M, Wiegertjes G, Heddergott N, Overath P. 2007. Hydrodynamic Flow-Mediated Protein Sorting on the Cell Surface of Trypanosomes 505–515. doi:10.1016/j.cell.2007.08.046

Engstler M, Stark H. 2015. Simulating the Complex Cell Design of Trypanosoma brucei and Its Motility **11**. doi:10.1371/journal.pcbi.1003967

Field MC, Carrington M. 2009. The trypanosome flagellar pocket. *Nat Rev Microbiol* **7**:775–786. doi:10.1038/nrmicro2221

Forlenza M, Nakao M, Wibowo I, Joerink M, Arts JAJ, Savelkoul HFJ, Wiegertjes GF. 2009. Nitric oxide hinders antibody clearance from the surface of Trypanoplasma borreli and increases susceptibility to complement-mediated lysis. *Mol Immunol* **46**:3188–3197. doi:10.1016/j.molimm.2009.08.011

Forlenza M, Scharsack JP, Kachamakova NM, Taverne-Thiele AJ, Rombout JHWM, Wiegertjes GF. 2008. Differential contribution of neutrophilic granulocytes and macrophages to nitrosative stress in a host-parasite animal model. *Mol Immunol* **45**:3178–3189. doi:10.1016/j.molimm.2008.02.025

Gibson W. 2017. KinetoplasteaHandbook of the Protists. pp. 1089–1138.

Griffiths S, Portman N, Taylor PR, Gordon S, Ginger ML, Gull K. 2007. RNA interference mutant induction in vivo demonstrates the essential nature of trypanosome flagellar function during mammalian infection. *Eukaryot Cell* **6**:1248–1250. doi:10.1128/EC.00110-07

Haag J, O'hUigin C, Overath P. 1998. The molecular phylogeny of trypanosomes: evidence for an early divergence of the Salivaria. *Mol Biochem Parasitol* **91**:37–49. doi:10.1016/S0166-6851(97)00185-0

Heddergott N, Krüger T, Babu SB, Wei A, Stellamanns E, Uppaluri S, Pfohl T, Stark H, Engstler M. 2012. Trypanosome Motion Represents an Adaptation to the Crowded Environment of the Vertebrate Bloodstream. *PLoS Pathog* **8**. doi:10.1371/journal.ppat.1003023

Hughes AL, Piontkivska H. 2003. Phylogeny of Trypanosomatidae and Bodonidae (Kinetoplastida) based on 18S rRNA: Evidence for paraphyly of Trypanosoma and six other genera. *Mol Biol Evol* **20**:644–652. doi:10.1093/molbev/msg062

Joerink M, Groeneveld A, Ducro B, Savelkoul HFJ, Wiegertjes GF. 2007. Mixed infection with Trypanoplasma borreli and Trypanosoma carassii induces protection: Involvement of cross-reactive antibodies. *Dev Comp Immunol* **31**:903–915. doi:10.1016/j.dci.2006.12.003

Krüger T, Engstler M. 2015. Seminars in Cell & Developmental Biology Flagellar motility in eukaryotic human parasites. *Semin Cell Dev Biol* **46**:113–127. doi:10.1016/j.semcdb.2015.10.034

Langousis G, Hill KL. 2014. Motility and more: The flagellum of Trypanosoma brucei. *Nat Rev Microbiol* **12**:505–518. doi:10.1038/nrmicro3274

Lom J. 1979. Biology of the trypanosomes and trypanoplasms of fishBiology of the Kinetoplastida. pp. 269–337. doi:10.1111/j.1550-7408.1980.tb04245.x

Lom J, Dyková I. 1992. Protozoan parasites of fishes. Amsterdam: Elsevier.

Losev A, Grybchuk-Ieremenko A, Kostygov AY, Lukeš J, Yurchenko V. 2015. Host specificity, pathogenicity, and mixed infections of trypanoplasms from freshwater fishes. *Parasitol Res* **114**:1071–1078. doi:10.1007/s00436-014-4277-y

Lukeš J, Skalický T, Týč J, Votýpka J, Yurchenko V. 2014. Evolution of parasitism in kinetoplastid flagellates. *Mol Biochem Parasitol* **195**:115–122. doi:10.1016/j.molbiopara.2014.05.007

Overath P, Haag J, Mameza MG, Lischke A. 1999. Freshwater fish trypanosomes: Definition of two types, host control by antibodies and lack of antigenic variation. *Parasitology* **119**:591–601. doi:10.1017/S0031182099005089

Overath P, Ruoff J, Stierhof YD, Haag J, Tichy H, Dyková I, Lom J. 1998. Cultivation of bloodstream forms of Trypanosoma carassii, a common parasite of freshwater fish. *Parasitol Res* **84**:343–347. doi:10.1007/s004360050408

Purcell EM. 1977. Life at low Reynolds number. *Am J Phys* **45**:3–11. doi:10.1119/1.10903

Ralston KS, Kabututu ZP, Melehani JH, Oberholzer M, Hill KL. 2009. The Trypanosoma brucei Flagellum: Moving Parasites in New Directions . *Annu Rev Microbiol* **63**:335–362. doi:10.1146/annurev.micro.091208.073353

Ralston KS, Lerner AG, Diener DR, Hill KL. 2006. Flagellar Motility Contributes to Cytokinesis in Trypanosoma brucei and Is Modulated by an Evolutionarily Conserved Dynein Regulatory System † **5**:696–711. doi:10.1128/EC.5.4.696

Rodríguez JA, Lopez MA, Thayer MC, Zhao Y, Oberholzer M, Chang DD, Kisalu NK, Penichet ML, Helguera G, Bruinsma R, Hill KL, Miao J. 2009. Propulsion of African trypanosomes is driven by bihelical waves with alternating chirality separated by kinks.

Shimogawa MM, Ray SS, Kisalu N, Zhang Y, Geng Q, Ozcan A, Hill KL. 2018. Parasite motility is critical for virulence of African trypanosomes. *Sci Rep* **8**:1–11. doi:10.1038/s41598-018-27228-0

Simpson AGB, Stevens JR, Lukeš J. 2006. The evolution and diversity of kinetoplastid flagellates. *Trends Parasitol* **22**:168–174. doi:10.1016/j.pt.2006.02.006

Steinhagen D, Kruse P, Korting W. 1990. Some haematological observations on carp, Cyprinus carpio L., experimentally infected with Trypanoplasma borreli Laveran & Mesnil, 1901 (Protozoa: Kinetoplastida). *J Fish Dis* **13**:157–162. doi:10.1111/j.1365-2761.1990.tb00768.x

Steinhagen D, Kruse P, Korting W. 1989. The Parasitemia of Cloned Trypanoplasma borreli Laveran and Mesnil , 1901 , in Laboratory- Infected Common Carp (Cyprinus carpio L .) Author (s): Dieter Steinhagen , Peter Kruse and Wolfgang Körting Source : The Journal of Parasitology , Vol . 75 , No. *J Parasitol* **75**:685–689.

Uppaluri S, Nagler J, Stellamanns E, Heddergott N, Herminghaus S, Engstler M, Pfohl T. 2011. Impact of microscopic motility on the swimming behavior of parasites: Straighter Trypanosomes are more directional. *PLoS Comput Biol* **7**:1–8. doi:10.1371/journal.pcbi.1002058

Wheeler RJ. 2017. Use of chiral cell shape to ensure highly directional swimming in trypanosomes. *PLoS Comput Biol* **13**:1–22. doi:10.1371/journal.pcbi.1005353

Woo P, Thomas P. 1991. Polypeptide and antigen profiles of Cryptobia salmositica, C. oullocki and C. catostomi (Kinetoplastida: Sarcomastigophora) isolated from fishes. *Dis Aquat Organ* **11**:201–205. doi:10.3354/dao011201

Woo PTK. 2003. Cryptobia (Trypanoplasma) salmositica and salmonid cryptobiosis. *J Fish Dis* **26**:627–646. doi:10.1046/j.1365-2761.2003.00500.x

CHAPTER 5

An uncontrolled inflammatory innate response is associated with susceptibility of zebrafish to trypanoplasma infections

Sem H. Jacobs[1,2], Laura C. Van Eyndhoven[1#], Sylvia Brugman[1], Marleen Scheer[1], Christelle Langevin[3], Geert F. Wiegertjes[1,4], Maria Forlenza[1]

[1] Cell Biology and Immunology Group, Department of Animal Sciences, Wageningen University & Research, Wageningen, The Netherlands
[2] Experimental Zoology Group, Department of Animal Sciences, Wageningen University & Research, Wageningen, The Netherlands
[3] Institut National de la Recherche Agronomique (INRA), Jouy-en-Josas, France
[4] Aquaculture and Fisheries Group, Department of Animal Sciences, Wageningen University & Research, Wageningen, The Netherlands
[#] Current address: Department of Biomedical Engineering, Immunoengineering, Eindhoven University of Technology, Eindhoven, The Netherlands

Manuscript in preparation

Abstract

We recently reported on the establishment of a trypanoplasma infection model in larval zebrafish using fish-specific *Trypanoplasma borreli* and visualised cellular attachment mechanisms and adaptation strategies of this biflagellate trypanoplasma to its vertebrate host. Here, taking advantage of both, the transparency of zebrafish larvae and the availability of transgenic zebrafish lines marking neutrophils and macrophages, we report on innate immune responses during the early phase of *T. borreli* infection. Based on total macrophage-related fluorescence intensity we differentiated infected larvae in groups of macrophage (MΦ)-low and MΦ-high individuals and noted macrophage numbers were inversely correlated with parasitaemia and susceptibility to the infection. Not only macrophage number but also distribution, morphology and activation state were different in MΦ-low and MΦ-high individuals. Although total (neutrophils) green fluorescence was also found to increase upon infection, this did not correlate to the macrophage response nor to trypanoplasma levels. Interestingly, exclusively in the caudal vein of MΦ-low individuals (i.e. larvae developing high parasitaemia), foamy macrophages were present, characterized by a strong pro-inflammatory profile. Our data provide an *in vivo* characterization of the differential response of two important innate immune cell types, neutrophils and macrophages, to trypanoplasma infection in the natural environment of a vertebrate fish host. We identify foamy macrophages as innate immune cell types potentially associated with an exacerbated immune response to extracellular protozoan parasites.

Introduction

Trypanoplasma (Cryptobia) borreli is an extracellular blood flagellate in the order Kinetoplastids, suborder Bodonids and naturally transmitted between cyprinid fish by leeches such as *Piscicola sp.* (Lom, 1979; Lukeš et al., 2014; Steinhagen et al., 1989). A well-studied and closely-related parasite of salmonid fish is *Trypanoplasma (Cryptobia) salmositica* (Woo, 2003; Woo and Ardelli, 2013). Both trypanoplasma can affect wild as well as farmed fish and cause comparable pathology between cyprinids and salmonids, including symptoms of anaemia and splenomegaly (Bunnajirakul et al., 2000; Lom, 1979; Losev et al., 2015; Steinhagen et al., 1990; Woo, 2003). Different from the well-known trypanosomes, *Trypanoplasma* have two flagella: the free flagellum emerges from the flagellar pocket, at the anterior side of the cell body, whereas the recurrent (cell-attached) flagellum emerges from the same anterior side, runs along the cell body to extend as free flagellum at the posterior end of the parasite (Lom, 1979). Of interest, under natural circumstances (cyprinid) fish can be found co-infected with both *Trypanosoma carassii* and *T. borreli* (Joerink et al., 2007; Lom, 1979). Studies on mixed parasite infections could be of great interest with respect to co-evolution of parasites but are complex and difficult to interpret without first performing studies on single infections. Until recently (Dóró et al., 2019, **Chapter 3** and **4**), exactly how uniflagellate *Trypanosomes* and biflagellate *Trypanoplasma* move and behave in their vertebrate host was unknown.

Zebrafish have become a powerful animal model species due to their genetic tractability, availability of various transgenic lines marking several immune cell types and transparency of developing embryos allowing for high-resolution *in vivo* visualisation of cell behaviour (Benard et al., 2015; Bertrand et al., 2010; Dóró et al., 2019; Ellett et al., 2011; Langenau et al., 2004; Lawson and Weinstein, 2002; Page et al., 2013; Petrie-Hanson et al., 2009; Renshaw et al., 2006; White et al., 2008). During the first 2-3 weeks of development zebrafish mostly lack mature T and B lymphocytes and thus offer the opportunity to study and target only innate immune responses (Torraca and Mostowy, 2018), especially those driven by neutrophils and macrophages. The true power of the zebrafish model however, lies in the possibility to visualise in real-time, *in vivo,* not only the progression of the infection, but also the interaction of pathogens with host immune cells and tissues as well as the host response to the infection. In fact, we recently reported on the establishment of experimental infections of *T. borreli* or *T. carassii* in zebrafish, a well-known cyprinid species closely related to the natural hosts of both pathogens (Dóró et al., 2019, **Chapter 3** and **4**). By combining the transparency of zebrafish larvae with high-resolution high-speed videography we could visualise, for the first time *in vivo,* novel swimming behaviours, attachment mechanisms and adaptation strategies of these parasites in the blood and tissues of a vertebrate host.

Previous studies in common carp, the main cyprinid and natural host of *T. borreli* infections revealed an early pro-inflammatory response with production of pro-inflammatory cytokines (Forlenza et al., 2011) and presence of classically-activated macrophages with associated

elevated levels of Nitric Oxide (Saeij et al., 2002) (Joerink et al., 2006), shown to negatively affect lymphocyte proliferation (Saeij et al., 2003b) and cause tissue nitration (Forlenza et al., 2008). Macrophages and neutrophils appear to contribute differentially to the inflammatory state and associated tissue damage (Forlenza et al., 2008). Although these *in vitro* and *ex vivo* studies revealed valuable information on the host response to *T. borreli*, *in vivo* kinetics of innate immune cell activation, including macrophages and neutrophils recruitment and relative contribution to the early pro-inflammatory response, development of parasitaemia and disease progression, have remained unexplored.

In the current study, we characterize in detail the early innate immune response to *T. borreli* in live transgenic zebrafish larvae marking neutrophils and macrophages. We observed a differential response of macrophages and neutrophils to *T. borreli* with respect to their tissue distribution and activation state. While initially both, macrophages and neutrophils respond to the infection by proliferation, only macrophages, depending on the infection level, are actively recruited to blood vessels, drastically change their morphology and activation state. As early as 2 days post-infection, we could assign larvae to groups of macrophage (MΦ)-low and MΦ-high individuals based on their total fluorescence. The macrophage response appeared related to parasitaemia. MΦ-high individuals not only had a high number of macrophages, but also low parasitaemia and always succeeded in controlling the infection. Conversely, MΦ-low individuals, had a lower number of macrophages, high parasitaemia and always succumbed to the infection. Most interestingly, exclusively in the caudal vein of MΦ-low larvae we observed the occurrence of foamy macrophages characterized by a strong inflammatory profile, as assessed through the use of *il1b* and *tnfa* transgenic zebrafish lines. This suggests that fish characterized by an early presence of foamy macrophages develop high parasitaemia and are relatively susceptible to infection. To our knowledge, this is the first study reporting on the *in vivo* visualisation and real-time characterization of the early innate immune response to the biflagellate *T. borreli* and the occurrence of foamy macrophages during *Trypanoplasma* infections.

Materials and methods

Zebrafish lines and maintenance

Zebrafish were kept and handled according to the Zebrafish Book (zfin.org) and local animal welfare regulations of The Netherlands. Zebrafish embryo and larvae were raised in egg water (0.6 g/L sea salt, Sera Marin, Heinsberg, Germany) at 27°C with a 12:12 light-dark cycle. From 5 days post fertilisation (dpf) until 14 dpf larvae were fed Tetrahymena once a day. From 10 dpf larvae were also daily fed dry food ZM-100 (ZM systems, UK). The following zebrafish lines used in this study: transgenic *Tg(mpx:GFP)*^{i114} (Renshaw et al., 2006), *Tg(kdrl:hras-mCherry)*^{s896} *referred as Tg(kdrl:caax-mCherry)* (Chi et al., 2008), *Tg(fli1:eGFP)*^{y1} (Lawson and Weinstein, 2002), *Tg(mpeg1:eGFP)*^{gl22}, (Ellett et al., 2011), *Tg(mpeg1.4:mCherry-F)*^{ump2Tg}, *Tg(il1b:eGFP-F)*^{ump3Tg} (Nguyen-

Chi et al., 2014), *Tg(tnfa:eGFP-F)*^{ump5Tg} (Nguyen-Chi et al., 2015) or crosses thereof. The latter three transgenic zebrafish lines express a farnesylated (membrane-bound) mCherry (mCherry-F) or eGFP (eGFP-F) under the control of the *mpeg1, il1b* or *tnfa* promoter, respectively.

***Trypanosoma borreli* culture and infection of zebrafish larvae**

Trypanoplasma borreli was cloned and characterized by Steinhagen *et al.* (1989) and maintained in our laboratory by syringe passage through common carp (*Cyprinus carpio*) as described previously (Forlenza et al., 2008). Infected blood was incubated overnight (o/n) at 4°C, during which period parasites accumulated at the interface between the plasma and red blood cells. Isolated *T. borreli* parasites cultures were resuspended in complete medium (22.5% MEM with glutamine and phenol red (Gibco), 22.5% Leibovitz's L-15 medium without L-glutamine, with phenol red (Lonza, Verviers, Belgium), 45% Hanks' Balanced Salt solution (HBSS) with phenol red (Lonza, Verviers, Belgium), 10% sterile water, completed with 10% pooled carp serum, 2% 200 mM glutamine (Fisher Scientific) and 1% penicillin-streptomycin solution (10.000:10.000, Fisher Scientific)). *T. borreli* cultures were kept at 27°C without CO_2 at a density below $5x10^6$/ml, and sub-cultured 1-3 times a week. In this way *T. borreli* could be kept in culture without losing infectivity for 1-2 months. The carp white blood cells eventually present in the enriched trypanoplasma fraction immediately after isolation, died within the first 3-5 days of culture and were removed prior to T. *borreli* injection into zebrafish. To this end, cells were centrifuged at 800xg for 5 minutes in a 50 ml Falcon tube and the tube was subsequently tilted in a 20^0 angle relative to the table surface, facilitating the separation of the motile trypanoplasma along the conical part of the tube from the static pellet of white blood cells at the bottom. For zebrafish infection, trypanoplasma were cultured for 1 week and no longer than 3 weeks. Zebrafish larvae (5 dpf) were anaesthetised with 0.017% MS-222 in egg water and injected intravenously in the Duct of Cuvier with n= 200 *T. borreli,* as described previously (Dóró et al., 2019 and **Chapter 4**). Injected larvae were directly transferred into pre-warmed egg water and kept at 27°C. Viability was monitored daily. Lethargic fish showing no escape reflex to a pipette, were confirmed to be heavily infected upon microscopic analysis. The escape reflex was therefore used to monitor morbidity and the progression of infection. When necessary, fish were removed from the experiment and euthanized with an overdose of anaesthetic (0.4% MS-222).

***In vivo* imaging and videography of zebrafish**

Prior to imaging, zebrafish larvae were anaesthetised in 0.017% MS-222 (Sigma-Aldrich). For total fluorescence acquisition, double transgenic *Tg(mpeg1:mCherryF;mpx:GFP)* were positioned on preheated flat agar plates (1% agar in egg water containing 0.017% MS-222) and imaged with Fluorescence Stereo Microscope (Leica M205 FA). The image acquisition settings were as follows: Zoom: 18.0-18.5, Gain: 2.5, Exposure time (ms): 300 (BF)/1000 (GFP)/6000 (mCherry), Intensity: 200 (BF)/100 (GFP)/230 (mCherry), Contrast: 255/255 (BF)/ 70/255 (GFP)/ 15/255 (mCherry).

Alternatively, anaesthetised larvae were embedded in 1.5% UltraPure LMP Agarose (Invitrogen) and positioned on the bottom of a 35 mm petri dish, (14 mm microwell, coverglass No. 0 (0.085-0.13mm), MatTek corporation) prior to imaging. Roper Spinning Disk Confocal (Yokogawa) on Nikon Ti Eclipse microscope equipped with a 40x (1.30 NA, 0.24 mm WD) OI objective, was used with the following settings: GFP excitation: 491nm, emission: 496-560nm, digitizer: 200 MHz (12-bit); 561 BP excitation: 561nm; emission: 570-620nm, digitizer: 200 MHz (12-bit); BF: digitizer: 200 MHz (12-bit). Z-stacks of 1 or 0.5 µm. Andor-Revolution Spinning Disk Confocal (Yokogawa) on a Nikon Ti Eclipse microscope equipped with 40x (0.75 NA, 0.66 mm WD) objective, 40x (1.15 NA, 0.61-0.59 mm WD) WI objective, 20x (0.75 NA, 1.0 mm WD) objective and 10x (0.50 NA, 16 mm WD) objective were used with the following settings: dual pass 523/561: GFP excitation: 488nm, emission: 510-540 nm, EM gain: 20-300 ms, digitizer: 10 MHz (14-bit); RFP excitation: 561 nm; emission: 589-628 nm, EM gain: 20-300 ms, digitizer: 10 MHz (14-bit); BF DIC EM gain: 20-300 ms, digitizer: 10 MHz (14-bit). Z-stacks of 1 µm. Images were analysed with ImageJ-Fijii (version 1.52p)

High-speed videography of *T. borreli* swimming behaviour *in vivo* was performed as described previously (Dóró et al., 2019) using an (8 bits) EoSens MC1362 (Mikrotron GmbH, resolution 1280 x 1024 pixels), with Leica HC 1x Microscope C-mount Camera Adapter controlled by XCAP-Std software (version 3.8, EPIX inc.). The high-speed camera was mounted on aDMi8 inverted digital microscope (Leica Microsystems), controlled by Leica LASX software (version 3.4.2.) and equipped with 40x (NA 0.6) and 20x (NA 0.4) long distance objectives (Leica Microsystems). Videos were acquired at 500 frames per second (fps). For livestream light microscopy (acquisitions at 20 fps) a DFC3000G camera (Leica Microsystems) was mounted on the DMi8 inverted digital microscope and controlled by the Leica LASX software. Images were acquired at a resolution of 720x576 or 1296 x 966 pixels.

Fluorescence quantification

Quantification of total cell fluorescence in zebrafish larvae was performed in ImageJ- Fijii (version 1.52p) software using the free-form selection tool and by accurately selecting the larvae area. Area integrated intensity and mean grey values of each selected larva were acquired. To correct for background fluorescence, three consistent black areas were selected in each image. Analysis was performed using the following formula: corrected total cell fluorescence (CTCF) = Integrated density – (Area X Mean grey background value). The Mean grey background value was the average of 3 mean grey values of selected background regions. Larvae with a CTCF equal or higher than 75 were classified as macrophage high (MΦ-high) whereas larvae with a CTCF equal or lower than 60 were classified as macrophage low (MΦ-low).

Assessment of the severity of infection

Careful monitoring of larval behaviour as well as observations during *in vivo* image analysis revealed that MΦ-high and MΦ-low generally displayed different infection levels. To objectively monitor parasitaemia in these two groups, we developed a clinical scoring system based on *in vivo* observation of parasite location and distribution in live individuals. We previously showed that *T. borreli* can be found in the blood and tissues of zebrafish and can extravasate as early as 1 dpi (**Chapter 4**). Differently from a previously characterized blood flagellate infecting zebrafish (*T. carassii*), *T. borreli* is not easily observed in small intersegmental capillaries in which the parasite-to-red blood cells ratio aided in the quantification of parasite load (Dóró et al., 2019). Instead, *T. borreli* is found preferentially in medium- and large-sized blood vessels such as the tail tip-vessel loop, the cardinal artery and vein. In fact, a clear difference between MΦ-high and MΦ-low individuals was observed when looking at the tail tip vessel-loop. When parasites were observed in this medium-sized vessel, the larva was categorised as high-infected since parasites were never observed in the tail tip vessel-loop of low-infected zebrafish. Anaemia and site of extravasation (e.g. fins, muscle, intraperitoneal cavity, and interstitial space lining the blood vessels) were recorded as well but did not correlate with parasitaemia levels.

Real-time quantitative PCR

Tg(mpeg1.4:mCherry-F;mpx:GFP) were injected intravenously at 5 dpf with n=200 *T. borreli or* with PVP. At 2 dpi larvae were separated in MΦ-high and MΦ-low individuals. At 5 dpi, based on the presence or absence of *T. borreli* in the tail tip vessel-loop, larvae were categorized in high- or low-infected individuals and sacrificed by an overdose of MS-222 anaesthetic (50 mg/L). N=4-5 pools/group, each composed of n=4-5 larvae, were made and transferred to RNA later (Ambion), kept at 4°C o/n and then transferred to -20°C for further storage. Total RNA was isolated with the Qiagen RNeasy Micro Kit (QIAgen, Venlo, The Netherlands) according to manufacturer's protocol, including an on-column DNase step. Next, 250-350 ng total RNA was used as template for cDNA synthesis using SuperScript III Reverse Transcriptase and random hexamers (Invitrogen, Carlsbad, CA, USA), following the manufacturer's instructions with an additional DNase step using DNase I Amplification Grade (Invitrogen, Carlsbad, CA, USA). cDNA was then diluted 25 times to serve as template for real-time quantitative PCR (RT-qPCR) using Rotor-Gene 6000 (Corbett Research, QIAgen), as previously described (Forlenza et al., 2012). Primers (*ef1a*-Fw: CTGGAGGCCAGCTCAAACAT, RV: ATCAAGAAGAGTAGTAGTACCG [ZDB-GENE-990415-52]; *T. bor. hsp70* FW: CAGCCGGTGGAGCGCGT, RV: AGTTCCTTGCCGCCGAAGA [FJ970030.1]) were obtained from Eurogentec (Liège, Belgium). Gene expression was normalized to the expression of *elongation factor-1 alpha* (*ef1a*) housekeeping gene and expressed relative to the PVP control at the same time point.

EdU labelling and Immunohistochemistry

To visualise dividing nuclei, iCLICK™ EdU (5- ethynyl-2'- deoxyuridine, component A) from ANDY FLUOR 555 Imaging Kit (ABP Biosciences), at a stock concentration of 10 mM, was diluted in PVP to 1.13 mM. Infected *Tg(mpeg1:eGFP)* or *Tg(mpx:GFP)* larvae at 2 dpi (7dpf) were injected in the heart cavity with 2 nl of solution and euthanized 30-32 hours later with an overdose of anaesthetic prior to fixation in 4% paraformaldehyde (PFA, Thermo Scientific) in PBS, o/n at 4°C. All subsequent steps were performed at room temperature (RT), unless stated otherwise. Fixed larvae were washed three times in buffer A (0.1% (v/v) tween-20, 0.05% (w/v) azide in PBS), followed by dehydration: 50% MeOH in PBS, 80% MeOH in H_20 and 100% MeOH, each for 15 min with gentle agitation. To remove background pigmentation, larvae were incubated in bleach solution (5% (v/v) H_2O_2 and 20% (v/v) DMSO in MeOH) for 1hr at 4°C, followed by rehydration: 100% MeOH, 80% MeOH in H2O, 50% MeOH in PBS each for 15 min with gentle agitation. Next, larvae were incubated three times for 5 minutes, each in buffer B (0.2% (v/v) triton-x100, 0.05% azide in PBS) with gentle agitation, followed by incubation in EdU iCLICK™ development solution for 30 min in the dark and three rapid washes in buffer B.

The described EdU development led to (partial) loss of GFP signal in the transgenic zebrafish. Therefore, to retrieve the position of neutrophils or macrophages, wholemount immunohistochemistry (IHC) was performed. All subsequent steps were performed at RT, unless stated otherwise. Larvae were blocked in 0.2% Triton-X100, 10% DMSO, 6% (v/v) normal goat serum (NGS) and 0.05% azide in PBS, for 3 hrs with gentle agitation. Next, the chicken anti-GFP (Aves labs.Inc.), diluted 1:500 in antibody buffer (0.2% tween-20, 0.1% heparin, 10% DMSO, 3% NGS and 0.05% azide in PBS), was added and incubated o/n at 37°C. After three rapid and three 5 min washes in buffer C (0.1% tween-20, 0.1% (v/v) heparin in PBS) with gentle agitation, goat anti-chicken-Alexa 488 (Abcam) was added, 1:500 diluted in antibody buffer, and incubated o/n at 37°C. After three rapid and three 5 minutes washes in buffer C with gentle agitation, larvae were imaged with Andor Spinning Disk Confocal Microscope as described above.

BODIPY injection

BODIPY™ FL pentanoic acid (BODIPY-FL5, Invitrogen) was diluted in DMSO to a 3 mM stock solution. Stock solution was diluted 100x (30 μM) with PVP. Infected larvae at 3 dpi (8 dpf) were anaesthetised, injected in the hart cavity with 1 nl of the solution and imaged 18-20 hours later.

Statistical analysis

Analysis of gene expression and total fluorescence data were performed in GraphPad PRISM 5. Statistical analysis of gene expression data was performed on Log(2) transformed values followed by Wilcoxon matched-pairs signed rank test. Analysis of total fluorescence

quantification was performed using a Two-way ANOVA followed by a Bonferroni post-hoc test or a Tukey's post-test. Analysis of EdU was performed using One-way ANOVA followed by Kruskall-Wallis test and Dunn's multiple comparison post-test (macrophage analysis) or Mann-Whitney t-test and Student's t-test (neutrophil analysis). In all cases, $p<0.05$ was considered significant.

Results

Susceptibility of zebrafish larvae to *T. borreli* infection

In **Chapter 4** we reported on the establishment of an experimental *T. borreli* infection in zebrafish larvae and described the swimming behaviour of this biflagellate *in vivo*, in the blood and tissue fluids of a vertebrate host. Here, we started by determining the kinetics of susceptibility and percent survival of zebrafish larvae infected at 5 dpf. Infection with *T. borreli* consistently led to the highest incidence of mortality between 5 and 7 days post-infection (dpi) (**Fig 1**) and to approximately 20% survival, indicating that individual zebrafish larvae, even in the absence of a fully developed immune system, can control the parasite infection.

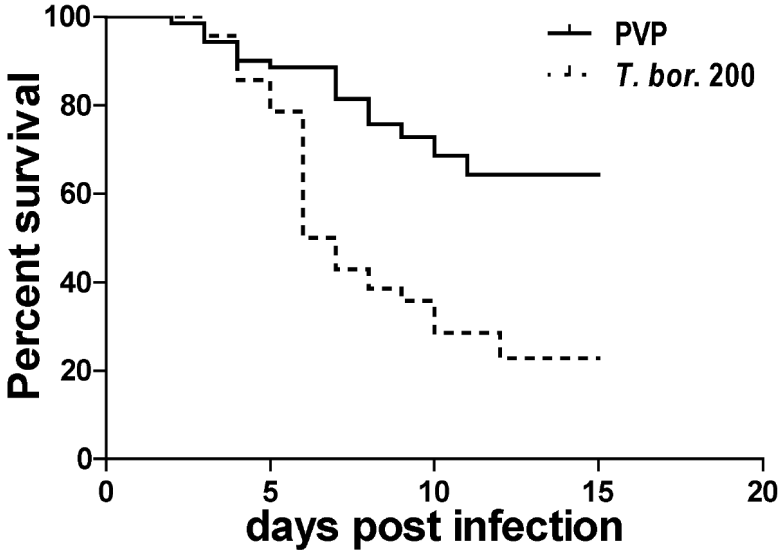

Fig 1. *T. borreli* infection of larval zebrafish.
Tg(mpeg1.4:mCherry-F;mpx:GFP) zebrafish larvae (5 dpf) were injected intravenously with n=200 *T. borreli* or with PVP. Survival was monitored over a period of 15 days.

Heterogeneous response of macrophages, but not neutrophils, to *T. borreli* infection

We investigated the early cellular innate immune responses in *T. borreli*-infected zebrafish larvae using double-transgenic zebrafish *Tg(mpeg1.4:mCh-F;mpx:GFP)* with macrophages visible in fluorescent red and neutrophils in fluorescent green. Already at 2 dpi, based on total fluorescence, we observed a more heterogeneous response for macrophages (red fluorescence) than for neutrophils. Some larvae displayed high red fluorescence, whereas others did not clearly differ from non-infected PVP controls (**Fig 2A**, middle and right panels). The heterogeneous response could not be explained by differences in the macrophage population prior to infection since larvae were always screened and selected based on their homogeneous red fluorescence (**Fig 2A**, left panel). Different from macrophages, the neutrophil response (green fluorescence) did not vary considerably among infected individuals and was always higher in infected than in non-infected PVP controls (**Fig 2B**). Based on these observations, we always categorized infected larvae as high-responders (MΦ-high), or low-responders (MΦ-low) based on total red fluorescence at 2 dpi (**Supplementary Fig 1**). Next, we analysed the total macrophage and neutrophil fluorescence over time in MΦ-high and MΦ-low larvae (**Fig 3**). In larvae categorized as MΦ-low, total red fluorescence did not change over time when compared to the respective PVP control group (**Fig 3A** and **3C**). In larvae categorized as MΦ-high, however, total red fluorescence increased significantly from 2 to 7 dpi (**Fig 3A** and **3C**). This indicated that the difference in fluorescence observed at 2 dpi between MΦ-low and MΦ-high individuals, is not due to individual differences in kinetics. Total green fluorescence moderately but significantly increased over time to a similar extent in MΦ-high and MΦ-low larvae (**Fig 3C** and **3D**). When comparing total macrophage (red) and neutrophil (green) fluorescence within the same individual, no correlation could be detected (**Supplementary Fig 1**). Thus, a MΦ-high individual did not present a high neutrophil CTCF or *vice versa*.

Fig 2. Heterogeneous macrophage response upon *T. borreli* infection. ►

Tg(mpeg1.4:mCherry-F;mpx:GFP) larvae (3 dpf) were screened and selected for homogeneity in red **(A)** and green **(B)** fluorescence (left panels). At 5 days post-fertilisation (dpf) larvae were injected intravenously with n=200 *T. borreli* or with PVP and imaged at 2 days post infection (dpi) (middle and right panels). Images were acquired with Leica M205FA Fluorescence Stereo Microscope with 18.5x zoom; numbers indicate Corrected Total Cell Fluorescence (CTCF) of the corresponding individual. From 2 dpi onwards, a heterogeneous CTCF was observed for macrophages; some infected larvae displayed high red fluorescence (CTCF ≥75), while others did not clearly differ from the non-infected PVP controls (CTCF ≤60, middle and right panels). Such heterogeneous response was not observed for neutrophils. Scale bar indicates 500 μm.

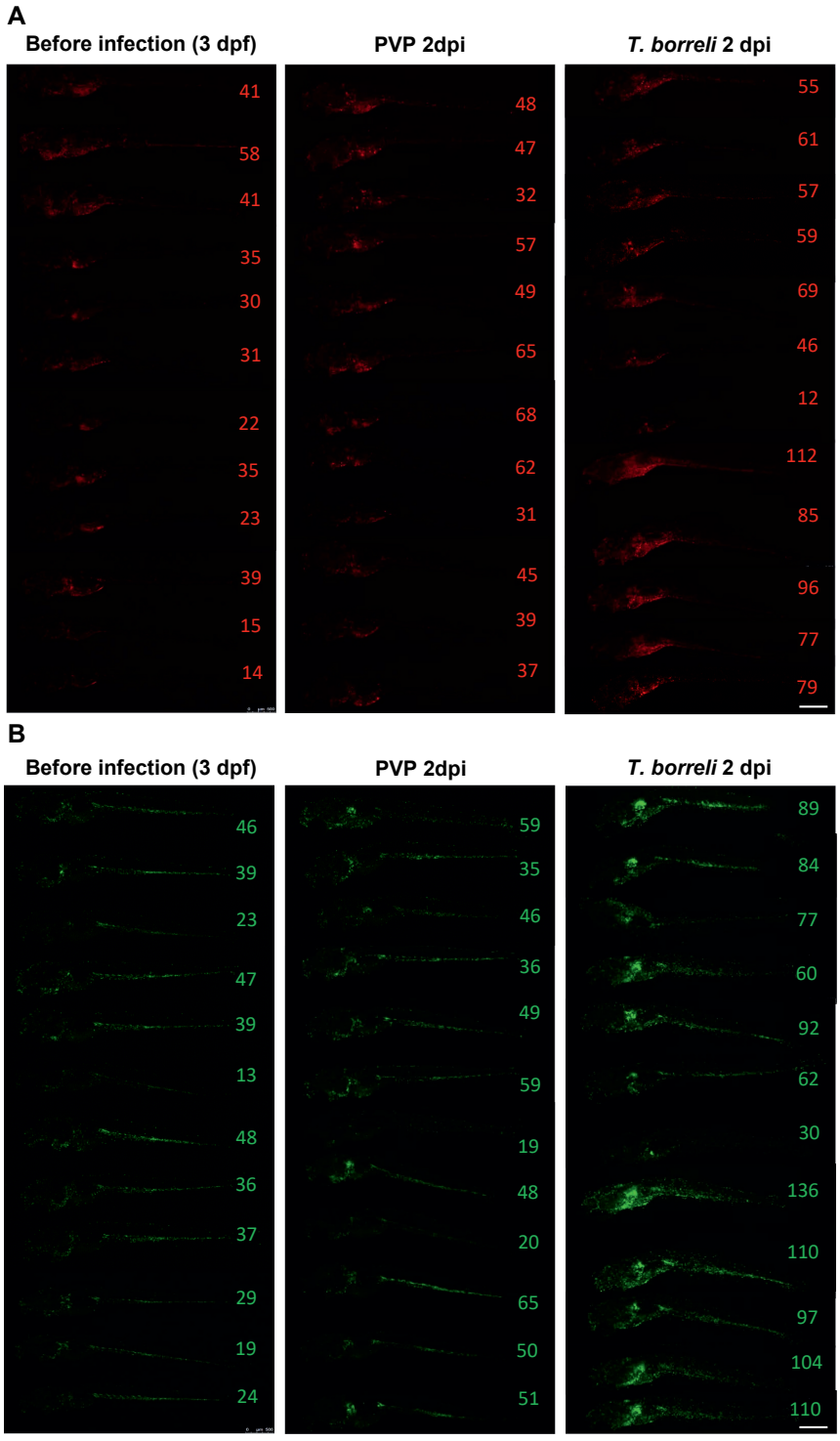
A
Before infection (3 dpf)
PVP 2dpi
T. borreli 2 dpi
41
58
41
35
30
31
22
35
23
39
15
14
48
47
32
57
49
65
68
62
31
45
39
37
55
61
57
59
69
46
12
112
85
96
77
79
B
Before infection (3 dpf)
PVP 2dpi
T. borreli 2 dpi
46
39
23
47
39
13
48
36
37
29
19
24
59
35
46
36
49
59
19
48
20
65
50
51
89
84
77
60
92
62
30
136
110
97
104
110

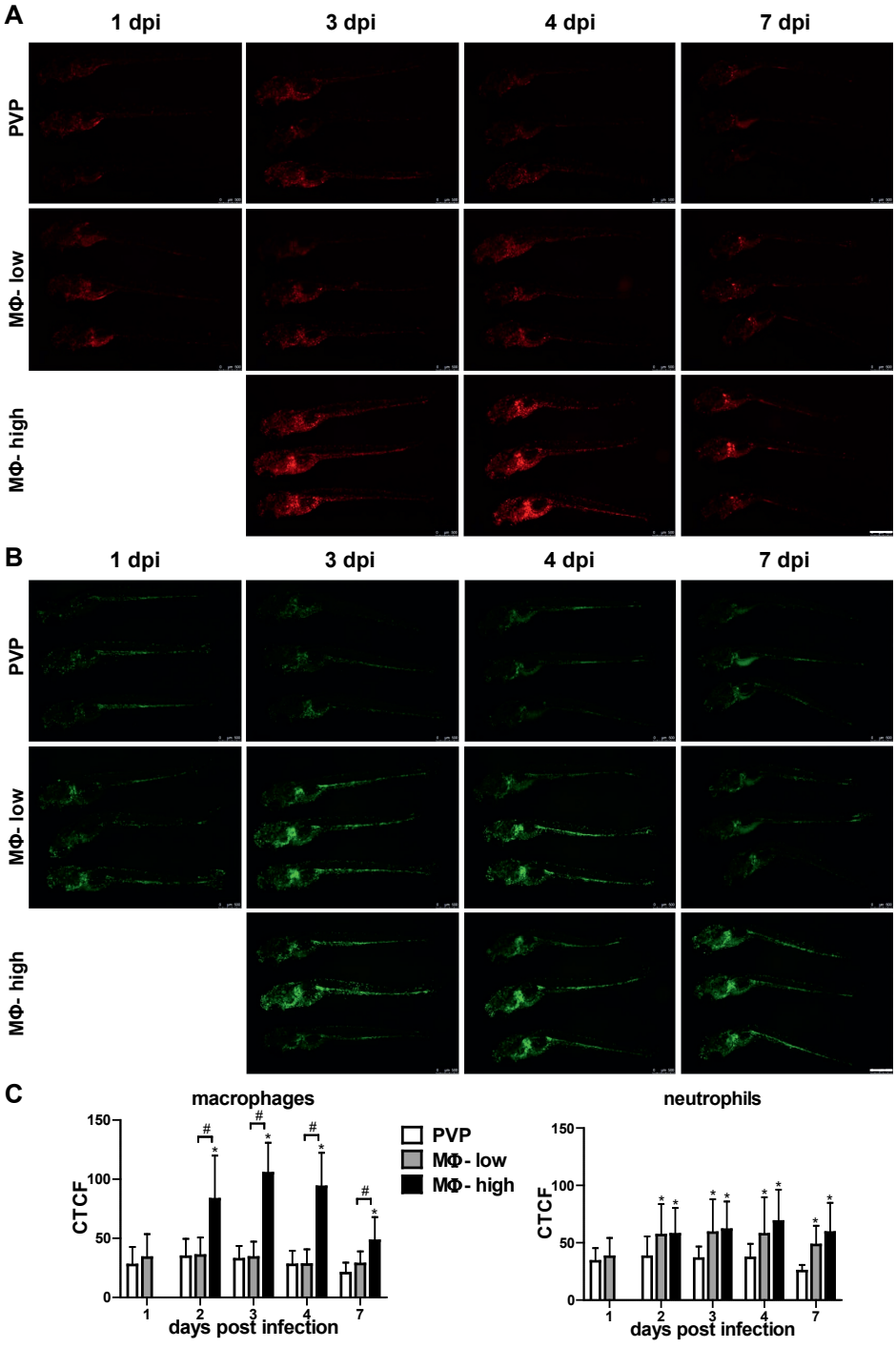
A
1 dpi
3 dpi
4 dpi
7 dpi
PVP
MΦ- low
MΦ- high
B
1 dpi
3 dpi
4 dpi
7 dpi
PVP
MΦ- low
MΦ- high
C
macrophages
neutrophils
PVP
MΦ- low
MΦ- high
CTCF
150
100
50
0
1
2
3
4
7
days post infection
#
*

◂ Fig 3. Kinetics of macrophage and neutrophil response to *T. borreli* infection.
Tg(mpeg1.4:mCherry-F;mpx:GFP) were screened for homogeneity of red fluorescence at 3 dpf and injected intravenously at 5 dpf with n=200 *T. borreli* or with PVP. At 2 dpi, larvae were separated in MΦ-high and MΦ-low individuals. **A-B)** Representative images of the overall macrophage (red) and neutrophil (green) response at the indicated time points, acquired with Leica M205FA Fluorescence Stereo Microscope with 18.5x zoom. Scale bar indicates 500 µm. **C)** Corrected Total Cell Fluorescence (CTCF) quantification of infected and non-infected larvae. Bars represent average and standard deviation of red and green fluorescence in n=14-18 larvae per group from two independent experiments. * and # indicate significant differences to the PVP control or to the corresponding MΦ-low group, respectively, as assessed by Two-way ANOVA followed by Bonferroni post-hoc test.

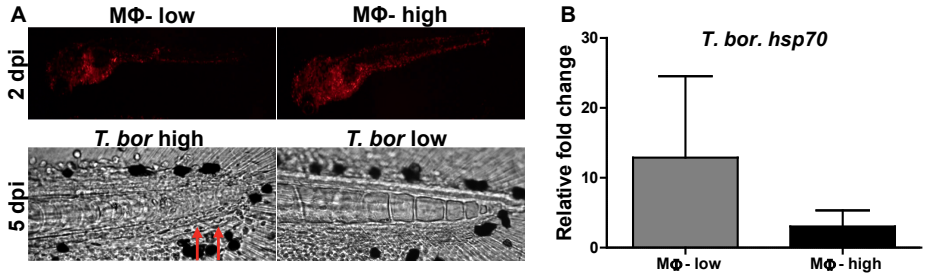

Fig 4. Assessment of *T. borreli* levels in MΦ-high or MΦ-low zebrafish larvae.
Tg(*mpeg1.4*:*mCherry-F;mpx*:*GFP)* were injected intravenously at 5 dpf with n=200 *T. borreli or* with PVP. At 2dpi larvae were separated in MΦ-high and MΦ-low individuals. At 5 dpi, based on the presence or absence of *T. borreli* in the tail tip vessel-loop, fish were categorized as high- or low-infected individuals and used for live microscopy or for gene expression analysis. **A)** Upper panels: representative images of a MΦ-low (left) and MΦ-high (right) individual, acquired with Leica M205 FA Fluorescence Stereo Microscope with 18.5x magnification; lower panels: representative frames extracted from the corresponding **Supplementary Video 1** showing the presence of *T. borreli* in the tail tip vessel-loop of MΦ-low but not of MΦ-high individuals. Images were acquired with a Leica DMi8 inverted microscope at a 40x magnification. **B)** Real-time quantitative PCR analysis of the *T. borreli*-specific *heat-shock protein-70* (*hsp70*) in n=4 MΦ-low (high-infected) and n=5 MΦ-high (low-infected) pools from two independent experiments. Relative expression ratio was normalized to *ef1α* and expressed relative to the corresponding non-infected PVP group. Bars represent mean and standard deviation.

Differential macrophage response is associated to differences in parasitaemia

After having established that individual larvae can respond heterogeneously to *T. borreli* infection, at least with respect to their macrophage response, we next investigated whether this was associated to differences in parasite load. To this end, clinical signs of infection, based on *in vivo* monitoring of physiological changes as well as parasitaemia, were used to determine the infection level of individual larvae and group them based on the severity

of infection. Anaemia, vasodilation and extravasation (e.g. fins, muscle, intraperitoneal cavity, and interstitial space lining the blood vessels) were observed and recorded (as also described previously, **Chapter 4**), but did not correlate with parasitaemia levels. Finally, although *T. borreli* was readily observed in large-sized blood vessels (cardinal artery and vein), in which it is not possible to rapidly assess parasite levels due to the rapid blood flow, clear differences between MΦ-high and MΦ-low individuals could be best detected when observing medium-sized vessels such as the tail tip vessel's loop. In fact, from 5 dpi onwards, we consistently observed that in MΦ-low individuals, parasites could always be detected in the tail tip vessel-loop, and larvae were thus categorised as high-infected (*T. borreli* high); conversely, in MΦ-high individuals, parasites were never detected in the tail tip vessel-loop, and larvae were thus categorised as low-infected (*T. borreli* low, **Fig 4A** and **Supplementary Video 1**). To validate the scoring system, *T. borreli*-specific gene expression was analysed at 5 dpi in pools of larvae previously (at 2 dpi) classified as MΦ-low or MΦ-high (**Fig 4B**). As expected, only in MΦ-low pools the *T. borreli*-specific gene was highly expressed, validating our scoring system and suggesting that MΦ-high individuals very quickly control parasitaemia. Thus, based on the aforementioned considerations, infection levels could be categorised based on two main criteria: 1) overall macrophage fluorescence from 2 dpi onwards, and 2) *T. borreli* presence or absence in tail tip vessel's loop (from 5 dpi onwards).

***T. borreli* infection promotes proliferation of macrophages and of neutrophils**

To prove that the observed increase in overall fluorescence was due to an increase in macrophage number and not only to, for example, activation of the *mpeg* or *mpx* promotor, Tg*(mpeg1:eGFP)* or *Tg(mpx:GFP*) zebrafish larvae were infected at 5 dpf with *T. borreli*, 2 days later were separated in MΦ-high and MΦ-low individuals, and injected with iCLICK™ EdU for identification of proliferating cells.

EdU^+ nuclei (red) could be seen throughout the body of developing larvae. When specifically looking at proliferating macrophages (**Fig 5**) we selected the area of the head (left panels) and trunk (right panels) region, where previously (**Fig 3A**) the highest increase in red and green fluorescence was observed. In agreement with the previous observation (**Fig 3C**), a higher number of macrophages (total green fluorescence in head and trunk) was observed in MΦ-high when compared to MΦ-low and PVP-injected individuals (**Fig 5A** and **5B**). For a reliable quantification of the total number of proliferating (EdU^+) macrophages, we focused on the trunk region. A significant increase was observed in MΦ-high individuals as opposed to a marginal, yet not significant, increase in MΦ-low individuals (**Fig 5C** and **Supplementary Video 2**).

When analysing neutrophils' proliferation (**Fig 6**), we focused on the overall neutrophil response in *T. borreli*-infected larvae and did not separate the larvae in MΦ-high and MΦ-low individuals; this because previously (**Supplementary Fig 1**) no correlation between macrophages and neutrophils response was observed. In agreement with the previous

observation (**Fig 3B**), a higher number of neutrophils (total green fluorescence in head and trunk) was observed in *T. borreli*-infected compared to non-infected PVP controls (**Fig 6A** and **6B**). In the trunk region, the total number of proliferating (EdU^+) neutrophils was significantly higher in infected than in PVP-injected individuals (**Fig 6C** and **Supplementary Video 3**). Altogether, these data confirm that both, macrophages and neutrophils respond to *T. borreli* infection by proliferating, and that, as expected, macrophage proliferation is higher in MΦ-high than in MΦ-low individuals.

Differential distribution of neutrophils and macrophages in blood vessels of *T. borreli*-infected zebrafish larvae

After having assessed that both, macrophages and neutrophils respond to the infection by proliferating (**Fig 5** and **6**), and that the overall macrophage response can be predictive of the infection level (**Fig 3** and **4**), we next investigated the distribution of macrophages and neutrophils during infection. Considering the haematic nature of the parasite, we focused on one of the major blood vessels, the cardinal caudal vein, at 4-6 dpi, a period during which clear differences in macrophage response (**Fig 2**) and in infection levels (**Fig 4**) were observed. To this end, we made use of double transgenic zebrafish with the blood vessel endothelium visible in fluorescent red and neutrophils in fluorescent green, *Tg(kdrl:caax-mCherry;mpx:GFP)*, and of double transgenic zebrafish with the blood vessel endothelium visible in fluorescent green and macrophages in fluorescent red, *Tg(fli1:eGFP x mpeg1.4 mCherry-F*). Longitudinal and orthogonal images of the blood vessel were analysed to visualise the exact location of cells along the cardinal caudal vein (**Fig 7** and **Supplementary Video 4** and **5**). In PVP-injected controls both, macrophages and neutrophils were exclusively located outside the blood vessel, in close contact with the outer layer of the vein or in the tissue adjacent the cardinal vein (**Fig 7A** and **7B**). In *T. borreli*-injected individuals, while neutrophils remained located exclusively outside the blood vessel (**Fig 7A**), macrophages could be seen both, inside (white arrows) and outside (blue arrows, **Fig 7B**). The proportion of macrophages inside or outside the vessel could vary among individuals, but macrophages were generally seen more frequently inside the vessel of MΦ-low than MΦ-high individuals. Altogether, our data indicate that upon infection, macrophages but not neutrophils are recruited inside the blood vessel, especially in MΦ-low (*T. borreli* high) individuals.

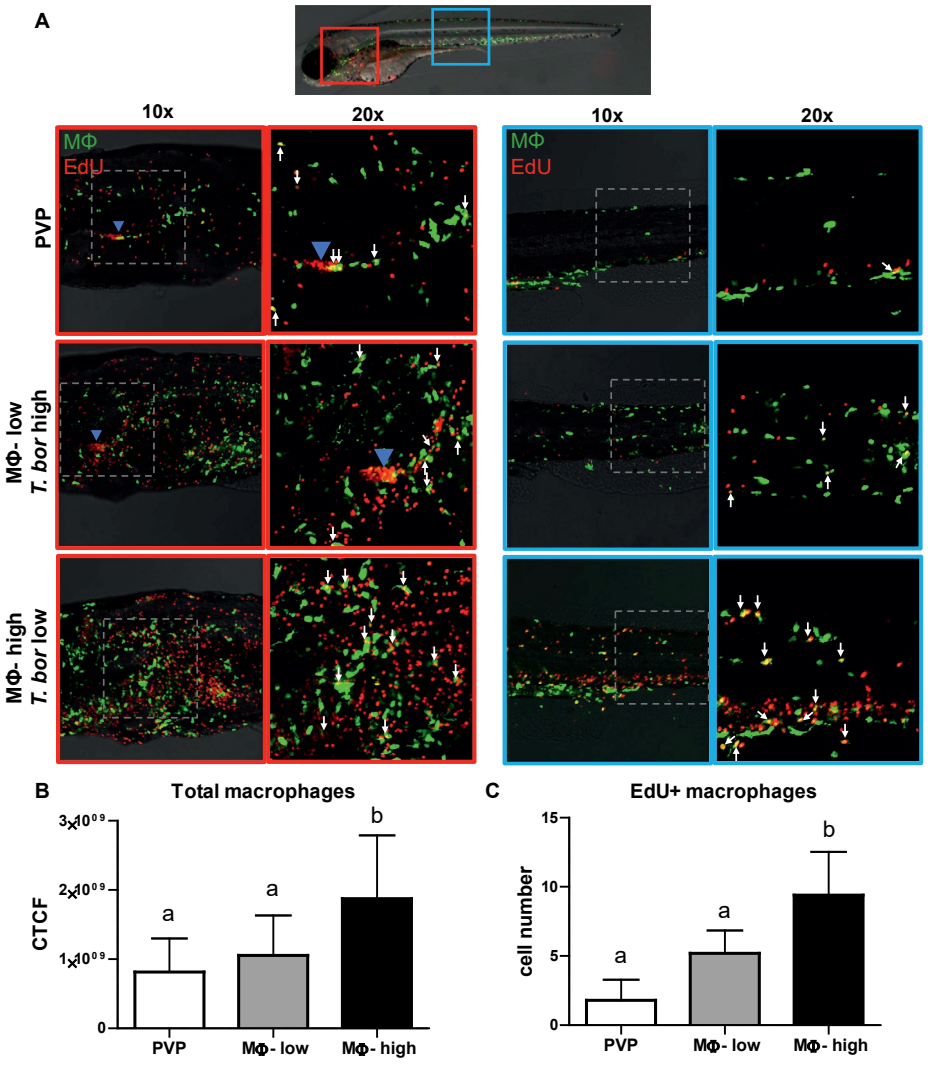
A
10x
20x
10x
20x
MΦ
EdU
PVP
MΦ- low
T. bor high
MΦ- high
T. bor low
B
Total macrophages
CTCF
3x10^09
2x10^09
1x10^09
0
a
a
b
PVP
MΦ- low
MΦ- high
C
EdU+ macrophages
cell number
15
10
5
0
a
a
b
PVP
MΦ- low
MΦ- high

◂ Fig 5. *T. borreli* infection triggers proliferation of macrophages.
Tg(mpeg1:eGFP) zebrafish larvae were infected intravenously at 5 dpf with n=200 *T. borreli* or with PVP control (n=5 larvae per group). At 2 dpi, larvae were separated in MΦ-high or MΦ-low individuals and received 2 nl of 1.13 mM iCLICK™ EdU; 30-32h later (~8 dpf) larvae were fixed and treated with iCLICK EdU ANDY FLUOR 555 development to identify EdU^+ nuclei and with chicken anti-GFP antibody to identify macrophages. Fish were imaged with an Andor Spinning Disc Confocal Microscope using 10x and 20x magnification. **A)** Representative maximum projection images (from n=3 independent experiments) of the head (left panels) and trunk (right panels), capturing macrophages (green) and EdU^+ nuclei (red) in PVP control, MΦ-low and MΦ-high individuals. The images acquired at a 10x magnification provide an overview of the macrophages and of EdU^+ nuclei present in these regions, whereas the 20x magnification allowed us to look into more details and perform the cell counts reported in C. EdU^+ macrophages (white arrows) were identified upon detailed analysis of the separate stacks used to generate the 20x overlay images, also provided in **Supplementary Video 2**. In the PVP control group, EdU^+ nuclei and GFP^+ macrophages rarely overlapped, indicating limited proliferation. In MΦ-low and MΦ-high individuals the number of EdU^+ macrophages increased, indicating proliferation of macrophages during *T. borreli* infection (20x). Blue arrowhead in the head, indicates the position of the thymus (when visible), an actively proliferating organ at this time point. **B)** Corrected total cell fluorescence (CTCF) calculated in the head and trunk region (n=5 larvae per group) using ImageJ. Bars represent average and standard deviation. Letters indicate significant differences as assessed by One-Way ANOVA followed by Tukey's post-test. **C)** Total EdU^+ macrophage in the trunk region (n= 5 larvae per group, 20x). Bars represent average and standard deviation. * indicates significant differences to the PVP control as assessed by Kruskall-Wallis test followed by Dunn's post-test.

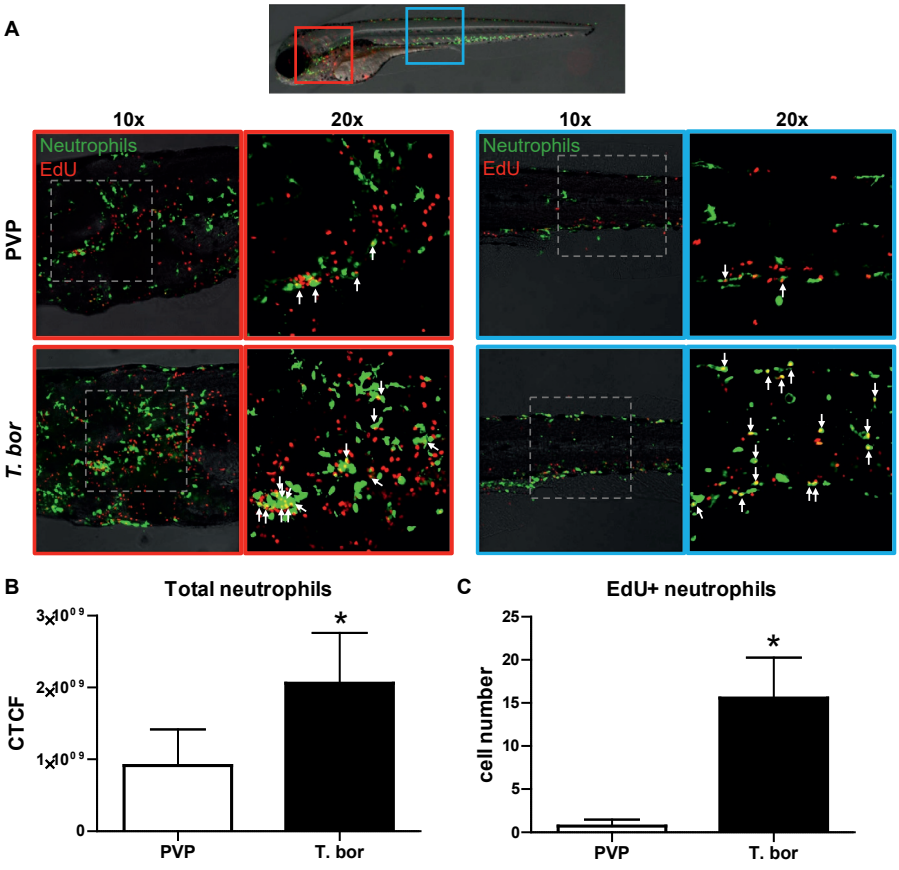
A
10x
20x
10x
20x
Neutrophils
EdU
Neutrophils
EdU
PVP
T. bor
B
Total neutrophils
CTCF
3x10^09
2x10^09
1x10^09
0
*
PVP
T. bor
C
EdU+ neutrophils
cell number
25
20
15
10
5
0
*
PVP
T. bor

◂ Fig 6. *T. borreli* infection triggers neutrophils proliferation.
Tg(mpx:GFP) were treated as described in Fig 5 (n=5 larvae per group). **A)** Representative images (from n=4 independent experiments) of the head (left panels) and trunk (right panels) region are shown, capturing neutrophils (green) and EdU$^+$ nuclei (red) in PVP and *T. borreli*-infected zebrafish. The images acquired at a 10x magnification provide an overview of the neutrophils and EdU$^+$ nuclei present in these regions. The identification of EdU$^+$ neutrophils (white arrows) was performed upon detailed analysis of the separate stacks used to generate the 20x overlay images, also provided in **Supplementary Video 3**. In the PVP control group, EdU$^+$ nuclei and GFP$^+$ neutrophils rarely overlapped, indicating limited proliferation of neutrophils. In the infected individuals the number of EdU$^+$ neutrophils increased, indicating proliferation of neutrophils during *T. borreli* infection. **B)** Corrected total cell fluorescence (CTCF) calculated in the head and trunk region (n=5 larvae per group) using ImageJ. Bars represent average and standard deviation. * indicates significant differences to the PVP control as assessed by Student's t-test. **C)** Total EdU$^+$ neutrophils in the trunk region of MΦ-low and MΦ-high individuals (n= 7 larvae per group, 20x). Bars represent average and standard deviation. * indicates significant differences to the PVP control as assessed by Mann–Whitney t-test.

High *T. borreli* infection levels trigger the formation of foamy macrophages

When looking in more details to the macrophages inside or outside the caudal vein in control and MΦ-low or MΦ-high individuals, clear differences could be observed not only in their location but also in their morphology. In PVP-injected controls, macrophages generally exhibited an elongated and dendritic morphology, were rarely observed inside the vessel, and in the trunk region were mostly located along the vessel wall, in the tissue between the cardinal vessels or in the ventral fin (**Fig 8A**, left panel). A similar dendritic morphology and distribution were observed also in MΦ-high individuals (*T. borreli* low) and only in rare cases, macrophages with rounded morphology were observed inside the vessel (**Fig 8A**, right panel). Strikingly, in MΦ-low individuals (*T. borreli* high), we consistently observed large, dark, granular and round macrophages located almost exclusively inside the cardinal vein on the dorsal luminal side. These dark macrophages were clearly visible already in bright field images due to their size, colour and location, and could be present as single cells or as aggregates (**Fig 8A**, middle panel). The occurrence of these large macrophages increased with the progression of the infection and were predominantly observed in high infected individuals (**Supplementary Video 6**).

The rounded morphology, the size and the dark appearance of these macrophages was reminiscent of that of foamy macrophages. Therefore, to further investigate the nature of these cells, the green fluorescent fatty acid BODIPY-FLC5 was used to track lipid accumulation in macrophages of infected larvae. Interestingly, administration of BODIPY-FL5 in MΦ-low (*T. borreli*-high) individuals, 1 day prior to the expected appearance of the large macrophages, confirmed the accumulation of lipids in these cells (**Fig 8B** and **Supplementary Video 6**). This result suggests that the large rounded macrophages in the cardinal caudal vein are indeed foamy macrophages and are induced in larvae with a high parasite load.

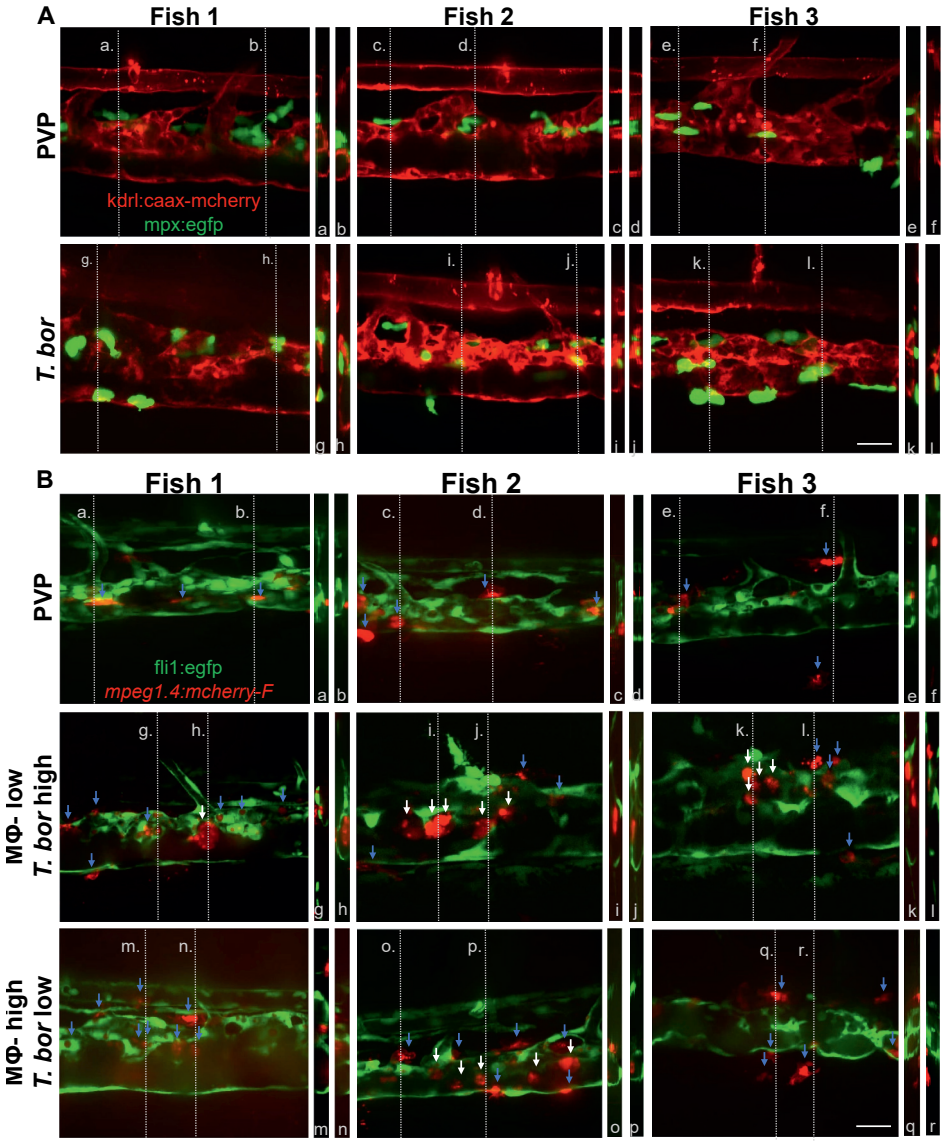
A
Fish 1
Fish 2
Fish 3
PVP
T. bor
kdrl:caax-mcherry
mpx:egfp
B
Fish 1
Fish 2
Fish 3
PVP
fli1:egfp
mpeg1.4:mcherry-F
MΦ- low
T. bor high
MΦ- high
T. bor low

◂ Fig 7. Macrophages, but not neutrophils, are recruited into the cardinal caudal vein of high-infected zebrafish larvae.

A) *Tg (kdrl:caax-mCherry;mpx:GFP)* zebrafish larvae were injected intravenously at 5 dpf with *n*=200 *T. borreli* or with PVP (n= 5 larvae per group). At 2 dpi larvae were separated into MΦ-high and MΦ-low individuals and imaged at 5 dpi with a Roper Spinning Disk Confocal Microscope using 40x magnification. Representative images from 3 individuals acquired over two independent experiments are shown, revealing neutrophils (green) located only outside the vessel (red) in both control and infected larvae. Orthogonal views are shown for the locations marked by the grey dashed lines (a-l), confirming that in all groups neutrophils are present exclusively outside the vessel. Scale bar indicates 25 µm. **Supplementary Video 4**, provides the stacks used for the orthogonal views. **B)** *Tg(fli1:eGFP x mpeg1.4:mCherry-F*) were treated as described in A (n=5 larvae per group). Representative images from 3 individuals acquired over two independent experiments are shown with macrophages (red) inside (white arrows) and outside (blue arrows) the cardinal caudal vein (green). Orthogonal views are shown for the locations marked by the grey dashed lines (a-r), confirming that in PVP-injected controls the majority of the macrophages are present outside the blood vessel. In MΦ-low individuals, although some macrophages can be seen outside the blood vessel, the majority of the macrophages resides inside. In MΦ-high individuals, macrophages were generally seen outside the blood vessel and only in rare cases, macrophages were seen inside the blood vessel (fish 2 lower panel). Scale bar indicates 25 µm. **Supplementary Video 5**, provides the stacks used for the orthogonal views.

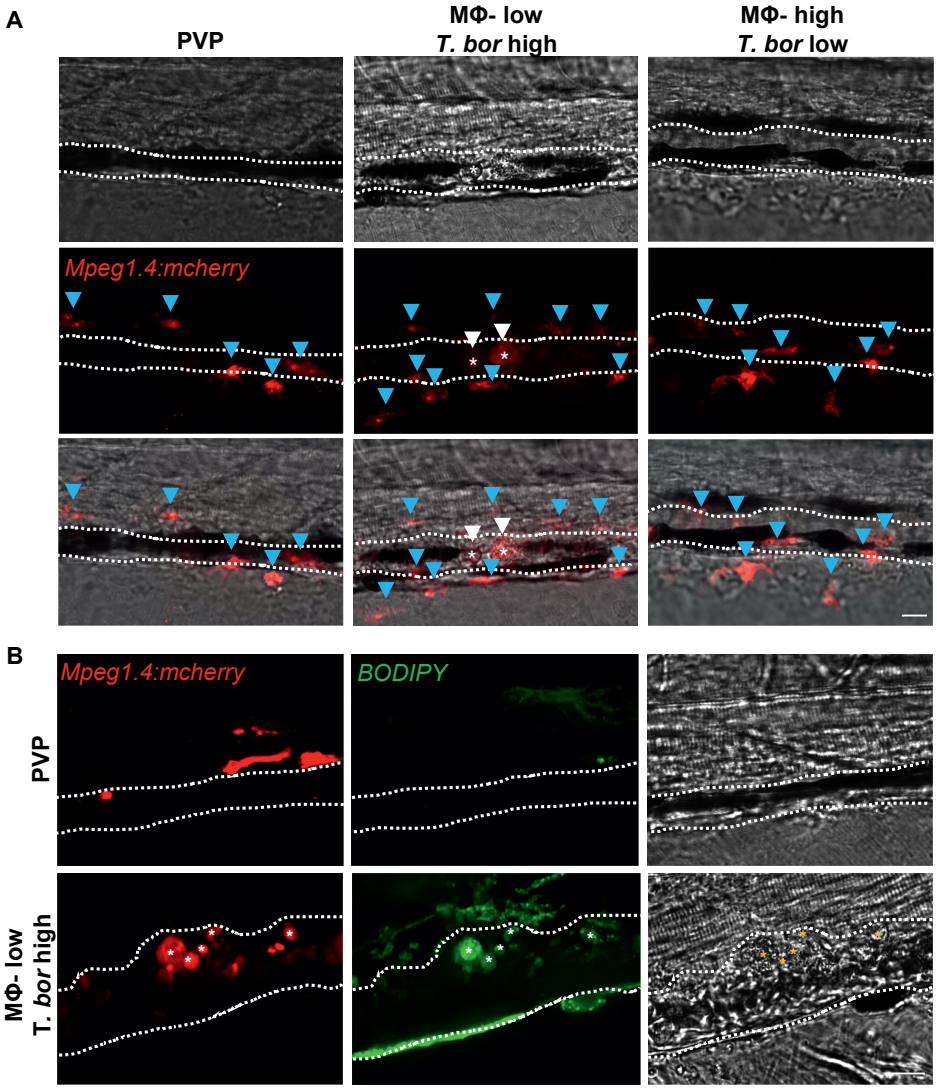
A
PVP
MΦ- low
T. bor high
MΦ- high
T. bor low
Mpeg1.4:mcherry
B
Mpeg1.4:mcherry
BODIPY
PVP
MΦ- low
T. bor high

◂ Fig 8. Occurrence of foamy macrophages in high-infected zebrafish larvae.
A) *Tg(mpeg1.4:mCherry-F;mpx:GFP)* zebrafish larvae were infected intravenously at 5 dpf with *n*=200 *T. borreli* or with PVP (*n*=5 larvae per group). At 2 dpi larvae were separated into MΦ-high and MΦ-low individuals and imaged at 4 dpi using a Roper Spinning Disc Confocal Microscope using 40x magnification. Representative images (from two independent experiments) are shown, with macrophages outside the vessel (blue arrowheads) or round macrophages inside (white arrowheads) the cardinal vein (dashed line). Scale bar indicates 25 µm. In PVP-injected controls and MΦ-high individuals, the majority of the macrophages are outside the vessel and have an elongated or dendritic morphology. In MΦ-low individuals, although macrophages with dendritic morphology can be seen outside the vessel, macrophages inside the vessel clearly have a rounded morphology. **B)** *Tg(mpeg1.4:mCherry-F)* were treated as in A (n=4-5 larvae per group). At 3 dpi, larvae received 1 nl of 30 µM BODIPY-FLC5 and were imaged 18-20 hours later using a Roper Spinning Disc Confocal Microscope using 40x magnification. Representative images from two independent experiments are shown. Scale bar indicates 25 µm. **Supplementary Video 6** provides details of the location and morphology of macrophages in A and B.

Foamy macrophages have a pro-inflammatory profile and are associated with susceptibility to the infection

To study in more detail the activation state of the foamy macrophages, we made use of double transgenic lines having macrophages in fluorescent red and *tnfa*- or *il1b*-expressing cells in fluorescent green, *Tg(tnfa:gfp-F;mpeg1.4:mCherryF)* or *Tg(il1b:gfp-F; mpeg1.4:mCherryF)* (**Fig 9**). We imaged the larvae at 4-6 dpi, the time period during which the appearance of foamy macrophages was observed in MΦ-low individuals (*T. borreli*-high).

For *tnfa* expression, in PVP-injected controls, all macrophages were outside the vessel, and only few *tnfa*-expressing macrophages could be observed (**Fig 9A**, left panel, white arrow heads) showing limited green fluorescence in discrete spots within the cytoplasm. In this transgenic line, in some individuals, a generalized background in the muscle or skin tissue could be observed, but this did not coincide with the presence of macrophages and varied between individuals. In MΦ-low individuals (*T. borreli*-high), all foamy macrophages were strongly positive for *tnfa* expression (**Fig 9A**, middle panel, asterisks), indicating a pro-inflammatory activation state. Conversely, in MΦ-high individuals (*T. borreli*-low), foamy macrophages were not observed, and the dendritic or lobulated macrophages outside or lining the vessel expressed low levels of *tnfa* (**Fig 9A** right panel, white arrowheads). Similar to what observed in PVP-injected controls, the green fluorescence was not distributed throughout the cytoplasm (white arrowheads).

For *il1b* expression, similar to what was observed for *tnfa*, in PVP-injected controls all macrophages were outside the vessel and only some macrophages displayed a low basal level of *Il1b* expression (**Fig 9B**, left panel, white arrowhead). In MΦ-low individuals (*T. borreli*-high), foamy macrophages inside the vessel were strongly positive for *il1b* (**Fig 9B**, middle panel, asterisks), confirming their pro-inflammatory profile. Macrophages in the tissue around the vessel did not express *il1b* (blue arrowhead). In MΦ-high individuals (*T. borreli*-low), *il1b*

expression level in macrophages was generally low (**Fig 9B**, right panel, white arrowheads), and the majority of macrophages did not express *il1b* (blue arrowheads). In infected individuals (independently of the infection level) besides macrophages, also endothelial cells expressed *il1b* and were visible as bright green rounded cells lining the vessel (**Fig 9B**, middle and right panel).

Finally, to investigate whether these profiles are associated to a differential susceptibility to the infection, *Tg(mpeg1.4:mCherry-F)* zebrafish larvae (5 dpf) were infected with *T. borreli*. At 2 dpi larvae were separated into MΦ-high and MΦ-low individuals and at 5 dpi parasitaemia was assessed by microscopic analysis as described earlier. The MΦ-high group had a relative percent survival (RPS) of 46% with a slow incidence of mortality, whereas the MΦ-low group clearly showed the lowest survival (RPS of 13%) with the highest incidence of mortality between day 5 and 7 post-infection, the period in which a clear difference in parasitaemia could be observed between the groups (**Fig 10**).

Fig 9. Individuals with a high infection level, have a strong inflammatory profile. ►
Zebrafish larvae (5dpf), *Tg(tnfa:eGFP-F; mpeg1.4:mCherryF)* (**A**) or *Tg(il1b:gfp-F; mpeg1.4:mcherryF)* (**B**), were infected with n=200 *T. borreli* or with PVP. At 2 dpi larvae were separated into MΦ-high and MΦ-low individuals and at 5 dpi parasite levels were assessed. **A)** Larvae were imaged at 5 dpi with an Andor Spinning Disk Confocal Microscope using 40x magnification (n=5-6 larvae per group). In non-infected PVP controls (left panel), all macrophages are outside the vessel, have a dendritic morphology, and the majority is negative for *tnfa* expression (blue arrowheads); only one cell is moderately positive for *tnfa* expression (white arrowhead). In MΦ-low, *T. borreli*-high, foamy macrophages (asterisks), always present within the vessel, are strongly positive for *tnfa* expression. In MΦ-high, *T. borreli*-low, macrophages are present outside and lining the vessel; their morphology resembled that of macrophages present in the PVP-injected controls and are only moderately positive for *tnfa* expression (white arrowheads). Scale bar indicates 25 μm. **B)** Larvae were imaged at 5 dpi with a Roper Spinning Disk Confocal Microscope using 40x magnification (n=4-6 larvae per group). *Il1b-gfp* expression is generally low in non-infected PVP controls and in MΦ-high individuals (*T. borreli*-low) and is mostly expressed in macrophages lining the vessels (white arrowheads). In MΦ-low, (*T. borreli*-high), foamy macrophages (asterisks) were positive for *il1b-gfp* expression. In MΦ-high (*T. borreli*-low), *il1b*-positive macrophages (white arrowheads) are present but are less numerous than in MΦ-low individuals and are mostly along the vessel. In both MΦ-high and MΦ-low individuals, endothelial cells in and around the cardinal caudal vein show high *il1b-gfp* expression (bright green cells in middle and right panel). Scale bar indicates 25 μm.

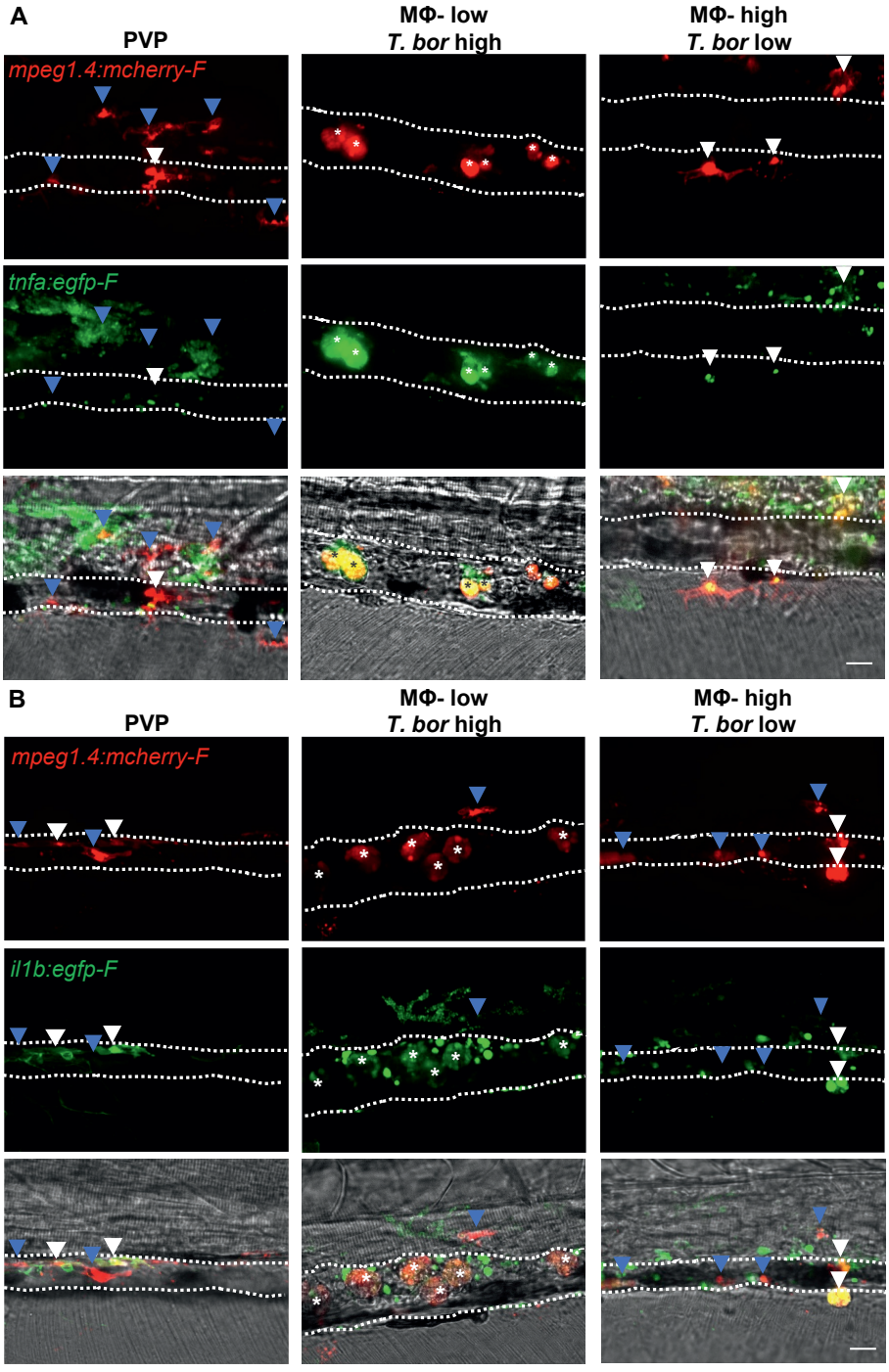
A
PVP
MΦ- low
T. bor high
MΦ- high
T. bor low
mpeg1.4:mcherry-F
tnfa:egfp-F
B
PVP
MΦ- low
T. bor high
MΦ- high
T. bor low
mpeg1.4:mcherry-F
il1b:egfp-F

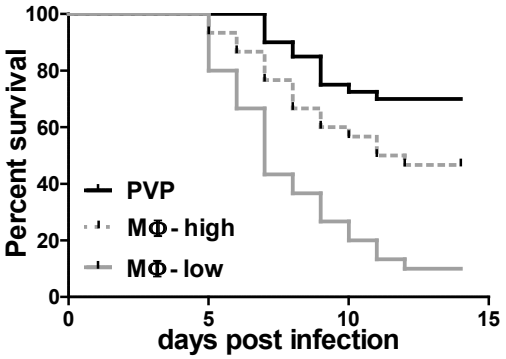

Fig 10. MΦ-high individuals show lower susceptibility to *T. borreli* infection.
Tg(Mpeg1.4:mCherry-F) zebrafish larvae (5 dpf, n= 30-40 per group) were injected intravenously with n=200 *T. borreli* or with PVP. At 2 dpi larvae were separated into MΦ-high and MΦ-low individuals based on their red fluorescence intensity and at 5 dpi parasitaemia was confirmed to be low in MΦ-high and high in MΦ-low individuals based on the presence or absence of *T. borreli* in the tail tip vessel-loop. Fish and survival were monitored over a period of 13 days.

Discussion

In this study, we describe the differential response of macrophages and neutrophils *in vivo,* during *Trypanoplasma borreli* infection of larval zebrafish. Upon infection, we were able to consistently differentiate infected zebrafish larvae in MΦ-high and MΦ-low individuals based on their total macrophage fluorescence and we observed that differences in fluorescence levels were due to increased macrophage proliferation in MΦ-high individuals. Although total (neutrophils) green fluorescence was also found to increase upon infection, this did not correlate to the macrophage response nor to trypanoplasma levels. Indeed, after having developed a scoring system to assess *T. borreli* load *in vivo* in (live) individual larvae, we were able to link macrophage responses to parasitaemia levels and to different disease outcome. When considering also the activation state of macrophages, measured as *tnfa* and *il1b* expression, altogether we could draw a picture in which infected fish that respond to the infection by triggering an early macrophage proliferation (MΦ-high individuals), succeed in controlling parasitaemia, display a low or moderate pro-inflammatory profile and are associated with resistance to the infection. Conversely, MΦ-low individuals, with a lower macrophage number, are not able to control parasitaemia, display a high pro-inflammatory profile characterized by the occurrence of foamy macrophages, and are ultimately associated with susceptibility to the infection.

Foamy macrophages are named after the lipid bodies accumulated in their cytoplasm, leading to their typical morphological appearance (Dvorak et al., 1983), they are enlarged in size and contain diverse cytoplasmic organelles (Melo et al., 2003). Foamy macrophages have been linked to various infectious diseases, such as Leishmaniasis, Chagas disease, tuberculosis and toxoplasmosis (reviewed in López-Muñoz et al., 2018; Vallochi et al., 2018), and are generally associated with inflammation, since their cytoplasmic lipid bodies are a source of eicosanoids, strong mediators of inflammation (Melo et al., 2006; Wymann and Schneiter, 2008). Our results are in line with these reports as we show the occurrence of foamy macrophages only in zebrafish that developed high parasitaemia, a strong pro-inflammatory response and succumbed to the infection. Interestingly, also in our previous study on innate immune responses to *Trypanosoma carassii* infections (**Chapter 3**), we report the presence of foamy macrophages in individuals displaying a strong pro-inflammatory response and high susceptibility to the infection. Altogether, these data suggest that foamy macrophages occur not only during intracellular pathogen infections, but also during extracellular parasite infections, at least in larval zebrafish. Whether foamy macrophages also occur during extracellular trypanosome infections in mice, humans or cattle is yet to be established. Our data on two different extracellular parasite infections, strongly suggest that it may be possible, and further emphasize the complementarity of the zebrafish model to other mammalian models of kinetoplastid infection. In fact, it is thanks to the transparency of zebrafish larvae that we were able to observe *in vivo*, individual differences within a heterogeneous zebrafish population, to detect the formation of foamy macrophages in some but not all individuals, and to correlate individual responses to specific disease outcomes. It is possible that if we were to bleed an individual to analyse its blood cell composition during an ongoing infection, as often done in mice studies or in others using large non-transparent animals, we likely would have missed the presence of these large cells that, at least in zebrafish, remained solidly attached to the luminal vessel wall of highly infected individuals.

As previously discussed (**Chapter 3**), further characterization of the specific role of macrophages during *T. borreli* infection by using metronidazole-mediate macrophage ablation in a Tg(*mpeg1:Gal4*^{gl2}/*UAS-E1b:Eco.NfsB-mCherry*^{c26}) line (Davison et al., 2007; Ellett et al., 2011), was hampered by: i) the silencing of the UAS promotor driving mCherry expression at time points later than 7 dpf (2 dpi), the period in which the difference between MΦ-high and MΦ-low individuals began to appear; ii) susceptibility of *T. borreli* to metronidazole itself. Furthermore, administration of liposome-encapsulated clodronate (Lipo-clodronate), previously used in 1-2 dpf larvae to transiently eliminate macrophages (Nguyen-Chi et al., 2017; Phan et al., 2018), when used in older larvae (>5 dpf), resulted in oedema formation. Therefore, currently, it was not possible to evaluate the specific contribution of macrophages to the differential response observed in MΦ-high and MΦ-low individuals.

Based on the sequence of events recorded during *T. borreli* infection of zebrafish, the differential macrophage response precedes the (lack of) control of parasitaemia. In fact, at 2 dpi, when clear differences in overall macrophage fluorescence were visible between MΦ-high and MΦ-low individuals, no differences in parasitaemia levels were observed. Thus, the early increase in macrophage number appears to be beneficial for survival, however, whether macrophages have a direct or an indirect role in parasite control requires further investigation. Although tempting to speculate that elimination of the parasite, possibly by phagocytosis, could have contributed to the early parasite control, we never observed (*in vitro* and *in vivo*) direct contact between *T. borreli* and macrophages nor neutrophils, confirming that, as previously reported for *T. borreli* and Trypanosome infections of mice (Caljon et al., 2018; Saeij et al., 2003a; Scharsack et al., 2003), phagocytes are not able to internalize live and motile parasites.

Besides the differential proliferative response, clear differences in the activation state, morphology and localization of macrophages in MΦ-high and MΦ-low individuals were observed. Clearly, MΦ-low individuals, which did not succeed in controlling parasitaemia, displayed an exacerbated pro-inflammatory response, whereas in MΦ-high individuals, the inflammation level as well as parasitaemia remained low. Previously, we reported that in carp Tnfα plays a dual role in *T. borreli* control *in vivo* (Forlenza et al., 2009). In fact, Tnfα depletion as well as overexpression of soluble Tnfα were detrimental to the host, whereas overexpression of the transmembrane form of Tnfα led to full protection. Furthermore, the study showed that carp and zebrafish Tnfα, similarly to mouse TNFα (Daulouede et al., 2001; Lucas et al., 1994; Magez et al., 1997), can directly lyse *Trypanosoma brucei (in vitro)* via its lectin-like activity. Whether Tnfα can also lyse *Trypanoplasma*, and thus directly contribute to parasite control, is yet to be ascertained. Possibly a (moderate) early Tnfα production (from 2 dpi onwards) in MΦ-high individuals could have played a beneficial role in controlling the parasitaemia levels. Conversely, the exacerbated pro-inflammatory response in MΦ-low individuals might have contributed to susceptibility to the infection. Whether such outcomes can be solely ascribed to Tnfα activities, or whether other humoral factors may contribute directly or indirectly to parasite control in some individuals, requires further investigation.

In the current study, we were not able to specifically address the activation state of neutrophils during infection. To our knowledge, transgenic lines specifically marking neutrophils in red fluorescence that can thus be combined with the available *Tg(il1b:eGFP-F)* ^{ump3Tg} or *Tg(tnfa:eGFP-F)*^{ump5Tg} lines, are currently not available. The *lysozymeC:DsRed* reporter line for example, marks a subset of macrophages and likely also granulocytes, but it is not specific for neutrophils only (Hall et al., 2007). Thus, in the future, it will certainly be interesting to also investigate the kinetics of neutrophils activation and their relative contribution to the inflammatory response.

Altogether, in this study we describe the innate immune response of zebrafish larvae to *T. borreli* infections. Considering its evolutionary position, parasitic nature, and ability to infect the same host as other aquatic trypanosomes (e.g *T. carassii*), our analysis contributes to the unravelling of conserved innate immune response strategies of vertebrates to kinetoplastid infections. The observation that a controlled early innate immune response is crucial for survival not only during (fish or mammalian) trypanosome but also during trypanoplasma infections provides further evidence of the complementarity of zebrafish to other mammalian models to study host-parasite interaction and the evolution of pathogenicity of kinetoplastids.

Acknowledgments

This work was supported by the Dutch Research Council (NWO), project number 022.004.005; Dr. Mai E. Nguyen-Chi from DIMNP, CNRS, University of Montpellier is gratefully acknowledged for her helpful advice and discussions about the transgenic zebrafish lines. The authors like to thank the CARUS Aquatic Research Facility of Wageningen University for fish rearing and husbandry and Wageningen Light Microscopy Centre and Montpellier Resources Imagerie facility for their assistance.

References

Benard EL, Racz PI, Rougeot J, Nezhinsky AE, Verbeek FJ, Spaink HP, Meijer AH. 2015. Macrophage-expressed perforins Mpeg1 and Mpeg1.2 have an anti-bacterial function in zebrafish. *J Innate Immun* **7**:136–152. doi:10.1159/000366103

Bertrand JY, Chi NC, Santoso B, Teng S, Stainier DYR, Traver D. 2010. Haematopoietic stem cells derive directly from aortic endothelium during development. *Nature* **464**:108–111. doi:10.1038/nature08738

Bunnajirakul S, Steinhagen D, Hetzel U, Körting W, Drommer W, Korting W, Drommer W. 2000. A study of sequential histopathology of Trypanoplasma borreli (Protozoa: Kinetoplastida) in susceptible common carp Cyprinus carpio. *Dis Aquat Organ* **39**:221–229. doi:10.3354/dao039221

Caljon G, Mabille D, Stijlemans B, Trez C De, Mazzone M, Tacchini-cottier F, Malissen M, Ginderachter JA Van, Magez S, Baetselier P De, Abbeele J Van Den. 2018. Neutrophils enhance early Trypanosoma brucei infection onset 1–11. doi:10.1038/s41598-018-29527-y

Chi NC, Shaw RM, Val S De, Kang G, Jan LY, Black BL, Stainier DYR. 2008. Expression and Atrioventricular Canal Formation. *Genes Dev* 734–739. doi:10.1101/gad.1629408.734

Daulouede S, Bouteille B, Moynet D, De Baetselier P, Courtois P, Lemesre JL, Buguet A, Cespuglio R, Vincendeau P. 2001. Human macrophage tumor necrosis factor (TNF)-alpha production induced by Trypanosoma brucei gambiense and the role of TNF-alpha in parasite control. *J Infect Dis* **183**:988–991.

Davison JM, Akitake CM, Goll MG, Rhee JM, Gosse N, Baier H, Halpern ME, Leach SD, Parsons MJ. 2007. Transactivation from Gal4-VP16 transgenic insertions for tissue-specific cell labeling and ablation in zebrafish. *Dev Biol* **304**:811–824. doi:10.1016/j.ydbio.2007.01.033

Dóró É, Jacobs SH, Hammond FR, Schipper H, Pieters RP, Carrington M, Wiegertjes GF, Forlenza M. 2019. Visualizing trypanosomes in a vertebrate host reveals novel swimming behaviours, adaptations and attachment mechanisms. *Elife* **8**:1–25. doi:10.7554/elife.48388

Dvorak AM, Dvorak HF, Peters SP, Shulman ES, MacGlashan DW, Pyne K, Harvey VS, Galli SJ, Lichtenstein LM. 1983. Lipid bodies: cytoplasmic organelles important to arachidonate metabolism in macrophages and mast cells. *J Immunol* **131**:2965–76.

Ellett F, Pase L, Hayman JW, Andrianopoulos A, Lieschke GJ. 2011. mpeg1 promoter transgenes direct macrophage-lineage expression in zebrafish. *Blood* **117**:49–57. doi:10.1182/blood-2010-10-314120.

Forlenza M, Fink IR, Raes G, Wiegertjes GF. 2011. Heterogeneity of macrophage activation in fish. *Dev Comp Immunol* **35**:1246–1255. doi:10.1016/j.dci.2011.03.008

Forlenza M, Kaiser T, Savelkoul HFJ, Wiegertjes GF. 2012. The use of real-time quantitative PCR for the analysis of cytokine mRNA levels.Methods in Molecular Biology (Clifton, N.J.). pp. 7–23. doi:10.1007/978-1-61779-439-1_2

Forlenza M, Magez S, Scharsack JP, Westphal A, Savelkoul HFJ, Wiegertjes GF. 2009. Receptor-Mediated and Lectin-Like Activities of Carp (Cyprinus carpio) TNF-α. *J Immunol* **183**:5319–5332. doi:10.4049/jimmunol.0901780

Forlenza M, Scharsack JP, Kachamakova NM, Taverne-Thiele AJ, Rombout JHWM, Wiegertjes GF. 2008. Differential contribution of neutrophilic granulocytes and macrophages to nitrosative stress in a host-parasite animal model. *Mol Immunol* **45**:3178–3189. doi:10.1016/j.molimm.2008.02.025

Hall C, Flores M, Storm T, Crosier K, Crosier P. 2007. The zebrafish lysozyme C promoter drives myeloid-specific expression in transgenic fish. *BMC Dev Biol* **7**:1–17. doi:10.1186/1471-213X-7-42

Joerink M, Forlenza M, Ribeiro CMS, de Vries BJ, Savelkoul HFJ, Wiegertjes GF. 2006. Differential macrophage polarisation during parasitic infections in common carp (Cyprinus carpio L.). *Fish Shellfish Immunol* **21**:561–571. doi:10.1016/j.fsi.2006.03.006

Joerink M, Groeneveld A, Ducro B, Savelkoul HFJ, Wiegertjes GF. 2007. Mixed infection with Trypanoplasma borreli and Trypanosoma carassii induces protection: Involvement of cross-reactive antibodies. *Dev Comp Immunol* **31**:903–915. doi:10.1016/j.dci.2006.12.003

Langenau DM, Ferrando AA, Traver D, Kutok JL, Hezel JPD, Kanki JP, Zon LI, Thomas Look A, Trede NS. 2004. In vivo tracking of T cell development, ablation, and engraftment in transgenic zebrafish. *Proc Natl Acad Sci U S A* **101**:7369–7374. doi:10.1073/pnas.0402248101

Lawson ND, Weinstein BM. 2002. In vivo imaging of embryonic vascular development using transgenic zebrafish. *Dev Biol* **248**:307–318. doi:10.1006/dbio.2002.0711

Lom J. 1979. Biology of the trypanosomes and trypanoplasms of fishBiology of the Kinetoplastida. pp. 269–337. doi:10.1111/j.1550-7408.1980.tb04245.x

López-Muñoz RA, Molina-Berríos A, Campos-Estrada C, Abarca-Sanhueza P, Urrutia-Llancaqueo L, Peña-Espinoza M, Maya JD. 2018. Inflammatory and pro-resolving lipids in trypanosomatid infections: A key to understanding parasite control. *Front Microbiol* **9**:1–16. doi:10.3389/fmicb.2018.01961

Losev A, Grybchuk-Ieremenko A, Kostygov AY, Lukeš J, Yurchenko V. 2015. Host specificity, pathogenicity, and mixed infections of trypanoplasms from freshwater fishes. *Parasitol Res* **114**:1071–1078. doi:10.1007/s00436-014-4277-y

Lucas R, Magez S, De Leys R, Fransen L, Scheerlinck JP, Rampelberg M, Sablon E, De Baetselier P. 1994. Mapping the lectin-like activity of tumor necrosis factor. *Science (80-)*. doi:10.1126/science.8303299

Lukeš J, Skalický T, Týč J, Votýpka J, Yurchenko V. 2014. Evolution of parasitism in kinetoplastid flagellates. *Mol Biochem Parasitol* **195**:115–122. doi:10.1016/j.molbiopara.2014.05.007

Magez S, Geuskens M, Beschin A, del Favero H, Verschueren H, Lucas R, Pays E, de Baetselier P. 1997. Specific uptake of tumor necrosis factor-alpha is involved in growth control of Trypanosoma brucei. *J Cell Biol* **137**:715–727.

Melo RCN, Ávila HD, Fabrino DL, Almeida PE, Bozza PT. 2003. Macrophage lipid body induction by Chagas disease in vivo: Putative intracellular domains for eicosanoid formation during infection. *Tissue Cell* **35**:59–67. doi:10.1016/S0040-8166(02)00105-2

Melo RCN, Fabrino DL, Dias FF, Parreira GG. 2006. Lipid bodies: Structural markers of inflammatory macrophages in innate immunity. *Inflamm Res* **55**:342–348. doi:10.1007/s00011-006-5205-0

Nguyen-Chi M, Laplace-Builhé B, Travnickova J, Luz-Crawford P, Tejedor G, Lutfalla G, Kissa K, Jorgensen C, Djouad F. 2017. TNF signaling and macrophages govern fin regeneration in zebrafish larvae. *Cell Death Dis* **8**:e2979. doi:10.1038/cddis.2017.374

Nguyen-Chi M, Laplace-Builhe B, Travnickova J, Luz-Crawford P, Tejedor G, Phan QT, Duroux-Richard I, Levraud JP, Kissa K, Lutfalla G, Jorgensen C, Djouad F. 2015. Identification of polarized macrophage subsets in zebrafish. *Elife* **4**:1–14. doi:10.7554/eLife.07288

Nguyen-Chi M, Phan QT, Gonzalez C, Dubremetz JF, Levraud JP, Lutfalla G. 2014. Transient infection of the zebrafish notochord with E. coli induces chronic inflammation. *DMM Dis Model Mech* **7**:871–882. doi:10.1242/dmm.014498

Page DM, Wittamer V, Bertrand JY, Lewis KL, Pratt DN, Delgado N, Schale SE, McGue C, Jacobsen BH, Doty A, Pao Y, Yang H, Chi NC, Magor BG, Traver D. 2013. An evolutionarily conserved program of B-cell development and activation in zebrafish. *Blood* **122**:1–11. doi:10.1182/blood-2012-12-471029

Petrie-Hanson L, Hohn C, Hanson L. 2009. Characterization of rag1 mutant zebrafish leukocytes. *BMC Immunol* **10**:1–8. doi:10.1186/1471-2172-10-8

Phan QT, Sipka T, Gonzalez C, Levraud JP, Lutfalla G, Nguyen-Chi M. 2018. Neutrophils use superoxide to control bacterial infection at a distance. *PLoS Pathog* **14**:1–29. doi:10.1371/journal.ppat.1007157

Renshaw SA, Loynes CA, Trushell DMI, Elworthy S, Ingham PW, Whyte MKB. 2006. A transgenic zebrafish model of neutrophilic inflammation. *Blood* **108**:3976–3978. doi:10.1182/blood-2006-05-024075

Saeij JPJ, Groeneveld A, Van Rooijen N, Haenen OLM, Wiegertjes GF. 2003a. Minor effect of depletion of resident macrophages from peritoneal cavity on resistance of common carp Cyprinus carpio to blood flagellates. *Dis Aquat Organ* **57**:67–75. doi:10.3354/dao057067

Saeij JPJ, Van Muiswinkel WB, Groeneveld A, Wiegertjes GF. 2002. Immune modulation by fish kinetoplastid parasites: A role for nitric oxide. *Parasitology* **124**:77–86. doi:10.1017/S0031182001008915

Saeij JPJ, Van Muiswinkel WB, Van De Meent M, Amaral C, Wiegertjes GF. 2003b. Different capacities of carp leukocytes to encounter nitric oxide-mediated stress: A role for the intracellular reduced glutathione pool. *Dev Comp Immunol* **27**:555–568. doi:10.1016/S0145-305X(02)00158-1

Scharsack JP, Steinhagen D, Kleczka C, Schmidt JO, Körting W, Michael RD, Leibold W, Schuberth HJ. 2003. Head kidney neutrophils of carp (Cyprinus carpio L.) are functionally modulated by the haemoflagellate Trypanoplasma borreli. *Fish Shellfish Immunol* **14**:389–403. doi:10.1006/fsim.2002.0447

Steinhagen D, Kruse P, Korting W. 1990. Some haematological observations on carp, Cyprinus carpio L., experimentally infected with Trypanoplasma borreli Laveran & Mesnil, 1901 (Protozoa: Kinetoplastida). *J Fish Dis* **13**:157–162. doi:10.1111/j.1365-2761.1990.tb00768.x

Steinhagen D, Kruse P, Korting W. 1989. The Parasitemia of Cloned Trypanoplasma borreli Laveran and Mesnil , 1901 , in Laboratory- Infected Common Carp (Cyprinus carpio L .) Author (s): Dieter Steinhagen , Peter Kruse and Wolfgang Körting Source : The Journal of Parasitology , Vol . 75 , No. *J Parasitol* **75**:685–689.

Torraca V, Mostowy S. 2018. Zebrafish Infection: From Pathogenesis to Cell Biology. *Trends Cell Biol* **28**:143–156. doi:10.1016/j.tcb.2017.10.002

Vallochi AL, Teixeira L, Oliveira K da S, Maya-Monteiro CM, Bozza PT. 2018. Lipid Droplet, a Key Player in Host-Parasite Interactions. *Front Immunol* **9**:1022. doi:10.3389/fimmu.2018.01022

White RM, Sessa A, Burke C, Bowman T, LeBlanc J, Ceol C, Bourque C, Dovey M, Goessling W, Burns CE, Zon LI. 2008. Transparent Adult Zebrafish as a Tool for In Vivo Transplantation Analysis. *Cell Stem Cell* **2**:183–189. doi:10.1016/j.stem.2007.11.002

Woo PTK. 2003. Cryptobia (Trypanoplasma) salmositica and salmonid cryptobiosis. *J Fish Dis* **26**:627–646. doi:10.1046/j.1365-2761.2003.00500.x

Woo PTK, Ardelli BF. 2013. Immunity against selected piscine flagellates. *Dev Comp Immunol* **43**:268–279. doi:10.1016/j.dci.2013.07.006

Wymann MP, Schneiter R. 2008. Lipid signalling in disease. *Nat Rev Mol Cell Biol*. doi:10.1038/nrm2335

Supplementary data

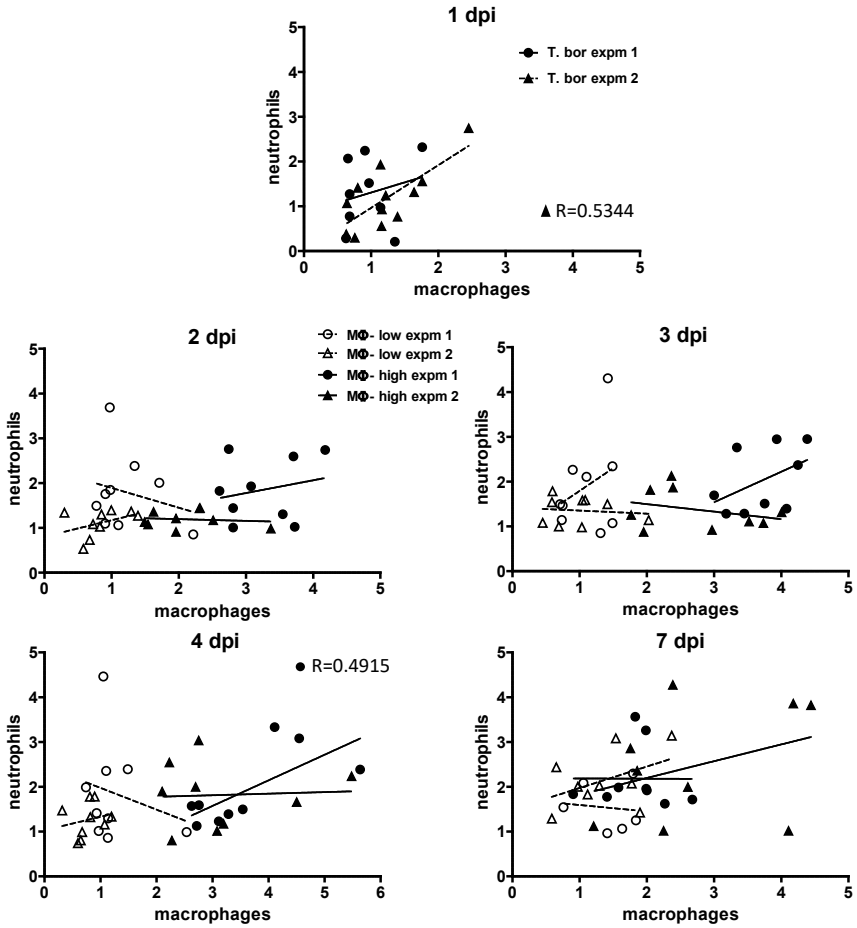

Supplementary Fig 1. Lack of correlation between total neutrophil and macrophage fluorescence in MΦ-high or MΦ-low individuals. *Tg(mpeg1.4:mCherry-F;mpx:GFP)* larvae were screened for homogeneity of red fluorescence at 3 dpf and injected intravenously at 5 dpf with n=200 *T. borreli* or with PVP. At 1 dpi, total fluorescence was acquired to confirm homogeneity of fluorescence among *T. borreli*-infected individuals prior their segregation in MΦ-high and MΦ-low individuals. At 2 dpi larvae were separated in MΦ-high and MΦ-low individuals. Total macrophage (red) and neutrophil (green) fluorescence of n=14-18 larvae per group, from two independent experiments, was acquired at the indicated time points. Symbols indicate the relative CTCF for macrophages and neutrophils in each individual, calculated relative to the PVP control at the respective time point. Open symbols indicate relative values in MΦ-low individuals and closed symbols indicate relative values in MΦ-high individuals, in experiment 1 (circles) and experiment 2 (triangles). No significant interaction was observed, except at 1 dpi in experiment 2, and at 4 dpi in MΦ-high individuals of experiment 1, although the correlation (R^2) was still low.

CHAPTER 6

General discussion

African trypanosomes and American trypanosomes are important causative agents of diseases of humans, livestock and cold-blooded species, including fish. The best-known trypanosomes cause human diseases, affecting millions of people in the developing world and lead to high morbidity and mortality rates. Various *in vitro, ex vivo* studies as well as experimental infection of mice with trypanosome, contributed to tremendous insights into the general biology of trypanosomes, their motility, their interaction with and evasion of the host immune system, as well as into various aspects related to vaccine failure, antigenic variation, and (uncontrolled) inflammation. One of the best-studied non-mammalian trypanosomes is *Trypanosoma carassii*. *T. carassii* often co-infects fish with *Trypanoplasma* species, and presently few, or even no studies have been performed to characterise the morphology, motility and host-pathogen interactions of trypanoplasma. For both trypanosomes and trypanoplasma, *in vivo* studies to visualise the parasite swimming behaviour and host immune response, in a natural host environment, have not been described. The overall **aim of this thesis** was to visualise and characterise blood flagellates infections, by studying: **1)** parasite motility *in vitro* and *in vivo* and **2)** the kinetics of innate immune responses *in vivo*.

By making use of the transparent zebrafish larvae, infected with the fish-specific *Trypanosoma carassii*, we revealed in **Chapter 2** novel attachment mechanisms and adaptation strategies of trypanosomes *in vivo* and we placed our observations in the framework of existing literature. In **Chapter 4** we describe for the first time *in vitro* and *in vivo,* the swimming behaviour of *Trypanoplasma borreli*. We performed a novel quantitative analysis to compare the swimming behaviour *in vitro* of *T. borreli* and the *T. carassii*. Further, the zebrafish model allowed us to study the differential response of innate immune cells to trypanosome and trypanoplasma infections, as reported in **Chapter 3** and **5**. In this final chapter, **Chapter 6**, the obtained knowledge will be discussed and future studies will be suggested, taking into consideration the strengths and weaknesses of our current work. At the end of this chapter, the results will be put into a broader perspective and the thesis will be discussed with respect to its overall relevance.

Mechanisms of trypanosomes and trypanoplasma to evade or manipulate the host' immune responses

Extravasation of *T. borreli* and *T. carassii* is one of the hallmarks during infection and since both parasites remain extracellular, they are continuously exposed to the hosts' immune response. However, we observed that as long as the parasites are motile, phagocytosis of *T. borreli* and *T. carassii* does not occur, neither *in vivo* nor *in vitro* (personal observation). Our observations were confirmed by other studies, as they reported to never observe direct

interaction of live parasites with macrophages or neutrophils, indicating that, as shown previously, elimination of the live trypanosomes and trypanoplasma by phagocytosis is very unlikely (Caljon et al., 2018; Saeij et al., 2003; Scharsack et al., 2003). Thus, the question arises: what mechanisms do trypanosomes and trypanoplasma use to evade or manipulate immune responses?

African trypanosomes show antigenic variation, an immune evasion mechanism, based on sequential switching of the major variant surface glycoprotein (VSG). VSGs are highly immunogenic and induce specific antibody production. By periodically changing their VSGs, trypanosomes are initially not recognized by antibodies against VSG epitopes displayed on the former surface coat. In this way, at population level, the trypanosomes escape from immune recognition (Antia et al., 1996; Cross, 1996; Morrison et al., 2009; Vickerman, 1969). VSGs are anchored in the trypanosome membrane by glycosylphosphatidylinositol (GPI) anchors, forming a thick barrier and protect from antibodies that might bind to buried conserved proteins (reviewed by Schwede et al., 2015). Motility of trypanosomes has been shown to be also important in immune evasion. *In vitro* studies described that *T. brucei* can clear antibodies, when present at low levels on its surface, during the early stages of infection by using hydrodynamic drag forces generated by directional swimming. The VSG-bound antibodies accumulate in the flagellar pocket at the posterior end and are endocytosed (Engstler et al., 2007).

Unlike VSG-expressing trypanosomes, little is known about the surface proteins and other virulence factors of non-VSG-expressing trypanosomes and trypanoplasma. Studies indicated that the surface of *Cryptobia salmositica*, a close relative of *T. borreli*, affecting salmonid fish, contains neuraminidase-sensitive sialic acid residues (Vommaro et al., 1997). For *T. carassii*, some surface proteins have been identified that could play a role in immune evasion or manipulation of immune responses. Examples of these are mucin-like glycoproteins and major surface proteases (MSPs), such as gp63 (Aguero et al., 2002; Lischke et al., 2000; Oladiran and Belosevic, 2012; Overath et al., 1999). Gp63 is suggested to have various roles in host- parasite interactions and immune modulation in *Leishmania*, *T. cruzi* and *T. brucei* (Brittingham et al., 1995; Cuevas et al., 2003; Gruszynski et al., 2006; McGwire et al., 2002). One of its roles in *Leishmania* species is to bind complement component C3 and proteolytically convert C3b to an inactive form, thus interrupting the complement cascade and in this way protecting the parasites against complement-mediated lysis (Brittingham et al., 1995; McGwire et al., 2002). Additionally, in *T. brucei*, it was suggested that gp63 on the cell surface is responsible for the shedding of VSG during differentiation from bloodstream stage to procyclic stage (Grandgenett et al., 2007; LaCount et al., 2003). *T. borreli* and *T. carassii* were shown to express a cathepsin L-like proteinase, phylogenetically closely related to cysteine proteinases of other Trypanosomatida, having the ability to cleave common carp IgM and other host proteins (Ruszczyk et al., 2008a, 2008b). Among these, cleavage

products of transferrin were shown to contribute to activation of macrophages towards a pro-inflammatory profile (Jurecka et al., 2009). Furthermore, it was shown that *T. borreli* uses a similar method of antibody clearance as observed for *T. brucei* (Forlenza et al., 2009b).

T. brucei can secrete or release immunosuppressive molecules like Kinesin Heavy Chain 1 (TbKHC1) and Adenylate Cyclase (tbAdC). TbKHC1 induces IL-10 release and the arginase pathway by myeloid cells, leading to the formation of alternatively (non-inflammatory) activated macrophages (M2) favouring parasite growth (De Muylder et al., 2013). Upon phagocytosis, in an act of altruistic death, *T. brucei* upregulate the expression of transmembrane receptor-like adenylate cyclase (TbAdC). This cyclase induces the cytosolic release of cAMP in phagocytic cells, activates protein kinase A and thus effectively prevents the production of the trypanolytic cytokine TNF and indirectly of other pro-inflammatory molecules (Salmon et al., 2012). It seems that the VSG-expressing trypanosomes have developed a mechanism where altruistic parasites are phagocytosed, and in this way disable the classical (inflammatory) activated macrophages (M1) needed for parasite control. Besides immunosuppressive molecules, some trypanosome strains express resistance proteins, such as serum resistance antigen (SRA) or a specific glycoprotein (TgsGP), counteracting host trypanosome lytic factors (reviewed by Stijlemans et al., 2016). In our studies, we observed during both *T. borreli* and *T. carassii* infections in zebrafish, two distinct groups of individuals; 1) low-infected individuals expressing low levels of pro-inflammatory cytokines, which were able to control parasite levels and as a result survived the infection, and 2) high-infected individuals expressing high levels of pro-inflammatory cytokine, which were unable to control the parasite infections, and eventually died as result of the infection (**Chapter 3** and **5**). We could speculate that the parasites in the surviving fish, in some way manipulated the host to prevent inflammation, and in this way avoid the exacerbated pro-inflammatory responses that were observed in the high-infected individuals. Further, the variation of the immune response between these two groups might be indicative of the intrinsic differences at individual level, which makes one fish more prone to develop a high pro-inflammatory response, whereas another fish is able to better control the response. the. It might be informative to analyse the various phenotypes of macrophages that are observed in the high- and low-infected individuals. To study this, relevant cell types of one individual can be grouped and compared to the same type of cells from another individual. Additionally, single cells could be isolated to investigate the differences between macrophages with different phenotypes within the same individual fish and how they could contribute to different responses to the infection.

During experimental and natural trypanosome infections, differences in pathology and parasite control were also observed. These differences were usually observed between different breeds and strains of animals. In cattle, differences have been identified related to the capacity to survive trypanosome infections and there are cattle breeds categorized

as trypanotolerant or trypanosusceptible. Trypanotolerant animals have a better capacity to control the parasitaemia and anaemia than trypanosusceptible animals (Naessens, 2006; Naessens et al., 2003). Likewise, the genetic background of different mice strains can also influence the susceptibility or tolerance to infection, although here parasitaemia levels were not necessarily correlated to anaemia and vice versa. C57BL/6 mice exhibited severe anaemia, but low parasitaemia, while BALB/c mice had greatly reduced anaemia, but higher parasitaemia (Magez et al., 2004). Interestingly, during our studies, we observed a differential response during both *T. borreli* and *T. carassii* infections in zebrafish larvae from one population of outbred zebrafish larvae. This, in combination with the ability to monitor the infection at the individual level, may contribute to the design of future studies to unravel against what parasite molecules host innate immune cells respond to and what mechanisms do non-VSG expressing trypanosomes and trypanoplasma use to evade or manipulate immune responses.

Next steps for *in vivo* visualisation of innate immune responses during trypanosome and trypanoplasma infections

A dual role for Tnfα during *T. carassii* and *T. borreli* infections?

Various mice studies studying trypanosome infections have shown that timely and controlled release of innate immune cytokines is crucial during the acute phase of trypanosome infections (Iraqi et al., 2001; Kaushik et al., 1999; Lucas et al., 1994; Magez et al., 2007; Namangala et al., 2001; Noel et al., 2002). TNF and nitric oxide (NO) play a crucial role in limiting trypanosome growth during the first peak of parasitaemia (Lopez et al., 2008; Magez et al., 2007, 2006; Sternberg and Mabbott, 1996), although overexpression of NO and TNFα can contribute to immunopathology (Brunet, 2001; Magez et al., 1999), indicating dual roles for both TNF and NO during trypanosome infections.

Our group previously reported that Tnfα is essential to control *T. borreli in vivo* in common carp, although overexpression of this cytokine was detrimental to the host (Forlenza et al., 2009). Furthermore, similar to mouse TNFα, this study showed that carp, zebrafish, rainbow trout and seabream Tnfα, could directly lyse *Trypanosoma brucei (in vitro)* via a lectin-like activity (Daulouède et al., 2001; Forlenza et al., 2009; Lucas et al., 1994; Magez et al., 1997). TNFα is able to bind via its lectin-like domain to mannose moieties present in the flagellar pocket of some African trypanosomes (Lucas et al., 1994) and to cause direct parasite lysis. The most distinct observation about the innate immune response during *T. borreli* and *T. carassii* infections during our current studies was the inverse correlation between parasite levels and the inflammatory (macrophage) response. During *T. carassii* infections, low-infected zebrafish larvae had a significant increase in macrophage number from 5

dpi onwards, whereas in high-infected individuals, a significant increase was observed only from 9 dpi onwards (**Chapter 3**). Similarly, by 2 dpi, *T. borreli*-infected zebrafish larvae could be categorised in MΦ-high and MΦ-low individuals, based on total red fluorescence, and 3 days later we could confirm that MΦ-high individuals had low infection levels and vice versa (**Chapter 5**). These observations suggest that an early increase in macrophage numbers is beneficial for survival. Possibly, (moderate) Tnfα production by these cells could have played a beneficial role in controlling the parasitaemia levels. Conversely, we observed an exacerbated pro-inflammatory response in high-infected or MΦ-low individuals, which is in agreement with the detrimental role of Tnfα when expressed at too high levels. There are various potential explanations for the inability of high-infected zebrafish larvae to control the parasitaemia and the increased inflammatory response. Mice studies have shown that the timely secretion of regulatory molecules, such a soluble TNFR2, might play an important role in inflammation control (Magez et al., 2004). Whether the susceptibility to *T. carassii* and *T. borreli* infections can be solely ascribed to Tnfα, needs further investigation.

Zebrafish have two *TNFα* homologues, *tnfa* and *tnfb* (Kinoshita et al., 2013), and it would be interesting to study the role of *tnfb* during *T. carassii* and *T. borreli* infections in zebrafish. The role of *tnfa* during infections in zebrafish is in general better studied. Zebrafish is used as an animal model to study human tuberculosis. Its natural pathogen, *Mycobacterium marinum,* shares major virulence factors with the human pathogen *Mycobacterium tuberculosis*. Various studies analysed in zebrafish the role of Tnfa in host defence against tuberculosis (Clay et al., 2008; Ramakrishnan, 2013; Roca et al., 2019, 2008). Both *tnfa* and *tnfb* were shown to be (pro-inflammatory) M1 macrophage markers in zebrafish. The transgenic zebrafish line *Tg(tnfa:eGFP-F*), allows visualisation of *tnfa* expressing cells (Nguyen-Chi et al., 2015). Currently, no transgenic zebrafish reporter line is available marking *tnfb* expressing cells. Additionally, in future studies, the (innate) immune response could be studied in the absence of macrophages or Tnfα, to investigate their role in protection and susceptibility to infection. As discussed in **Chapter 3** and **5**, it was currently not possible for us to evaluate the contribution of macrophages. Tnfα knock-out zebrafish (*tnfa*-/- of *tnfb*-/-) could be used in the future to study the role of Tnfα. For a timely, transient downregulation of *tnfa in vivo* zebrafish, treatment with pentoxifylline (PTX) could be used (Nguyen-Chi et al., 2017). Altogether, in mammalian but possibly also in zebrafish models of trypanosome infections Tnfa seems to play a prominent role in the early innate response. The genetic tractability and amenability of zebrafish therefore, offers a valuable complementary tool to not only investigate the role but also visualise the ensuing immune response triggered upon manipulation of Tnfa activities.

Nitric oxide during *T. carassii* and *T. borreli* infections: immune suppressor or immune effector?

Our group previously showed that *in vitro* nitric oxide (NO) hinders clearance of surface-bound antibody through its trypanostatic effect on *T. borreli* (Forlenza et al., 2009). Considering that *T. borreli* was shown to trigger very high levels of NO production *in vivo,* NO may play a protective role, especially early during infection, by contributing to the accumulation of antibodies on the parasite's surface and thus to antibody-dependent complement-mediated lysis (Forlenza et al., 2009). Additionally, it was observed *in vitro* that not NO, but peroxinitrite ($ONOO^-$) has a strong cytotoxic effect on the parasite (Forlenza et al., 2008). On the other hand, *in vivo*, the ability of *T. borreli* to induce high levels of NO was shown to cause extensive tissue nitration, inflammation and inhibition of lymphocyte proliferation, whereas *T. borreli* itself is not affected (Forlenza et al., 2009; Saeij et al., 2003; Saeij et al., 2002). Inducing high levels of NO, could be a strategy of *T. borreli* to immunosuppress and evade the host immune response (Forlenza et al., 2008). In carp, administration of an iNOS inhibitor showed to be beneficial to the host, since it resulted in lower parasitaemia levels and higher survival (Saeij et al., 2002). These observations show that NO is an important player in host-parasite interactions, with a possible dual role as an immune suppressor or immune effector. In contrast, it was shown that *in vivo*, *T. carassii* did not induce NO production in carp and even inhibited LPS-induced NO production *in vitro* (Saeij et al., 2002).

Tyrosine nitration is a marker for nitrosative stress (tissue damage) and is caused by the release of reactive oxygen and nitrogen species by activated macrophages and neutrophils. The generation of these agents can lead to the formation of peroxynitrate, which can nitrate phenolic groups, leading to the formation of nitrotyrosine (Forlenza et al., 2008; Hurst and Hurst, 2002). Myeloperoxidase (MPO)-catalysed oxidation of nitrite can as well contribute to the production of nitrotyrosine *in vivo* (Eiserich et al., 1997; Forlenza et al., 2008). To investigate whether also during *T. borreli* infection of zebrafish larvae macrophages and/or neutrophils contribute to nitrosative stress, we performed a preliminary experiment where *Tg(mpeg1:eGFP)* or *Tg(mpx:GFP*) zebrafish larvae were infected with *T. borreli*; at 3 dpi, larvae were separated in MΦ-low (high parasitaemia) and MΦ-high (low parasitaemia) individuals, followed by immune-staining of the head and trunk region with anti-GFP (macrophages or neutrophils) and anti-nitrotyrosine antibodies.

Tyrosine nitration could be detected in both, non-infected and infected individuals as diffused staining, frequently as scattered discrete spots throughout the head, or along the cardinal caudal vein in the trunk region (**Fig 1A**). Nitrotyrosine levels were slightly higher in MΦ-high and MΦ-low infected individuals than in the PVP-injected controls (**Fig 1B**) indicating that *T. borreli* infection leads to cell and tissue nitration. Next we analysed tyrosine nitration specifically in macrophages and neutrophils (**Fig 2**). In PVP-injected controls only few nitrotyrosine$^+$ macrophages were observed. Upon infection, in both MΦ-high and MΦ-low individuals we observed an increased number of nitrotyrosine$^+$ macrophages. Tyrosine

nitration however, was not observed in all macrophages, suggesting a differential macrophage activation upon infection (**Fig 2A**). We observed nitrotyrosine^{+} neutrophils in PVP-injected control groups, possibly due to background activity of endogenous myeloperoxidase (MPO), which is able to also nitrate tyrosine residues in the absence of peroxynitrate (Elks et al., 2013; Forlenza et al., 2008). Upon infection, we observed an increase in the levels of nitrotyrosine immunoreactivity, especially in the head region (**Fig 2C**). The nitrotyrosine was both observed in the cytoplasmic compartments and immediately surrounding the neutrophils indicating release of peroxynitrate upon infection, which is responsible for the nitration of surrounding proteins (**Fig 2B** and **2C**). During this experimental set up we were not able to determine if the nitrotyrosine outside the neutrophils can exclusively be ascribed to the neutrophils, since it could be due to neighbouring macrophages, which were not visible in the same individual fish. Additionally, more fish need to be analysed to quantify the differences between tyrosine nitration levels of macrophages and neutrophils, since for this preliminary study we only analysed two fish per group. For further analysis it would be interesting to perform a three colour immune-staining, allowing identification of nitrotyrosine, macrophages and neutrophils in one individual fish. We were currently not able to perform a three colour immune-staining to label macrophages, neutrophils and nitrotyrosine, since two of ours primary antibodies (anti-nitrotyrosine and anti-mCherry) where raised in rabbit, while the anti-GFP antibody was raised in chickens. This study provides a first insight in the occurrence of tissue nitration during *T. borreli* infections in zebrafish, due to the release of peroxynitrate or MPO by macrophages or neutrophils. However, further studies are needed to specify the contribution of macrophages and neutrophils in tissue nitration and analyse the role of nitric oxide (NO) during *T. borreli* and *T. carassii* infections of zebrafish.

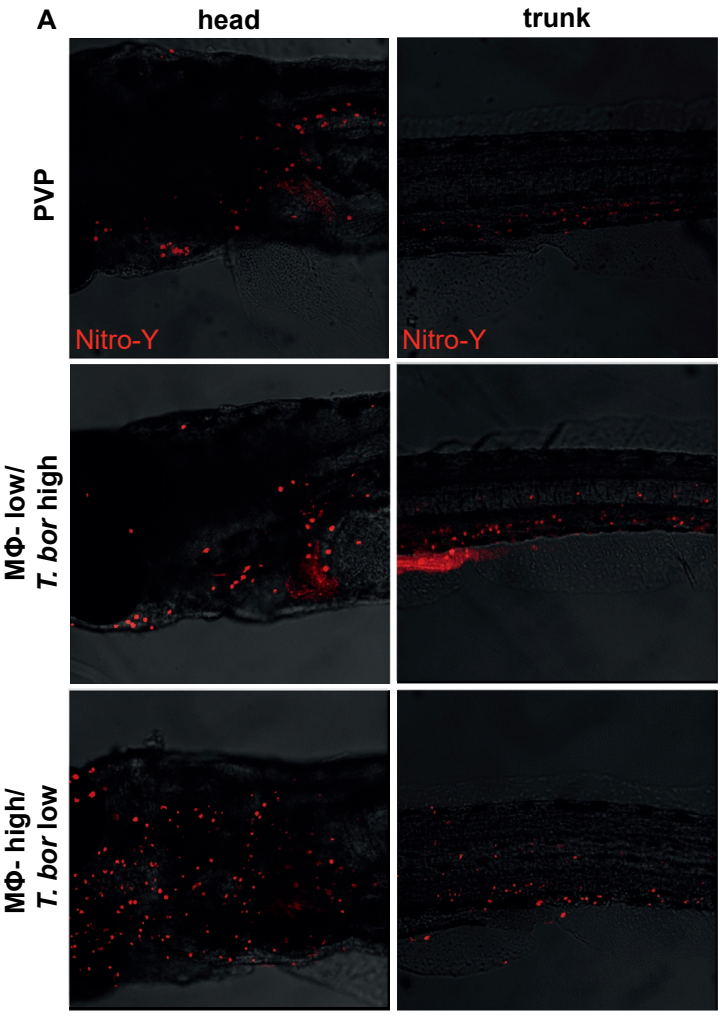
A
head
trunk
PVP
Nitro-Y
Nitro-Y
MΦ- low/
T. bor high
MΦ- high/
T. bor low
B
Total nitro-Y
Head
Trunk
CTCF
8.0x10^8
6.0x10^8
4.0x10^8
2.0x10^8
0
PVP
MΦ- low
MΦ- high

◂ **Fig 1. Tissue nitration during *T. borreli* infections in zebrafish.**
Tg(mpeg1:eGFP) zebrafish larvae were infected intravenously at 5 dpf with n=200 *T. borreli* or with PVP control. At 3 dpi, larvae were fixed and threated with anti-nitrotyrosine antibody (Bio-connect, Upstate The Netherlands, 1:150), followed by goat anti-rabbit-Alexa 594 (Invitrogen, 1:500) to identify production of nirotyrosine. Fish were imaged with Andor Spinning Disc Confocal Microscope using 10x. **A)** Representative maximum projection images of the head and trunk regions are shown, capturing nitrotyrosine (red) in PVP-injected control, MΦ-low and MΦ-high zebrafish. **B)** Corrected total cell fluorescence (CTCF) calculated in the both head and trunk region (n=2 larvae per group) using ImageJ.

Mixed infections with *T. carassii* and *T. borreli*: a model for macrophage polarization?

In this thesis we report the development of an infection model of *T. carassii* or *T. borreli* in a vertebrate host and we studied the innate immune responses during mono-parasitic infections in zebrafish larvae. Natural mixed infections of these two parasites have been reported frequently, but have not been studied in detail. Both parasites occur naturally in the blood of cyprinid fish, as single infections as well as mixed infections (Lom and Dyková, 1992). Our group previously established a mixed infection model in common carp by injecting fixed numbers of both parasites. Interestingly, single infections of *T. borreli* lead to higher parasitaemia levels than during mixed infections and the survival rates were increased during the mixed infections compared to mono-infections with *T. borreli*. Additionally, a significantly early and higher antibody production was observed, compared to mono-parasitic infections. The increased survival during the mixed infection could partially be due to production of cross-reactive antibodies, since the presence of *T. carassii* prior to *T. borreli* showed increased resistance to the infection with *T. borreli*. This study indicated a protective effect of co-infection with *T. carassii* on the resistance to *T. borreli*, possibly mediated by cross-reactive antibodies (Joerink et al., 2007).

In many parasitic infections both classically activated macrophages (M1) and alternatively activated macrophages (M2) play a pivotal role. Experimental mono-parasitic infections of common carp with *T. borreli* or *T. carassii* have shown that these parasites induce different immune responses. *T. borreli* preferentially induces the production of NO and the development of classically activated macrophages (M1) whereas *T. carassii* does not induce the production of NO but rather stimulates an increased arginase activity involved in the alternative activation of macrophages (M2) (Fink et al., 2015; Forlenza et al., 2009b, 2008; Joerink et al., 2006; Saeij et al., 2002).

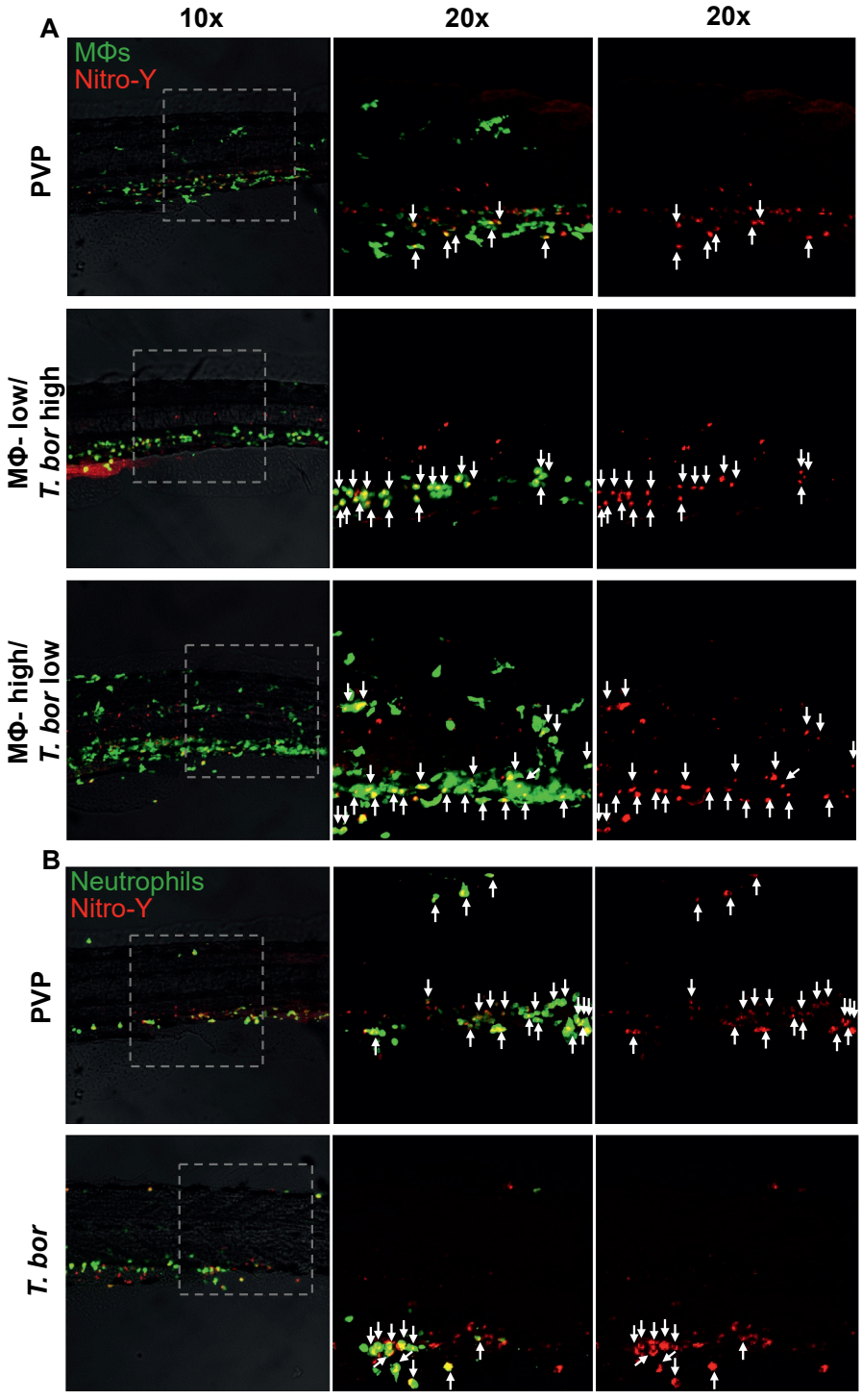
A
10x
20x
20x
MΦs
Nitro-Y
PVP
MΦ- low/
T. bor high
MΦ- high/
T. bor low
B
Neutrophils
Nitro-Y
PVP
T. bor

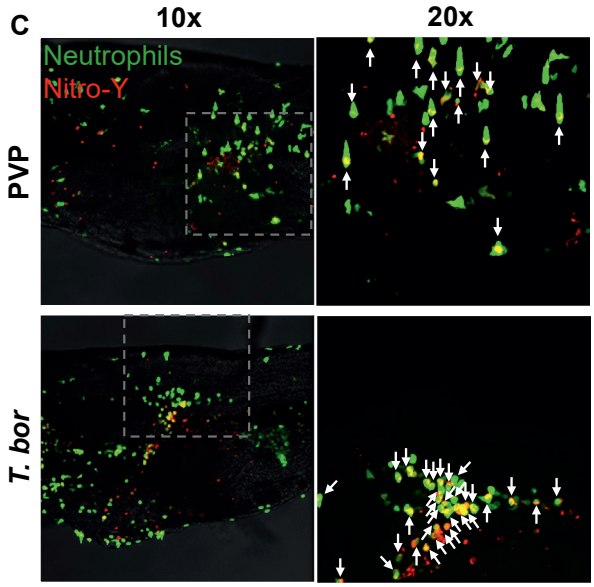

Fig 2. Increased nitrotyrosine immunoreactivity of macrophages and neutrophils during *T. borreli* infection.

Tg(mpeg1:eGFP) and *Tg(mpx:GFP)* zebrafish larvae were infected intravenously at 5 dpf with n=200 *T. borreli* or with PVP control. At 3 dpi, larvae were fixed and threated with anti-nitrotyrosine antibody (Bio-connect, Upstate The Netherlands, 1:150), followed by goat anti-rabbit-Alexa 594 (Invitrogen, 1:500) and anti-GFP antibody Chicken anti-GFP (1:500), followed by goat anti-chicken-Alexa 488 (Abcam, 1:500) to identify production of nitrotyrosine and macrophages or neutrophils. Fish were imaged with Andor Spinning Disc Confocal Microscope using 10x and 20x magnification. **A)** Representative maximum projection images of the trunk regions are shown, capturing macrophages (green) and nitrotyrosine (red) in PVP-injected control, MΦ-low and MΦ-high zebrafish. White arrows indicate nitrotyrosine$^+$ and GFP$^+$ macrophages. **B-C)** Representative maximum projection images of the trunk B) and head C) regions are shown, capturing neutrophils (green) and nitrotyrosine (red) in PVP-injected control and *T. borreli* infected zebrafish. White arrows indicate nitrotyrosine$^+$ and GFP$^+$ neutrophils.

Zebrafish infected with either *T. borreli* or *T. carassii* did not induce such clear overall differences in macrophage polarisation as seen in carp. We observed during both *T. borreli* and *T. carassii* infections in zebrafish two distinct groups of individuals. The differences in inflammatory responses between these two groups could indicate that there are two different inflammatory phenotypes present during the infection, but in different individual fish; the low-infected individuals displayed overall a more 'controlled inflammatory' profile (less M1-like), compared to the high-infected individuals, which displayed overall strong pro-inflammatory profile (more M1-like). The zebrafish larvae allowed us to visualise, *in vivo* in real-time, the individual innate immune responses. The studies performed in carp might possibly not been able to pick up these individual

differences, and therefore have only looked at the predominant (macrophage) response. It cannot be excluded that in adult carp, adaptive immunity also played a role in modulating the innate inflammatory response.

Besides differences in the overall macrophage responses between individual zebrafish, we also observed heterogeneity between macrophages within one individual. It would be interesting to investigate the transcription profiles of the different macrophage phenotypes during the course of the infection and being able to analyse the differences between the macrophages that are responsible for the early Tnfα release in the early phase of infection, the ones that do not express Tnfα and the foamy macrophages in the later stage of infection. It was demonstrated in zebrafish that aseptic wounding and *Escherichia coli* inoculation recruited unpolarized macrophages to the sites of inflammation, where they become polarized into M1 cells and over time these macrophages were converted into an M2-like macrophage subtype, presumably to help clear up the inflammation (Nguyen-Chi et al., 2015). Currently, no zebrafish transgenic reporter lines specifically marking M1 and M2 macrophages are available. Tnfα is a putative, although not unique, marker for M1 macrophages. The possibility to develop M1 (e.g., NOS-2+) and M2 (e.g., ARG-2+, TGFβ1+) zebrafish transgenic lines using different fluorescent markers, in combination with other markers as suggested by Nguyen-Chi et al (2015), would make the zebrafish *T. borreli* and *T. carassii* (mixed) infection model very suited to study macrophage polarization *in vivo,* in real-time at individual cell level and allows visualisation of how macrophage polarization might be influenced by the presence of both parasites (Elks et al., 2013; Nguyen-Chi et al., 2015; Wiegertjes et al., 2016).

Trypanosomes during co-infections and their effect on (memory) B cells

Studies revealed that African trypanosomes have developed several protective adaptations in case they do get recognized by host antibodies. Ample evidence exists that trypanosomes can induce B cell exhaustion. This is caused by a reduction in B cell lymphopoiesis in the bone marrow and marginal zone B cells (transitional and IgM^+ B cells) in the spleen, followed by gradual depletion of follicular B cells (Bockstal et al., 2011; Radwanska et al., 2008). Marginal zone B cells are the first line of defense against blood-borne pathogens and follicular B cells are the main source of the development of antibody producing plasma cells and memory B cells. When follicular B cell depletion is complete, it is impossible for the host to produce new antibodies against new VSGs and additionally, B cell exhaustion has a secondary detrimental effect; the elimination of vaccine-induced immunological memory (Radwanska et al., 2008). This effect of trypanosome infections on the vaccine efficacy of non-related diseases has been reported during both animal and human trypanosomiasis (Holland et al., 2003, 2001; Ilemobade et al., 1982; Mwangi et al., 1990; Rurangirwa et al., 1983, 1979; Sharpe et al., 1982). The zebrafish could be a suitable complementary model to study B cell dysfunction and associated elimination of memory responses, *in vivo*.

In African trypanosomiasis, co-infections are often observed, including those with pathogens causing malaria, helminthiasis, typhoid, urinary tract infections, HIV, and tuberculosis (Kagira et al., 2011). One of the most successful zebrafish disease model is the one based on *Mycobacterium marinum*, a close relative to the causative agent of human tuberculosis (*M. tuberculosis*) (reviewed by Cronan and Tobin, 2014; Meijer, 2016; Tobin and Ramakrishnan, 2008). In the future, it would be interesting to use the zebrafish as a model to study mixed infections with *M. marinum* and *T. carassii* or *T. borreli* and study how the differential macrophage activation and the absence of B cell memory during trypanosome infection would affect the mycobacterium infection and vice versa. To study these mixed infections, both embryonic/larval and juvenile zebrafish can be used. The embryonic and larval zebrafish (2-7dpf) stages provide a time frame to study the innate immune responses, while around 3 weeks post fertilization (wpf), both innate and adaptive immune cell types are present in the developing juvenile zebrafish (Langenau et al., 2004; Page et al., 2013). The juvenile stage closely resembles that of the adult, but sexual maturity takes until approximately 90 dpf. The advantage of this life stage (around 3-4 wpf), compared to the adult stage, is the presence of the adaptive immune cells whist the zebrafish are still relatively transparent allowing *in vivo*, real-time imaging. Some transgenic zebrafish lines fluorescently marking B cells (subsets) are already available (Liu et al., 2017; Page et al., 2013) and currently more are being developed.

Contribution and activation state of neutrophils during trypanosome and trypanoplasma infections

In the studies presented in this thesis, we were not able to specifically address the contribution and activation state of neutrophils during *T. carassii* and *T. borreli* infections. During *T. carassii* infections we did observe that neutrophils also responded to the infection by proliferating, although to a much lesser extent than macrophages. The total number of neutrophils however, was comparatively low and likely did not contribute to the total cell fluorescence measured in our whole larvae analysis (**Chapter 3**). During *T. borreli* infections we observed neutrophils responding to the infection by proliferation and the total (neutrophils) green fluorescence was also found to increase upon infection. However, this increase in total fluorescence did not correlate to the macrophage response nor to trypanoplasma levels (**Chapter 5**). Neutrophils were recently implicated in promoting the onset of tsetse fly-mediated trypanosome infections in mouse dermis, however macrophage-derived immune mediators, such as NO and TNFα were confirmed to play a more prominent role in the control of first-peak parasitaemia and in the regulation of the overall inflammatory response (Caljon et al., 2018). To our knowledge, transgenic lines specifically marking neutrophils in red fluorescence that can be combined with the available *Tg(il1b:eGFP-F)* ^{ump3Tg} or *Tg(tnfa:eGFP-F)*^{ump5Tg} lines, are currently not available. For

example, the *lysozymeC:DsRed* reporter line, marks a subset of macrophages and likely also granulocytes, and is therefore not specific for neutrophils only (Hall et al., 2007). In the future, it will certainly be interesting to investigate the activation of neutrophils and their contribution to the inflammatory response.

Role of sialic acid in *T. carassii* and *T. borreli* attachment/adhesion

Sialic acid on the trypanosome cell surface and host cells

The cell membrane of non-VSG-containing trypanosomes, such as *Trypanosoma cruzi*, are dominated by carbohydrate-rich coats of GPI-anchored mucin-like glycoproteins. These contain sialic acid, a monosaccharide that is cleaved and transferred from host serum components (glycoconjugates) to parasite surface molecules by a trypanosomal neuraminidase called trans-sialidase (Pereira-Chioccola et al., 2000; Schenkman et al., 1991; Schenkman and Eichinger, 1993). The VSG-containing *T. brucei* have sialic acid and trans-sialidases on their cell surface only in the procyclic trypomastigote stage (tsetse fly stage) and not in the mammalian bloodstream forms (Engstler et al., 1995, 1993; Engstler and Schauer, 1993). Sialic acid on the *T. cruzi* cell surface was shown to be involved in the prevention of parasite lysis in the vertebrate host, since the large amount of sialylated mucins form a protective surface coat (Pereira-Chioccola et al., 2000). In the absence of sialic acid substitution, the antibodies isolated from Chagasic patients were able to bind with high affinity to α-galactosyl epitopes present in the mucin molecules on the cell membrane. When bound to the cell membrane, these antibodies caused extensive structural perturbation of the parasite coat with formation of large blebs, caused by aggregation of the mucins, ultimately leading to irreversible surface damage and parasite lysis. The observation that sialylation prevents mucin clustering, could possibly be explained by electrostatic repulsion of negatively charged sialic acid molecules (Pereira-Chioccola et al., 2000). Studies showed that the neuraminidases produced by trypanosomes are responsible for removal of sialic acids on endothelial cells and erythrocytes and could be transferred to the parasite surface molecules (Schenkman et al., 1991; Schenkman and Eichinger, 1993). The desialylation of the major surface sialo-glycoproteins on erythrocytes, the glycophorins, is able to trigger erythrophagocytosis during *T. vixax* infections (Guegan et al., 2013). Other studies suggested that desialylated erythrocytes are subject to lysis by the classical or alternative pathway of complement (Brown et al., 1983; Jancik and Roland, 1974; Tomlinson et al., 1992), which was also described for *T. cruzi* infections (Libby et al., 1986; Pereira, 1983). The desialylation of erythrocytes by trypanosomal neuraminidases therefore seems to contribute to anaemia and appears to be an aspect regularly observed during trypanosome infections.

Studies for *T. congolense* analysed the role of sialic acid present on the host cells and revealed that this monosaccharide is involved in parasite adherence to erythrocytes and to endothelial cells of the vasculature (Hemphill et al., 1994; Hemphill and Ross, 1995). The involvement of sialic acid in attachment of *T. congolense* was investigated by means of wheat-germ agglutinin (WGA), WGA-gold, neuraminidases and trypsin treatments. Incubation of bovine endothelial cell monolayers with neuraminidases or with WGA, which binds N-acetylglucosamine and N-acetylneuraminic acid (sialic acids), caused inhibition of parasite adhesion (Hemphill et al., 1994; Hemphill and Ross, 1995). These studies suggested that *T. congolense* used sialic acid residues on the endothelial cell membrane for adhesion. It was shown that the attachment of *T. congolense* does involve extensive modifications of the membrane-attached flagellum (Beattie and Gull, 1997; Hemphill and Ross, 1995), but which molecules present on the parasite cell surface and flagellum interact with the sialic acids on the host cells has not been shown. Overall, sialic acids on the host cell surfaces might serve as a receptors for the attachment of *T. congolense*, while other studies showed that the surface coat trypanosomes and trypanoplasma also contain sialic acid residues and neuraminidases.

Sialic acid on the cell surface of *T. carassii* and *T. borreli*

As described in **Chapter 2** and **Chapter 4**, we observed that *T. carassii* and *T. borreli* are able to adhere *in vitro*, to the glass surface or to erythrocytes, and *in vivo*, to endothelium of the cardinal caudal vein. Based on our observations that the parasites attach to a glass surface, which does not contain sialic acids and on previous studies showing that sialic acid residues are present on the cell surface of *T. cruzi*, *T. carassii*, *C. salmositica* and *T. borreli* (Aguero et al., 2002; Lischke et al., 2000; Overath et al., 2001; J. P. Saeij et al., 2003; Vommaro et al., 1997), we were interested if the sialic acid present on the parasite cell surface was involved in the attachment. We performed a preliminary study where we incubated *T. carassii* and *T. borreli* with WGA-488 (molecular probes conjugated to Alexa Fluor-488, Invitrogen). We imaged the parasites on non-coated glass slides to visualise the WGA-488 surface labeling (**Fig 3A**) and counted the number of parasites adhering to the slide. Despite a reduction in the number of parasites adhering to the glass surface, attachment was not completely abolished by WGA treatment. In this experiment, no endothelial cells were present to mimic the *in vivo* situation, as described for the experiments by Hemphill et al (1994; 1995). Previously, it was observed that *T. brucei* was able to remove antibodies bound to its surface by hydrodynamic sorting, followed by endocytosis. This process is most effective at 37^{0}C and became less effective at temperatures below 24^{0}C (Engstler et al., 2007). The natural host of *T. borreli* and *T. carassii* is carp, which are ectothermic animals and generally live at temperatures between 4^{0}C and 25^{0}C. Additionally, it was observed *in vitro* that antibody clearance from the surface of *T. borreli* could not be completely halted even at 4ºC. The lack of complete inhibition of attachment in our study could have been influenced by the incubation at room temperature. In a follow up experiment, we incubated *T. borreli* with WGA-488 on ice and injected them intravenously in zebrafish larvae, followed by imaging from

1 hour post injection (hpi) onwards. We observed fewer WGA-labeled parasites adhering to the cardinal caudal vein endothelium when compared to non-labelled parasites (data not shown). These two preliminary experiments suggest the involvement of sialic acid in the attachment of *T. borreli* and *T. carassii* to endothelial surfaces of their host. In follow up studies it would be interesting to remove the sialic acids on the parasite cell surface by e.g. desialylation or analyse which molecules on the endothelial cells in the host are responsible for the adherence of the parasites (Tomlinson et al., 1994).

We observed that *T. carassii* attached through the posterior end, leaving the cell body and flagellum free to move (**Chapter 2**), and *T. borreli* attached through a very discrete portion of its cell membrane approximately in the centre of its cell body, leaving both flagella free to move (**Chapter 4**). Both parasites therefore use very small portions of their cell body to adhere to surfaces and the difference in location of attachment might be due to differences in cell body shape and rigidity. To identify the specific anchoring site of *T. carassii* and *T. borreli,* parasites were incubated with the CellBrite red dye, (CBR, Biotium), which is incorporated into the phospholipid layer of eukaryotic cells, labelling cytoplasmic and intercellular membrane structures. Labelled parasites were directly imaged live or fixed (4% PFA) on non-coated glass slides. As expected, for *T. carassii* we observed red labelling in a region close to the flagellum base, likely the flagellar pocket (**Fig 3B**, yellow arrow). Accumulation of the CBR dye in the flagellar pocket is likely due to the intrinsic ability of trypanosomes to rapidly endocytose membrane molecules in their flagellar pocket, the only phagocytic site of the cells, and thus to engulf any surface-bound molecule. Interestingly, for some of the parasites, we observed one additional organelle stained at the posterior tip of the cell body, localised more posterior than the flagellar pocket (**Fig 3B**, white arrow). This region seemed to co-localise with the posterior tip, the site where we observed attachment to erythrocytes or the glass surface (**Fig 3C**). Hence, the anchoring point for attachment is most likely not the flagellar pocket or the flagellar pocket neck as originally thought (**Chapter 2**, Dóró et al., 2019). Interestingly, the red labelling at the most posterior tip of *T. carassii* seems to coincide with the site of expression of XMAP215 protein in *T. brucei* (**Fig 3D**, white arrow), a marker for plus ends of microtubules marking the posterior end of the cell body in *T. brucei* parasites (Halliday et al., 2019; Wheeler et al., 2013). Visualising CBR-labelled *T. borreli* was more challenging, since after PFA fixation the cell body morphology was lost and we were unable to reliably locate the stained organelles. In live parasites however, we observed the presence of CBR in a region that is likely the flagellar pocket and one or two additional undefined regions (data not shown).

The involvement of the posterior end of *T. carassii* during attachment was confirmed also *in vivo,* and can potentially be involved in extravasation (**Chapter 2**, Dóró et al., 2019), although we were unable so far to capture the exact extravasation moment of *T. carassii in vivo*. *In vivo* attachment would have been difficult to visualise in other infection models such as mice. The observation that specific proteins seem to localise to the posterior tip of *T. carassii* during attachment and this location seems to overlap with the posterior end protein XMAP215, offers a possibility for future studies to analyse (*in vivo*) the proteins that might be involved in attachment.

Visualising blood flagellate infections in zebrafish: societal relevance and scientific impact.

Trypanosomes infect a variety of hosts and cause various infectious diseases in humans and animals. Well known examples are the fatal human diseases Sleeping Sickness, caused *by T. brucei* and Chagas' disease, caused by *T. cruzi*. Numerous *in vitro* studies and mice infection studies contributed tremendously to the insights into the general biology of trypanosomes, their interaction with and evasion of the host immune system, as well as into various aspects related to vaccine failure, antigenic variation, and (uncontrolled) inflammation. Additionally, trypanosome morphology was observed to be essential for their motility, adaptation to their host's environment and pathogenesis. How the arms race between trypanosomes and their mammalian host exactly develops in the early phase of infection, is currently unknown. This could largely be due to the inability to visualise, *in vivo*, the parasites and host cells.

In this thesis we describe for the first time blood flagellate infections *in vivo* in the natural environment of a vertebrate host. By making use of the transparent zebrafish larvae, infected with the fish-specific *Trypanosoma carassii*, we revealed in Chapter 2 novel attachment mechanisms and adaptation strategies of trypanosomes *in vivo* and we placed our observations in the framework of existing studies and literature. In Chapter 4 we describe *in vitro* and *in vivo* the swimming behaviour of *Trypanoplasma borreli*. Although the uniflagellate *T. carassii* and biflagellate *T. borreli* have major morphological differences, they are both able to the successfully infect the same natural host. We performed a novel quantitative analysis to compare the *in vitro* parasite motility (in two dimensions) of *T. borreli* and *T. carassii*. Parasite motility and attachment to the blood vessel wall are crucial for establishment and maintenance of infection, making them potential drug targets. Although the zebrafish is a suitable model to visualise *in vivo* novel parasite swimming behaviours, we were unable with our current setup to record the swimming behaviour in three dimensions and this did not yet allow us to perform a quantitative detailed analysis *in vivo*. Further, the zebrafish model allowed us to observe a differential response of innate immune cells to trypanosome and trypanoplasma infections, as reported in Chapter 3 and 5. We suggested that an early increase in macrophages upon infection appears to be beneficial for survival and we observed the occurrence of foamy macrophages, which could potentially be associated with inflammation-associated pathology. The *T. carassii* and *T. borreli* zebrafish infection model is a promising complementary model to existing animal models and *in vitro* studies, and can contribute to fundamental mechanistic insights into host-parasite interactions. Further, the model will not only help to understand parasite behaviour, but also the mechanisms of its immune evasion and the host immune response.

In the longer term, the results from this thesis could contribute to the improvement of human health and agriculture systems of emerging economies. Trypanosomiasis control presently relies on a combination of case detection, treatment and vector control. However, the current drugs available are suboptimal (Büscher et al., 2017). Additionally, fish trypanosomes and

trypanoplasma may cause heavy losses in economically important fishes (reviewed by Woo and Ardelli, 2013). Understanding the role of the innate immune response and the parasite behaviour mechanisms *in vivo* will aid in the development of novel therapeutic strategies and vaccines that can effectively limit the disease spread. In this thesis, we show that the blood flagellate-zebrafish infection model paves the way for both, fundamental and applied studies that in the future can contribute to human and animal trypanosomiasis elimination.

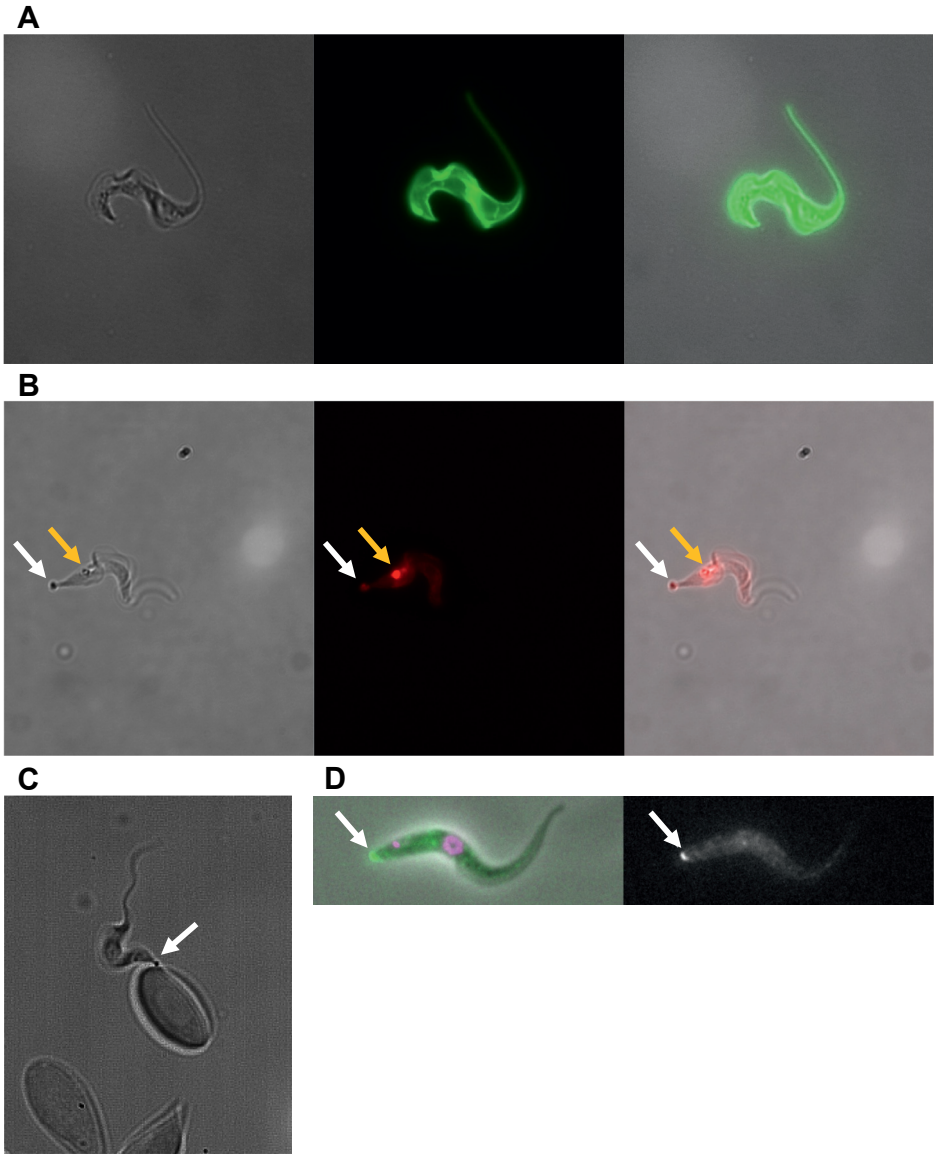

◂ Fig 3. Involvement of posterior tip *T. carassii* in attachment.
A) *T. carassii* incubated with WGA-488 surface labelling (Invitrogen) in culture medium for 25 minutes, followed by 3 washing steps. Parasites were imaged with a DM6b upright digital Leica microscope using 100x magnification. **B)** *T. carassii* incubated with CellBrite red (CBR), imaged with a DM6b upright digital Leica microscope using 100x magnification. CBR dye labelled the flagella pocket (yellow arrow) and one additional organelle, co-localising with the posterior tip of the cell body (white arrow). This region seemed to co-localise with the posterior tip, involved attachment. **C)** *T. carassii* attached via posterior tip (white arrow) to blood cell, image acquired with a DM6b upright digital Leica microscope using 100x magnification. **D)** Procyclic trypomastigote form *T. brucei,* visualising microtubule plus end binding protein XMAP215 at the posterior tip (bright green, white arrow) and DNA stained by Hoechst (magenta), imaged with a DM5500 B Leica microscope using a 63x magnification (Halliday et al., 2019) (http://tryptag.org/?query=Tb927.6.3090).

References

Aguero F, Campo V, Cremona L, Jager A, Noia JM Di, Overath P, Sanchez DO, Frasch AC. 2002. Gene Discovery in the Freshwater Fish Parasite. *Society* **70**:7140–7144. doi:10.1128/IAI.70.12.7140

Antia R, Nowak MA, Anderson RM. 1996. Antigenic variation and the within-host dynamics of parasites. *Proc Natl Acad Sci U S A* **93**:985–989. doi:10.1073/pnas.93.3.985

Beattie P, Gull K. 1997. Cytoskeletal architecture and components involved in the attachment of Trypanosoma congolense epimastigotes. *Parasitology* **115 (Pt 1**:47–55.

Bockstal V, Guirnalda P, Caljon G, Goenka R, Telfer JC, Radwanska M, Magez S, Black SJ. 2011. T . brucei Infection Reduces B Lymphopoiesis in Bone Marrow and Truncates Compensatory Splenic Lymphopoiesis through Transitional B-Cell Apoptosis **7**. doi:10.1371/journal.ppat.1002089

Brittingham A, Morrison CJ, McMaster WR, McGwire BS, Chang K-P, Mosser DM. 1995. Role of the Leishmania surface protease gp63 in complement fixation, cell adhesion, and resistance to complement-mediated lysis. *Parasitol Today* **11**:445–446. doi:10.1016/0169-4758(95)80054-9

Brown EJ, Joiner KA, Frank MM. 1983. Interaction of desialated guinea pig erythrocytes with the classical and alternative pathways of guinea pig complement in vivo and in vitro. *J Clin Invest* **71**:1710–1719. doi:10.1172/JCI110925

Brunet LR. 2001. Nitric oxide in parasitic infections. *Int Immunopharmacol* **1**:1457–1467. doi:10.1016/S1567-5769(01)00090-X

Büscher P, Cecchi G, Jamonneau V, Priotto G. 2017. Human African trypanosomiasis. *Lancet* **390**:2397–2409. doi:10.1016/S0140-6736(17)31510-6

Clay H, Volkman HE, Ramakrishnan L. 2008. Tumor Necrosis Factor Signaling Mediates Resistance to Mycobacteria by Inhibiting Bacterial Growth and Macrophage Death. *Immunity* **29**:283–294. doi:10.1016/j.immuni.2008.06.011

Cronan MR, Tobin DM. 2014. Fit for consumption: Zebrafish as a model for tuberculosis. *DMM Dis Model Mech* **7**:777–784. doi:10.1242/dmm.016089

Cross GAM. 1996. Antigenic variation in trypanosomes: Secrets surface slowly. *BioEssays* **18**:283–291. doi:10.1002/bies.950180406

Cuevas IC, Cazzulo JJ, Sánchez DO. 2003. gp63 homologues in Trypanosoma cruzi: Surface antigens with metalloprotease activity and a possible role in host cell infection. *Infect Immun* **71**:5739–5749. doi:10.1128/IAI.71.10.5739-5749.2003

Daulouède S, Bouteille B, Moynet D, De Baetselier P, Courtois P, Lemesre JL, Buguet A, Cespuglio R, Vincendeau P. 2001. Human Macrophage Tumor Necrosis Factor (TNF)–α Production Induced by Trypanosoma brucei gambiense and the Role of TNF-α in Parasite Control . *J Infect Dis* **183**:988–991. doi:10.1086/319257

De Muylder G, Daulouède S, Lecordier L, Uzureau P, Morias Y, Van Den Abbeele J, Caljon G, Hérin M, Holzmuller P, Semballa S, Courtois P, Vanhamme L, Stijlemans B, De Baetselier P, Barrett MP, Barlow JL, McKenzie ANJ, Barron L, Wynn TA, Beschin A, Vincendeau P, Pays E. 2013. A Trypanosoma brucei Kinesin Heavy Chain Promotes Parasite Growth by Triggering Host Arginase Activity. *PLoS Pathog* **9**:1–14. doi:10.1371/journal.ppat.1003731

Dóró É, Jacobs SH, Hammond FR, Schipper H, Pieters RP, Carrington M, Wiegertjes GF, Forlenza M. 2019. Visualizing trypanosomes in a vertebrate host reveals novel swimming behaviours, adaptations and attachment mechanisms. *Elife* **8**:1–25. doi:10.7554/elife.48388

Eiserich JP, Hristova M, Cross CE, Jones AD, Freeman BA, Halliwell B, Van der Vliet A. 1997. Formationof nitric oxide- derived inflammatoryoxidants bymyeloperoxidase in neutrophils. *Nature* **22**:393–397. doi:10.1038/246170a0

Elks PM, Brizee S, van der Vaart M, Walmsley SR, van Eeden FJ, Renshaw SA, Meijer AH. 2013. Hypoxia Inducible Factor Signaling Modulates Susceptibility to Mycobacterial Infection via a Nitric Oxide Dependent Mechanism. *PLoS Pathog* **9**:1–16. doi:10.1371/journal.ppat.1003789

Engstler M, Pfohl T, Herminghaus S, Boshart M, Wiegertjes G, Heddergott N, Overath P. 2007. Hydrodynamic Flow-Mediated Protein Sorting on the Cell Surface of Trypanosomes 505–515. doi:10.1016/j.cell.2007.08.046

Engstler M, Reuter G, Schauer R. 1993. The developmentally regulated trans-sialidase from Trypanosoma brucei sialylates the procyclic acidic repetitive protein. *Mol Biochem Parasitol* **61**:1–13. doi:10.1016/0166-6851(93)90153-O

Engstler M, Schauer R. 1993. Sialidases from African trypanosomes. *Parasitol Today* **9**:222–225. doi:10.1016/0169-4758(93)90018-B

Engstler M, Schauer R, Brun R. 1995. Distribution of developmentally regulated trans-sialidases in the Kinetoplastida and characterization of a shed trans-sialidase activity from procyclic Trypanosoma congolense. *Acta Trop* **59**:117–129. doi:10.1016/0001-706X(95)00077-R

Fink IR, Elks PM, Wentzel AS, Spaink HP, Wiegertjes GF. 2015. Polarization of immune responses in fish: The 'macrophages first' point of view. *Mol Immunol* **69**:146–156. doi:10.1016/j.molimm.2015.09.026

Forlenza M, Magez S, Scharsack JP, Westphal A, Savelkoul HFJ, Wiegertjes GF. 2009a. Receptor-Mediated and Lectin-Like Activities of Carp (Cyprinus carpio) TNF-α. *J Immunol* **183**:5319–5332. doi:10.4049/jimmunol.0901780

Forlenza M, Nakao M, Wibowo I, Joerink M, Arts JAJ, Savelkoul HFJ, Wiegertjes GF. 2009b. Nitric oxide hinders antibody clearance from the surface of Trypanoplasma borreli and increases susceptibility to complement-mediated lysis. *Mol Immunol* **46**:3188–3197. doi:10.1016/j.molimm.2009.08.011

Forlenza M, Scharsack JP, Kachamakova NM, Taverne-Thiele AJ, Rombout JHWM, Wiegertjes GF. 2008. Differential contribution of neutrophilic granulocytes and macrophages to nitrosative stress in a host-parasite animal model. *Mol Immunol* **45**:3178–3189. doi:10.1016/j.molimm.2008.02.025

Grandgenett PM, Otsu K, Wilson HR, Wilson ME, Donelson JE. 2007. A function for a specific zinc metalloprotease of African trypanosomes. *PLoS Pathog* **3**:1432–1445. doi:10.1371/journal.ppat.0030150

Gruszynski AE, van Deursen FJ, Albareda MC, Best A, Chaudhary K, Cliffe LJ, del Rio L, Dunn JD, Ellis L, Evans KJ, Figueiredo JM, Malmquist NA, Omosun Y, Palenchar JB, Prickett S, Punkosdy GA, van Dooren G, Wang Q, Menon AK, Matthews KR, Bangs JD. 2006. Regulation of surface coat exchange by differentiating African trypanosomes. *Mol Biochem Parasitol* **147**:211–223. doi:10.1016/j.molbiopara.2006.02.013

Guegan F, Plazolles N, Baltz T, Coustou V. 2013. Erythrophagocytosis of desialylated red blood cells is responsible for anaemia during Trypanosomavivax infection. *Cell Microbiol* **15**:1285–1303. doi:10.1111/cmi.12123

Hall C, Flores M, Storm T, Crosier K, Crosier P. 2007. The zebrafish lysozyme C promoter drives myeloid-specific expression in transgenic fish. *BMC Dev Biol* **7**:1–17. doi:10.1186/1471-213X-7-42

Halliday C, Billington K, Wang Z, Madden R, Dean S, Sunter JD, Wheeler RJ. 2019. Cellular landmarks of Trypanosoma brucei and Leishmania mexicana. *Mol Biochem Parasitol* **230**:24–36. doi:10.1016/j.molbiopara.2018.12.003

Hemphill A, Frame I, Ross CA. 1994. The interaction of Trypanosoma congolense with endothelial cells. *Parasitology* **109**:631–641. doi:10.1017/S0031182000076514

Hemphill A, Ross CA. 1995. Flagellum-mediated adhesion ofTrypanosoma congolense to bovine aorta endothelial cells. *Parasitol Res* **81**:412–420. doi:10.1007/bf00931503

Holland W., Do T., Huong N., Dung N., Thanh N., Vercruysse J, Goddeeris B. 2003. The effect of Trypanosoma evansi infection on pig performance and vaccination against classical swine fever. *Vet Parasitol* **111**:115–123. doi:10.1016/S0304-4017(02)00363-1

Holland WG, My LN, Dung TV, Thanh NG, Tam PT, Vercruysse J, Goddeeris BM. 2001. The influence of T. evansi infection on the immuno-responsiveness of experimentally infected water buffaloes. *Vet Parasitol* **102**:225–234. doi:10.1016/S0304-4017(01)00534-9

Hurst JK, Hurst JK. 2002. Whence nitrotyrosine ? *J Clin Invest* **109**:1287–1289. doi:10.1172/JCI200215816. Commentary

Ilemobade AA, Adegboye DS, Onoviran O, Chima JC. 1982. Immunodepressive effects of trypanosomal infection in cattle immunized against contagious bovine pleuropneumonia. *Parasite Immunol* **4**:273–282. doi:10.1111/j.1365-3024.1982.tb00438.x

Iraqi F, Sekikawa K, Rowlands J, Teale A. 2001. Susceptibility of tumour necrosis factor-α genetically deficient mice to trypanosoma congolense infection. *Parasite Immunol* **23**:445–451. doi:10.1046/j.1365-3024.2001.00401.x

Jancik J, Roland S. 1974. Sialic Acid — a Determinant of the Life-Time of Rabbit Erythrocytes. *Hoppe-Seyler´s Zeitschrift für Physiol Chemie*. doi:10.1515/bchm2.1974.355.1.395

Joerink M, Forlenza M, Ribeiro CMS, de Vries BJ, Savelkoul HFJ, Wiegertjes GF. 2006. Differential macrophage polarisation during parasitic infections in common carp (Cyprinus carpio L.). *Fish Shellfish Immunol* **21**:561–571. doi:10.1016/j.fsi.2006.03.006

Joerink M, Groeneveld A, Ducro B, Savelkoul HFJ, Wiegertjes GF. 2007. Mixed infection with Trypanoplasma borreli and Trypanosoma carassii induces protection: Involvement of cross-reactive antibodies. *Dev Comp Immunol* **31**:903–915. doi:10.1016/j.dci.2006.12.003

Jurecka P, Irnazarow I, Stafford JL, Ruszczyk A, Taverne N, Belosevic M, Savelkoul HFJ, Wiegertjes GF. 2009. The induction of nitric oxide response of carp macrophages by transferrin is influenced by the allelic diversity of the molecule. *Fish Shellfish Immunol* **26**:632–638. doi:10.1016/j.fsi.2008.10.007

Kagira JM, Maina N, Njenga J, Karanja SM, Karori SM, Ngotho JM. 2011. Prevalence and types of coinfections in sleeping sickness patients in Kenya (2000/2009). *J Trop Med* **2011**. doi:10.1155/2011/248914

Kaushik RS, Uzonna JE, Gordon JR, Tabel H. 1999. Innate resistance to Trypanosoma congolense infections: Differential production of nitric oxide by macrophages from susceptible BALB/c and resistant C57B1/6 mice. *Exp Parasitol* **92**:131–143. doi:10.1006/expr.1999.4408

Kinoshita S, Biswas G, Kono T, Hikima J, Sakai M. 2013. Presence of two tumor necrosis factor (tnf)-α homologs on different chromosomes of zebrafish (Danio rerio) and medaka (Oryzias latipes). *Mar Genomics*. doi:10.1016/j.margen.2013.10.004

LaCount DJ, Gruszynski AE, Grandgenett PM, Bangs JD, Donelson JE. 2003. Expression and Function of the Trypanosoma brucei Major Surface Protease (GP63) Genes. *J Biol Chem* **278**:24658–24664. doi:10.1074/jbc.M301451200

Langenau DM, Ferrando AA, Traver D, Kutok JL, Hezel JPD, Kanki JP, Zon LI, Thomas Look A, Trede NS. 2004. In vivo tracking of T cell development, ablation, and engraftment in transgenic zebrafish. *Proc Natl Acad Sci U S A* **101**:7369–7374. doi:10.1073/pnas.0402248101

Libby P, Alroy J, Pereira MEA. 1986. A neuraminidase from Trypanosoma cruzi removes sialic acid from the surface of mammalian myocardial and endothelial cells. *J Clin Invest* **77**:127–135. doi:10.1172/JCI112266

Lischke A, Klein C, Stierhof YD, Hempel M, Mehlert A, Almeida IC, Ferguson MAJ, Overath P. 2000. Isolation and characterization of glycosylphosphatidylinositol-anchored, mucin-like surface glycoproteins from bloodstream forms of the freshwater-fish parasite Trypanosoma carassii. *Biochem J* **345**:693–700. doi:10.1042/0264-6021:3450693

Liu X, Li Y-S, Shinton SA, Rhodes J, Tang L, Feng H, Jette CA, Look AT, Hayakawa K, Hardy RR. 2017. Zebrafish B Cell Development without a Pre–B Cell Stage, Revealed by CD79 Fluorescence Reporter Transgenes. *J Immunol* **199**:1706–1715. doi:10.4049/jimmunol.1700552

Lom J, Dyková I. 1992. Protozoan parasites of fishes. Amsterdam: Elsevier Science Publishers.

Lopez R, Demick KP, Mansfield JM, Paulnock DM. 2008. Type I IFNs Play a Role in Early Resistance, but Subsequent Susceptibility, to the African Trypanosomes. *J Immunol* **181**:4908–4917. doi:10.4049/jimmunol.181.7.4908

Lucas R, Magez S, Leys R De, Fransen L, Lucas R, Magez S, Leys R De, Fransen L, Scheerlinck J, Rampelberg M, Sablon E. 1994. Mapping the Lectin-Like Activity of Tumor Necrosis Factor Published by : American Association for the Advancement of Science Stable URL : http://www.jstor.org/stable/2882928 JSTOR is a not-for-profit service that helps scholars , researchers , and student **263**:814–817.

Magez S, Geuskens M, Beschin A, Del Favero H, Verschueren H, Lucas R, Pays E, De Baetselier P. 1997. Specific uptake of tumor necrosis factor-α is involved in growth control of Trypanosoma brucei. *J Cell Biol* **137**:715–727. doi:10.1083/jcb.137.3.715

Magez S, Radwanska M, Beschin A, Sekikawa K, De Baetselier P. 1999. Tumor necrosis factor alpha is a key mediator in the regulation of experimental Trypanosoma brucei infections. *Infect Immun* **67**:3128–3132.

Magez S, Radwanska M, Drennan M, Fick L, Baral TN, Allie N, Jacobs M, Nedospasov S, Brombacher F, Ryffel B, Baetselier PD. 2007. Tumor Necrosis Factor (TNF) Receptor–1 (TNFp55) Signal Transduction and Macrophage-Derived Soluble TNF Are Crucial for Nitric Oxide–Mediated Trypanosoma congolense Parasite Killing . *J Infect Dis* **196**:954–962. doi:10.1086/520815

Magez S, Radwanska M, Drennan M, Fick L, Baral TN, Brombacher F, Baetselier PD. 2006. Interferon-γ and Nitric Oxide in Combination with Antibodies Are Key Protective Host Immune Factors during Trypanosoma congolense Tc13 Infections . *J Infect Dis* **193**:1575–1583. doi:10.1086/503808

Magez S, Truyens C, Merimi M, Radwanska M, Stijlemans B, Brouckaert P, Brombacher F, Pays E, Baetselier PD. 2004. P75 Tumor Necrosis Factor–Receptor Shedding Occurs as a Protective Host Response during African Trypanosomiasis. *J Infect Dis* **189**:527–539. doi:10.1086/381151

McGwire BS, O'Connell WA, Chang KP, Engman DM. 2002. Extracellular release of the glycosylphosphatidylinositol (GPI)-linked Leishmania surface metalloprotease, gp63, is independent of GPI phospholipolysis. Implications for parasite virulence. *J Biol Chem* **277**:8802–8809. doi:10.1074/jbc.M109072200

Meijer AH. 2016. Protection and pathology in TB: learning from the zebrafish model. *Semin Immunopathol* **38**:261–273. doi:10.1007/s00281-015-0522-4

Morrison LJ, Marcello L, McCulloch R. 2009. Antigenic variation in the African trypanosome: Molecular mechanisms and phenotypic complexity. *Cell Microbiol* **11**:1724–1734. doi:10.1111/j.1462-5822.2009.01383.x

Mwangi DM, Munyua WK, Nyaga PN. 1990. Immunosuppression in caprine trypanosomiasis: Effects of acuteTrypanosoma congolense infection on antibody response to anthrax spore vaccine. *Trop Anim Health Prod* **22**:95–100. doi:10.1007/BF02239832

Naessens J. 2006. Bovine trypanotolerance: A natural ability to prevent severe anaemia and haemophagocytic syndrome? *Int J Parasitol* **36**:521–528. doi:10.1016/j.ijpara.2006.02.012

Naessens J, Leak SGA, Kennedy DJ, Kemp SJ, Teale AJ. 2003. Responses of bovine chimaeras combining trypanosomosis resistant and susceptible genotypes to experimental infection with Trypanosoma congolense. *Vet Parasitol* **111**:125–142. doi:10.1016/S0304-4017(02)00360-6

Namangala B, Noel W, De Baetselier P, Brys L, Beschin A. 2001. Relative contribution of interferon-gamma and interleukin-10 to resistance to murine African trypanosomosis. *J Infect Dis* **183**:1794–1800.

Nguyen-Chi M, Laplace-Builhé B, Travnickova J, Luz-Crawford P, Tejedor G, Lutfalla G, Kissa K, Jorgensen C, Djouad F. 2017. TNF signaling and macrophages govern fin regeneration in zebrafish larvae. *Cell Death Dis* **8**:e2979. doi:10.1038/cddis.2017.374

Nguyen-Chi M, Laplace-Builhe B, Travnickova J, Luz-Crawford P, Tejedor G, Phan QT, Duroux-Richard I, Levraud JP, Kissa K, Lutfalla G, Jorgensen C, Djouad F. 2015. Identification of polarized macrophage subsets in zebrafish. *Elife* **4**:1–14. doi:10.7554/eLife.07288

Noel W, Gh GH, Raes G, Namangala B, Daems I, Brys L, Brombacher F, Baetselier P De, Beschin A. 2002. Infection Stage-Dependent Modulation of Macrophage Activation in. *Society* **70**:6180–6187. doi:10.1128/IAI.70.11.6180

Oladiran A, Belosevic M. 2012. Recombinant glycoprotein 63 (Gp63) of Trypanosoma carassii suppresses antimicrobial responses of goldfish (Carassius auratus L.) monocytes and macrophages. *Int J Parasitol* **42**:621–633. doi:10.1016/j.ijpara.2012.04.012

Overath P, Haag J, Lischke A, O'hUigin C. 2001. The surface structure of trypanosomes in relation to their molecular phylogeny. *Int J Parasitol* **31**:468–471. doi:10.1016/S0020-7519(01)00152-7

Overath P, Haag J, Mameza MG, Lischke A. 1999. Freshwater fish trypanosomes: Definition of two types, host control by antibodies and lack of antigenic variation. *Parasitology* **119**:591–601. doi:10.1017/S0031182099005089

Page DM, Wittamer V, Bertrand JY, Lewis KL, Pratt DN, Delgado N, Schale SE, McGue C, Jacobsen BH, Doty A, Pao Y, Yang H, Chi NC, Magor BG, Traver D. 2013. An evolutionarily conserved program of B-cell development and activation in zebrafish. *Blood* **122**:1–11. doi:10.1182/blood-2012-12-471029

Pereira-Chioccola VL, Acosta-Serrano A, De Almeida IC, Ferguson MAJ, Souto-Padron T, Rodrigues MM, Travassos LR, Schenkman S. 2000. Mucin-like molecules form a negatively charged coat that protects Trypanosoma cruzi trypomastigotes from killing by human anti-α-galactosyl antibodies. *J Cell Sci* **113**:1299–1307.

Pereira MEA. 1983. A Developmentally Regulated Neuraminidase Activity in Trypanosoma cruzi Published by : American Association for the Advancement of Science Stable URL : https://www.jstor.org/stable/1689985 **219**:1444–1446.

Radwanska M, Guirnalda P, Trez C De, Ryffel B, Black S, Magez S. 2008. Trypanosomiasis-Induced B Cell Apoptosis Results in Loss of Protective Anti-Parasite Antibody Responses and Abolishment of Vaccine-Induced Memory Responses **4**. doi:10.1371/journal.ppat.1000078

Ramakrishnan L. 2013. The zebrafish guide to tuberculosis immunity and treatment. *Cold Spring Harb Symp Quant Biol* **78**:179–192. doi:10.1101/sqb.2013.78.023283

Roca FJ, Mulero I, López-Muñoz A, Sepulcre MP, Renshaw SA, Meseguer J, Mulero V. 2008. Evolution of the Inflammatory Response in Vertebrates: Fish TNF-α Is a Powerful Activator of Endothelial Cells but Hardly Activates Phagocytes. *J Immunol* **181**:5071–5081. doi:10.4049/jimmunol.181.7.5071

Roca FJ, Whitworth LJ, Redmond S, Jones AA, Ramakrishnan L. 2019. TNF Induces Pathogenic Programmed Macrophage Necrosis in Tuberculosis through a Mitochondrial-Lysosomal-Endoplasmic Reticulum Circuit. *Cell* **178**:1344-1361.e11. doi:10.1016/j.cell.2019.08.004

Rurangirwa FR, Musoke AJ, Nantulya VM, Tabel H. 1983. Immune depression in bovine trypanosomiasis: effects of acute and chronic Trypanosoma congolense and chronic Trypanosoma vivax infections on antibody response to Brucella abortus vaccine. *Parasite Immunol* **5**:267–276. doi:doi:10.1111/j.1365-3024.1983.tb00743.x

Rurangirwa FR, Tabel H, Losos GJ, Tizard IR. 1979. Suppression of antibody response to Leptospira biflexa and Brucella abortus and recovery from immunosuppression after Berenil treatment. *Infect Immun* **26**:822–826.

Ruszczyk A, Forlenza M, Joerink M, Ribeiro CMS, Jurecka P, Wiegertjes GF. 2008a. Trypanoplasma borreli cysteine proteinase activities support a conservation of function with respect to digestion of host proteins in common carp. *Dev Comp Immunol* **32**:1348–1361. doi:10.1016/j.dci.2008.05.002

Ruszczyk A, Forlenza M, Savelkoul HFJ, Wiegertjes GF. 2008b. Molecular cloning and functional charactrisation of a cathepsin L-like proteinase from the fish kinetoplastid parasite Trypanosoma carassii. *Fish Shellfish Immunol* **24**:205–214. doi:10.1016/j.fsi.2007.10.015

Saeij JP, de Vries BJ, Wiegertjes GF. 2003. The immune response of carp to Trypanoplasma borreli: kinetics of immune gene expression and polyclonal lymphocyte activation. *Dev Comp Immunol* **27**:859–874.

Saeij JPJ, Van Muiswinkel WB, Groeneveld A, Wiegertjes GF. 2002. Immune modulation by fish kinetoplastid parasites: A role for nitric oxide. *Parasitology* **124**:77–86. doi:10.1017/S0031182001008915

Saeij JPJ, Van Muiswinkel WB, Van De Meent M, Amaral C, Wiegertjes GF. 2003. Different capacities of carp leukocytes to encounter nitric oxide-mediated stress: A role for the intracellular reduced glutathione pool. *Dev Comp Immunol* **27**:555–568. doi:10.1016/S0145-305X(02)00158-1

Salmon D, Vanwalleghem G, Morias Y, Denoeud J, Krumbholz C, Lhommé F, Bachmaier S, Kador M, Gossmann J, Dias FBS, De Muylder G, Uzureau P, Magez S, Moser M, De Baetselier P, Van Den Abbeele J, Beschin A, Boshart M, Pays E. 2012. Adenylate cyclases of Trypanosoma brucei inhibit the innate immune response of the host. *Science (80-)* **337**:463–466. doi:10.1126/science.1222753

Schenkman S, Eichinger D. 1993. Trypanosoma cruzi trans-sialidase and cell invasion. *Parasitol Today* **9**:218–222. doi:10.1016/0169-4758(93)90017-A

Schenkman S, Jiang MS, Hart GW, Nussenzweig V. 1991. A novel cell surface trans-sialidase of trypanosoma cruzi generates a stage-specific epitope required for invasion of mammalian cells. *Cell* **65**:1117–1125. doi:10.1016/0092-8674(91)90008-M

Schwede A, Macleod OJS, MacGregor P, Carrington M. 2015. How Does the VSG Coat of Bloodstream Form African Trypanosomes Interact with External Proteins? *PLoS Pathog* **11**:1–18. doi:10.1371/journal.ppat.1005259

Sharpe RT, Langley AM, Mowat GN, Macaskill JA, Holmes PH. 1982. Immunosuppression in bovine trypanosomiasis: response of cattle infected with Trypanosoma congolense to foot-and-mouth disease vaccination and subsequent live virus challenge. *Res Vet Sci* **32**:289–293. doi:10.1016/S0034-5288(18)32382-8

Sternberg JM, Mabbott NA. 1996. Nitric oxide-mediated suppression of T cell responses during Trypanosoma brucei infection: Soluble trypanosome products and interferon-γ are synergistic inducers of nitric oxide synthase. *Eur J Immunol*. doi:10.1002/eji.1830260306

Stijlemans B, Caljon G, Van Den Abbeele J, Van Ginderachter JA, Magez S, De Trez C. 2016. Immune evasion strategies of Trypanosoma brucei within the mammalian host: Progression to pathogenicity. *Front Immunol* **7**. doi:10.3389/fimmu.2016.00233

Tobin DM, Ramakrishnan L. 2008. Comparative pathogenesis of Mycobacterium marinum and Mycobacterium tuberculosis. *Cell Microbiol* **10**:1027–1039. doi:10.1111/j.1462-5822.2008.01133.x

Tomlinson S, Carvalho LP De, Vandekerckhove F, Nussenzweig V. 1992. Resialylation of sialidase-treated sheep and human erythrocytes by Trypanosoma cruzi trans-sialidase: Restoration of complement resistance of desialylated sheep erythrocytes. *Glycobiology* **2**:549–551. doi:10.1093/glycob/2.6.549

Tomlinson S, Pontes de Carvalho LC, Vandekerckhove F, Nussenzweig V. 1994. Role of sialic acid in the resistance of Trypanosoma cruzi trypomastigotes to complement. *J Immunol* **153**:3141–7.

Vickerman K. 1969. On the Surface Coat and Flagellar Adhesion in Trypanosomes. *J Cell Sci* **5**:163–193.

Vommaro RC, Attias M, Silva Filho FC, Woo PTK, De Souza W. 1997. Surface charge and surface carbohydrates of Cryptobia salmositica virulent and avirulent forms and of C. bullocki (Kinetoplastida: Cryptobiidae). *Parasitol Res* **83**:698–705. doi:10.1007/s004360050322

Wheeler RJ, Scheumann N, Wickstead B, Gull K, Vaughan S. 2013. Cytokinesis in trypanosoma brucei differs between bloodstream and tsetse trypomastigote forms: Implications for microtubule-based morphogenesis and mutant analysis. *Mol Microbiol* **90**:1339–1355. doi:10.1111/mmi.12436

Wiegertjes GF, Wentzel AS, Spaink HP, Elks PM, Fink IR. 2016. Polarization of immune responses in fish: The 'macrophages first' point of view. *Mol Immunol* **69**:146–156. doi:10.1016/j.molimm.2015.09.026

Woo PTK, Ardelli BF. 2013. Immunity against selected piscine flagellates. *Dev Comp Immunol* **43**:268–279. doi:10.1016/j.dci.2013.07.006

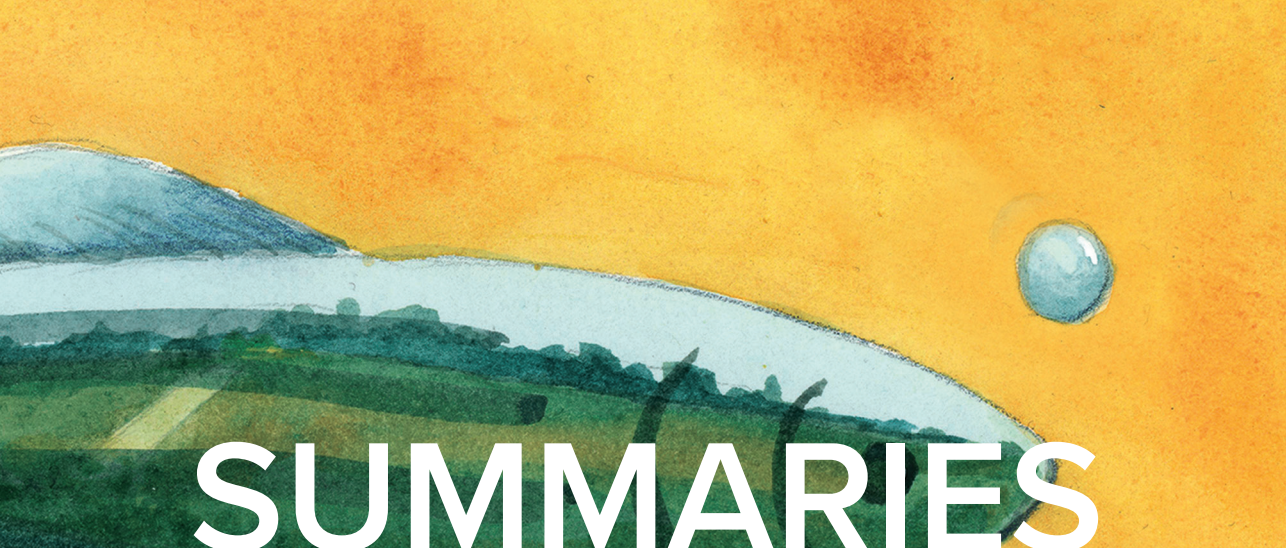

SUMMARIES

Summary (English)
Samenvatting (Nederlands)

Summary

Trypanosomes of the *Trypanosoma* genus are blood flagellates, and important causative agents of diseases of humans, livestock and cold-blooded species. Numerous *in vitro* studies and infection studies in mice contributed enormously to the insights into the biology of trypanosomes, their interaction with and evasion of the host immune system, as well as into various aspects related to vaccine failure and (uncontrolled) inflammation. A tight regulation of the early innate immune response to trypanosome infections was shown to be critical to obtain a balance between parasite control and inflammation-associated pathology. Trypanosome morphology was observed to be essential for their motility, the adaptation to their host's environment and pathogenesis. One of the best-studied non-mammalian trypanosomes is *Trypanosoma carassii*, which presents many morphological similarities to mammalian trypanosomes. *T. carassii* is regularly observed co-infecting fish with *Trypanoplasma spp* such as *T. borreli*. Currently, few or no *in vitro* studies have been performed to unravel the swimming behaviour and host-pathogen interaction of *Trypanoplasma* species. For both trypanosomes and trypanoplasma, *in vivo* studies to visualize the parasite motility and host immune response have not been reported so far. In light of this, aim of this thesis was to visualize and characterise blood flagellates infections, by studying: 1) parasite motility *in vitro* and *in vivo* and 2) the kinetics of innate immune responses *in vivo*.

In **Chapter 1**, I provide a framework for this thesis by first introducing the Kinetoplastid order, including the aquatic extracellular blood flagellates *Trypanosoma carassii* and *Trypanoplasma borreli*. Next, I describe the suitability of the zebrafish as a disease model, because of its transparency during larval life stages, the sequential development of the immune system and the availability of mutant and transgenic lines. Then I highlight the current knowledge about the early innate immune responses of the host during trypanosome infections. Subsequently, I highlight the most common immune evasion and manipulation strategies of trypanosomes, followed by a reflection on what is known about the innate immune response and immune evasion or manipulation mechanisms in the less characterised *Trypanoplasma* species. Motility is one of the most crucial aspects of trypanosome and trypanoplasma pathogenesis. All the studies currently performed to investigate host-pathogen interactions, the differential immune responses upon infection and trypanosome motility have been performed *in vitro* or *ex vivo*. In general, thanks to these studies, information about the morphology, swimming behaviour, flagellar motility and host-pathogen interaction of trypanosomes is available, however, there are limited studies performed on *Trypanoplasma* species.

Currently, detailed analysis of trypanosome motility, morphology and parasite-host cell interaction has been restricted to *in vitro* or *ex vivo* studies, using conditions that mimic the host environment. In **Chapter 2**, we established a *T. carassii* infection model in zebrafish, allowing

us to visualize, for the first time *in vivo*, novel swimming behaviours, attachment mechanisms and adaptation strategies of trypanosomes in the blood and tissues of a vertebrate host. First, the swimming behaviour of trypanosomes *ex vivo* in carp blood was described, and we observed that the majority of the trypanosomes were found to be tumbling swimmers. This suggested that the tumbling behaviour could be a typical feature of trypanosomes residing in the vasculature of their host. *In vivo* analysis of the swimming behaviour of *T. carassii* however, showed that it was not possible to assign a specific swimming behaviour to trypanosomes in the blood, since in the presence of an intact blood flow, we observed the trypanosomes to be passively dragged by the flow along with blood cells. Thus, with an intact blood flow, trypanosomes were never observed to tumble or swim directionally faster than the flow. When extravasated outside the blood vessels, or in conditions where the blood stream or the number of blood cells was reduced or absent, trypanosomes were able to adapt their swimming behaviour to the changing environment. For example in the fin, with very restricted space, trypanosomes were observed to swim directionally and inverting their swimming direction by backward swimming. In less compact tissue trypanosomes were observed to both tumble and swim directional, and they could invert their swimming direction by a "whip-like" motion or backwards swimming. Finally, we describe a novel attachment mechanism, by which trypanosomes anchor themselves to host cells or tissue.

The current knowledge about the early innate immune response upon infection with trypanosomes was obtained from studies performed in several mice models with limited possibility to visualize the infection *in vivo*, due to the lack of transparency of the host. We established in Chapter 2 the *T. carassii* infection model in zebrafish and consequently, in **Chapter 3** we studied *in vivo* the innate immune response of zebrafish larvae to *T. carassii* infections. First, we developed a clinical scoring system, based on various criteria, which allowed us to consistently divide individual larvae into high- or low-infected groups. Between these two groups, we did not only observe differences between macrophage and neutrophil number and distribution, but also in macrophage morphology and activation state. In high- and low-infected individuals, differences were observed in the inflammatory response of macrophages and in the susceptibility to the infection. Interestingly, exclusively in the cardinal caudal vein of high-infected fish, large granular macrophages, rich in lipid droplets, appeared. Lipid staining confirmed these cells were foamy macrophages, characterised by a strong pro-inflammatory profile as assessed using *tnfa* and *il1b* transgenic zebrafish lines. This strong pro-inflammatory profile was associated with susceptibility of the host to the infection.

T. carassii are regularly observed co-infecting cyprinid fish with *T. borreli.* Although several aspects of trypanosome motility are described previously by *in vitro* or *ex vivo* studies, and more recently *in vivo* in our studies (**Chapter 2**), the swimming behaviour of biflagellate

trypanoplasma remains rather unexplored. Trypanosomes, like *T. carassii*, have the flagellar pocket on the posterior end and a recurrent flagellum running along the cell body, ending free on the anterior (leading) end. For *T. borreli,* both flagella originate from a single flagellar pocket that is located at the anterior end of the cell body. The recurrent flagellum runs from the flagellar pocket along the cell body and ends free at the posterior end, whereas the non-cell attached flagellum is free to move at the anterior end of the parasite. In **Chapter 4**, we compared the motility of the biflagellate *T. borreli* with the motility of uniflagellate *T. carassii*, by performing a quantitative analysis comparing their *in vitro* swimming behaviour, cell body characteristics and flagella behaviour. We described that *T. borreli* swim more directionally and have larger, more variable and flexible cell bodies compared to *T. carassii.* Additionally, the anterior flagellum of both parasites displayed comparable behaviours, although one is cell-attached in *T. carassii* and the other is non-cell attached in *T. borreli*. Additionally, we made use of experimental infection of zebrafish with *T. borreli* to visualize *in vivo* the trypanoplasma swimming behaviour in the bloodstream and tissues of a vertebrate host. We showed that, like *T. carassii*, *T. borreli* was also able to anchor itself to host cells and tissue, although the attachment did occur in a different manner than that observed for *T. carassii.*

In **Chapter 5**, we took again advantage of the transparency of zebrafish larvae and of the availability of transgenic lines marking innate immune cells, as we studied the innate immune response of zebrafish larvae to *T. borreli* infections. We reported on the differential response of neutrophils and macrophages during the early phase of the infection. Furthermore, based on total macrophage-related fluorescence intensity, we differentiated infected larvae in groups of macrophage (MΦ)-low and MΦ-high individuals. We confirmed that differences in total macrophage fluorescence directly correlated with differences in macrophage numbers and observed that macrophage numbers were inversely correlated with parasitaemia and susceptibility to the infection. Exclusively in the cardinal caudal vein of MΦ-low larvae (with high infection levels), we again observed the occurrence of foamy macrophages. These macrophages were characterized by a strong inflammatory profile, and were associated to susceptibility to the infection. Conversely, MΦ-high individuals (with low infection levels), showed a low inflammatory profile and were able to control the infection.

Finally, in **Chapter 6**, the results of previous chapters are integrated in a larger framework and the implications of these results for future research is described, taking into consideration the strengths and weaknesses of our current work. I start with reflecting on the observation that live, motile trypanosomes and trypanoplasma were never observed to directly interact with macrophages or neutrophils and describe mechanisms that are used by trypanosomes and trypanoplasma to evade immune responses or manipulate their immune recognition. I propose a future study that could be performed in zebrafish to analyse whether trypanosomes and trypanoplasma, in some way, manipulated the host to prevent inflammation, and

subsequently promote parasite growth and settlement. Subsequently, the next steps for *in vivo* visualization of innate immune responses during trypanosome and trypanoplasma infections are discussed. Results of this thesis indicate that a (moderate) Tnfα production by the early responding macrophages could have played a beneficial role in controlling the parasitaemia levels and approaches to study in the future the involvement of Tnfα (subsets) during trypanosome and trypanoplasma infections are proposed. Additionally, I describe preliminary work studying the contribution of innate immune cells to tissue nitration, which is caused by the release of reactive oxygen and nitrogen species upon *T. borreli* infection. Next, I propose mixed *T. carassii* and *T. borreli* infections of zebrafish as a potential tool to study macrophage polarization *in vivo*. I propose that the zebrafish might be a suited model to investigate the effect of trypanosomes on vaccine efficacy during co-infections (with for example *Mycobacterium marinum*). Finally, the current knowledge about the role of sialic acid and trans-sialidases in the attachment of trypanosomes and trypanoplasma is defined. I describe the results of two preliminary studies that we performed to identify the specific anchoring site of *T. carassii* and *T. borreli* and to study the involvement of sialic acids in the attachment, both *in vitro* and *in vivo*. Furthermore, I suggest how the preliminary results of these studies can help us in the future to analyse which molecules might be involved in the attachment of these extracellular blood flagellates.

In this thesis we describe for the first time blood flagellate infections *in vivo* in the natural environment of a vertebrate host. The *T. carassii* and *T. borreli* zebrafish infection models are promising complementary models to existing (mammalian) animal models, and can contribute to fundamental mechanistic insights into host-parasite interactions.

Samenvatting

Trypanosomen van het geslacht *Trypanosoma* zijn bloedflagellaten en belangrijke veroorzakers van ziekten bij mensen, vee en koudbloedige diersoorten. Talrijke *in vitro* studies en infectieonderzoeken bij muizen hebben enorm bijgedragen aan de inzichten in de biologie van trypanosomen, hun interactie met en ontwijking van het immuunsysteem van de gastheer, evenals in verschillende aspecten met betrekking tot vaccinatie falen en (ongecontroleerde) ontsteking. Een strakke regulering van de vroege aangeboren immuunrespons op trypanosoom infecties bleek van cruciaal belang om een evenwicht te vinden tussen parasiet controle en ontsteking-gerelateerde pathologie. De morfologie van trypanosomen werd vastgesteld als een essentiële factor voor hun beweeglijkheid, de aanpassing aan de omgeving van hun gastheer en de pathogenese. Een van de best bestudeerde niet-zoogdierlijke trypanosomen is *Trypanosoma carassii*, dat veel morfologische overeenkomsten vertoont met zoogdierlijke trypanosomen. *T. carassii* co-infecteert vissen met *Trypanoplasma spp* zoals *T. borreli*. Momenteel zijn er weinig of geen *in vitro* onderzoeken uitgevoerd met het doel het zwemgedrag en de interactie tussen gastheer en pathogeen van *Trypanoplasma* soorten te ontrafelen. Voor zowel trypanosomen als trypanoplasma zijn tot nu toe geen *in vivo* onderzoeken gerapporteerd om de motiliteit van de parasiet en de immuunrespons van de gastheer te visualiseren. In het licht hiervan was het doel van dit proefschrift het visualiseren en karakteriseren van infecties met bloedflagellaten, door het bestuderen van: 1) motiliteit van parasieten *in vitro* en *in vivo* en 2) de kinetiek van aangeboren immuunreacties *in vivo*.

In **Hoofdstuk 1** geef ik een kader voor dit proefschrift door eerst de Kinetoplastid order te introduceren, inclusief de aquatische extracellulaire bloedflagellaten *Trypanosoma carassii* en *Trypanoplasma borreli*. Vervolgens beschrijf ik de geschiktheid van de zebravis als ziektemodel, vanwege de transparantie tijdens de larvale levensstadia, de opeenvolgende ontwikkeling van het immuunsysteem en de beschikbaarheid van mutante en transgene lijnen. Vervolgens belicht ik de huidige kennis over de vroege aangeboren immuunreacties van de gastheer tijdens trypanosoom infecties. Verder belicht ik de meest voorkomende strategieën voor immuun ontduiking en manipulatie van trypanosomen, gevolgd door een reflectie op wat bekend is over de aangeboren immuunrespons en immuun ontduiking of manipulatiemechanismen bij de minder gekarakteriseerde *Trypanoplasma* soorten. Motiliteit is een van de meest cruciale aspecten van de pathogenese van trypanosomen en trypanoplasma. Alle onderzoeken die momenteel zijn uitgevoerd om interacties tussen gastheer en pathogeen, de differentiële immuunreacties na infectie en de trypanosoom motiliteit te onderzoeken, zijn *in vitro* of *ex vivo* uitgevoerd. In het algemeen is dankzij deze studies informatie beschikbaar over de morfologie, zwemgedrag, flagellum motiliteit en gastheer-pathogeen interactie van trypanosomen, maar er zijn beperkte studies uitgevoerd met *Trypanoplasma* soorten.

Momenteel is gedetailleerde analyse van de beweeglijkheid, morfologie van trypanosomen en interactie tussen parasiet en gastheercel beperkt tot *in vitro* of *ex vivo* studies, waarbij gebruik wordt gemaakt van omstandigheden die de gastheeromgeving nabootsen. In **Hoofdstuk 2** hebben we een *T. carassii* infectiemodel in zebravis vastgesteld, waarmee we voor het eerst *in vivo* nieuw zwemgedrag, hechtingsmechanismen en aanpassingsstrategieën van trypanosomen in het bloed en de weefsels van een gewervelde gastheer kunnen visualiseren. Eerst werd het zwemgedrag van trypanosomen *ex vivo* in karper bloed beschreven, en we zagen dat de meerderheid van de trypanosomen tuimelende zwemmers bleken te zijn. Dit suggereerde dat het tuimelgedrag een typisch kenmerk zou kunnen zijn van trypanosomen die zich in het vaatstelsel van hun gastheer bevinden. *In vivo* analyse van het zwemgedrag van *T. carassii* toonde echter aan dat het niet mogelijk was om een specifiek zwemgedrag toe te kennen aan trypanosomen in het bloed, aangezien we in aanwezigheid van een intacte bloedstroom zagen dat de trypanosomen passief werden voortgesleept de bloedstroom samen met bloedcellen. Dus, met een intacte bloedstroom, werd nooit waargenomen dat trypanosomen sneller tuimelden of directioneel zwommen dan de stroming. Bij extravasatie buiten de bloedvaten, of in omstandigheden waarbij de bloedstroom of het aantal bloedcellen was verminderd of afwezig, konden trypanosomen hun zwemgedrag aanpassen aan de veranderende omgeving. Bijvoorbeeld, in de vin, met zeer beperkte ruimte, werd waargenomen dat trypanosomen directioneel zwommen en hun zwemrichting omkeerden door achteruit te zwemmen. In minder compact weefsel werden trypanosomen waargenomen die zowel tuimelen als directioneel zwemmen, en ze konden hun zwemrichting omkeren door een ‘zweepachtige beweging’ of achterwaarts zwemmen. Ten slotte beschrijven we een nieuw hechtingsmechanisme, waarbij trypanosomen zichzelf verankeren aan gastheercellen of -weefsel.

De huidige kennis over de vroege aangeboren immuunrespons na infectie met trypanosomen werd verkregen uit studies uitgevoerd in verschillende muizenmodellen met beperkte mogelijkheid om de infectie *in vivo* te visualiseren, vanwege het gebrek aan transparantie van de gastheer. We hebben in Hoofdstuk 2 het *T. carassii* infectiemodel bij zebravissen vastgesteld en daarom hebben we in **Hoofdstuk 3** *in vivo* de aangeboren immuunrespons van zebravis larven op *T. carassii* infecties bestudeerd. Ten eerste hebben we een klinisch scoresysteem ontwikkeld op basis van verschillende criteria, waardoor we individuele larven consistent konden verdelen in hoog of laag geïnfecteerde groepen. Tussen deze twee groepen hebben we niet alleen verschillen waargenomen tussen het aantal en de distributie van macrofagen en neutrofielen, maar ook in de morfologie van de macrofagen en de activeringsstatus. Bij individuen met een hoge en een lage infectie werden verschillen waargenomen in de ontstekingsreactie van macrofagen en in de gevoeligheid voor de infectie. Interessant is dat, exclusief in de kardinale caudale ader van sterk geïnfecteerde vissen, grote granulaire macrofagen, rijk aan lipide druppeltjes, verschenen. Lipide kleuring

bevestigde dat deze cellen 'foamy' macrofagen waren, gekenmerkt door een sterk pro-inflammatoir profiel, zoals beoordeeld met behulp van transgene zebravislijnen van *tnfa* en *il1b*. Dit sterke pro-inflammatoire profiel ging gepaard met de gevoeligheid van de gastheer voor de infectie.

T. carassii wordt regelmatig waargenomen dat het cypriniden co-infecteert met *T. borreli*. Hoewel verschillende aspecten van de beweeglijkheid van trypanosomen eerder zijn beschreven door *in vitro* of *ex vivo* studies, en meer recentelijk *in vivo* in onze studies (Hoofdstuk 2), blijft het zwemgedrag van biflagellate trypanoplasma tamelijk onbekend. Trypanosomen, zoals *T. carassii*, hebben de flagellaire pocket aan het achterste uiteinde en een terugkerend flagellum dat langs het cellichaam loopt en vrij eindigt aan het voorste (leidende) uiteinde. Voor *T. borreli* zijn beide flagella afkomstig van een enkele flagellaire pocket die zich aan het voorste uiteinde van het cellichaam bevindt. Het terugkerende flagellum loopt van de flagellaire pocket langs het cellichaam en eindigt vrij aan het achterste uiteinde, terwijl het niet-celgebonden flagellum vrij kan bewegen aan het voorste uiteinde van de parasiet. In **Hoofdstuk 4** hebben we de motiliteit van het biflagellaat *T. borreli* vergeleken met de motiliteit van uniflagellaat *T. carassii*, door een kwantitatieve analyse uit te voeren die hun *in vitro* zwemgedrag, cellichaam kenmerken en flagella-gedrag vergelijkt. We beschreven dat *T. borreli* meer directioneel zwemt en een groter, meer variabel en flexibel cellichaam heeft vergeleken met *T. carassii*. Bovendien vertoonde het voorste flagellum van beide parasieten vergelijkbaar gedrag, hoewel de ene celgebonden is in *T. carassii* en de andere niet-celgebonden is in *T. borreli*. Daarnaast hebben we gebruik gemaakt van experimentele infectie van zebravissen met *T. borreli* om *in vivo* het trypanoplasma-zwemgedrag in de bloedbaan en weefsels van een gewervelde gastheer te visualiseren. We toonden aan dat *T. borreli*, net als *T. carassii*, ook in staat was om zich te hechten aan gastheercellen en -weefsel, hoewel de hechting op een andere manier gebeurde dan die waargenomen voor *T. carassii*.

In **Hoofdstuk 5** hebben we opnieuw gebruik gemaakt van de transparantie van zebravis larven en van de beschikbaarheid van transgene lijnen die aangeboren immuun cellen markeren, en we hebben zo de aangeboren immuunrespons van zebravislarven op *T. borreli* infecties bestudeerd. We rapporteerden over de differentiële respons van neutrofielen en macrofagen tijdens de vroege fase van de infectie. Verder hebben we, gebaseerd op de totale macrofaag-gerelateerde fluorescentie-intensiteit, geïnfecteerde larven onderscheiden in groepen van macrofaag (MΦ) -lage en MΦ-hoge individuen. We bevestigden dat verschillen in totale macrofaagfluorescentie direct correleerden met verschillen in macrofaaggetallen en zagen dat macrofaaggetallen omgekeerd gecorreleerd waren met infectieniveaus en gevoeligheid voor de infectie. Exclusief in de kardinale caudale ader van MΦ-lage larven (met hoge infectieniveaus), hebben we opnieuw het verschijnen van 'foamy' macrofagen

waargenomen. Deze macrofagen werden gekenmerkt door een sterk ontstekingsprofiel en waren geassocieerd met gevoeligheid voor de infectie. Omgekeerd vertoonden MΦ-hoge individuen (met lage infectieniveaus) een laag inflammatoir profiel en konden ze de infectie onder controle houden.

Ten slotte worden in **Hoofdstuk 6** de resultaten van eerdere hoofdstukken geïntegreerd in een groter kader en worden de implicaties van deze resultaten voor toekomstig onderzoek beschreven, rekening houdend met de sterke en zwakke punten van ons huidige werk. Ik begin met het reflecteren over de observatie dat nooit werd waargenomen dat levende, beweeglijke trypanosomen en trypanoplasma rechtstreeks interageren met macrofagen of neutrofielen en beschrijf mechanismen die worden gebruikt door trypanosomen en trypanoplasma om immuunreacties te omzeilen of hun immuun herkenning te manipuleren. Ik stel een toekomstige studie voor die zou kunnen worden uitgevoerd bij zebravissen om te analyseren of trypanosomen en trypanoplasma op een of andere manier de gastheer manipuleerden om ontstekingen te voorkomen en vervolgens de groei en afwikkeling van parasieten te bevorderen. Vervolgens worden de volgende stappen besproken voor *in vivo* visualisatie van aangeboren immuunreacties tijdens trypanosoom en trypanoplasma infecties. Resultaten van dit proefschrift geven aan dat een (matige) Tnfα-productie door de vroeg reagerende macrofagen een gunstige rol zou kunnen hebben gespeeld bij het beheersen van de infectieniveaus en testen om in de toekomst de betrokkenheid van Tnfα (subsets) tijdens trypanosoom- en trypanoplasma-infecties te bestuderen worden voorgesteld. Daarnaast beschrijf ik voorbereidend werk dat de bijdrage van aangeboren immuun cellen aan weefselnitratie bestudeert, die wordt veroorzaakt door het vrijkomen van reactieve zuurstof- en stikstofsoorten bij infectie met *T. borreli*. Vervolgens stel ik gemengde *T. carassii* en *T. borreli* infecties van zebravissen voor als een potentieel hulpmiddel om macrofaagpolarisatie *in vivo* te bestuderen. Ik stel voor dat de zebravis een geschikt model zou kunnen zijn om het effect van trypanosomen op de werkzaamheid van vaccins tijdens co-infecties (met bijvoorbeeld *Mycobacterium marinum*) te onderzoeken. Ten slotte wordt de huidige kennis over de rol van sialic acid en trans-sialidasen bij de aanhechting van trypanosomen en trypanoplasma gedefinieerd. Ik beschrijf de resultaten van twee voorbereidende onderzoeken die we hebben uitgevoerd om de specifieke verankeringsplaats van *T. carassii* en *T. borreli* te identificeren en om de betrokkenheid van sialic acids bij de hechting te bestuderen, zowel *in vitro* als *in vivo*. Verder stel ik voor hoe de voorlopige resultaten van deze onderzoeken ons in de toekomst kunnen helpen analyseren welke moleculen mogelijk betrokken zijn bij de aanhechting van deze extracellulaire bloedflagellaten.

In dit proefschrift beschrijven we voor het eerst bloedflagellate infecties *in vivo* in de natuurlijke omgeving van een gewervelde gastheer. De *T. carassii* en *T. borreli* zebravis infectie modellen zijn veelbelovende complementaire modellen voor bestaande (zoog) diermodellen en kunnen bijdragen aan fundamentele mechanistische inzichten in interacties tussen gastheer en parasiet.

ABOUT THE AUTHOR

Curriculum vitae
List of publications
Overview of completed training activities
Acknowledgements

Curriculum Vitae

Sem was born in Sittard on the 1st of September 1990. While growing up, Sem always enjoyed the company of animals. Therefore, it was a logic step for Sem to start in 2009 the Bachelor Animal Sciences in Wageningen. During this study, Sem followed the Minor “Biology of infectious diseases” and for her BSc thesis she studied the influence of a simple and complex starter microflora on the development and health of caesarean derived piglets (Adaptation Physiology group).

After finishing her Bachelor, Sem gained more interest in research related to host- (vector-) pathogen interaction and the health of humans and animals. During her first MSc thesis, Sem investigated the role of skin bacterial odours on the attractiveness of Anopheles mosquitoes (Laboratory of Entomology). After this, she had her first contact with trypanosome and zebrafish research, when she performed her Major MSc thesis for 9 months at the Cell Biology and Immunology Group, where she worked on the *in vitro* characterization of zebrafish soluble and membrane-bound TNFα. Sem finished her Masters with an internship of 6 months, where she investigated the relationship between subcellular localisation and function of the XRNA 5’ to 3’ exoribonuclease in trypanosomes (Department of Biochemistry, University of Cambridge, United Kingdom).

Winning the NWO-WIAS PhD graduate programme grant, which was part of the Research Master cluster, gave Sem the opportunity to start her PhD in November 2015 at the Cell Biology and Immunology Group and Experimental Zoology Group. The aim of the project was to study *Trypanosoma carassii* and *Trypanoplasma borreli* infections in zebrafish. The results of her PhD project can be found in this thesis. During her project there was collaboration with the research groups Virologie et Immunologie Moléculaires, INRA (France) and Dynamique des Interactions Membranaires Normales et Pathologiques, CNRS, University of Montpellier (France), with an exchange period in both labs of 4 weeks.

From April 2020 Sem works as a Study Director at the Discovery & Environmental Sciences Department at Charles River Laboratories (the Netherlands).

List of publications

Dóró, E.; **Jacobs, S.H.**; Hammond, F.R.; Schipper, H.; Pieters, R.P.M.; Carrington, M; Wiegertjes, G.F.; Forlenza, M. Visualizing trypanosomes in a vertebrate host reveals novel swimming behaviours, adaptations and attachment mechanisms. *Elife* (2019)
DOI: https://doi.org/10.7554/eLife.48388.001

Jacobs, S.H.; Dóró, E.; Hammond, F.R; Scheer, M.; Nguyen- Chi, M.E.; Lutfalla, G.; Wiegertjes, G.F.; Forlenza, M. Differential response of macrophages and neutrophils to trypanosome infections in zebrafish: occurrence of foamy macrophages.
Submitted for publication

Jacobs, S.H.; Lankheet, M.J.M.; Van Dijk, K.S.E.; Arditti, F.; Pieters, R.P.M.; Schipper,H.; Wiegertjes, G.F.; Forlenza, M. Swimming behaviour of the biflagellate *Trypanoplasma borreli*, a comparison to the uniflagellate *Trypanosoma carassii.*
Manuscript in preparation

Jacobs, S.H.; Van Eyndhoven, L.C.; Brugman, S.; Scheer, M.; Langevin, C.; Wiegertjes, G.F.; Forlenza, M. An uncontrolled inflammatory innate response is associated with susceptibility of zebrafish to trypanoplasma infections.
Manuscript in preparation

Overview of completed training activities

The Basic Package	**3 ECTS**
WIAS Introduction Day	2015
Course on philosophy of science and/or ethics	2016
Course on essential skills	2016
Disciplinary Competences	**12 ECTS**
Preparing research review	2016
Advanced Immunology course UMC, Utrecht	2016
EMBL Advanced Fluorescence Microscopy course, Heidelberg, Germany	2016
(Zebra)Fish Vaccination Immunology Workshop, Wageningen	2017
KNAW species-specific laboratory fish course, Utrecht	2017
Professional Competences	**9 ECTS**
Supervising MSc thesis work	2017
WIAS Science Day committee member	2016-2017
Project and Time Management	2017
Interpersonal Communication for PhD candidates	2017
WAPS Council member	2017-2018
Scientific Writing	2019
Presentation Skills	**4 ECTS**
Famelab, Wageningen	2016
WIAS Science Day, Wageningen (poster)	2016
ZDM conference, Leiden (poster)	2018
ISDCI conference, Santa Fe (poster)	2018
Fish Immunology Workshop, Wageningen (oral)	2019
ISFSI conference, Gran Canaria (oral)	2019
Teaching competences	**6 ECTS**
BSc course: Cell Biology I (4x)	2015-2018
Fish Immunology Workshop (4x)	2016-2019
Supervising major Master thesis (2x)	2016-2019
Supervising Bachelor thesis	2016
Education and Training total:	**34 ECTS**

Completion of the training activities is in fulfilment of the requirements for the education certificate of the Graduate School of the Wageningen Institute of Animal Sciences (WIAS). One ECTS equals a study load of 28 hours.

Acknowledgements

Now remains the last, but certainly not the less important part of my thesis: Acknowledgements. During more than four years of research, I was privileged to meet or collaborate with many amazing, kind, inspiring, smart and helpful people, who contributed, each in their own way, to this thesis. I would like to thank some of them in particular.

First, my daily supervisor and promotor, **Maria**. Thank you for all your dedication, science-enthusiasm, knowledge and support, while guiding me through my thesis. There were never issues or difficulties, only 'challenges'. Your door was always open, and I was always welcome when I had a question or wanted to discuss some results. I very much enjoyed our 'doggy' / 'animal' chats before or after our meetings. Thank you, I learned a lot from you.

Ten tweede, natuurlijk mijn andere promotor, **Geert**. Bedankt voor al je enthousiasme, wijsheden, humor en grapjes, niet alleen tijdens onze ('Fish-unit') meetings, maar ook tijdens congressen en andere uitjes met de groep. Ook jouw deur stond altijd open voor korte (en minder korte) vragen. Later tijdens mijn thesis werden je ideeën en 'nieuwe ogen' voor mijn hoofdstukken en papers zeer gewaardeerd.

Dan mijn co-promotor, **Martin**. Al spreken we niet altijd elkaars 'taal', we begrepen elkaar uiteindelijk wel altijd. Bedankt voor je geduld, alle interessante en ontspannen meetings en de mogelijkheid dat ik altijd even binnen kon komen vallen voor een vraag(je) over de FFT (vele vragen), betekenis van termen of parameters, grafieken en hun lay-out.

Graag wil ik alle technicians en studenten bedanken die hebben meegeholpen aan mijn thesis. **Marleen, Trudi, Carolien, Henk** en **Remco**, heel erg bedankt voor jullie hulp, betrokkenheid en ideeën. Ook wil ik graag **Truus, Sander, Tom, Emily, Wian** en **Menno** bedanken voor al jullie hulp met de zebravissen in Carus. **Sep, Laura** en **Kaylee**, jullie waren alle drie enthousiaste en gemotiveerde studenten. Heel erg bedankt voor jullie bijdrage en inzet! Ik vind het heel leuk dat sommigen van jullie nu ook je PhD carrière zijn gestart of gaan starten.

Dear (Ex) E-wing PhDs from CBI and EZO; **Annelieke, Jules, Olaf, Sandra, Éva, Mirelle, Paulina, Mojtaba, Julia, Carmen, Christine, Esther, Adrià, Mark, Marloes, Awatif, Cornelius, Cees, Antoine, Wouter, Pulkit, Pim, Mike, Uros, Julian, Andres, Myrthe, Lana, Tiffany, Noraly**. I had a great time with you all during the last four years. Thank you for all the fun lunches, coffee breaks, (thank-you) dinners, drinks, PhD weekends, Labuitjes, parties and other activities.

Éva and **Sylvia**, thank you for your support and teaching me the zebrafish/parasite ins and outs.

Of course I am also thankful for my paranymphs; **Adrià** and **Mark**. It was always great to have you as my officemates and fellow (zebra)fish buddies. Your friendliness, positivity and calmness I appreciated a lot! We had regularly nice chats and you were there to listen to me when I was stressed or wanted to share some good news. Thank you, I am happy you are by my side (perhaps remotely) and agreed to be my paranymphs.

I also would like to thank of course all other CBI and EZO colleagues. Thank you for your interest, help, kindness, jokes and fun. I had four amazing years being your colleague!

Annemiek, Myrte, Eva, Marit, Tania, Floor, Marike en **Kitty**, sommigen van jullie heb ik al leren kennen toen we ‘ op kot gingen’ in Antwerpen, anderen tijdens de start van mijn studie in Wageningen. Bedankt voor het aanhoren van al mijn PhD avonturen en uitdagingen afgelopen jaren en jullie interesse en support, al de gezelligheid, leuke uitjes en etentjes!

Dan mijn ouders, **Frank** en **Marij**, bedankt voor jullie steun, betrokkenheid, hulp en liefde. Jullie staan altijd voor me klaar en staan me bij met raad en daad. Ik kijk altijd uit naar de leuke, gezellige, ontspannen weekendjes in Echt (en nu Stevensweert), samen met jullie en de beestjes.

Roberto, Bety e **Ricardo**, vocês estiverem sempre ao meu lado, mesmo que a distância, durante todo o doutorado. Obrigado por seu apoio e interesse.

Lieve **Felipe**, at the beginning you supported me during my studies and PhD at distance from Brazil. When you moved to Wageningen, you and Sjefke became my daily support team during my busy PhD period. Thank you for your help, love and especially patience and understanding. You helped me a lot by making me see things in perspective ;).

Colophon

The research described in this thesis was financially supported by the Dutch Research Council (NWO) (project number 022.004.005).

Financial support from Wageningen University for printing this thesis is gratefully acknowledged.

Cover design by © evelienjagtman.com
Lay-out by © evelienjagtman.com
Printed by ProefschriftMaken